

THE UNIVERSITY OF Hull

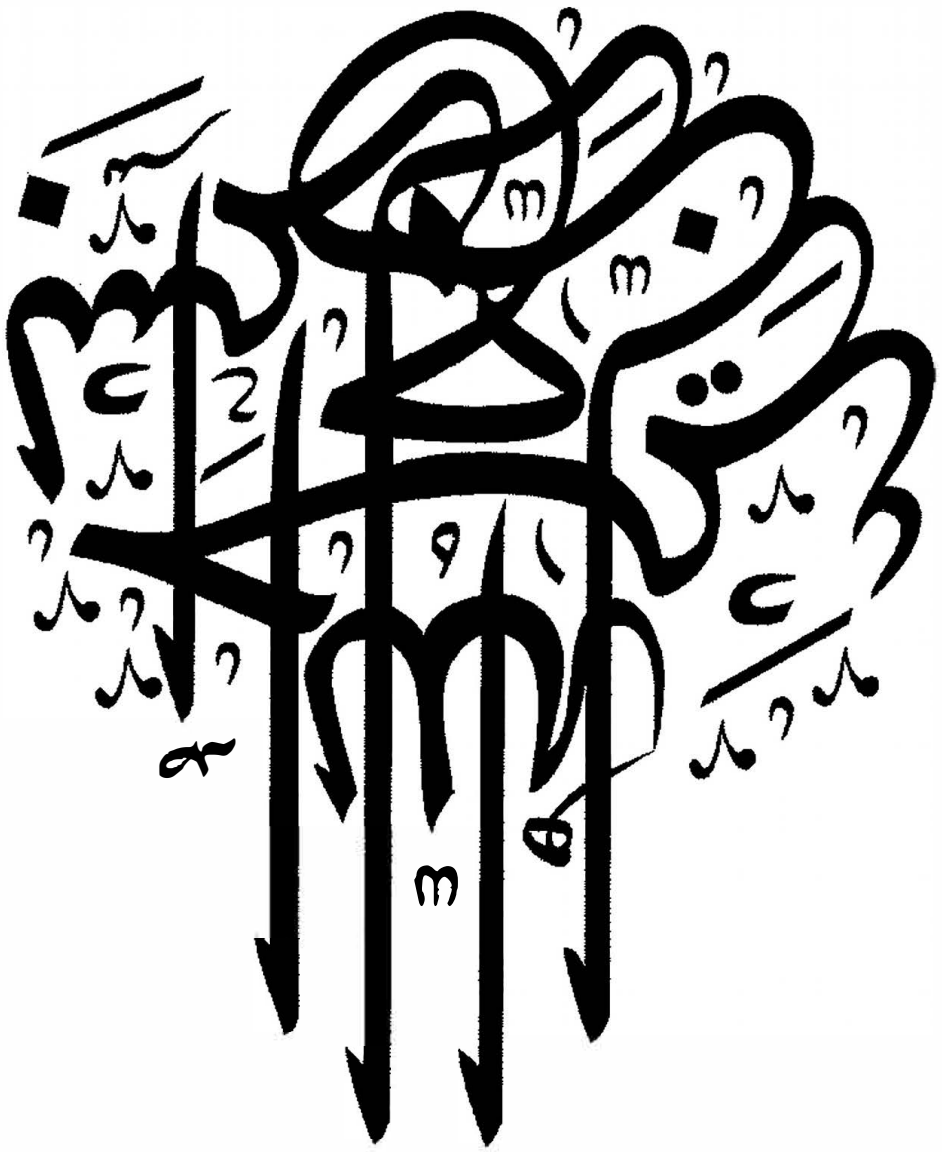
Spectrum Measurement, Sensing, Analysis and Simulation in the Context of Cognitive Radio

Being a Thesis submitted for the Degree of
Doctor of Philosophy
in the University of Hull

By

Meftah A Mehdawi
University of Hull, UK

August, 2015



To the memory of my Father, who
always advised me to read and read.

Also to my wife and Mother, who
suffered a lot due to my absence for so long period
of study, but prayed and wished
for me to complete this degree successfully

Abstract

The radio frequency (RF) spectrum is a scarce natural resource, currently regulated locally by national agencies. Spectrum has been assigned to different services and it is very difficult for emerging wireless technologies to gain access due to rigid spectrum policy and heavy opportunity cost. Current spectrum management by licensing causes artificial spectrum scarcity. Spectrum monitoring shows that many frequencies and times are unused. Dynamic spectrum access (DSA) is a potential solution to low spectrum efficiency. In DSA, an unlicensed user opportunistically uses vacant licensed spectrum with the help of cognitive radio. Cognitive radio is a key enabling technology for DSA. In a cognitive radio system, an unlicensed Secondary User (SU) identifies vacant licensed spectrum allocated to a Primary User (PU) and uses it without harmful interference to the PU. Cognitive radio increases spectrum usage efficiency while protecting legacy-licensed systems.

The purpose of this thesis is to bring together a group of CR concepts and explore how we can make the transition from conventional radio to cognitive radio. Specific goals of the thesis are firstly the measurement of the radio spectrum to understand the current spectrum usage in the Humber region, UK in the context of cognitive radio. Secondly, to characterise the performance of cyclostationary feature detectors through theoretical analysis, hardware implementation, and real-time performance measurements. Thirdly, to mitigate the effect of degradation due to multipath fading and shadowing, the use of wideband cooperative sensing techniques using adaptive sensing technique and multi-bit soft decision is proposed, which it is believed will

introduce more spectral opportunities over wider frequency ranges and achieve higher opportunistic aggregate throughput.

Understanding spectrum usage is the first step toward the future deployment of cognitive radio systems. Several spectrum usage measurement campaigns have been performed, mainly in the USA and Europe. These studies show locality and time dependence. In the first part of this thesis a spectrum usage measurement campaign in the Humber region, is reported. Spectrum usage patterns are identified and noise is characterised. A significant amount of spectrum was shown to be underutilized and available for the secondary use. The second part addresses the question: how can you tell if a spectrum channel is being used? Two spectrum sensing techniques are evaluated: Energy Detection and Cyclostationary Feature Detection. The performance of these techniques is compared using the measurements performed in the second part of the thesis. Cyclostationary feature detection is shown to be more robust to noise. The final part of the thesis considers the identification of vacant channels by combining spectrum measurements from multiple locations, known as cooperative sensing. Wideband cooperative sensing is proposed using multi resolution spectrum sensing (MRSS) with a multi-bit decision technique. Next, a two-stage adaptive system with cooperative wideband sensing is proposed based on the combination of energy detection and cyclostationary feature detection. Simulations using the system above indicate that the two-stage adaptive sensing cooperative wideband outperforms single site detection in terms of detection success and mean detection time in the context of wideband cooperative sensing.

Preface and Acknowledgements

This PhD thesis investigates the relationship between the radio spectrum today (command and control) and radio spectrum tomorrow (Dynamic Spectrum Access/Cognitive Radio). The topic of this thesis can be traced back to some eight years ago. I was in process of finishing my studies in Electronic Engineering at Tripoli University, Libya, and was provided with the opportunity to do my final project at GPTC Company on the subject of “Radio Frequency Spectrum Management (VHF&UHF)”. After graduating I took part in several training courses including a nine months training programme in Germany (Spectrum Monitoring and Direction Finder), six months in Iran (Microwave Link), three months in Egypt (Computer Security Network) and one month in UK (Data Analysis). In 2009 I was provided with opportunity to get my Masters degree at the University of Hull and the title of my Master thesis was System Model for the Evaluation of Interference (Cosite Analysis Model). Nick Riley acted as supervisor. After graduating I took part in a six months training program in GPTC Company in telecommunication called “Install and measurement radio mobile cellular”.

In 2012 I was provide with the opportunity to study for my PhD degree at University of Hull. The proposal was to follow with my Master thesis subject area “Wireless System Technologies” but with different topic. Nick Riley acted as supervisor. Motived by advances in wireless technology and after a lot of discussion we agreed to consider the challenge of spectrum today and spectrum tomorrow (Dynamic Spectrum Access/Cognitive Radio). This new proposal

became the beginning of this PhD research (see chapter 1). In the last 3 years I worked in several studies on this topic which result in the presented thesis. For most of this period I carried out my research working at spectrum measurement and spectrum sensing in the context of cognitive radio, from both practical and simulation point of view.

Several people have been influential during my PhD research. Nick Riley acted as supervisor in my Master degree. After this period he stimulated me to continue doing research on cognitive radio and to write a PhD thesis. I benefitted from his suggestions and support through the years, particularly, in the writing up stage. He also stimulated me to work together with researchers outside the University. Kevin Paulson also helped me considerably during the years. During my PhD I contributed to several meetings at COST Action IC0905 TERRA, led by Arturas Medeisis. He supported me in number of ways, for instance stimulating me to go to get a grant to present my work at several meetings and workshops as well as to attend training courses. Besides Arturas, three more people have supported within Cost Action project. They are Oliver Holland, Keith Nolan and Alexander M. Wyglinsk. I am also grateful to the members of my PhD committee for their useful comments.

Last but not the least, I would also like to thank my family for the support they provided me through my entire life and in particular, I must acknowledge my Wife and my Mother, without whose love, encouragement and editing assistance, I would not have finished this thesis.

List of Contents

Abstract	i
Preface and Acknowledgements.....	iii
List of Contents.....	v
List of Tables	x
List of Figures.....	xi
List of Abbreviations.....	xiv
Chapter1: Introduction	1
1.1 Overview	1
1.2 Motivation and Objectives	3
1.3 Thesis Outline	5
1.4 Thesis Contributions.....	8
1.5 Collaboration and Presentations (C & P).....	9
1.6 Publications	10
Part I: Radio Spectrum Today and Radio Spectrum Tomorrow	
Chapter2: The Radio Spectrum and Dynamic Spectrum Access.....	14
2.1 Background.....	14
2.2 History of Radio Spectrum	14
2.2.1 Approaches for Radio Spectrum Regulation	15
2.2.2 Basic Rules of Spectrum Regulation	16
2.3 Organisations that Regulate the Radio Spectrum	16
2.3.1 International Telecommunication Union, ITU (Global Co-ordination).....	17
2.3.2 European Union (EU).....	17
2.3.3 Examples of National Spectrum Management Authorities.....	18
2.4 Licensed and Unlicensed Spectrum.....	19

2.4.1	The Difficulty of Spectrum Licensing	20
2.4.2	Unlicensed Spectrum as an Alternative	20
2.4.3	Tragedy of Radio Spectrum Regulation	21
2.5	Dynamic Spectrum Access (Radio Spectrum Tomorrow).....	22
2.5.1	Dynamic Spectrum Exclusive Use Model	22
2.5.2	Open Sharing Model.....	23
2.5.3	Hierarchical Access Model.....	23
2.6	Key Parameters	24
2.7	Chapter Summary.....	26
Chapter3: Introduction to Software Defined Radio and Cognitive Radio		27
3.1	Introduction.....	27
3.2	Microelectronics Evolution and its Impact on Communication Technology	28
3.3	Software Defined Radio	29
3.3.1	History of SDR Development.....	29
3.3.2	Main Components of SDR-Based System Architecture	30
3.3.3	SDR Technology	32
3.3.4	Available SDR Platforms	34
3.4	Cognitive Radio.....	37
3.4.1	Cognitive Radio Definition.....	37
3.4.2	Cognitive Radio Network Architecture.....	38
3.4.3	Cognitive Capability of a Cognitive Radio.....	39
3.5	Chapter Summary.....	41

Part II: Measurement Phase Using Low Time Resolution (Spectrum Analyser)

Chapter4: Historical Spectrum Occupancy Measurements and Lesson Learned in the Context of CR		43
4.1	Introduction.....	43
4.2	Global Spectrum Occupancy Measurements (Previous Campaigns)	44
4.3	Shared Spectrum Company (SSC).....	45
4.3.1	SSC Campaigns During 2003.....	45
4.3.2	SSC Campaigns During 2004.....	45
4.3.3	SSC Campaigns During 2005.....	46
4.3.4	SSC Campaigns During 2007.....	46
4.3.5	SSC Campaigns During 2009.....	46
4.3.6	Comparing Global Spectrum Occupancy Measurements	47
4.4	Lessons Learned During Measurements Setup.....	49
4.4.1	Influence of Antenna Selection	50
4.4.2	Influence of Spectrum Analyser on the Measurements	53
4.4.3	Influence of Frequency and Time Dimension.....	56

4.4.3.1	Influence of Frequency Dimension	56
4.4.3.2	Influence of Time Dimension	59
4.4.4	Data Post-Processing.....	60
4.5	Threshold Impact.....	61
4.5.1	An Adaptive Threshold Setting Approach	63
4.6	Chapter Summary.....	64
Chapter5: Spectrum Occupancy Survey in Cognitive Radio: Measurement and Analysis.....		65
5.1	Introduction.....	65
5.2	Radio Spectrum Measurement	66
5.2.1	Measuring Radio Spectrum Usage	66
5.2.2	Spectrum Study	66
5.2.3	Spectrum Measurement System	67
5.2.4	Measurement Sites	68
5.2.5	Data Acquisition	72
5.3	Measurement Setup.....	73
5.4	Data Processing	74
5.5	Analysis of Spectrum Occupancy	75
5.5.1	General View of Spectrum Occupancy.....	75
5.5.2	Occupancy Metrics.....	76
5.5.3	Urban Area High Point (Location 1).....	77
5.5.3.1	Result and Main Observations	81
5.5.4	Urban, Suburban and Rural (Using Vehicle).....	82
5.5.4.1	Urban Area Ground Points.....	82
5.5.4.2	Rural, Suburban Locations	85
5.6	Chapter Summary.....	86

Part III: Spectrum Sensing and Analysis Using High Time Resolution (USRP2)

Chapter6: Spectrum Sensing Technology		89
6.1	Introduction.....	89
6.2	Passive Awareness and Active Awareness	90
6.2.1	Passive Awareness.....	90
6.2.2	Active Awareness	91
6.3	Spectrum Sensing Techniques.....	92
6.4	Primary Transmitter Detection (Non-Cooperative Sensing)	94
6.4.1	Energy Detection	95
6.4.2	Cyclostationary Feature Detection.....	98
6.4.3	Matched Filtering	100
6.4.4	Other Sensing Methods.....	101

6.4.5	Performance Assessment of Well-Known Spectrum Sensing Techniques ED, CFD, MF and Other Techniques	103
6.4.6	Simulation Platform for Spectrum Sensing Techniques ED, CFD and MF	104
6.5	Comparison of Various Sensing Methods	105
6.6	Cooperative and Two-Stage Adaptive Sensing.....	107
6.7	Chapter Summary.....	107
Chapter7:	Cyclostationary Feature Detection	109
7.1	Introduction.....	109
7.2	Goals, Framework and Approach.....	111
7.3	Cyclostationary Process	112
7.3.1	Model of the Cyclostationary Signal	113
7.3.1.1	Cyclic Autocorrelation Function (CAF).....	113
7.3.1.2	Spectral Correlation Density Function (SCF)	114
7.3.1.3	Spectral Coherence Function (SOF)	115
7.3.2	Benefits of the SCF/SOF.....	116
7.3.3	Evaluation of Cyclic Spectral Analysis Algorithms	117
7.3.3.1	Time Smoothed FFT Method	117
7.3.3.2	FFT Accumulation Method (FAM).....	118
7.3.3.3	Strip Spectral Correlation Algorithm (SSCA)	119
7.4	Channel Noise Analysis.....	120
7.4.1	Path Loss Model and Ranging	121
7.4.2	Path Loss Exponent Estimation	122
7.5	Methodology	123
7.5.1	Cyclostationary Feature Analysing System.....	123
7.5.2	Experimental Setup	125
7.6	Analysis and Results	126
7.6.1	Performance Measurement Overview.....	126
7.6.2	Path Loss Exponent Analysis	128
7.6.2.1	Open Sky Scenario (LOS Football Field)	129
7.6.2.2	Open Sky Scenario (Reflector and Shadowing).....	130
7.6.2.3	Indoor Scenario (LOS/NLOS)	131
7.6.2.4	RF Shielded Room	134
7.6.2.5	Brief summary.....	134
7.6.3	SNR and Observation Time.....	135
7.7	Chapter Summary.....	136

Part IV: Simulation Phase, Cooperative Wideband Spectrum Sensing

Chapter8:	Cooperative Wideband Spectrum Sensing.....	139
8.1	Introduction.....	139
8.2	Challenges in Non-Cooperative Sensing.....	141

8.3	Cooperative Sensing.....	142
8.3.1	Centralised and Distributed Sensing	142
8.3.2	Data and Decision Fusion	142
8.4	Wideband Spectrum Sensing	144
8.4.1	Dual-stage Spectrum Sensing	145
8.4.2	Wideband Cooperative Sensing	146
8.5	Proposed System Model for Wideband Cooperative Spectrum with Multi-Bit Hard Decision in Cognitive Radio using MRSS Technique.	146
8.5.1	Multi-Resolution Spectrum Sensing Method	147
8.5.1.1	Wavelet-based MRSS	148
8.5.2	Performance Analysis of Multi Threshold using Multi-bit Hard Combination Technique	149
8.5.3	Proposed Algorithm using MRSS technique	151
8.5.4	Simulation Results and Discussion	152
8.5.4.1	Coarse and Fine Resolution Sensing Results for a Node	152
8.5.4.2	Effect of Number of Nodes and Number of Transmitters	153
8.5.4.3	Comparing Three-Bit Hard Combination with traditional Hard Combination.....	154
8.6	Proposed System Model for Two-stage Adaptive Spectrum Sensing	156
8.6.1	Performance Assessment and Comparison of Two-stage Detector with One Stage Detector.....	159
8.6.2	Performance of Adaptive Two-Stage Combined Sensing.....	160
8.6.3	Optimisation of Mean Detection Time using Two-Stage Adaptive Sensing.....	162
8.7	Proposed System Model for Wideband Cooperative Spectrum Sensing with Multi-Bit Hard Decision using Two-stage adaptive sensing.	164
8.7.1	System Description.....	165
8.7.2	Simulation Results and Discussion	167
8.8	Chapter Summary.....	168

Part IV: Conclusion and Future work

Chapter9: Conclusion and Future Work.....	172
--	------------

9.1	Future Research Directions	175
-----	----------------------------------	-----

References.....	177
------------------------	------------

Appendix: Spectrum Measurement Platform, Simulink Model and Matlab

Code.....	191
------------------	------------

A.1	Control Subsystem (Spectrum Analyser)	191
-----	---	-----

A.1.2	Algorithm Control Script (Spectrum Analyser).....	193
-------	---	-----

A.2	Cyclostationary Feature Detection)	194
-----	--	-----

A.2.1	Design of Experiments (USRP2)	194
-------	-------------------------------------	-----

A.2.2	Simulink Model	194
-------	----------------------	-----

A.3	Simulation Model (Cooperative Wideband Spectrum Sensing)	196
-----	--	-----

List of Tables

Table 3.1: Comparison of DSPs, GPP, FPGAs and ASICs [49].....	32
Table 4.1: Characteristics of Antennas.....	50
Table 4.2: Impact of Amplification on the Activity Detected for Wireless Band.	55
Table 4.3: Impact of the Amplification Configuration.....	56
Table 4.4: Impact of the RBW on the Activity Detected Between 137 and 400MHz.....	59
Table 4.5: Calculate Thresholds and Corresponding Duty Cycles.	62
Table 5.1: Location of Measurement Sites Urban/Suburban Sites.....	71
Table 5.2: Location of Measurement Sites Rural Sites.....	71
Table 5.3: Spectrum Analyser Configuration.....	73
Table 5.4: Average Duty Cycle Statistics.....	81
Table 5.5: Top Level Measurement Statistic.	83
Table 7.1: Three Important Functions Derived in Cyclostationary Feature Detection.	116
Table 7.2: Time Smoothed Method Design Parameters [167].....	120
Table 7.3: Path Loss Exponents for Different Environments [180].	122
Table 7.4: Location Factor.	124
Table 7.5: Path Loss Exponents in Each Locations, Path Loss Exponent Difference & Variance.	135

List of Figures

Figure 1-1: Thesis organisation.....	6
Figure 1-2: Platform Architecture Overview.	6
Figure 2-1: Classification of Dynamic Spectrum Access Schemes [12, 31].....	22
Figure 2-2: Opportunistic Spectrum Access Concept [36].....	24
Figure 3-1: Main Components of SDR-Based System Architecture.....	31
Figure 3-2: Radio Block Diagram, Highlighting the Separation between Digital, and Analog Parts, Programmable, Configurable and Fixed Hardware Parts [50].	33
Figure 3-3: Cognitive Radio Network Architecture [73]	38
Figure 3-4: Cognitive Cycle of Cognitive Radio [15].	40
Figure 4-1: Bar Graph of the Spectrum Occupancy in Each Band (30-960 MHz).....	48
Figure 4-2: Bar Graph of the Spectrum Occupancy in Each Band (960-2900 MHz).....	48
Figure 4-3: Measurement Setup.....	50
Figure 4-4: Average Received Signal with/without External Amplifier over the Full TV Band.	52
Figure 4-5: Average Received Signal at CH30 and CH33.	53
Figure 4-6: Influence of the Frequency Bin on the Activity GSM1800.....	57
Figure 4-7: Influence of the Frequency Bin on the Activity Band UMTS.....	57
Figure 4-8: Average Duty Cycle per Hour for TV Broadcasting and GSM Band.....	59
Figure 4-9: Flow Chart of Post-Processing.....	61
Figure 4-10: Average Duty Cycle as Function of the Decision Threshold for Different Systems.	62
Figure 5-1: Measurement Equipment Employed in this Study: Antenna, Preamplifier and Spectrum Analyser at Urban Area (Hull University).	69
Figure 5-2: Measurement Equipment Employed in this Study: Antenna, Preamplifier and Spectrum Analyser at Rural Area (Humber region).	70
Figure 5-3: Measurement Locations in Urban Environment (Hull city).	72

Figure 5-4: Measurement Locations in Suburban/ Rural Environment (Humber region).	72
Figure 5-5: Data Processing Procedure.	74
Figure 5-6: Received Power versus the Frequency Band (80 MHz-2700 MHz).	76
Figure 5-7: Occupancy Measurement from 180 MHz to 400 MHz.	79
Figure 5-8: Occupancy Measurement from 470 MHz to 850 MHz.	79
Figure 5-9: Occupancy Measurement from 880 MHz to 960MHz.	80
Figure 5-10: Occupancy Measurement from 1710 MHz to 1880MHz.	80
Figure 5-11:Occupancy Measurement from 1900MHz to 2500MHz	80
Figure 5-12:Band By Band Average Duty Cycle Statistics.	81
Figure 5-13:Average Duty Cycle Statistics in Locations 2-15 for TV Band Compared to Location 1.	84
Figure 5-14:Normalised Average DC Statistics in Locations 2-15 for TV Bands (470-860 MHz).	85
Figure 5-15:Average DC Statistics in Locations 17 To 31 for TV Bands: TV (470-862 MHz).	85
Figure 6-1: Spectrum Awareness.	90
Figure 6-2: Classification of Spectrum Sensing Techniques.	93
Figure 6-3: Block Diagram of Energy Detection.	95
Figure 6-4: Threshold Setting in ED: Trade-off between Missed Detection and False Alarm.	97
Figure 6-5: Block Diagram of Cyclostationary Feature Detection.	99
Figure 6-6: Block Diagram of Matched Filter Detection.	100
Figure 6-7:(A)Comparison of Spectrum Sensing&(B)Performance of the Spectrum sensing.	103
Figure 6-8:Probability of Detection vs Probability of False Alarm Spectrum Sensing Techniques ED, MF, CFD with SNR=0dB And SNR=6dB.	105
Figure 6-9:Comparison of Spectrum Sensing Methods	106
Figure 7-1: SCF of BPSK under different SNR/observation time compared with PSD, using 27 , 213and 217BPSK Symbols [154].	110
Figure 7-2: Fourier Expansion of Periodic Signal for Feature Extraction.	113
Figure 7-3: Theoretical SCF Magnitude for BPSK, QPSK and SQPSK with Carrier Frequency [170].	116
Figure 7-4: Practical Implementation of Time Smoothed FFT Method [176].	118
Figure 7-5: Time Smoothed FFT Method [143], [7].	118
Figure 7-6: Description of the FFT Accumulation Method Algorithm [173].	119
Figure 7-7: Description of the SSCA Method Algorithm [166], [167].	120
Figure 7-8: Different Kinds of Fading Processes Such as Path Loss, Shadowing and Multipath that can occur in a Real Scenario.	121
Figure 7-9: Framework Structure of Cyclostationary Feature Analysing System.	123
Figure 7-10: Test Bed for Experiments.	125
Figure 7-11: Matlab System Block Diagram.	125
Figure 7-12: Received Power vs Frequency and Cyclic Frequency	128
Figure 7-13: Experiment Setup for Path-Loss Measurement Locations at Hull University...	129
Figure 7-14: A) SCF/PSD Path Loss at Football Field with LOS B) Photographs B) Fit Curve Slopes	130

Figure 7-15: SCF/PSD Path Loss outside Building with NLOS.	131
Figure 7-16: SCF/PSD Path Loss outside Building with LOS.....	131
Figure 7-17: SCF/PSD Path Loss at PhD Researcher Room.....	133
Figure 7-18: SCF/PSD Path Loss at Hallway Gate with LOS.	133
Figure 7-19: SCF/PSD Path Loss at Hallway Gate with NLOS.....	133
Figure 7-20: SCF/PSD Path Loss at Anechoic Chamber.	134
Figure 7-21: SCF Vs PSD with Varying SNR and Observation Time.....	136
Figure 8-1: Comparison of the Performance of proposed Data Fusion Rules.....	143
Figure 8-2: Block Diagrams for MRSS Wideband Sensing Algorithms.....	148
Figure 8-3: Energy Distribution of Primary User Signal and Noise.	149
Figure 8-4: Energy Regions of Softened Three Bits Hard Combination.....	150
Figure 8-5: Block Diagram of the Cooperative Wideband Sensing of the Proposed Scheme.	152
Figure 8-6: Result of Coarse Sensing Of 430-530 MHz Band.....	152
Figure 8-7: (A) Detection versus SNR for Four Different Numbers of Nodes, (B) Detection of Transmitter 3 versus SNR for Three Different Scenarios.....	153
Figure 8-8: (A)Detection versus SNR (B) False Alarm versus SNR	155
Figure 8-9: Two-Stage Adaptive Spectrum Sensing Detectors.....	157
Figure 8-10: Detection Performance against SNR Comparison of the Two Stage Detector with One Stage Detector.....	160
Figure 8-11: Mean Detection Time Comparison of Proposed Spectrum Sensing Cyclostationary Detector, Energy Detector and Two-Stage Adaptive.....	162
Figure 8-12: Probability Of Detection of the Proposed Two-Stage Adaptive Detector As Compared to A Single Stage ED And Cyclostationary Detector.....	162
Figure 8-13: Mean Detection Time Comparison for Varying P_K and Δ	164
Figure 8-14: Architecture of Wideband Cooperative Sensing Using Two Stage Adaptive Detection.....	165
Figure 8-15: ROC Curves Comparison of Non- Wideband Cooperative Detector With Wideband Cooperative Detector under Different Fusion Rule.	168
Figure 8-16: Detection Performance against SNR Comparison of Two-Stage Adaptive Detection Non-Cooperative Detector with Cooperative Detector.....	168

List of Abbreviations

ADC	Analogue to Digital Conversion
AWGN	Additive White Gaussian Noise
BB	Base Band
BS	Base Station
BW	Bandwidth
BWA	Broadband Wireless Access
CAF	Cyclic Autocorrelation Function
CCDF	Complementary Cumulative Distribution Function
CDF	Cumulative Distribution Function
CEPT	European Conference of Postal and Telecommunications Administration
CORVUS	Cognitive Radio Approach for Usage of Virtual Unlicensed Spectrum
CPC	Cognitive Pilot Channel
CPS	Cyclic Power Spectrum
CSS	Cooperative Spectrum Sensing
CR	Cognitive Radio
CFD	Cyclostationary Feature Detection
CRN	Cognitive Radio Network
DAB	Digital Audio Broadcasting
DAC	Digital to Analogue Conversion
DARPA	Defence Advanced Research Projects Agency
DC	Duty Cycle
DCS	Digital Cellular System
DCT	Downlink Continuous Transmission
DECT	Digital Enhanced Cordless Telecommunications
DFS	Dynamic Frequency Selection
DL	Downlink
DRIVE	Dynamic Radio for IP-Services in Vehicular Environments
DS	Downstream
DMR	Digital Modular Radio
DSA	Dynamic Spectrum Access
DSP	Digital Signal Processor
DTT	Digital Terrestrial Television
DUT	Device Under Test
ED	Energy Detection
ECC	Electronic Communications Committee

E-GSM	Extended Global System for Mobile Communications
ETSI	European Telecommunications Standards Institute
FCC	Federal Communications Commission
FDD	Frequency Division Duplex
FFT	Fast Fourier Transform
FIR	Finite Impulse Response
FM	Frequency Modulation
FAM	FFT Accumulation
FSK	Frequency Shift Keying
FPGA	Field-Programmable Gate Array
FTP	File Transfer Protocol
GMDSS	Global Maritime Distress and Safety System
GMSK	Gaussian Minimum Shift Keying
GPS	Global Positioning System
GSM	Global System for Mobile Communications
GPU	Graphics Processing Unit
HF	High Frequency
IEEE	Institution of Electrical and Electronics Engineers
IETF	Internet Engineering Task Force
IF	Intermediate Frequency
IMT	International Mobile Telecommunications
ISM	Industrial, Scientific and Medical
ITU	International Telecommunication Union
ITU-RR	ITU Radio Regulations
ITS	Intelligent Transport System
JTRS	Joint Tactical Radio System
KUAR	Kansas University Agile Radio
LOS	Line Of Sight
MAC	Medium Access Control
MEMS	Microelectromechanical Systems
MLE	Maximum Likelihood Estimation
MRSS	Multi Resolution Spectrum Sensing
NLOS	Non-Line Of Sight
NSF	National Science Foundation
NRNRT	National Radio Network Research Testbed
NRA	National Regulatory Authorities
NTIA	National Telecommunications and Information Administration
Ofcom	Office of Communications, Regulation Authority in United Kingdom,
OSA	Opportunistic Spectrum Access
PAMR	Public Access Mobile Radio
PC	Personal Computer
PDF	Probability Density Function
PDSP	Programmable Digital Signal Processor
PFA	Probability of False Alarm
PHY	Physical Layer
PMR	Private/Professional Mobile Radio
PSD	Power Spectral Density
PTM	Point-To-Multipoint
QoS	Quality of Service
RAN	Radio Access Network
RBW	Resolution Bandwidth
REM	Radio Environment Map
RF	Radio Frequency
RMSE	Root Mean Square Error
ROC	Receiver Operating Characteristic

ROSHT	Recursive One-Sided Hypothesis Testing
RRS	Reconfigurable Radio Systems
RSPG	Radio Spectrum Policy Group
RSS	Received Signal Strength
SCA	Software Communication Architecture
SCC	Standards Coordinating Committee
SCPI	Standard Commands for Programmable Instruments
SDR	Software Defined Radio
SCF	Spectral Correlation Function
CFD	Cyclostionary Feature Detection
SFDR	Spurious-Free Dynamic Range
SOF	Spectral Coherence Function
SNR	Signal-To-Noise Ratio
SSC	Shared Spectrum Company
SSCA	Strip Spectral Correlation Algorithm
SSE	Sum of Square Errors
TAJPSP	Tactical Anti Jam Programmable Signal Processor
TS-CSS	Two-Step Compressed Spectrum Sensing
TDD	Time Division Duplex
TDMA	Time Division Multiple Access
TETRA	Terrestrial Trunked Radio
TPC	Transmit Power Control
TV	Television
UDP	User Datagram Protocol
UL	Uplink
UMTS	Universal Mobile Telecommunications System
USB	Universal Serial Bus
USRP	Universal Software Radio Peripheral
UWB	Ultra Wide Band
VBW	Video Bandwidth
VI	Virtual Instrument
VHF	Very High Frequency
VISA	Virtual Instrument Standard Architecture
WARP	Berkeley Emulation Engine3 (BEE3)
WCDMA	Wideband Code Division Multiple Access
WRCs	World Radio communication Conference
Wifi	Wireless Fidelity
Wimax	Worldwide Interoperability for Microwave Access
WLAN	Wireless Local Area Network
WRAN	Wireless Regional Area Network
WMAN	Wireless Metropolitan Area Network

Chapter

1 Introduction

1.1 Overview

The rapid proliferation of wireless technologies along with greater bandwidth demands from users is expected to increase the demand for radio spectrum by orders of magnitude over the next decade. This demand for spectrum has been clearly reflected in spectrum auctions concluded in several countries [1, 2, 3] where exorbitant prices have been paid to obtain licenses for the small vestige of the radio spectrum. The other reason for this spectrum shortage is that propagation effects and technologies limit the natural frequency spectrum. The entire radio spectrum is already allocated to various wireless services, making it difficult for emerging wireless technologies to obtain spectrum for their operation. This increases the opportunity cost of the spectrum. The spectrum scarcity is not real but artificial and largely due to inefficient static spectrum allocation policies [4]. Current inefficiencies in spectrum utilisation might arise from a number of factors including: use of excessive guard bands between channels or services; permanent assignments which are infrequently used and excessive geographical coordination distances. The early spectrum measurement campaigns conducted in USA showed the shocking result of underutilisation of spectrum which further confirms the claim of the inefficient spectrum allocation. Overall, similar findings were reported by various authors and studies, such as [5, 6, 7]. These occupancy studies suggest that the problem with spectrum scarcity arises not from the physical availabilities of spectrum being insufficient, but from the fact that allocated spectrum is poorly utilised. The outcome of these studies puts a question mark on the ability of the prevailing spectrum allocation policy to fulfil the growing demand

for spectrum for the future wireless services. The current spectrum management system is excessively rigid. It provides a license, which offers slow, cumbersome, and inefficient access to the spectrum. For instance, measurements made by the Federal Communication Commission (FCC), USA and Office of Communications regulator in the UK (Ofcom) within the TV bands have shown that a great part of the spectrum, although allocated, is virtually unused [8]. Such unused portions of the spectrum vary from place to place and time to time. Also, Ofcom revealed that over 50% of locations in the United Kingdom have more than 150 MHz of TV spectrum virtually available to be used [9]. For these reasons, in the last few years, several countries including the USA have already switched off analogue TV broadcasting in favour of Digital Terrestrial Television (DTT) broadcasting systems [10] and digital switchover plans have driven a thorough review of TV spectrum exploitation. Even after the redeployment of the digital TV channels, the problem of an efficient utilisation of the allocated frequencies is still far from being solved. For example, there are still large terrestrial areas in which, although allocated, the TV channels remain unused, due to coverage problems. New spectrum allocation approaches such as the Dynamic Spectrum Access (DSA) method have been studied. This new concept implies that the radio terminals have the capacity to monitor their own radio environment and consequently adapt to the transmission conditions on whatever frequency bands are available (adaptive radio). If this concept is supplemented with the capacity to analyse the surrounding radio environment in search of underutilised spectrum (white spaces), the term adaptive radio is extended to Cognitive Radio (CR). The efficient application of CR techniques along with software radio would enable an effective dynamic spectrum sharing environment for coexistence.

The purpose of this thesis is to bring together a group of CR concepts and explore how we can make the transition from conventional radio to cognitive radio. Specific goals of the thesis are firstly the measurement of the radio spectrum to understand the current spectrum usage in the context of cognitive radio. Secondly, to investigate spectrum sensing techniques including use of simulation techniques and experimental measurement, specifically energy detection and cyclostationary feature detection. Thirdly, to mitigate the effect of degradation due to multipath fading and shadowing, the use of wideband cooperative sensing techniques is proposed, which it is believed will introduce more spectral opportunities over wider frequency ranges and achieve higher opportunistic aggregate throughput.

1.2 Motivation and Objectives

During recent decades, the demand for more radio spectrum has increased with the development of wireless communications. With the deployment of more wireless communications systems, most of the available spectrum has been statically allocated. However, recent measurements show an opposite situation: many licensed services transmit only sporadically, giving an overall spectrum occupancy of roughly 35%, even in the most crowded areas. It is precisely this inefficiency in the use of the frequency resources which has motivated the current research in cognitive radio technology. Ideally, cognitive radios have a perfect picture of the spectrum usage in a given place and at a given time, being able to smartly adapt the transmission scheme to perform opportunistic communication.

Despite cognitive radio technology holding considerable promise in the proliferation of new wireless services, there still exist many technical challenges. These include understanding the current spectrum, reliable sensing of spectrum opportunities, interference free spectrum sharing, efficient spectrum handoff and coordination among CR users for secondary use of licensed spectrum. There is still a long way to go before the CR vision becomes a reality. More precisely, this thesis has focussed on a variety of problems involved in: Understanding the current spectrum usage of the different wireless services, characterising and experimentally evaluating detection methods with respect to minimum detectable signal levels, evaluation of the sensing time needed, robustness to noise uncertainty and implementation complexity and feasibility; and investigating improvements offered by a number of wideband collaborative radios, different fusion and threshold rules and spatial separation between cognitive radios.

Empirical measurement of the radio environment to promote understanding of the current spectrum usage of the different wireless services is the first step towards deployment of future CR networks. Many measurement campaigns [11, 12] have been conducted worldwide in the context of cognitive radio. The results show underutilisation of the licensed spectrum temporally and spatially. The CR research attained further momentum from the outcome of these spectrum occupancy measurement campaigns. The results of the above mentioned campaigns are not directly applicable to general locations since the geographical characteristics, and the social environment, have an impact on the spectrum use. Empirical modelling of spectrum utilisation in the context of cognitive radio is a research area that still requires much more effort. The knowledge of the spectrum usage of licensed bands from the measurement campaigns will form the input for regulatory bodies to adapt spectrum reframing in certain

bands and provide motivation to introduce emerging technologies like cognitive radio for efficient spectrum utilisation.

Spectrum sensing is the key issue in cognitive radio systems [13, 14]. Without a robust widely applicable spectrum sensing method, secondary users (without license) may cause intolerable interference to primary users (having license) or frequently introduce false alarms in their own communications. Two main methods have been exploited for spectrum sensing, namely energy detection [15] and cyclostationary features detection [16]. Energy detection is adopted in many studies due to its simplicity; however, it suffers from the uncertainty of noise level [15] in low signal-to-noise ratio (SNR) regimes. An alternative approach is to exploit the periodic structure of the primary user's signal, i.e. cyclostationary features, by carrying out cyclic spectral analysis [17]. By using cyclostationary feature detection, noise can be significantly suppressed, thus achieving more robustness than energy detection. Even though there has been investigation of cyclostationary feature detection under noise, they are limited by the features in the propagation environment, its evaluation technique and its scope. Therefore, the characteristics of cyclostationary feature detection with real world signals in the presence of channel noise need to be investigated in detail, which quantify the performance of cyclostationary feature sensing techniques in various conditions.

The essential requirements for spectrum sensing are fast, robust and reliable signal detection in a low signal-to-noise ratio (SNR) environment. In cognitive radio networks (CRN), the sensing performance of a single CR is often reduced by multipath fading, shadowing, and receiver uncertainty in the channel. To mitigate these effects, cooperative or in multiuser sensing techniques are being used [18, 19]. CR can detect the signals in a single/narrow frequency band or multiple/wide frequency bands. While present narrowband spectrum sensing algorithms have focused on exploiting spectral opportunities over a narrow frequency range, cognitive radio networks will eventually be required to exploit spectral opportunities over a wide frequency range from hundreds of Megahertz (MHz) to several Gigahertz (GHz) for achieving higher opportunistic throughput. Hence, as distinct from narrowband spectrum sensing, wideband spectrum sensing aims to find more spectral opportunities over a wide frequency range and achieve higher opportunistic aggregate throughput.

The research objectives of this PhD thesis address three main working parts:

- 1) Empirical spectrum occupancy measurements in the Humber region, UK, and associated modelling and analyses of cognitive radio potentials.
- 2) Investigation of the characteristics of

cyclostationary feature detection with real world signals under channel noise. 3) Proposal of new cooperative wideband spectrum sensing schemes with multi-bit hard decision in cognitive radio, which lead to energy-efficient and time-saving using two stages in the spectrum sensing process.

In more detail these three areas are:

- 1) The main goal of the empirical research work is to conduct spectrum occupancy measurements in the Humber region, UK to identify typical low occupancy bands suitable for deploying cognitive radio technology. The analytical research work includes discussion of the potential of cognitive radio based on measurement and the resulting need for spectrum for the addressed services. Overall, this activity is intended to contribute to mitigation of spectrum scarcity.
- 2) The goal of this part of the research is to evaluate the performance of cyclostationary feature detection from a practical implementation point of view to identify and characterise the spectral correlation function (SCF) of a modulated signal under real world channel noise and in particular to examine the performance of the SCF under low SNR conditions. This part included a comparison between energy detection and cyclostationary feature detection performance.
- 3) In this part, wideband cooperative spectrum sensing algorithms are presented. The distinct features and contributions of this section are a proposed system model for wideband cooperative spectrum sensing with multi-bit hard decision in cognitive radio using dual-stage sensing technique, where the power consumption and the time taken for sensing are considerably reduced.

1.3 Thesis Outline

This thesis is divided into five parts, as illustrated in Figure 1.1. A platform architecture overview of the thesis is illustrated in Figure 1.2. In part I, Chapter 1 explains the motivation behind this research. Chapter 2 reviews existing wireless communication technologies that lead to the development of cognitive radio. Chapter 3 gives an introduction to software defined radio and cognitive radio and some examples of implementation and applications.

The central part of this thesis is organised in three parts II, III and IV along with the corresponding conclusions in Part V. Parts II and III deal respectively with low and high resolution measurements (Spectrum analyser and USRP2) and specify the methodological

aspects of the two spectrum measurement platforms employed in the context of this thesis. Part IV presents simulation techniques to further develop wideband cooperative sensing technique. Consisting each in future detail:

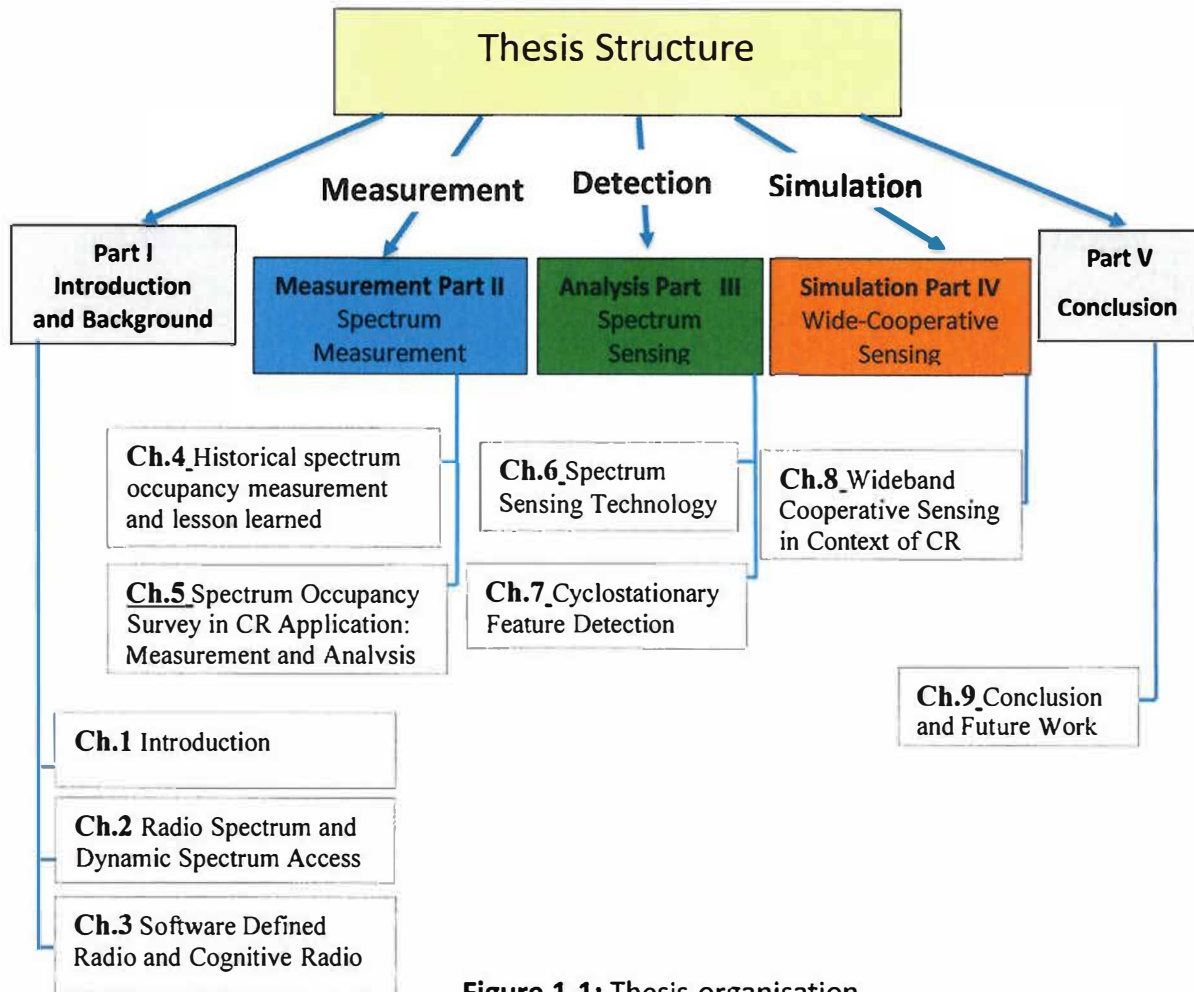


Figure 1-1: Thesis organisation.

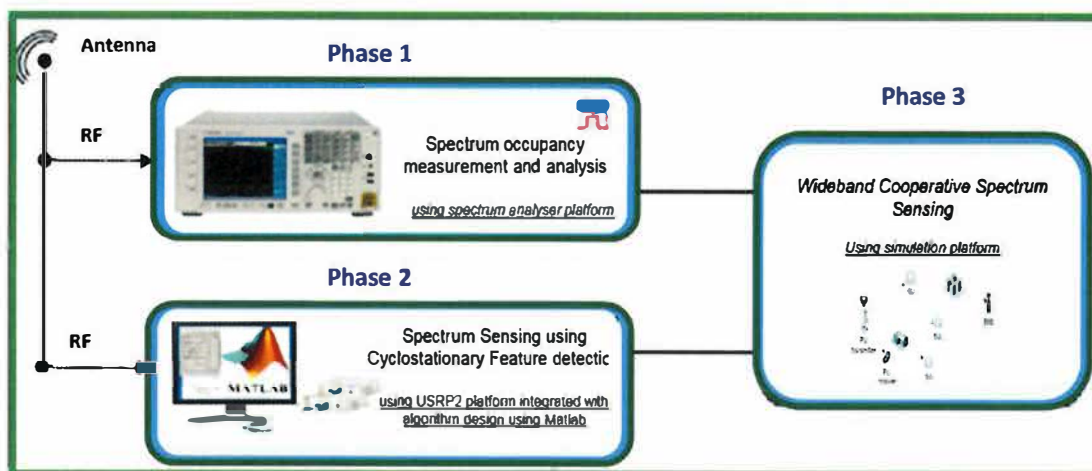


Figure 1-2: Platform Architecture Overview.

Part II Introduces historical spectrum occupancy measurements, and deals with various aspects related to the first employed measurement platform. Next, we evaluate the spectrum occupancy measurement over two chapters. First, Chapter 4 introduces and compares global spectrum occupancy measurements. We start with measurement challenges and methodological aspects to cope with the major drawback of previous spectrum occupancy studies by providing a unifying methodological framework for future spectrum measurement campaigns. Chapter 5, presents the results of an extensive spectrum measurement campaign that was carried out, taking into account the findings of Chapter 4, over a wide variety of locations and scenarios within in the Humber region, UK. Measurement results are exhaustively analysed in order to identify potential bands of interest for the future deployment of the DSA/CR technology.

Part III starts by presenting a state-of-the-art survey of spectrum sensing techniques. It then deals with various specific aspects related to the second measurement platform, based on the Universal Software Radio Peripheral (USRP) and Matlab architecture, which is used to compare the performance of cyclostationary feature detection with energy detection from a practical implementation point of view. This part involves two chapters: Chapter 6 provides an in-depth review of the operation of spectrum sensing. Aspects of spectrum sensing such as primary transmitter detection methods are discussed; Chapter 7 evaluates the performance of cyclostationary feature detection (CFD) estimation from a practical implementation point of view to identify and characterise the SCF features of modulated signal under real world channel noise and examine the performance of the SCF under low SNR environment with real world signal and compares it with energy detection. The outcome of this study concludes that under real world noise, SCF feature analysis shows improved performance under low SNR environment compared with the PSD method.

In Part IV, Chapter 8, we proposed cooperative wideband spectrum sensing schemes with multi-bit hard decision in cognitive radio. First, we proposed a system model for wideband cooperative spectrum sensing with multi-bit hard decision in cognitive radio using multi resolution spectrum sensing (MRSS) technique. Next, based on this first, another algorithm is proposed using a two-stage adaptive sensing technique. The results show that the sensing time and energy consumption are both reduced significantly in the proposed schemes.

Part V, Chapter 9 summarises the main conclusions derived from the investigation carried out in the thesis and suggests possible directions for future work.

1.4 Thesis Contributions

The main contribution of the work presented in this thesis is the study of the spectrum usage variation in frequency, time and special domain within Humber region, UK through extensive empirical spectrum measurement campaigns. Moreover, this thesis investigates the cyclostationary feature sensing method by considering practical demonstrations and experimentations. Finally, in order to combat some practical challenges in spectrum sensing such as low SNR, fading and noise uncertainty, all of which significantly degrade the performance of primary signal detection, we propose a new cooperative wideband detection scheme with an optimal fusion rule for cognitive radio based networks.

The main thesis contributions (TCs) are as follows:

- [TC.1] Introduce and compare global spectrum occupancy measurements and address the major drawbacks of previous spectrum occupancy studies by providing a unifying methodological framework for future spectrum measurement campaigns.
- [TC.2] Investigate the spectrum utilisation of different bands at different geographical locations within the Humber region, UK and identify potential spectrum bands for the future deployment of CR technology.
- [TC.3] Compile a comprehensive study of potential signal detection techniques for spectrum sensing in CR systems. Specifically, outline the state-of-the-art research results, challenges and future perspectives of spectrum sensing in CR systems and also present a comparison of different methods.
- [TC.4] Design and implement the framework to identify and characterise cyclostationary feature detection in real time using SCF features of the modulated signal and examine the performance of SCF under low SNR conditions with real world signals as compared with energy detection using power spectral density (PSD).
- [TC.5] Propose a system model for wideband cooperative spectrum sensing with multi-bit hard decision in cognitive radio using multi MRSS technique, where the power consumption and the time of sensing are considerably reduced.
- [TC.6] Propose a system model for wideband cooperative spectrum sensing with multi-bit hard decision algorithm using a two-stage adaptive sensing technique. The algorithm uses an adaptive technique along with first stage coarse detection, providing more sensing accuracy when compared to the first algorithm whilst maintaining reliable detection performance.

1.5 Collaboration and Presentations (C & P)

While the majority of the research described here was undertaken at the University of Hull, there were opportunities for collaborative study with, and presentations to external partners. Throughout the three-year study period the author conducted research in an area of great interest to companies, organisations and the University to combine his knowledge and innovation and to bring results to the widest possible audience. Author participation in network-building activities, mobility and collaboration, was undertaken at various levels within the cognitive radio research hierarchy. The work carried out also linked to various research collaboration programmes and initiatives, which are detailed below:

Research Collaboration (C)

- [C.1] Collaboration between the author and Keysight (Agilent) has brought significant benefit to the author. The author was able to attend several RF measurement training and workshop sessions. The most beneficial aspect was the opportunity for the author to borrow equipment such as a portable spectrum analyser. This equipment helped the author to make several measurements at different locations with less complexity, as well as checking the calibration of our measurement platform.
- [C.2] COST Action IC0905 TERRA organisation meetings broadened the scope of educational benefits for the author, although the author attended only the last several meetings. The author obtained a number of grants to contribute by presentations during COST Action meetings and by attending summer school training. Following this summer school the author was able to enrol in a wider sequence of online measurement training offered by participating Dublin University. Given that the Dublin platform was developed by the COST Action it is available by distance learning, so geographic separation of universities was not a barrier. The use of distance learning technologies adds flexibility; for example, the author accessed Web-based course material at his convenience. This approach gives access to a much broader range of disciplines and experts than traditional programs based within a single university.
- [C.3] Another type of collaboration occurred with PhD students employed at several universities including Northumbria University, Newcastle, De-Montfort University, Leicester and Belgrade University, Serbia. De-Montfort and Belgrade

University have a limited number of platforms to do real time spectrum occupancy measurements as promotion for their research. So our real time measurements within the Humber region were exchangeable. Furthermore, the author collaborated with Newcastle University and took advantage of opportunities to network and learn from one another. Although the topics were different the same platform was used in both universities (USRP platform measurement using Matlab and LabVIEW). These links have been explored in the thesis, taking advantage of active research programs with these universities

Presentations (P)

- [P.1] Two Years of Research in Cognitive Radio (Wideband Spectrum Measurement and Wideband Cooperative Sensing). Meeting of the Cost Action IC0905 (TERRA), 30 April 2014 (Vilnius, Lithuania).
- [P.2] Energy Efficiency using Wide Band Cooperative Sensing. Meeting of the Cost Action IC0905 (TERRA), Biel, Switzerland, 26-27 Nov. 2013.
- [P.3] Characterising Cyclostationary Features of Digital Modulated Signals with Empirical Measurements using Spectral Correlation Function-TELFOR2014, Belgrade Serbia, 24-28 Nov.2014.
- [P.4] Spectrum Occupancy Measurements, analysis and Lesson Learned in the Context of Cognitive Radio. The 5th PhD Experience Conference 2014. University of Hull, 14-15 April 2014.
- [P.5] Evaluation of Interference between Antennas using Cosite Analysis Model. International conference in Advance Communication and Information Technology. Amsterdam, October 2012.

1.6 Publications

Spanning a period of three, the research for this thesis and related research has produces a number of papers in international journals, conferences, meetings and workshops. First we list the works that are already published and then we list the papers under evaluation.

Journal Publications

- [JP.1] **Mehdawi, M.**, Riley, N. G., Paulson, K., Fanan, A., & Ammar, M. (2013). Spectrum occupancy survey in Hull-UK for cognitive radio applications: measurement & analysis. *International Journal of Scientific & Technology Research*, 2(4), 231-236.

Conference Publications

- [CP.1] **Mehdawi, M.**, Riley, N. G., Ammar, M., & Zolfaghari, M. (2012, November). Comparing historical and current spectrum occupancy measurements in the context of cognitive radio. In Telecommunications Forum (TELFOR), 2012 20th(pp. 623-626). IEEE.
- [CP.2] **Mehdawi, M.**, Riley, N. G., Ammar, M., Fanan, A., & Zolfaghari, M. (2013, November). Cooperative wideband spectrum sensing with multi-bit hard decision in cognitive radio. In Telecommunications Forum (TELFOR), 2013 21st (pp. 220-223). IEEE.
- [CP.3] **Mehdawi, M.**, Riley, N. G., Ammar, M., Fanan, A., & Zolfaghari, M. (2014, November). Experimental detection using cyclostationary feature detectors for Cognitive Radios. In Telecommunications Forum Telfor (TELFOR), 2014 22nd(pp. 272-275). IEEE.
- [CP.4] **Mehdawi, M.**, Riley, N. G., Ammar, M., Fanan, A., (2015, November). Spectrum sensing and lesson learned in the context of cognitive radio. In Telecommunications Forum Telfor (TELFOR), 2015 23nd (INSPEC Accession Number: 15701030). IEEE.
- [CP.5] **Mehdawi, M.**, Riley, N. G., Fanan, A., The influence of antenna selection on measured TV band occupancy in context of in the context of cognitive radio networks. In Telecommunications Forum Telfor (TELFOR), 2016 24nd.IEEE
- [CP.6] Ammar, M., **Mehdawi, M.**, Riley, N. G., Fanan, A., Paulson, K., & Zolfaghari, M. "A Spectrum Sensing Test Bed based on Matlab and USRP2".(2013). Int'l Conference Image Processing, Computers and Industrial Engineering (ICICIE'2014) Jan. 15-16, 2014 Kuala Lumpur (Malaysia).
- [CP.7] A.M. Fanan, N.G. Riley, **M. Mehdawi**, M. Ammar, and M. Zolfaghari, "Survey: A Comparison of Spectrum Sensing Techniques in Cognitive Radio", Int'l Conference Image Processing, Computers and Industrial Engineering (ICICIE'2014) Jan. 15-16, 2014.
- [CP.8] Ammar, M., Riley, N. G., **Mehdawi, M.**, A. F., & Zolfaghari, M. Physical Layer Security in Cognitive Radio Networks. International Conference on Artificial Intelligence, Energy and Manufacturing Engineering (ICAEME'2015) Jan. 7-8, 2015 Dubai (UAE).

- [CP.9] A.M. Fanan, N.G. Riley, **M. Mehdawi**, “Comparison of Propagation Models with Real Measurements Around Hull, UK”, In Telecommunications Forum Telfor (TELFOR), 2016 24nd. IEEE
- [CP.10] Zolfaghari,M., Riley, N. G., **Mehdawi, M.**, & Shen, J. (2013, November). A slot-loaded reduced-size CPW-fed aperture antenna for UWB applications. In Antennas and Propagation Conference (LAPC), 2013 Loughborough (pp.611-614). IEEE.

Papers under Evaluation

- [PUE.1] Energy-efficient and time-saving using wide-band cooperative spectrum sensing using Multi-bit decision with adaptive technique in cognitive radio networks. To be submitted for publication, IEEE Journals Transactions & Magazines (undergoing of review by author).
- [PUE.2] Hybrid Detection Method for Improving Spectrum Sensing Performance in Cognitive Radio. To be submitted for publication, Telecommunications Forum, November 2017 (undergoing of review by author).
- [PUE.4] The performance of the cyclostationary feature detection method compared with the energy detection method under different real time measurement of channel impairment. To be submitted for publication, Elsevier Journal (undergoing review by author).

Part I: Radio Spectrum Today and Radio Spectrum Tomorrow

*If radios were intelligent and active, rather than dumb and
passive, vastly more information could be made available
through the airwaves*

Hal Abelson

This part contains two chapters

CHAPTER 2: Radio spectrum and Dynamic spectrum Access

CHAPTER 3: introduction to Software Defined Radio and Cognitive Radio

Chapter

2 The Radio Spectrum and Dynamic Spectrum Access

2.1 Background

Radio spectrum is a natural resource which is used for a wide variety of services with some special characteristics [20]. The key characteristics of the radio spectrum are the propagation features and the amount of information that signals can carry. Utilisation of the radio spectrum usually means emitting electromagnetic radiation at radio frequency (between 30 kHz and 300 GHz). This may be needed for the intended services, but may often cause undesirable effects including interference for other services. For example, when communicating using commercial radio devices, unacceptable interference could be caused for dissimilar, neighbouring, radio receivers that may be sharing the same or similar spectrum. One of the more sensitive cases is radio astronomy, where the required signals are at low levels and can easily suffer significant interference from conventional transmitters, even if they are distant from the radio astronomy receiver. Until today, radio spectrum regulation has been used to mitigate all such undesirable effects and is therefore, considered essential in order to enable reliable and efficient spectrum usage. By introducing this research topic we hope to illustrate that this situation may change with the establishment of cognitive radio and dynamic spectrum access.

2.2 History of Radio Spectrum

In 1865, the physicist, Maxwell, demonstrated the theory of electromagnetic energy, which includes the phenomenon known as radio waves [21]. His theory was confirmed by Henrich Hertz in 1888 when Hertz caused an electric discharge between two metal balls, from which

he projected radio waves across to a wire loop detection apparatus [22]. In 1895, Marconi realised the communication possibilities of artificially generated radio waves. In 1899 Marconi sent his first message across the English Channel and by 1901 he had spanned the Atlantic.

The first time that the world recognised the importance of radio communication was in April 1912, when the passenger liner Titanic, which represented the largest passenger steamship in the world in that time, hit an iceberg during its first voyage ever, and sank within only a couple of hours. This tragedy was not only one of the worst maritime disasters in history, but also because used as an early example of the need to introduce radio spectrum regulation. During that time many passengers were rescued because another ship received the radio emergency signals, but at the same time many passengers were lost because the radio receiver on board the nearest the ship was not operating during the night of disaster [23]. From that time, the use of radio communications has gained popularity as a result of Marconi's pioneering demonstrations and their role in the rescue of hundreds of lives during the tragic sinking of the Titanic. Hence radio became a topic of international debate, and was soon regulated by national authorities. For example, radio spectrum regulation in US was legalised as the Communication Act of 1934. The object of this Act was to guarantee services to the public. This process was adopted as radio spectrum regulation and since the beginning of the twentieth century, communication services like telephony, radio and terrestrial broadcast television, have been regulated according to this model [24].

2.2.1 Approaches for Radio Spectrum Regulation

As the spectrum is a finite resource the regulation of radio spectrum is essential. In this context the radio spectrum can also be thought of as a non-renewable resource insofar as the timescale required, due to the large investment in infrastructure, for change of use of any part of the spectrum is long, typically 10 to 20 years. The regulation of spectrum can be differentiated into four approaches: Licensed spectrum for exclusive usage, licensed spectrum for shared usage, unlicensed spectrum and open spectrum [25].

Licensed spectrum for exclusive usage is imposed and protected through the regulator. The licensee has exclusive and transferable flexible usage rights for specific spectrum. This exclusive licensing was established to protect licensee's signals. For instance, the spectrum of frequency used by universal mobile telecommunication system (UMTS) which was sold in Europe is one example of an exclusive right for a license of spectrum. Licensed spectrum for shared usage is restricted only to specific technology. The spectrum assigned to digital

enhanced cordless telecommunication (DECT) which is used in Europe is an example of this model. A further example is the spectrum used for public safety services, where exclusivity is vital for reliable service conditions. In the case of unlicensed spectrum, the responsibility for technical compliance is transferred to the producer of the radio products which may be freely used by the purchaser. Although this is limited spectrum, this low-regulation approach lets innovators deliver millions of unlicensed offerings such as Wi-Fi hotspots. In Europe this type is known as ‘license-exempt spectrum’. Using this band doesn’t involve any right of the user for protection from interference. Open spectrum, also known as free spectrum is available for use by all. Open spectrum allows anyone to access this range of spectrum without any restriction. However, even this type of spectrum requires a minimum set of rules that are required for sharing spectrum.

2.2.2 Basic Rules of Spectrum Regulation

According to [26] radio spectrum regulation promotes the development of spectrum access standards to balance six objectives:

- ❖ Sufficient quality of service should be realisable to all radio systems depending on support application;
- ❖ No radio should be blocked from spectrum access and from transmission for any extended time duration;
- ❖ Spectrum regulation and standards must not slow down innovation in economically successful and rapidly changing wireless communication markets.
- ❖ Available spectrum should be used efficiency, including spatial reuse of spectrum and solving the “tragedy of commons”;
- ❖ Spectrum should be used in a dynamically adaptive way, taking the local communication environment including spectrum usage policies into account;
- ❖ The cost of commercial radio devices should not be made to increase significantly through adoption of techniques mandated by radio regulation.

2.3 Organisations that Regulate the Radio Spectrum

Decisions relating to the choice of licensed spectrum for exclusive or shared usage, and declarations of spectrum as unlicensed or even open spectrum are undertaken by national and international institutions which are referred to as ‘regulators’. In the following section, significant regulators will be briefly introduced.

2.3.1 International Telecommunication Union, ITU (Global Co-ordination)

The ITU is known as the specialised agency of the United Nation which is responsible for information and communication technology. It is responsible for global coordination and sharing of the radio spectrum and prompts international cooperation to improve telecommunication infrastructure in the developing world as well as establishing worldwide standards. It has three sectors: Radiocommunication, Standardisation and Development. The ITU Radiocommunication sector (ITU-R) is one of the three sectors of the ITU and is responsible for radio communication. Globally, for all the regions of the world, frequency allocation processes are harmonised with the help of ITU-R. ITU agreement on spectrum allocation is set out in the ITU Radio Regulations (ITU RR). The Radio Regulations is the inter-governmental treaty text of the International Telecommunication Union [27]. The regulations cover both legal and technical issues. The planning, revision and adoption of the radio regulations are the responsibility of the World Radiocommunication Conferences (WRCs) of ITU, that take place every 2-3 years. These international conferences cope with many emerging services, with conflicting interests and business models in an attempt to modernise spectrum usage [27].

The ITU goals are to work as closely as possible with its members in order to define its activities to meet the ever-increasing and diverse needs of the world's developing and least developed countries. There are six regional groups that develop proposals at the regional level to be brought to the WRC, which include regional offices in Addis Ababa (for Africa), Brasilia (for Americas), Cairo (for the Arab States), Bangkok (for Asia and Pacific), a Europe coordination unit at the ITU headquarters (for European Countries), and several area offices, including Moscow (for CIS countries), all of which help maintain direct, sustained contact with national authorities, regional telecommunication organisations and other key stakeholders.

2.3.2 European Union (EU)

The spectrum regulation in European is carried out by the Electronic Communications Committee (ECC), which is responsible for radiocommunication and telecommunication of the European Conference of Postal and Telecommunications Administrations (CEPT). The CEPT was established in 1959 by 19 countries, which expanded to 26 during its first ten years. CEPT's activities include cooperation on commercial, operational, regulatory and technical standardisation issues. Today 48 countries are members of CEPT. The ECC produces four main

deliverables: ECC Decisions, ECC Recommendations, ECC Reports, and CEPT Reports. These are the results of the policy work and technical studies conducted to harmonise the use of spectrum across Europe and to improve market efficiency. All of their deliverables are developed in collaboration with national administrations and industry and are subject to public consultation. The main mission of ECC is provide common policies and regulation, harmonise the efficient use of radio spectrum and promote the interests of Europe on a worldwide basis. Everything decided by ECC is usually realised by CEPT member countries [26]. To assist the commission, two complementary bodies were set up following the Radio spectrum decision in 2002, to facilitate consultation and to develop and support an EU Radio spectrum policy: The Radio Spectrum Policy Group (RSPG) approves the CEPT reports and associated technical implementation measure prepared by the commission. Next, the Radio Spectrum Committee (RSC), was setup to facilitate consultation and to develop and support radio spectrum policy.

In 1988, ETSI, the European Telecommunications Standards Institute, was created under the care of CEPT, which transferred all of its telecommunication standardisation activities to ETSI. The ECC has a strong cooperation with ETSI in order to ensure coherence between ECC decisions and ETSI harmonised standards. ETSI is a non-profit organisation, whose mission is to produce globally-applicable standards for Information and Communications Technologies (ICT), including fixed, mobile, radio, converged, broadcast and internet technologies. As noted above, CEPT deliverables are non-binding. This gives the National Regulatory Authorities (NRA) a large degree of flexibility when it comes to adapting these to country specific conditions, legacy usages and circumstances.

2.3.3 Examples of National Spectrum Management Authorities

Based on the international allocations and regulatory provisions the NRAs grant access to spectrum for users. For instance, an EU member state has the right to set conditions on the use of spectrum under the framework directive. These conditions can include appropriate limits that aim to avoid harmful interference to other radio services. These conditions can be harmonised on a European wide basis either through a European Commission spectrum decision or by an ECC decision or recommendation. Alternative, if no mandatory harmonised guidance is available, a regulatory deliverable can be developed on a national basis.

At the national level, the use of radio spectrum in most countries is currently being managed by government agencies rather than by market forces. The biggest two telecommunications

regulatory authorities worldwide are UK, Office of Communications (Ofcom) and the US, Federal Communications Commission (FCC). Ofcom represents the regulatory authority in the United Kingdom (UK) and is responsible for regulation, management, licensing and assignment of radio spectrum. Ofcom was established in 2003 (taking over the radio –related work of the former Radiocommunication Agency (RA) as well as other UK regulatory bodies) and operates with a process of regulator consultation. Spectrum regulation in Ofcom involves three main supports:

- ❖ Spectrum should be free of technology and usage constraint as far as possible, but this policy constraint should be only used where it can be justified;
- ❖ It should be simple and transparent for a license holder to change the ownership and use of spectrum;
- ❖ The right of the spectrum user should be clearly defined and users should feel comfortable that that right will not be changed without good cause.

The FCC and the National Telecommunication and Information Administration (NTIA) are both responsible for spectrum regulation in the USA. The FCC is responsible for spectrum used for non-government purposes and NTIA is responsible for spectrum used by government including military use. In 2003 the FCC identified three steps to improve the spectrum utilisation:

- ❖ Improve the access in space, time and frequency domains;
- ❖ Enable flexible regulation in permitting controlled access to licensed spectrum;
- ❖ Stimulate efficient spectrum usage through policy.

2.4 Licensed and Unlicensed Spectrum

Most of the radio spectrum is allocated in licensed radio services. Generally this is identified as exclusive usage plus command and control. The licensed spectrum covers the exclusive access to spectrum and spectrum sharing within the licensed spectrum. In the case of exclusive spectrum usage, a license owner typically pays a fee for this benefit. The exclusive access has the advantage of preventing potential interference from different radio systems. In the case of spectrum scarcity, licensed spectrum is highly valuable, usually leading to economic profits for the licensee as consumers need to pay to use it. The auctions in the countries of Europe for licensing spectrum of 3G systems in 2000 are an example of this. Nowadays a frequently used licensing model is to license spectrum for shared usage restricted to specific technology, as well known as the command and control model. Emission parameters like maximum

transmission power and interference to neighbouring frequencies (such as out of band emissions) are restricted by the regulators. Regulation takes care of protection against interference and sometimes supports elementary coexistence capabilities such as dynamic channel selection [28].

2.4.1 The Difficulty of Spectrum Licensing

Spectrum licensing is very expensive, takes time and may be difficult to organise. As the number of new technologies increase dramatically, the licensing process constrains innovation, becoming a difficult barrier to overcome. Moreover, the inflexibility of exclusive usage rights arising from licensing spectrum in this way leads to inefficient spectrum utilisation, as the license prohibits the usage, by others, of the spectrum if it is underutilised or even unused by the license holder. Another problem with licensing is the duration of a license. Spectrum licenses typically expire after a decade and have to be renewed. The temporal license gives the regulator the opportunity of intervening if the spectrum is underutilised or wasted. For example, the regulator could answer market demands in shifting, extending or reissuing licenses, and can thus accelerate the introduction of new technologies. On the other hand, a danger of temporal licenses is that uncertainty about future regulatory decisions may hold back investments.

2.4.2 Unlicensed Spectrum as an Alternative

As the technologies of radio communication increase so quickly, and consequent user demand for bandwidth increase the availability of an adequate amount of radio spectrum is crucial. The commercial success of wireless technologies operating in unlicensed band opened the door to rethinking about regulation policy. WLANs, Wi-Fi, WPANs and Bluetooth are examples. The term “unlicensed spectrum” refers to the frequency bands for which no exclusive licenses are granted and on which unregistered users potentially may operate wireless devices without specific user authorisations. Users of these spectrum bands do not enjoy exclusivity and can be subject to interference from other users, although regulators typically restrict the transmission power in these bands to limit interference. This is allowed for radio devices that satisfy certain technical (MPT specification) standards that mitigate potential interference. The usage rights of unlicensed spectrum are flexible and no dedicated spectrum access method is specified or required.

Currently, there are many unlicensed frequency bands over the world, but two are considered to be the important: The Industrial, Scientific and Medical (ISM) band from 2400 to 2483MHz and frequency band between 5GHz and 6GHz. Despite the fact that the regulatory restriction

for the some bands are the same throughout different regulatory domains in world, regulation of some unlicensed spectrum differs essentially when comparing between countries. Recently, as TV bands in US and in UK, are underutilised, FCC and Ofcom proposed allowing unlicensed systems to have secondary usage of this spectrum. This principle will be discussed in detail in section 2.5.

2.4.3 Tragedy of Radio Spectrum Regulation

The success of unlicensed spectrum is drawing to a close, as the severe Quality of Service (QoS) constraints to spectrum access imposed by the upcoming multimedia applications cannot be fulfilled with today's means for coexistence. In the case of short distance wireless communication, spectrum demand is extremely localised and often sporadic. In such a scenario, the competition for shared spectrum is limited. Therefore, the regulatory instrument of restricting transmission, e.g., limiting the maximum emission power, is successful. In all other deployment scenarios, as for instance WLANs, unlicensed spectrum usage is a victim of its own success: too many parties and different technologies are using the same unlicensed spectrum so that it is getting overused and thus less usable for all. In economics the phenomenon is referred to as "tragedy of commons". Additionally we can introduce the 'tragedy of the anticommons' which refers to inefficient spectrum utilisation because of too restrictive regulation [29]. The tragedy of commons and the associated inefficient overuse of spectrum results in less investment in improved technology, and directly challenges the open access approach. Therefore, regulators impose restrictions such as limiting transmission powers. As a consequence, many alternative radio systems are not permitted to operate in such spectrum, which results again in inefficient underutilisation of spectrum. In [30] it is concluded that limiting spectrum sharing through spectrum regulation is the only way out of this tragedy. After we introduce the concept of dynamic spectrum access/cognitive radio in the next section, we will recognise that such statements are not really needed, as spectrum coordination can be realised with more flexible alternatives than restricting the amount of spectrum sharing. So what is the reality of spectrum usage? How intensively is our radio spectrum utilised? Is the radio spectrum completely crowded? Is it really a scarce resource that we have to protect against too many undesirable usage scenarios?

We will show in Chapter 4 and Chapter 5 results of measurement campaigns, conducted around Hull and elsewhere in order to find the answers to these questions. Our results (Chapter 5) confirm what is already known from literature: the reality is different to what might be expected:

many frequency bands are not used at all, and the spectrum appears to be under-utilised for most of the time, in most locations.

2.5 Dynamic Spectrum Access (Radio Spectrum Tomorrow)

Standing for the opposite of current static spectrum management policy, dynamic spectrum access methods are the tools that provide regulators with the flexibility needed in order to achieve a more efficient spectrum usage. The term dynamic spectrum access (DSA) has been coined to refer to an innovative solution proposing a procedure or scheme to share spectrum among wireless operators, technology and services in order to increase the overall spectrum utilisation. The concept of DSA is the essence of simplicity: listen to a channel, decide if it is being used, use it for a while, and keep checking to make sure no one who is entitled to its primary use or another cognitive radios (CR) are attempting to use it. As illustrated in Figure 2.1, dynamic spectrum access strategies can be generally categorised under three models [31]: Dynamic Spectrum Exclusive Use Model, Open Sharing Model and Hierarchical Access Model.

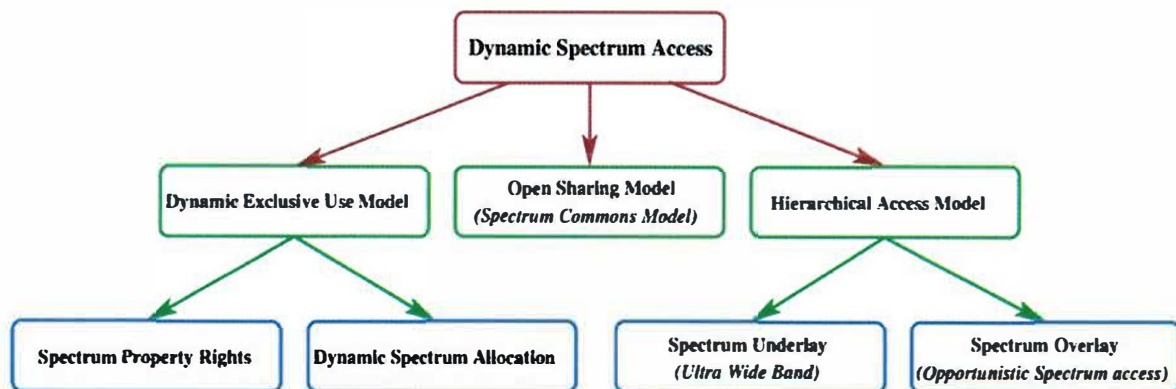


Figure 2-1: Classification of Dynamic Spectrum Access Schemes [12, 31].

2.5.1 Dynamic Spectrum Exclusive Use Model

In the exclusive use model for spectrum access, the radio spectrum is licensed to user/service to be exclusively used under certain rules. The basic plan of this type is to introduce flexibility in order to improve spectrum efficiency. Two approaches have been proposed under this model: spectrum property rights and dynamic spectrum allocation. Firstly; spectrum usage rights [32] can be transferred among users in different ways, as can other assets. This approach allows licensees to sell or lease some portion of their licensed spectrum and to freely choose the technology to be employed. This model plays an important role in driving the most profitable use of spectrum under this scheme. Although the licensees have right to lease and sell the spectrum, such sharing is not mandated by the regulation policy. Secondly; dynamic spectrum

allocation, as brought forth by the European DRiVE project [33, 34]. The main idea of this approach is to improve spectrum efficiency through dynamic spectrum assignment by exploiting the spatial and temporal traffic of different services. Similar to the current static spectrum allocation policy, such strategies allocate, at a given time and region, a portion of the spectrum to a radio access network for its exclusive use. This allocation, however, varies on a much faster scale than with the current policy.

2.5.2 Open Sharing Model

In the shared use spectrum access model, the radio spectrum can be simultaneously shared between a primary user (licensed user) and a secondary user (unlicensed user). It is referred to as spectrum commons. Supporters of this model draw support from the phenomenal success of wireless services operating in the unlicensed industrial, scientific, and medical (ISM) radio band (e.g., Wi-Fi). On the other hand, opponents of this proposal argue that it ultimately would result in a depletion of the shared limited resource in a scenario where too many nodes over-exploit the common good and degrade its quality.

2.5.3 Hierarchical Access Model

Built upon a hierarchical access structure with primary and secondary users, this model can be considered as a hybrid of the above two. It is adopted as a hierarchical structure that could distinguish between primary (licensed users) PU and secondary (license-exempt users) SU. The main idea from this model is to open licensed spectrum to secondary users while limiting the interference perceived by primary users. Two approaches to spectrum sharing between primary and secondary users have been considered: Spectrum Underlay and Spectrum Overlay.

❖ Spectrum Underlay

In the case of a spectrum underlay system, a secondary user can transmit concurrently with primary user. An example of this is ultra-wide band (UWB). This approach allows secondary users to potentially achieve short-range high data rates with very low transmission power. An advantage of such a system is that radios can be “dumb” since they do not need to sense the channel in order to defer to primary users [36].

❖ Spectrum Overlay

In the case of spectrum overlay, a secondary transmitter has knowledge of the primary user’s transmitted data sequence and how this sequence is encoded. Similar ideas apply when there are multiple secondary and primary users [35]. Therefore, to access the spectrum band, a secondary user has to perform spectrum sensing to detect the activity

of primary users in that band as illustrated in Figure 2.2. This approach is also identified as opportunistic spectrum access (OSA) [36].

In particular, the spectrum overlay/OSA is one of the most popular rapidly growing research fields, impacting not only the engineering community but also political, regulatory and economical mechanisms. Although spectrum overlay/OSA is a particular model for DSA, it is frequently referred to as DSA.

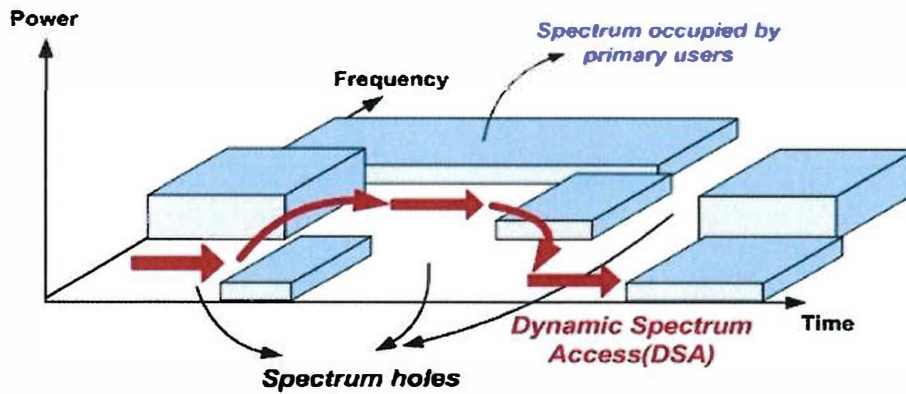


Figure 2-2: Opportunistic Spectrum Access Concept [36].

2.6 Key Parameters

The main goal of this section is to define and discuss the key parameters, which will be used in the next chapters. This especially includes Duty Cycle and Spectrum Occupancy, Spectrum Usage, Spectrum Hole, White Space, PSD, Blind PSD, FFT bin, Resolution Bandwidth, Probability Distributions of Signal and Noise and Confused region.

Occupancy is the percentage of time that the measured signal power exceeds a specified threshold. Spectrum Occupancy Rate is marked as the probability that the signal strength of a certain frequency bandwidth is occupied which means the signal is occupied when its signal power is above a particular threshold.

Spectrum Holes is represent the potential opportunities for non-interfering (safe) use of spectrum and can be considered as multidimensional regions within frequency, time, and space.

Duty Cycle (Measured occupancy) is used to measure spectrum occupancy. Duty cycle indicates how often the signal is seen on each channel during a simple period. The duty cycle is defined as the percentage of time a channel is occupied. Given a time-series of channel power measurements, the duty cycle can be calculated using:

$$Duty\ Cycle(DC) = \frac{Signal\ Occupancy\ Period}{Total\ Measurement\ Duration} \times 100\%$$

Band Spectrum Occupancy defined to be the average duty cycle of the channels within a band. The amount of spectrum occupied is then the product of the band spectrum occupancy and the bandwidth.

White Space is refers to portions of licensed radio spectrum that licensees do not use all of the time or in all geographical locations. Several regulators around the world are moving towards allowing unlicensed access to these frequencies, subject to the proviso that licensed transmissions are not adversely affected.

White Space (TV-Band) is a portion of spectrum in a band allocated to the broadcasting service and used for television broadcasting that is identified by an administration as available for wireless communication at a given time in a given geographical area on a non-interference and non-protected basis with regard to other services with a higher priority on a national basis.

Sensing threshold (TV) is the maximum received power level from TV towers allowed to consider a channel free. If received power detected is above this threshold, the channel is occupied, if it is below it is available.

Power Spectral Density (PSD) shows the strength of the variations (energy) as a function of frequency. In other words, it shows at which frequencies variations are strong and at which frequencies variations are weak. Computation of PSD is done directly by the method called FFT or computing autocorrelation function and then transforming it.

Fast Fourier transform (FFT) algorithm computes the discrete Fourier transform (DFT) of a sequence, or its inverse. Fourier analysis converts a signal from its original domain (often time or space) to a representation in the frequency domain and vice versa. Frequency Range and Resolution on the frequency axis of a spectrum graph depends on the sampling rate and the size of the data record. The FFT size defines the number of bins used for dividing the window into equal strips, or bins. Hence, a bin is a spectrum sample, and defines the frequency resolution of the window.

Resolution Bandwidth (RBW) determines the fast Fourier transform (FFT) bin size, or the smallest frequency that can be resolved. RBW is a fundamental form of measurement in the realm of spectral analysis, as it delivers the frequency accuracy, or precision, of a given measurement.

Confused Region is the area which lies between two thresholds (between PU and noise curve or under upper bound threshold, λ_1 and lower bound threshold, λ_2). In this region using single threshold detection of noise and PU signal is very difficult. It indicates that more parameters are required to quantify the reliability of each SU.

Blind Sensing is the technique which do not rely upon a specific feature of the primary signal air interface. Non-blind schemes require primary signal signatures as well as noise power estimation to reliably detect PU. Total blind, requiring no a priori information to determine PU activity.

2.7 Chapter Summary

In this Chapter, we presented an overview of radio spectrum today– regulation and spectrum usage, including history and terminology, institutions that regulate the radio spectrum, and the concepts of licensed and unlicensed bands. We concluded that the current spectrum management model operates at both national and international level. In the current paradigm all decisions are made by spectrum regulator. This traditional spectrum management model is therefore commonly referred to as command and control, and has been shown to have its limitations. Furthermore, we discussed how current spectrum management approaches that divide spectrum into either licensed or unlicensed bands do not appear to be working well. However, sharing of spectrum appears to offer a way ahead but it can be difficult to gain the licence owners agreement to this. Hence, the idea of unlicensed access to licensed bands – which will be called dynamic spectrum access (radio spectrum tomorrow) was introduced. The objective of dynamic spectrum access is to achieve a more efficient utilisation of the radio spectrum without interfering with primary users. Dynamic spectrum access strategies were presented and categorised under three models, exclusive use model, open sharing model and hierarchical access model. With respect to all dynamic spectrum access types, opportunistic spectrum access (OSA) was considered as the core technique of dynamic spectrum access (DSA), which has been extensively researched recently.

Chapter

3

Introduction to Software Defined Radio and Cognitive Radio

3.1 Introduction

As we mentioned in the previous chapter, today's wireless networks are characterized by a fixed spectrum assignment policy. However, a large portion of the assigned spectrum is used sporadically and geographical variations in the utilization of assigned spectrum ranges from 15% to 85% with a high variance in time. To this end, many approaches to Dynamic Spectrum Cognitive Radio (CR) and software-defined radio (SDR) concepts have been proposed. CR and SDR, are two of the most discussed topics in contemporary spectrum management [37]. The terms SDR and CR were introduced by J.Mitola in 1992 [38] and 1999 [39], respectively. Software defined radio is a radio communication system where components that in the past have been typically implemented in hardware are instead implemented by means of software. Cognitive Radio, usually built upon an SDR platform, is the technology allowing radio equipment to obtain knowledge of its radio environment and to dynamically adjust its operational parameters in order to improve its performance [40]. SDR and CR promise to bring about substantial benefits: Better utilisation of the radio spectrum (spectrum scarcity problem), opening the door for broadband usage, enabling open portability among different network technologies and allowing for economies of scale by their potential to harmonisise the needs of commercial, public safety and military users.

The rest of this Chapter is organised as follows: Section 3.2 delivers an overview around the evolution of microprocessor technology; Section 3.3 provides a brief summary of software defined radio including the history of SDR, main components of SDR, SDR technology and available SDR platforms. Section 3.4 provides an introduction to cognitive radio and cognitive radio network architecture. Section 3.5 summarises the Chapter.

3.2 Microelectronics Evolution and its Impact on Communication Technology

There has been a rapid evolution of microelectronics over the past few decades. For example, Moore's Law has described the long-term trend of the number of transistors accommodated on an integrated circuit. The doubling of the number of transistors per integrated circuit (per square cm) approximately every two years has improved processing speed and memory. The microelectronics industry has significantly influenced the digital communication systems sector. As result digital communication transceivers are becoming more flexible, powerful, and portable. Microelectronics improvements have given rise to the possibility of implementing software-defined radio technology and baseband radio functions can now be entirely implemented in digital logic and software as well as some Intermediate Frequency (IF) functions. There are several types of microelectronics for software-defined radio implementation [41]: of which the following are significance

Firstly, the general purpose microprocessor. This is very flexible in terms of configurability, allows easy implementations of new digital communication modules, is not specialised for mathematical computations, and is potentially power inefficient. Secondly, Digital Signal Processor (DSP) is specialised for performing mathematical computations, allows easy to implementations of new digital communication modules, is potentially slow for computationally intensive processes but can be power efficient (e.g., used in cellular telephones). Thirdly, Field Programmable Gate Array (FPGA), is computationally powerful, but power inefficient and does not allow flexible easy to implementations of new modules. Fourthly, graphics processing unit (GPU), extremely powerful computationally, but does not permit easy implementations of new modules.

A change of the hardware design of microelectronics paradigm will accelerate the appearance of mobile SDR terminals. A system wide co-design will result in less power consumption, smaller chip area and higher integration density of future SDR terminals. SDR-based architecture and SDR technology will be introduced in more detail in the next section.

3.3 Software Defined Radio

The rapid evolution of microelectronics will support the feasibility of SDR. An SDR is a class of reconfigurable/reprogrammable radio whose physical layer characteristics can be significantly modified by software changes. It is capable of implementing different functions at different times on the same platform, it defines in software various baseband radio features, (e.g., modulation, error correction coding), and it possesses some level of software control over RF front-end operations, (e.g., transmission carrier frequency). A number of definitions can be found to describe software defined radio, also known as software radio. Software defined radio may be defined as:

- ❖ A software defined radio is a radio transceiver where only the actual RF part is done in hardware, but the modulation, coding and media access part in software. This has become possible in part by the rise of both affordable as well as powerful Digital Signal Processors (DSPs) [42]. The key feature of SDR is agility, power efficiency, and ease of manufacturing and ease of upgrading.

Although definitions may vary to a certain degree regarding what constitutes an SDR platform, several key characteristics that generally define an SDR can be summarised in the following list [43]:

- ❖ Multifunctionality: Possessing the ability to support multiple types of radio function using the same digital communication system platform;
- ❖ Global mobility: transparent operation with different communication networks located in different parts of the world;
- ❖ Compactness and power efficiency: Many communication standards can be supported with just one SDR platform;
- ❖ Ease of manufacturing: Baseband functions are a software problem, not hardware problem.
- ❖ Ease of upgrading : Firmware updates can be performed on the SDR platform to enable functionality with the latest communication standards

3.3.1 History of SDR Development

In fact, SDR is not new technology, it has been available since the 1980s. The term ‘software radio’ has been first used by the employees of E-Systems Inc. in a company newsletter in 1984. One of the first public software radio initiatives was the U.S. DARPA-Air Force military project named SPEAKEASY [44]. The primary goal of the SPEAKEASY project was to use programmable processing to emulate more than 10 existing military radios,

operating in frequency bands between 2 and 2000 MHz. Another SPEAKEASY design goal was to be able to easily incorporate new coding and modulation standards in the future and was the first SDR platform to involve FPGA modules for implementing digital baseband functionality. The main goal of SPEAKEASY Phase I (1992-1995) was to demonstrate a radio for the U.S. Air Force tactical ground air control party that could operate from 2 MHz to 2 GHz, and thus could interoperate with ground force radios (ability to develop a reconfigurable modem with an open architecture and demonstrate its feasibility). The objectives were to prove the potential of the SDR to solve interoperability issues and problems related to product lifecycle shortening, due to rapidly evolving technologies. In SPEAKEASY phase II, the first goal was to get a more quickly reconfigurable architecture, which allowing several conversations at once, in an open software architecture, with cross-channel connectivity. The secondary goals were to make it smaller, cheaper, and weigh less. Joint Tactical Radio System (JTRS) is a family of military software radios. They are modular, multi-band and multi-mode networked radio systems. Examples of implementations of the JTRS for different purposes include the navy Digital Modular Radio (DMR) [45], WITS [46] by Motorola, the SDR-3000 [47] by Spectrum Signal Processing Inc. and the NRL software radio, which is an outgrowth of the JCIT. The JCIT is another military SDR, whereas the CHARIOT and SpectrumWare were academic projects, although funded by DARPA[48].

3.3.2 Main Components of SDR-Based System Architecture

Figure 3.1 shows the main components that play a vital role to enable the SDR concept. These key components, which have been identified in the literature [49] are as follows: Intelligent antenna, programmable RF modules, digital-to-analog (DAC) and analog-to-digital Converters (ADC), digital signal processor and interconnect technologies.

- 1) The intelligent antenna front end can be split into the basic antenna elements, the related array configuration and processing blocks. Antenna size is inversely proportional to the operating radio frequency. The main activities in the antenna domain to enable the SDR concept (to support the broad range of frequencies with the same antenna elements) are in the array processing blocks and techniques to improve the antenna system performance and intelligence.

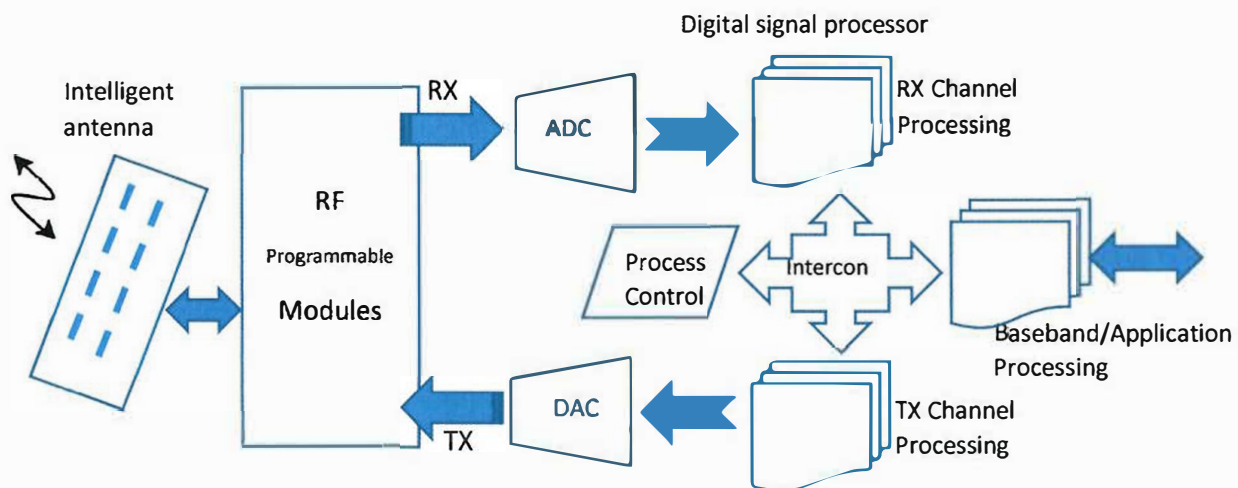


Figure 3-1: Main Components of SDR-Based System Architecture.

2) Programmable RF modules: It is a challenging task to cover the entire frequency band with the same piece of equipment. The essential RF components both in transmitters and receivers are band pass filters. In the SDR-based RF domain the real challenge is to design programmable band pass filters. One of the techniques employed for existing SDR systems is to use a bank of RF modules. The wideband synthesiser, Microelectromechanical systems (MEMS) and superconductor technologies and low noise high performance semiconductor processes are the subjects of active research in this domain recently.

3) DAC and ADC are the doors between the physical and digital domains. The realisation of a true SDR-based system depends upon their performance. In related literature, it is said that the goal of the SDR concept is to connect the converters directly to the antenna elements. The traditional converters are pushing the envelope to achieve better resolution and faster conversion rates. The super-conductivity and optical sampling techniques are the area of active research to achieve even higher performance. The optical sampling technique is a novel method to perform time-resolved measurements of optical data signals at high bit rates with a bandwidth that cannot be reached by conventional photodetectors and oscilloscope. However, the use of this optical technique has disadvantage of optical imperfection and high cost.

4) DSP is the key element to realise software defined radio based systems. The sampling techniques, rate conversion and multi-rate processing DSP techniques have been instrumental in the progress of SDR. To implement DSP algorithms to facilitate SDR, the candidate technologies are Programmable Digital Signal Processors (DSP),

Application-Specific Integrated Circuits (ASICs), Field-Programmable Gate Arrays (FPGAs) and a mixture of them.

5) Interconnect Technologies are required for an SDR enabled system to have the ability to connect various independent functional blocks to set up a radio link. The interface standards need` to be developed within the framework of an interconnect technology. Three main interconnect architectures are Bus, Switch fabric and Tree.

Table 3.1 below summarizes the several aspects of the digital hardware performance associated with software radios. Developers have a variety of architectures to choose from when developing digital signal processing applications. Embedded systems generally use four different types of advance processing devices to execute digital signal processing: ASICs, FPGAs, general-purpose processors (GPPs) and DSPs. When selecting architectures for specific applications, developers must balance cost, power, performance, flexibility and reliability to meet the demands of their mission-critical operations. For each architecture, there is a different set of tradeoffs [49]. In addition, SoC FPGAs are a powerful new class of programmable devices that are applicable to a wide range of electronic designs. SoC FPGA devices integrate both processor and FPGA architectures into a single device. Consequently, they provide higher integration, lower power, smaller board size, and higher bandwidth communication between the processor and FPGA. They also include a rich set of peripherals, on-chip memory, an FPGA-style logic array, and high-speed transceivers.

Table 3.1: Comparison of DSPs, GPP, FPGAs and ASICs [49].

Decision Table for Designers of Real-Time Applications							
	Time to Market	Performance	Price	Development Ease	Power	Feature Flexibility	Summary
ASIC	Poor	Excellent	Excellent	Fair	Good	Poor	Fair
DSP	Excellent	Excellent	Good	Excellent	Excellent	Excellent	Excellent
FPGA	Good	Excellent	Poor	Excellent	Poor	Good	Fair
GPP	Good	Good	Fair	Good	Fair	Excellent	Good

3.3.3SDR Technology

The different components of a radio system are illustrated in Figure 3.2 referenced from [50]. Clearly, all of the digital components may be not be programmable, but the larger the programmable part (DSP/FPGA part on Figure 3.2), the more software the radio is. Dedicated circuits are usually needed, for which the term configurable is more apt than programmable. In

a typical SDR, the analog part is limited to frequency translation: from Radio Frequency (RF) to Intermediate Frequency band (IF), and from IF to baseband. The baseband is sampled and all the signal processing is done digitally. It is not always likely or practicable to develop a radio that incorporates all the features of a fully software defined radio. Some radios may only support a few features associated with software defined radios, whereas others may be fully software defined [50].

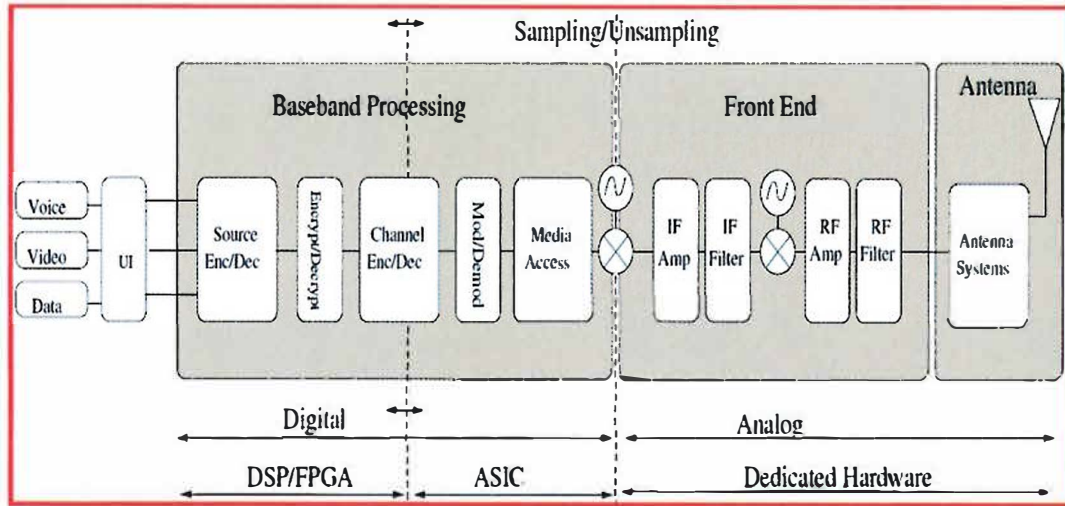


Figure 3-2: Radio Block Diagram, Highlighting the Separation between Digital, and Analog Parts, Programmable, Configurable and Fixed Hardware Parts [50].

In order to further the development of software defined radios and the Software Communication Architecture (SCA), industry at large formed the SDR Forum (recently renamed the Wireless Innovation Forum). This consortium of industry partners has been active in furthering the research and development of SDR and furthermore has continued to grow and evolve. To encourage a common meaning for the term ‘SDR’, the SDR Forum proposes to classify SDR into five tiers [50].

Tier 0 corresponding to hardware radio which cannot be changed by software; Tier 1 corresponds to software controlled radio with control functions implemented in software ; Tier 2 corresponds to software defined radio with digital baseband processing implemented in software; Tier 3 is the ideal software radio with sampling at the antenna to process the radio frequency signal in software; Tier 4 corresponds to the ultimate software radio which extends these capabilities with fast transition (millisecond) from one protocol to another. Tier 3 is the most popular definition of SDR: the radio includes software control of modulation, bandwidth frequency range and frequency bands. Tier 3 and Tier 4 are not realistic today.

Building an SDR terminal includes the choosing of a computing platform for the digital part, a sampling frequency and a radio front-end. In addition to the careful choice of a computing platform, the designer must make a trade-off between the sampling frequency and terminal complexity. For instance, sampling a signal at 4.9 GHz (hence with a necessary 10 GHz sample rate) is today not available with reasonable power consumption. Even with an evolution to lower power ADC, a high bandwidth ADC would produce more samples, hence require a more powerful or specialised platform.

3.3.4 Available SDR Platforms

There are various types of software defined radio platforms using various technologies. These technologies are often mixed and sometimes the term configurable is more appropriate than programmable for them. Note that when designing a complete SDR system from scratch, it is very important to have a hardware platform that is both sufficiently programmable and computationally powerful, as well as a software architecture that can allow a communication system designer to implement a wide range of different transceiver realisations. In this section, we first study some of well-known SDR hardware platforms followed by the software architectures.

SDR Hardware Platforms:

Universal Software Radio Peripheral (USRP): One of the most well-known of all SDR hardware platforms. It is a product of Matt Ettus (Ettus Research LLC), which is considered to be a relatively inexpensive hardware for enabling SDR design and development [51]. All the baseband digital communication algorithms and digital signal processing are implemented on a computer workstation. USRP is open source, which allows for user customisation and fabrication. The USRP1 and USRP2 platforms are a first and second generation of the USRP respectively. The USRP is composed of high frequency ADC/DACs which sample the signal at an intermediate frequency. A FPGA converts and stores the baseband signal. Most of the signal processing is done by a CPU connected to the FPGA by a USB link (USRP1) or an Ethernet link (USRP2). The platform is in widespread use and supported by third party software. It is aimed to work with GNU radio, but is also compatible with National Instruments LabVIEW and Mathworks Matlab. Following the success of the USRP1 & USRP2, Ettus Research officially released several new versions of the platform recently. USRPxx platform is optimised for designing and deploying next generation wireless communications

systems and for RF applications from DC to 6 GHz, and provides options for GPS Disciplined Synchronisation, MIMO configurations and embedded systems. Example application areas include white space radios, mobile phones, public safety radio, land mobiles, broadcast TV, FM radio, satellite navigation and amateur radio bands.

Other well-known SDR hardware platforms are Kansas University Agile Radio (KUAR), Rice Wireless Open-Access Research Platform (WARP), Berkeley Emulation Engine3 (BEE3) and Intelligent Transport System (ITS). The KUAR hardware [52] has been promoted through the Defense Advanced Research Projects Agency (DARPA) as a next generation (XG) program. The complete system was developed in simulink and implemented in Xilinx VHDL by generating the VHDL code from Simulink models using a modalism of mentor graphics. The WARP (wireless open-access research platform of Rice University) is a scalable and extensible programmable platform, built for prototyping advanced wireless networks [53]. It has programmability of both physical and network layer protocols on a single platform. The BEE3 is new generation of Berkeley Emulation Engine-2[54]. It is jointly developed by Microsoft Research, UC Berkeley and BEE cube Inc. It is useful for most computationally intensive real-time applications, employing a high-speed multiple FPGA-based real-world prototyping and development platform. ITS is from National Institute of Information and Communications Technology (NICT) of Japan, who developed a software-defined radio platform so-called NISTITS. It is specially designed for mobile communication, wireless LAN and digital terrestrial TV [55].

SDR Software Platforms:

MathWorks offers support for the USRP with the communications system toolbox, which supports Universal Hardware Driver (UHD) to provide a real-time connection to the USRP family of radios directly from Matlab and Simulink. RF signals can be received from a USRP radio, and the data processed in real-time using Matlab functions or Simulink blocks [56]. Similarly, RF signals can be transmitted from Matlab or Simulink by streaming data to USRP radios. Parameters such as centre frequency, gain and interpolation or decimation rates can be configured directly from Matlab or Simulink. Other software environments that support USRP are GNU Radio, LabVIEW and OpenBTS (open source software).

Other well-known software platforms are GNU Radio, Open-Source SCA Implementation Embedded (OSSIE), Wireless Open-Access Research Platform for Network (WARPnet) and Cognitive Radio Open Source System (CROSS). GNU Radio is an open source software development toolkit that provides the signal processing runtime and processing blocks to implement software radios using readily-available, low cost external RF hardware and commodity processors [51]. The radio applications are written in Python, while the performance critical signal processing components are implemented in C++. GNU Radio Companion (GRC) is a graphical tool for creating signal flow graphs and generating flow-graph source code. Thus, the developer is able to implement real-time, high throughput radio systems in a simple-to-use, rapid-application development environment. OSSIE is Virginia Tech open source software whose core framework is based on the JTRS software communications architecture (SCA) [57]. The OSSIE is an object-oriented SCA operating environment, where signal processing components are written in C++. The operating environment, often referred to as the core framework, implements the management, configuration, and control of the radio system. Every OSSIE component is considered as having two parts: one part realising the signal processing and another managing the SCA infrastructure. The OSSIE waveforms are described in an XML that is used to describe component properties and interconnections between components in a waveform. WARPnet is an SDR framework that is built around client server architecture in Python [58]. The WARPnet uses PCAP (Packet Capture) application programming interface to communicate with the WARP board directly. To allow the Python-based client/server to access PCAP, the Python Pcap extension (Pcapy) module is required. With WARPLab, one can interact with WARP nodes directly from the Matlab workspace and signals generated in Matlab can be transmitted in real-time over-the-air using WARP nodes. CROSS is open source cognitive radio architecture [59]. It consists of five core component categories (modules); cognitive radio shell (CRS), cognitive engine (CE), policy engine (PE), service management layer (SML), and software-defined radio host platform. The CROSS is a modular cognitive radio system framework that uses socket connections for inter-component communication. The cognitive radio shell library and API are implemented in C++, the other modules can be implemented in any language that support a TCP/IP socket interface.

3.4 Cognitive Radio

Cognitive radio (CR) is one of the new long term developments taking place in radio receiver and radio communications technology. After SDR which is slowly becoming more of a reality, CR and cognitive radio technology will be the next major step forward enabling more effective radio communications systems to be developed. The idea for cognitive radio has come out of the need to utilise the radio spectrum more efficiently, and to be able to maintain the most efficient form of communication for the prevailing conditions. By using the levels of processing that are available today, it is possible to develop a radio that is able to look at the existing spectrum, detect which frequencies are clear, and then implement the best form of communication for the required conditions. In this way cognitive radio technology is able to select the frequency band, the type of modulation, and power levels most suited to the requirements, prevailing conditions and the regional regulatory requirements.

3.4.1 Cognitive Radio Definition

Cognitive radio is a broad concept and has different meanings in different contexts [60,61, 62]. The term cognitive radio has been coined by Mitola as an intelligent radio which is aware of its surrounding environment and capable of changing its behavior to optimise the user experience [62, 63]. Therefore, a cognitive radio has three important characteristics: awareness, cognition, and adaptability. Slightly different cognitive radio characterisations are given in [64,65]. Awareness is the ability of the radio to measure, sense, and be aware of its environment and internal states. A radio may exhibit different levels of awareness such as spectrum awareness, location awareness, user awareness, network awareness, etc. Cognition, is the ability to process information, learn about the environment, and make decisions about its operating behavior to achieve predefined objectives. Adaptability, is the capability of adjusting operating parameters for the transmission on the fly without any modifications on the hardware components. This capability enables the cognitive radio to adapt easily to the dynamic radio environment. More pertinent definitions of a cognitive radio are given by Haykin [63,66] and by Jondral [67]:

- S. Haykin [63,66]: “Cognitive radio is an intelligent wireless communication system that is aware of its surrounding environment (i.e. its outside world), and uses the methodology of understanding-by-building to learn from the environment and adapt its internal states to statistical variations in the incoming RF stimuli by making corresponding changes in certain operating parameters (e.g. transmit power, carrier-frequency and modulation strategy) in real-time, with two primary objectives in mind:

highly reliable communications whenever and wherever needed and efficient utilisation of the radio spectrum.”

• F. K. Jondral [67]: “A CR is an SDR that additionally senses its environment, tracks changes, and reacts upon its findings. A CR is an autonomous unit in a communications environment that frequently exchanges information with the networks it is able to access as well as with other CRs.”

From these definitions, two main characteristics of CR can be identified: cognitive capability, i.e. the ability to capture information from the radio environment, and reconfigurability, which enables the transmitter parameters to be dynamically programmed and modified according to the radio environment.

3.4.2 Cognitive Radio Network Architecture

The components of the infrastructure-based CR architecture, as shown in Figure 3.3, can be classified in two groups as the primary network and the CR network [73]. The primary network is referred to as the legacy network that has an exclusive right to certain spectrum bands. Examples include the common cellular and TV broadcast networks. In contrast, the CR network does not have a license to operate in the desired band. Hence, the spectrum access is allowed only in opportunistic manner.

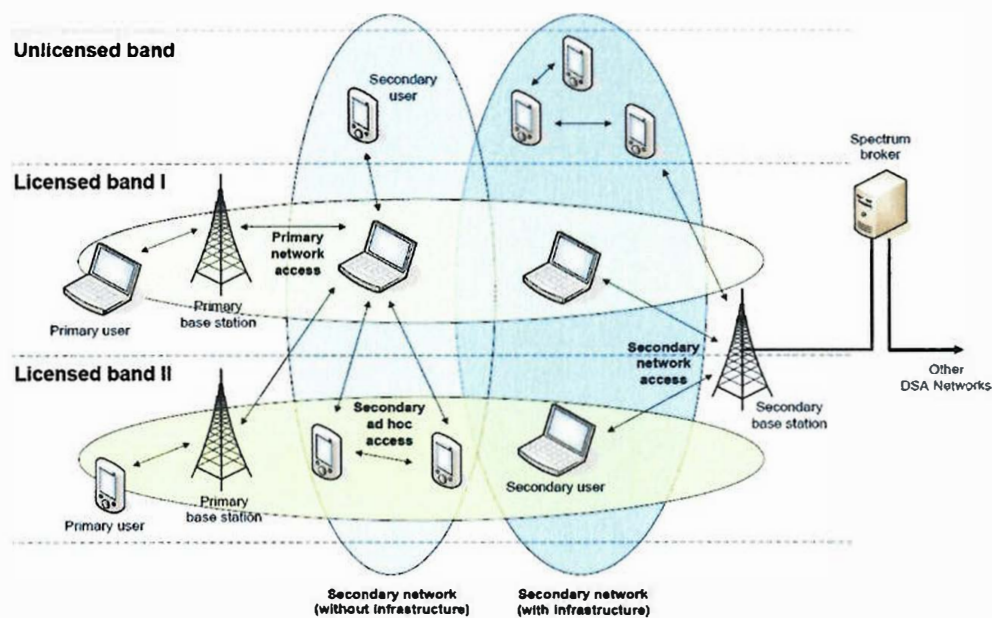


Figure 3-3: Cognitive Radio Network Architecture [73]

A primary network is defined as an existing network infrastructure that has a license for exclusively accessing a certain spectrum band. Examples include the common cellular and TV broadcast networks. The basic components of primary networks are as follow:

Primary user and Primary base station: A primary user has a license to operate in a certain spectrum band. This access can only be controlled by a primary base station and should not be affected by the operations of any CR users. A primary base station is a fixed infrastructure network component that has a spectrum license, such as the base station transceiver system (BTS) in a cellular system. In principle, these do not have any CR capability for sharing spectrum with CR users.

A secondary or unlicensed network is defined as a network, with fixed infrastructure or based on ad hoc communication principles, without license to operate in a desired band. Hence, spectrum access is allowed only in an opportunistic. A secondary network is composed of:

CR user, base station and spectrum broker: A CR user has no spectrum license. Hence, additional functionality is required to share the licensed spectrum band. In infrastructure-based networks, the CR users may only be able to sense a certain portion of the spectrum band through local observations. They do not make decisions on spectrum availability and just report their sensing results to the CR base station. A CR base station is a fixed infrastructure component with CR capabilities. It provides single-hop connection, without a spectrum access license, to CR users within transmission range and exerts control over them. A spectrum broker (or scheduling server) is a central network entity that plays a role in sharing the spectrum resources among different networks. It is not directly engaged in spectrum sensing. It just manages the spectrum allocations among different networks according to the sensing information collected by each network.

Alternatively, CR network can also have the cognitive nodes communicating with each other via ad-hoc point-to-point connections “without infrastructure” over either the licensed or the unlicensed bands as shown in as shown in Figure 3.3. While alleviating the infrastructure cost, such infrastructureless CR networks have increased networking complexity. In the absence of a controlling centralized entity, cognitive radio nodes in a distributed CR networks jointly coordinate their spectrum access decisions to share the available spectral opportunities. Thus, global mechanisms such as network-wide synchronization might be needed for spectrum access coordination.

3.4.3 Cognitive Capability of a Cognitive Radio

The cognitive capability of a cognitive radio is defined as the ability of the cognitive radio transceiver to sense the surrounding radio environment, analyse the captured information and

accordingly decide the best course of action(s) in terms of which spectrum bands are to be used and the best transmission strategy to be adopted. Such a cognition capability allows a cognitive radio to continually observe the dynamically changing surrounding radio environment in order to interactively formulate appropriate transmission plans to be used. However, in order to achieve these objectives, cognitive radio is required to adaptively modify its characteristics and to access radio spectrum without causing interference to the primary licensed users. The cognitive cycle of cognitive radio operation as a secondary radio system is shown in Figure 3.4. Steps of the cognitive cycle are: spectrum sensing, spectrum decision, spectrum sharing and spectrum mobility [73].

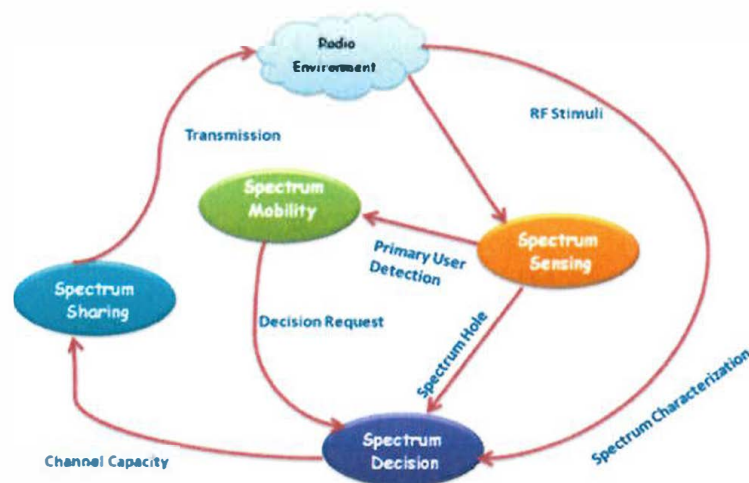


Figure 3-4: Cognitive Cycle of Cognitive Radio [15].

- ❖ Spectrum sensing: A CR user can allocate only an unused portion of the spectrum. Therefore, a CR user should monitor the available spectrum bands, capture their information, and then detect spectrum holes. Spectrum sensing may be performed in cooperative and non-cooperative fashions.
- ❖ Spectrum decision: Based on the spectrum availability, CR users can allocate a channel. This allocation not only depends on spectrum availability, but is also determined based on internal (and possibly external) policies. The spectrum decision function is divided into two steps: the characteristics of the spectrum holes detected in different spectrum bands are analysed and, the operating band is then selected based on the user Quality of Service (QoS) requirements
- ❖ Spectrum sharing: Because there may be multiple CR users trying to access the spectrum, this function is aimed at providing a fair spectrum access to the coexisting secondary users and/or networks by coordinating the access to the available spectrum holes.

- ❖ **Spectrum mobility:** Since CR users are regarded as visitors to the spectrum, the objective of the spectrum mobility function is to ensure a seamless communication during transitions between different spectrum bands while avoiding harmful interference. Also, transfer of CR to a different available channel and/or spectrum band may be triggered by other reasons (preservation or improvement of the QoS, for example).

3.5 Chapter Summary

Due to the command and control approach used in traditional spectrum licensing, the radio spectrum cannot be utilised efficiently. Therefore, a new spectrum licensing approach is being developed which improves the flexibility of spectrum access. This flexibility will be achieved through the use of cognitive radio implemented using software defined radio. Overall, in this Chapter, we firstly provide some insight into the various microprocessor technologies that are currently available to be implemented as part of an SDR hardware prototype. Secondly, we give a brief history of and motivating factors for, SDR, including the SPEAKEASY program that proved the potential of the SDR concept for military radios and the ongoing JTRS program. JTRS will replace the hardware intensive military radios with the more flexible, interoperable SDRs in the future. Next, the main components of SDR, SDR technology and SDR hardware platform and software architectures are introduced. Finally, we gave a literature survey of cognitive radio including different CR definition. Additionally, cognitive radio network architecture and cognitive capability of cognitive radio was discussed.

Part II: Measurement Phase Using Low Time Resolution (Spectrum Analyser)

'We don't see things as they are, we see them as we are.'

Anais Nin

This part contains two chapters

CHAPTER 4: Historical Spectrum Measurements and Lesson Learned in Context of CR.

CHAPTER 5: Spectrum Occupancy Survey in Cognitive Radio: Measurement and Analysis.

Chapter

4 Historical Spectrum Occupancy Measurements and Lesson Learned in the Context of CR

4.1 Introduction

We have suggested in previous Chapter that cognitive radio and SDR technology leads to result in efficient spectrum utilisation. However, before we attempt to assess the potential improvement available through use of CR we need to understand and recognise the actual occupancy of the licensed bands. Detailed and long term spectrum occupancy campaigns provide understanding and prediction of primary user activity, which is considered an essential step toward improving accuracy and the decision making process in cognitive radio. Actual measurements clearly show that the licensed spectrum is underutilised continuously across time and space; many white spaces which are not utilised may be identified readily [74]. Although previous spectrum measurement campaigns followed broadly similar approaches, a detailed analysis reveals the lack of a common and appropriate evaluation methodology. As pointed out in [75], different measurement strategies can result in widely divergent answers. Therefore, the availability of a common and reliable evaluation methodology would be desirable not only to prevent inaccurate results but also to enable the direct comparison of results from different sources and different campaigns. The main objective of this Chapter is to introduce and compare global spectrum occupancy measurements, and to mitigate the major drawback of previous spectrum occupancy studies by providing a unifying methodological framework for future spectrum measurement campaigns.

The rest of the Chapter can be grouped as follows: In section 4.2 we give an overview of global spectrum occupancy measurements. Since the Shared Spectrum Company (SSC) is the leading developer of spectrum management solutions, section 4.3 discusses the spectrum occupancy investigation by SSC. Next, comparison between global spectrum occupancy measurements are illustrated. In section 4.4 we discuss lessons learned during these measurements, which involve various factors to be considered when defining strategies for specific radio spectrum measurements such as antenna selection, influence of spectrum analyser and data post processing. Finally, section 4.5 summarises the conclusions.

4.2 Global Spectrum Occupancy Measurements (Previous Campaigns)

Summarising the results of measurement campaigns for spectrum utilisation involves examining several spectrum surveys covering a wide frequency range at different locations and scenarios to determine the actual spectrum utilisation. Several spectrum surveys have been conducted with some covering a wide frequency range and some more specific to a particular radio technology. For greater detail [76] summarises previous spectrum measurement and the main technical aspects of various broadband spectrum measurement campaigns. This section reviews some of the campaigns performed in different parts of the world in the context of cognitive radio application. The first spectrum occupancy measurements campaign to be considered here was performed in USA by the National Telecommunication and Information and Administration (NTIA) [77]. The next large scale spectrum occupancy measurement was done by Marc McHenry and funded by the National Science Foundation (NSF) [78]. The occupancy in many American cities was found to be always below 25% and it is suggested that this is due to the higher detection threshold used, between -90 and -105 dBm. Robin Chiang et.al conducted spectrum occupancy measurements in New Zealand [11]. This campaign, conducted in the frequency range between 806 MHz and 2750 MHz, indicated that, on average, the actual spectral usage in this band is only about 6.2%. The average occupancy for the band 80 MHz and 5850MHz was found to be only 4.5% in the spectrum survey of Singapore [79]. The spectrum occupancy measurements conducted in the frequency range from 75 MHz to 3 GHz in an outdoor urban environment of Barcelona, Spain is presented in [80]. The measurements are analysed and compared to the official spectrum regulations. A common finding among these studies is that a significant amount of spectrum available is indeed heavily underutilised at the moment. Since the Shared Spectrum Company (SSC), a pioneer in the development of spectrum management solutions, has been promoting the more efficient use of

RF spectrum, we are reviewing the campaigns of SSC in more detail in the following section as good examples of campaigns to date.

4.3 Shared Spectrum Company (SSC)

SSC may be considered as the first company to file comments at the Federal Communications Commission (FCC) proposing the shared use of “white spaces” in the television band for broadband Internet access. Over the past 12 years, SSC has become a leading expert and innovator in the development of cognitive radio technologies. SSC pioneered the research and development of dynamic spectrum access (DSA) technology for the U.S. Department of Defence. The company’s spectrum utilisation measurements are among the most cited in the wireless industry, and it has operated a spectrum observatory globally. Given the keen interest in the prime RF spectrum bands between 30 MHz and 3 GHz, SSC collected worldwide spectrum usage data at its spectrum observatory in these bands over last decade, mostly in America. Other studies have been also carried out in Europe. The following description of spectrum occupancy measurements campaigns undertaken by SSC (section 4.3.1 to 4.3.6) are based upon data extracted from references [68-72].

4.3.1 SSC Campaigns During 2003

Campaigns done between 10 - 12 June 2003 by Mark McHenry of Shared Spectrum and Max Viliimpoc from New America measured the utilisation of the radio frequency spectrum in the immediate vicinity of New America’s offices [68]. The location of the measurement site in an urban and highly pedestrian area just north of Dupont Circle, Washington offered an ideal vantage from which to measure spectrum utilisation during peak business hours. Accordingly, the analysis was performed over a range of frequencies covering both civilian and military use. Measurements were made in all bands in the 30 MHz to 3000 MHz range. The total spectrum occupied divided by the total spectrum available in the bands is used to find the overall occupancy value of 38%.

4.3.2 SSC Campaigns During 2004

The spectrum occupancy measurements of SSC’s 2004 campaign were performed in Vienna, Virginia. From this site, data was collected from 7 April 2004 until 16 April 2004[69]. The spectrum occupancy measurements were made over multiple bands from 30 MHz to 3000 MHz. The overall average occupancies were 3.4%, 6.9% and 13.1 % at Great Falls, Tyson’s Corner and Arlington in Virginia respectively, and the occupied spectrum was 87.62 MHz, 178.24 MHz and 292.57 MHz from total band of 3000MHz. Next, as part of National Science Foundation National Radio Network Research Testbed (NRNRT) program, Shared Spectrum

Company made extensive spectrum occupancy measurements from August 30 to 16 December, 2004 in one of the most densely populated areas in the United States, New York City, as well as in Vienna City, Virginia. These locations and events were specifically selected for study of spectrum occupancy during a period of extraordinarily high communications use. Measurements were made in all bands in the 30 MHz to 3000 MHz range. The total spectrum occupied divided by the total spectrum in the bands is used to find the overall occupancy value of 13%.

4.3.3 SSC Campaigns During 2005

Reference [70] describes spectrum occupancy measurements performed by the Shared Spectrum Company in conjunction with the Wireless Interference Lab of the Illinois Institute of Technology in Chicago, Illinois from November 16 to 18, 2005. Based on results of the study, it was concluded that the overall average spectrum usage during the measurement period was 17.4%. Occupancy varied from less than 1% in the 1240- 1300 MHz Amateur Band, to 70.9% in the 54 MHz – 88 MHz band. Thus, no more than 17.4% of the spectrum opportunities (in frequency and in time) were utilised in Chicago during a high use period when measured from an elevated location.

4.3.4 SSC Campaigns During 2007

In 2007 the spectrum occupancy measurements were performed by Shared Spectrum Company with a receiver at the top of the Commission for Communications Regulation building in Dublin, Ireland from April 16 through to April 18, 2007[71]. Dublin is the most densely populated city in Ireland and in this report it is shown that the spectrum occupancy during a high usage period in a normal work week is only 13.6% in this city. Next, spectrum occupancy measurements were performed by Shared Spectrum Company at the Loring Commerce Centre, Limestone, Maine from September 18 to 20, 2007. These measurements were made during a normal work week and it was concluded that the average spectrum usage during the measurement period was 1.7%. Occupancy varied from less than 1% to 24.65% (470- 512 MHz) in the measurement period.

4.3.5 SSC Campaigns During 2009

Given the keen interest in the prime RF spectrum bands between 30 MHz and 3 GHz, SSC collected spectrum usage data at its spectrum observatory in these bands over a three-and-a-half day period in the autumn 2009[72]. Two data collection antennas were placed on the rooftop of its seven-story, Vienna, Virginia headquarters building. The building is located in a dense urban area near Washington, DC. It was concluded that the average spectrum usage

during the measurement period was 21 %. Occupancy varied from less than 0.1% to 77 % (174-216 MHz) in the measurement period.

4.3.6 Comparing Global Spectrum Occupancy Measurements

In this section we have the collected and grouped together all data collected by SSC during the campaigns described above, to compare global results and draw conclusions. Figure 4.1 and Figure 4.2 provide graphic comparisons of the band by band occupancy in USA and Europe with the results of study performed from 2003 to 2009 in a different cities. The aggregate results of this comparison shows that spectrum utilisation average is very low. This proves that the inefficient usage of frequency spectrum is a problem not only in USA, but also in European countries. We believe that dynamic spectrum access technology can be used to harvest a large amount of this unoccupied spectrum worldwide.

Overall, this survey has presented data and briefly discussed some of the conclusions the can be drawn from them. Spectrum usage data was collected from 30 MHz to 3 GHz at a single location or multi locations. An analysis of the data indicates that a number of spectrum bands may be excellent candidates for reallocation and/or spectrum sharing. Given the urgent need to identify more additional spectrum for mobile broadband applications, this data should serve as a motivation to perform a more detailed analysis to confirm the results herein.

We conclude that any future analysis should include the following.

- ❖ Measurements should be taken at numerous locations. This would eliminate any bias introduced by the single location used in the current analysis.
- ❖ Some measurements should focus on urban areas while others would be wide area. Wide area results could be made aerially using planes or balloons. The wide area measurements should focus on rural areas and help underscore any differences with urban spectrum usage. The relation between measurements made at high points and at ground level is discussed in section 5.5.4.1.
- ❖ Measurements should be taken at fixed and mobile locations and should be taken indoors and outdoors.
- ❖ More in-depth analysis should be undertaken of selected bands (e.g., TV auxiliary, etc.) that offer the greatest potential for sharing. Analysis parameters such as the detection threshold should be optimised for each band, and non-measurement factors (e.g., the challenges involved in protecting receive-only satellite stations) should be accounted for where necessary.

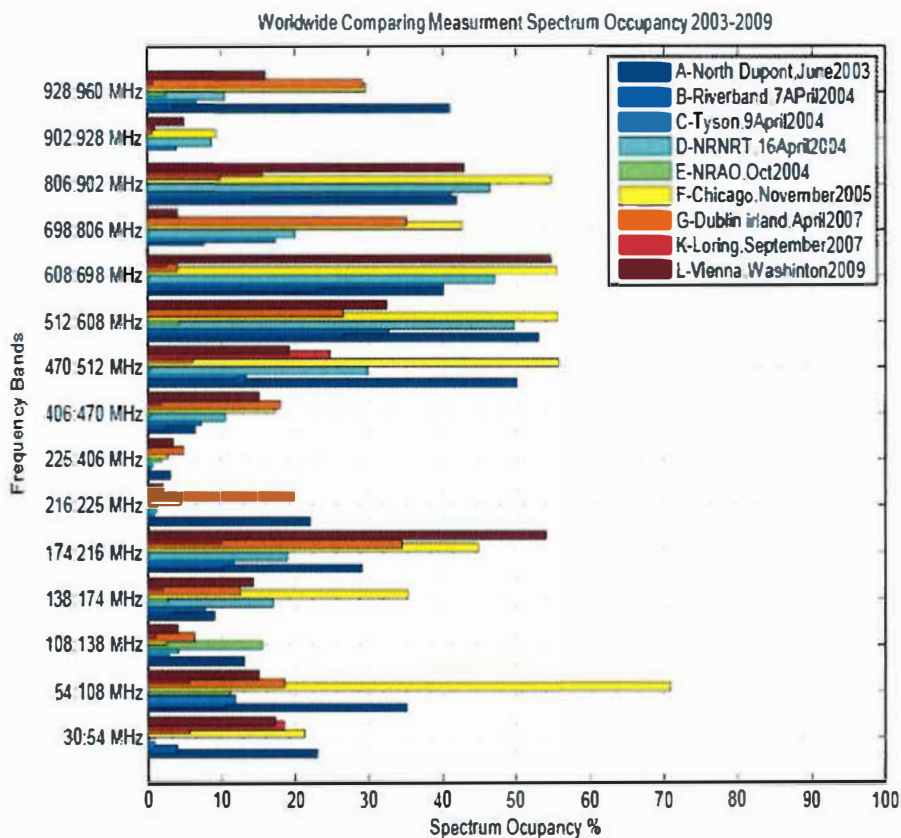


Figure 4-1: Bar Graph of the Spectrum Occupancy in Each Band (30-960 MHz).

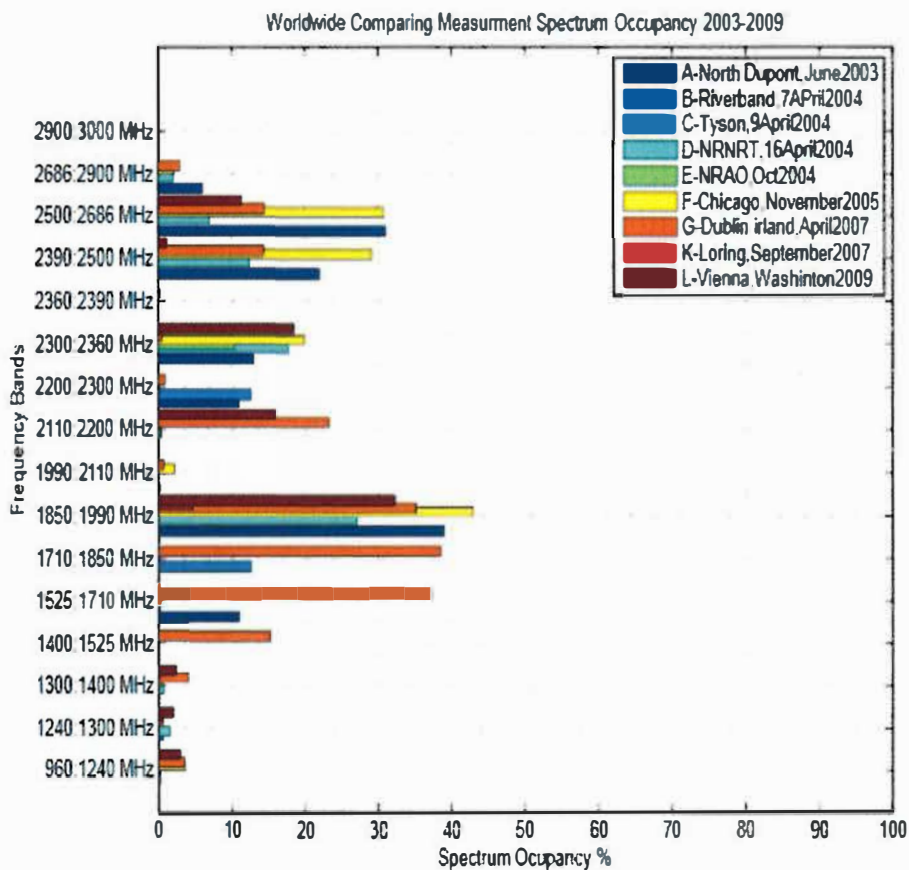


Figure 4-2: Bar Graph of the Spectrum Occupancy in Each Band (960-2900 MHz).

4.4 Lessons Learned During Measurements Setup

There are various factors to be considered while defining strategy for specific radio spectrum measurements which are mentioned in [75]. Some of these are basic parameters that every spectrum measurement strategy should clearly specify: frequency (frequency span and frequency points to be measured), resolution bandwidth, location (measurement site selection), direction (antenna pointing angle) and time (sampling rate and measurement period). In previous measurements, different configurations have been used ranging from simple steps, which connect antenna direct by to a spectrum analyser [82] to more sophisticated and complex designs [81,83]. The study presented in this thesis is based on a spectrum analyser setup where an external device is added in order to improve the detection capabilities of the system, which leads to more accuracy and reliability. A detailed scheme is shown in Figure 4.3. The design is composed of four broad band antennas covering the frequency from range from 30 to 3000 MHz, and a low noise preamplifier to enhance the overall sensitivity and the ability to detect weak signals, and spectrum analyser connected to a computer to record the spectrum activity data.

Selecting the right antenna plays a crucial role in determining the overall performance of measurement system to understand and to improve the received signal. Degradations and failures in the antenna system will cause poor measurement. Furthermore, to obtain additional measurement signal to noise ratio (SNR) amplification is used. The existing trade-off between sensitivity and dynamic range must be taken into account. Thus, the correct pre-amplifier has to be chosen based on the specific measurement needs (which are also related to the needs of the CR system itself). Although most spectrum analysers include an internal amplifier, in some measurement conditions an external amplifier is also preferred. The reason behind this is that some measurement SNR is lost between the antenna port and spectrum analyser. However, to improve the system Noise Figure (NF) a low noise pre-amplifier is often located very close to the antenna. This amplifier will compensate for cable loss and increase the system sensitivity. This condition only applies if the measurement system is limited by internal noise, which is indeed the case above about 30 MHz. On the other hand, it is worth noting that choosing an amplifier with the highest possible gain is not always the best option in broadband spectrum surveys where a wide range of input signals may present. Overall, the reasonable design criterion when selecting the antenna and pre-amplifier to be used is to guarantee that the different received signal strengths lie within the overall system dynamic range. In the next subsections the influence of antenna selection, influence of spectrum analyser, influence of

spectrum measurement and influence of frequency and time aspects will be introduced in more detail.

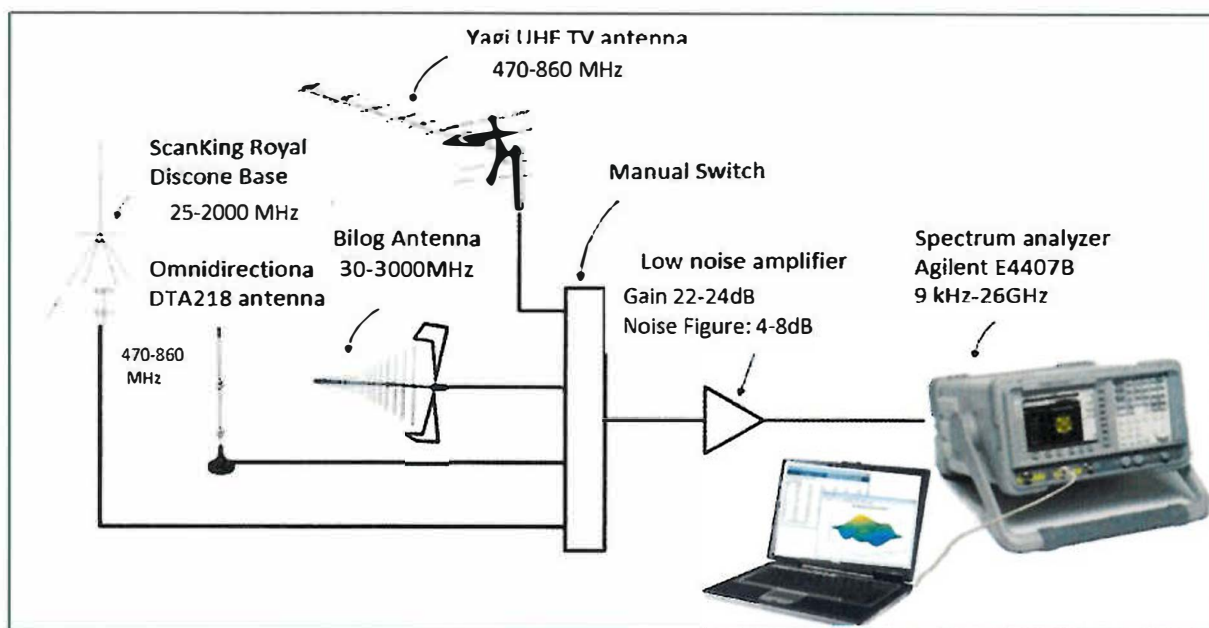


Figure 4-3: Measurement Setup.

4.4.1 Influence of Antenna Selection

An antenna is simply an electronic component designed to transmit and receive radio frequency signals (broadcast radio, TV, etc.). Different antenna types are used for different radio frequencies and for different coverages. Antenna selection can be one of the most confusing parts of designing a spectrum measurement platform. The two core types of antennas are omnidirectional and directional. A typical problem encountered with modern wideband measurement is the choice of suitable antennas. Table 4.1 reviews some of the characteristics of basic antennas that will be used for our signal measurements throughout our research.

Table 4.1: Characteristics of Antennas.

Type and product IDs	Gain	Class of antenna	Bandwidth
Discone Antenna (D130NJ)	Low/ 2.2dBi	Omnidirectional	25-2000 MHz
Digital Antenna (DTA218)	Low/ 3.5dBi	Omnidirectional	470-860MHz
Bilog Antenna (CBL6143)	Medium/ 6-7dB	Directional	30-3000MHz
Yagi TV antenna (RX20A/B/T)	High/ 12.5dBi	Directional	470-862 MHz

In the course of choosing the optimal antenna we always find ourselves comparing manufacturer's specifications. An alternative approach is to simply compare the measured signal levels of one antenna to another. In the following experiment we compare the

relative field performance of four antennas and choose the most suitable and accurate. The four antenna types that have been employed in this study are a Bilog Antenna (CBL6143 ,designed by Prof. Andy Marvin and Dr. Stuart Porter of the University of York), Omnidirectional Discone antenna (DTA218 Digital antenna) and a Yagi antenna (TV antenna RX20A/B/T) . The platform in this scheme was configured as in Figure 4.3. Overall, the antennas covered the range from 30 to 3000 MHz connected by a 1m RF cable to the preamplifier. The GPIB bus was used for logging the trace data onto the hard disk of a PC and for transferring control command sequences to the spectrum analyser. A manual switch was used to choose a given antenna. All measurements of antennas are made back to back, as quickly as possible, in order to minimise the error contribution from time variant signals and environmental conditions. The only parameter being compared here is received signal level, a function of an antenna's sensitivity and gain. Antennas were located at exactly the same spot and at exactly the same height (with one qualifier as follows), were carefully positioned using the same cables and same amplifier were used, and the elapsed time between measurements was minimised as much as possible. The spectrum analyser being used is the Agilent E4407B. The measurements were performed on the roof top of the Applied Science building at the University of Hull. This measurement site (GPS location latitude 53.74° North, longitude 0.34° West) was used to investigate TV band signals. Occupied channels available at the measurement location include channels 22, 25, 27, 28, 30, 33, 35, 53 and 60. The only thing being measured here is the relative received level of one antenna compared to another.

The general characterisation of the traffic density at the TV frequency bands with different antennas is described in this section. The spectrum occupancy measurements have been conducted with four different antennas, to investigate the effect of the antenna on the spectrum activity a cross whole TV band and with specific TV channels. The first and second measurements were conducted using Discone antenna and DTA218 Digital antennas, respectively, which are considered as omnidirectional antennas. The third measurement was performed using the Yagi antenna. The fourth measurement was conducted using the Bilog antenna. Antennas 3 and 4 are consider as directional antennas. We compare the performance of received signals measured over the TV band using the four antennas as shown in Figure 4.4. As expected, a higher received signal is observed with directional antennas than the omnidirectional antennas. A significantly higher spectral activity is observed by using an external amplifier for both the directional antennas and omnidirectional antennas. We have also noted that the duty cycle of spectrum occupancy of the TV band (470-862 MHz) using the

Bilog antenna is greater than with the other antennas. This may be due to another channel being received from another broadcasting aerial since that antenna combines electromagnetic characteristics of both biconical and log periodic antennas into one assembly.

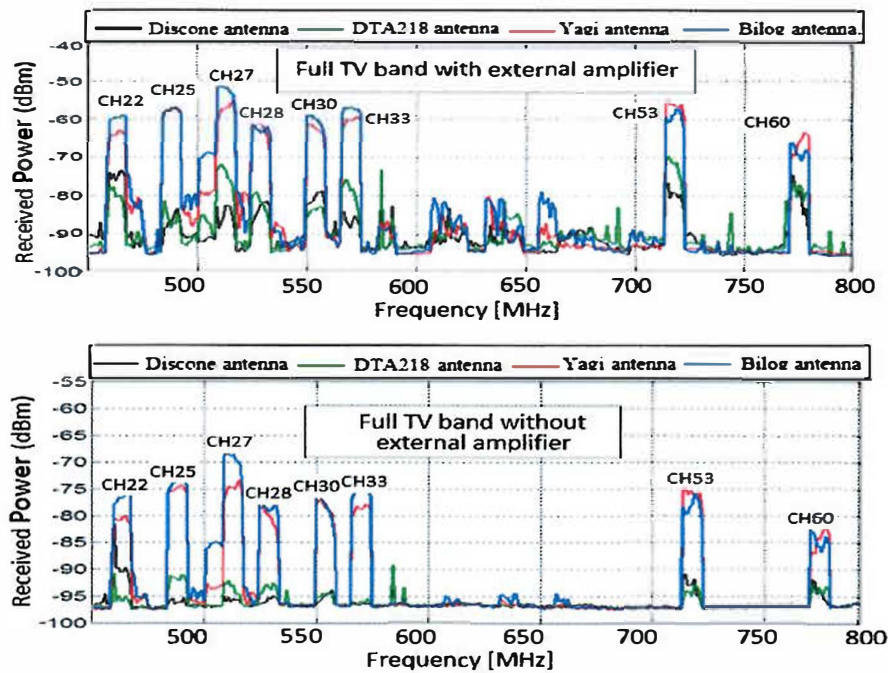


Figure 4-4: Average Received Signal with/without External Amplifier over the Full TV Band.

More specifically, Figure 4.5 compares the performance of receive antenna signals at specific channels (CH30, centre frequency 545MHz, and CH33, centre frequency 570MHz) for the four different antennas. Firstly, the analysis compares the Discone antenna (2.2dBi gain) with DTA218 antenna (3.5dBi gain). We see that the omnidirectional DTA218 provides better sensitivity, since the received signal is 2-4 dB higher at CH 33(and at the rest of the TV channels). Secondly, the analysis compares the Bilog Antenna (6-7dBi gain) with the Yagi UHF TV antenna (12.5dBi gain). Both are models of directional antenna and capable of measuring the complete TV frequency band. Although the Yagi has 5-6dBi gain more than Bilog antenna, the Bilog antenna provides better sensitivity, since this received signal has a 4 dB higher. Moreover, the Bilog antenna has about 3 to 4 dB better sensitivity than the Yagi UHF TV antenna across the majority of the TV band spectrum as shown in shown in Figure 4.4. One exception is at CH53 and CH60, where the Bilog sensitivity slightly drops off at the low end channel (beginning of Frequency Channel), but at the high end channel (ending of Frequency Channel), the measured channel responses where similar. Taking into account all the received signal power over all TV channels with and without external amplifier we could conclude that the Bilog antenna sensitivity is compares well to the others. The significant

differences observed for the TV channels captured are as follows: at CH33 the observations show that the Bilog antenna exhibits about 1-3 dB stronger response compared to the Yagi antenna, and that the Bilog antenna exhibits about 10-18 dB stronger response compared to omnidirectional antennas. As we mentioned previously, this is due to the specification of the Bilog antenna which combines unmatched accuracy with very high gain over the complete frequency range. It also combines the advantages of a biconical antenna and those of a log periodic antenna in a single high end EMC/EMI antenna with an extremely high accuracy over the full specified frequency range.

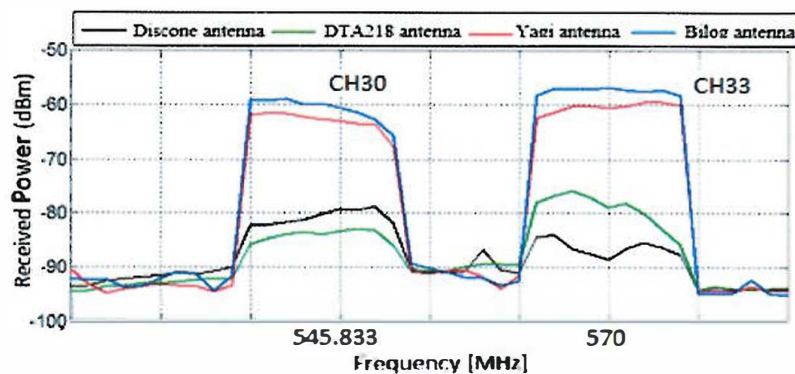


Figure 4-5: Average Received Signal at CH30 and CH33.

Generally, our system comprises four broadband receiving antennas, which are wideband antennas with directional and omnidirectional receiving patterns. The exceptionally wideband coverage (allowing a reduced number of antennas in broadband spectrum studies) and the omnidirectional feature (allowing the detection of licensed signals coming from any directions) make Bilog and DTA218 antennas attractive for radio measurement and monitoring applications. In this studies, directive antennas e.g., Bilog antennas may be used at fixed locations to improve the system's sensitivity at the cost of an increased complexity in the measurement procedures. However, to reduce complexity where a secondary user needs to detect licensed signals coming from any direction and different locations positions to avoid interference with the primary user, and the DTA218 omnidirectional antennas are preferable.

4.4.2 Influence of Spectrum Analyser on the Measurements

To get accurate measurements with an undistorted input signal, the spectrum analyser settings must be correctly set for application-specific measurements, and the measurement procedure optimised to take best advantage of the specifications. A spectrum analyser's ability to measure low-level signals is limited by the noise generated inside the spectrum analyser. This sensitivity to low-level signals is affected by the analyser settings. To measure the low-level signal, the spectrum analyser's sensitivity must be improved by minimising the input attenuator,

narrowing down the resolution bandwidth (RBW) filter, and using a preamplifier. These techniques effectively lower the displayed average noise level (DANL) and reveal the low-level signal. In this section, firstly, we will quantify the impact of sensitivity on the detected primary activity by taking the account of the average duty cycle of each band of PSD to provide simple characterisation of the temporal behaviour of a channel. Secondly, the effect of the amplification configuration on the outcome of the measurement will be illustrated.

1) The effect of amplification on the results from measurements on the GSM900 and wireless band (900-1300MHz) will be discussed in two cases: The GSM900 uplink and the GSM900 downlink has been chosen since, contrary to the TV band, GSM channels exhibit considerable time variability as calls come and go and provide the opportunity to study duty cycle in the context of CR. The wireless band (900-1300) has been chosen since it has very weak signal activity.

In case of GSM900, when the GSM uplink direction is measured without any amplification, some PSD signals are detected resulting in an overall average Duty Cycle (DC) for the GSM900 uplink of 2.0 % for the entire band. When only the external amplifier is connected, a higher number of primary signals are detected and the resulting average DC of GSM900 uplink is 8.1%. These results indicate that, when measuring the GSM uplink primary activity at our measurement location, an estimation error of nearly 6.0% was observed due to insufficient amplification. When the downlink GSM downlink is measured, the results obtained without amplification conclude that the GSM downlink band is subject to moderate/high usage levels with average duty cycle 63.34%, whereas the results obtained with amplification reveal that such band is actually overcrowded, with an average DC of 92.5 %, thus resulting in an absolute estimation error of $92.5\% - 63.3\% = 29.2\%$. Hence, poor sensitivity levels resulted in severe underestimation of primary activity since an estimation error of 29.2% was observed in this case.

In the case of wireless band (900-1300 MHz, with exception of the GSM downlink), we compared the amplification with four different scenarios: without amplification, with internal amplification only, and external amplification only and with both internal and external amplification. Without amplification the average duty cycle of band was around 3.1%. By including the internal amplifier (Average DC around 7.3%) and external amplifier (Average DC around 11.2%) and comparing the average duty cycle

it can be confirmed that the use of external amplifier provides better sensitivity improvements than the use of the spectrum analyser's built-in amplifier as shown in table 4.2. The external pre-amplifier enables the detection of some signals that are not detected with the spectrum analyser's built-in amplifier. On the other hand, both amplifiers are required in order to properly detect the presence of licensed systems (Average DC around 16.0%).

These measurements were investigated using fixed threshold to estimate the average duty cycle of spectrum occupancy measurement with four different scenarios. The results indicate that amplification by itself is not enough: an appropriate amplification configuration is required in order to accurately estimate spectrum usage.

Table 4.2: Impact of Amplification on the Activity Detected for Wireless Band.

Spectrum analyser	Average Duty cycle of wireless band 900-1300 MHz
Without amplification	3.1%
With internal amplification	7.3%
With external amplification	11.2%
With internal and external amplification	16.0%

2) The effect of the amplification configuration on the outcome measurements will be discussed in this section. This investigation was done during the Agilent (Keysight) Technologies workshop held in September 2104 in Shipley, Bradford. The workshop was a one day training involving signal measurement and signal analysis. During this workshop the spectrum analyser was tested with internal and external amplifiers. General, the use of amplification is a time-tested way to improve measurement sensitivity and accuracy for small signals, especially those near the noise floor. As can be appreciated, spectrum analysers are in general characterised by high noise figures, which limit the minimum signal power that can be detected. By using amplifiers with lower noise figures internal preamps alone or along with those external to signal analysers, the sensitivity of the spectrum analyser may be improved, allowing measurement of low level signals. To quantify the detection capabilities under different amplification configurations, to develop our spectrum measurement platform, the signal was detected using four different scenarios (without amplifier, with internal amplifier only, with external low noise amplifier only and both amplifiers). As we can see in table 4.3, the best sensitivity is achieved when both amplifiers are simultaneously employed. It is worth noting that the use of amplifiers not only can reduce the overall noise figure but also the system's dynamic range. As it can be

appreciated in Table 4.3, the use of either the internal or external amplifier does not reduce the effective spurious-free dynamic range significantly. However, when both amplifiers are simultaneously activated, the resulting overall gain causes an appreciable reduction of the dynamic range, thus imposing a trade-off between the sensitivity and the dynamic range. So, by using an appropriate preamplifier with the spectrum analyser, we can obtain significant benefit to the system performance. Based on the table of results a suitable measurement strategy is to employ both amplifiers whenever possible (this provides the best possible sensitivity) and to deactivate the internal or external amplifiers (preferably in this order) in the presence of overloading signals received above the maximum tolerable input power (this can avoid the appearance of spurious responses while still improving sensitivity). Overall, noise is unavoidable in any measurement system. In the case of spectrum analysers, which are primarily designed for high dynamic range rather than low noise, a preamplifier is usually required to produce good quality measurements in many applications. In summary, a low-noise preamplifier may be beneficial if the measurement device under test has low gain or has a high noise figure. But if a measurement device under test already has significant positive gain, a preamplifier should not be used as adding further gain will increase the input noise levels and may also drive the instrument into the non-linear region or exceed the maximum input power to the instrument and thus damaging it.

Table 4.3: Impact of the Amplification Configuration.

Amplifiers	None	Internal	External	Both
Noise Figure(dB)	30.0	16.0	8.0	5.0
Sensitivity(dBm/1kHz)	-118.0	-128.0	-138.0	-140.0
Dynamic range (dB)	88.0	86.0	87.0	84.0

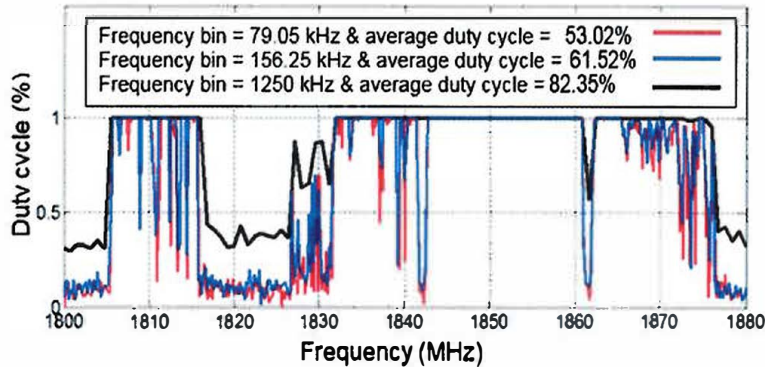
4.4.3 Influence of Frequency and Time Dimension

Despite the fact that the previous sections dealt with basic principles of spectral analysis, this section will discuss the proper selection of configuration parameters related to the influence of frequency and time aspects.

4.4.3.1 Influence of Frequency Dimension

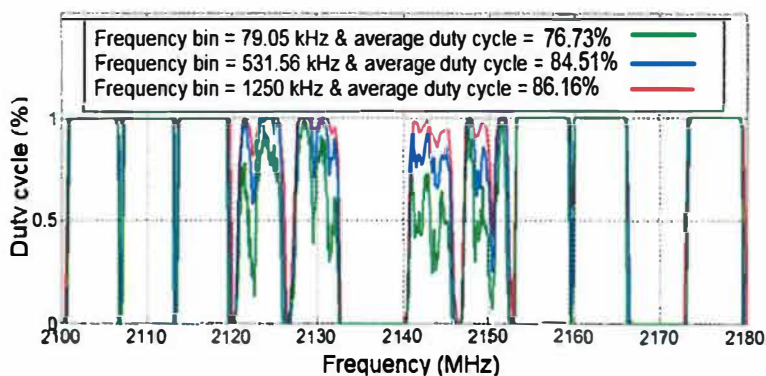
Frequency dimension is an obvious parameter that can be adjusted in the measurement program. The two main frequency dimension parameters are: Frequency range and Resolution Bandwidth (RBW). Where frequency range is the span of frequencies specified for making a measurement and RBW determines the fast Fourier transform (FFT) bin size, or the smallest frequency that can be resolved.

Firstly, in order that no signals will be missed by skipping over them in frequency, the band must be scanned in steps smaller than the resolution bandwidth. In previous spectrum measurement campaigns, the relation between the frequency range and signal bandwidth has received little attention. However, to achieve results with reasonable accuracy classifying emissions in bands with different channel widths this is important. Selecting a frequency bin size narrower than the signal bandwidth can give better accuracy results. Note that a bin is a spectrum sample, and defines the frequency resolution of the window, where $N(Bins) = FFT_{size} / 2$ and frequency resolution $FR = F_{max} / N(Bins)$. Examples are measurement of GSM1800 and the UMTS downlink bands shown in Figure 4.6 and 4.7 respectively. In the case of GSM1800, higher frequency bins tend to result in higher observed spectrum occupancy rates, as seen in Figure 4.6 and Figure 4.7. But, the behaviour in each case is different. In the case of the GSM1800 band, for frequency bins lower than the bandwidth of the transmitted signal (200 kHz), the average DCs (53.02% and 61.52%) indicate that the band is subject to moderate usage levels. For a frequency bin of 1.250 MHz, which is quite a bit large than the signal bandwidth, the obtained DC of 82.35% incorrectly concludes that the same band experiences a high level of utilisation.



Frequency bin	GSM1800 downlink
Frequency bin 79.05 kHz	53.02%
Frequency bin 156.25kHz	61.52%
Frequency bin 1250 kHz	82.35

Figure 4-6: Influence of the Frequency Bin on the Activity GSM1800.



Frequency bin	UMTS downlink
Frequency bin 79.05 kHz	76.73%
Frequency bin 531.56 kHz	84.51%
Frequency bin 1250 kHz	86.16%

Figure 4-7: Influence of the Frequency Bin on the Activity Band UMTS.

This phenomenon can be clarified as follows. Frequency bin values (e.g. frequency bin of 1250 kHz) larger than the signal bandwidth (200 kHz active channel) lead to important overestimations of spectrum occupancy in regions with moderate activity levels, which in turn results in greater average DCs for the entire band. In the case of UMTS the studies where the frequency bins are always lower than the signal bandwidth (5 MHz), the average DC increases with the frequency bin, and the difference is less significant (only 9.43% between 79.05kHz and 1250 kHz), as shown in Figure 4.7. This difference can indeed be qualified to the fact that for the lower frequency bins some frequency points lie within the UMTS channels' guard bands, where the DC is zero. As a result we could recognise that if the frequency bin is larger than the bandwidth of the signal being measured, spectrum occupancy is notably overestimated. On the other hand, occupancy estimation is reasonably accurate as long as the frequency bin size remains acceptably narrower than the signal bandwidth.

A second parameter is based on consideration of Resolution Bandwidth (RBW). Narrowing the RBW increases the system's ability to resolve signals in frequency and decreases the noise floor, which in turn improves the ability to detect weak signals at the cost of increased measurement times. Table 4.4 shows the influence of the resolution bandwidth on the activity in the band between 137 and 400 MHz. This band represents transmission from several radio systems with various signal bandwidths, such as private mobile radio networks (12.5/25 kHz), wireless microphones (200 kHz) and digital audio broadcasting (1.54MHz). From table 4.4 we could conclude that a 10-kHz RBW can be considered as an adequate trade-off between detection capability (represented by the average DC) and measurement time (represented by the average sweep time). For instance, the 10kHz RBW configuration only misses the detection of $22.05\% - 19.41 = 2.6\%$ of licensed signals with respect to the 3kHz RBW configuration while it is able to capture $12.745s / 1.147s = 11.17$ times more PSD samples within the same measurement period. Wider RBWs result in shorter average sweep times but higher estimation errors, up to 18.42% for the 300 kHz RBW configuration. In addition, since signal bandwidths of less than 10 kHz are unusual, a 10 kHz RBW is sufficient to resolve signals in frequency for most of the existing radio technologies. Based on the table results and observations, 10 kHz RBW can be considered as the most suitable choice for broadband spectrum research, offering trade-off between detection capability and required measurement time. This RBW will be used through the rest of our measurement campaign.

Table 4.4: Impact of the RBW on the Activity Detected Between 137 and 400MHz.

RBW	Average duty cycle	Average sweep time
1kHz	27.13%	114.73s
3kHz	22.05%	12.74s
10kHz	19.41%	1.147s
30kHz	14.01%	1.771s
100kHz	12.81%	11.47ms
300kHz	8.71%	5.5ms

4.4.3.2 Influence of Time Dimension

Time-domain analysis of spectrum measurements shows how a signal changes over time and is commonly defined by two parameters, sampling rate and the measurement period. Although sampling rate is controlled by the measurement device, measurement period can be easily controlled manually. Very different measurement periods have been considered in previous spectrum measurement campaigns, as it can be appreciated in [76]. The selected measurement period depends on the trade-off between the overall time required to complete the measurement campaign and the particular objectives of the measurement study. Some previous studies have been aimed at identifying spectrum usage patterns over long periods and understanding any potential seasonality in the visible spectrum usage. In former measurement campaigns different periods have been considered. For instance [84,85], suggested long-term measurement campaigns with measurement periods of several years to identify spectrum usage patterns over long periods. On the other hand, by considering the issue of resource utilisation the short-term evaluation and classification of spectrum usage is frequently more interesting since in practice it has impact on the behaviour and performance of cognitive radio. In such a case, long-term measurements are not necessary. In the context of cognitive radio we need to know how long spectrum should be measured to obtain a descriptive estimate of the actual spectrum usage. In order to answer this question the effects of the measurement of the TV band (CH22) and GSM900 was examined with time period of 1 hour, and of 24 hours. Results obtained during measurement campaign are different in these bands as shown in Figure 4.8.

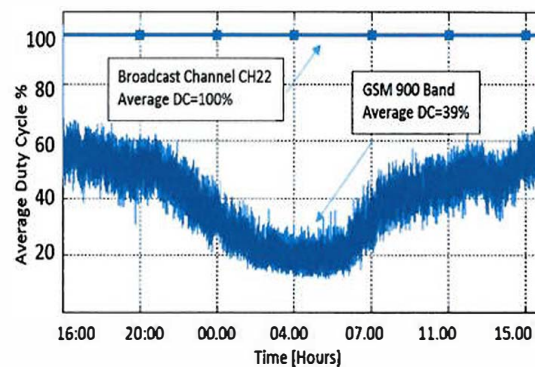


Figure 4-8: Average Duty Cycle per Hour for TV Broadcasting and GSM Band.

The utilisation of the TV band (CH22) indicate that the average DC for entire measured frequency point was a close to 100% as expected. This is because most occupancy data in our measurement bands (CH22 TV Channel) are stationary which do not vary with time and hence the instantaneous DCs matches the average value at every time instant. This conclusion is valid not only for TV but in general for transmitters with a constant temporal activity. However, GSM band exhibits an oscillating behaviour over time. When the entire band is considered, the instantaneous DC then notably differs from the average value. The utilisation of the GSM900 MHz band varies with time throughout the day. The minimum value was between 23:00 and 6:00 with an average DC of 19% to 21% while measurements between 16:00 and 22:00 report average DC of 50% to 60%. The average DC usage of band over the 24-hours is 39%. Overall, data show that the 24 h seasonal pattern is caused by the peak traffic of each day in 10:00–17:00 local time. Although the common monitoring durations are 24h, working hours or another appropriate period hours in order to account for potential daily temporal patterns, our investigations show that the optimum duration of monitoring depends on the purpose of the occupancy measurement and the available a priori knowledge about the behaviour of the radio systems using the spectrum resource.

4.4.4 Data Post-Processing

Data post-processing is a way to filter significantly data from the mass of measurements. Therefore, this section will discuss methods used for post processing during measurements and examine the impact of such methods on the obtained spectrum usage information. Regardless of the objective of the measurement campaign, one of the key steps of data processing is to determine which captured PSD samples correspond to busy and ideal channels. Although there are several techniques for signal detection (referred to as spectrum sensing techniques), when there is no a prior information available probably the easiest method to both understand and to detect whether a channel is used by a licensed user is energy detection [87]. Spectrum detection methods will be introduced in more detail in Chapter 6. Throughout this work, the energy in the received waveform over an observation interval (sensing time) is measured and compared to a threshold value. If such an energy based spectrum sensing technique is used to analyse spectrum occupancy, then there are two distinct classes of data, represented by the noise and the signal itself. As a result, setting the decision threshold between these classes is basically a single threshold classification process to determine the average duty cycle. Figure 4.9 illustrates the general case of post-processing and data management. Firstly (part 1, in the figure), a reliability check is necessary because some information could have been lost during

the measurement process. Measurement information such as start frequency, stop frequency and RBW are loaded from the measurement information file. These values are also checked directly from the measured data. After this, the specific measured values corresponding to one cycle were loaded from the file containing measured data. The consistent data are saved as a binary data file for future analysis. This type of file consumes less space and is easy to operate with. At this point (part 2, in the figure), the threshold level value (threshold) is set. The measured values for frequency points above this level are marked as “occupied” by another service (primary user). Finally (part 3, in the figure), the quantifying parameters are evaluated. The most common parameter describing utilisation of the frequency spectrum is the Duty Cycle [88, 89, 90].

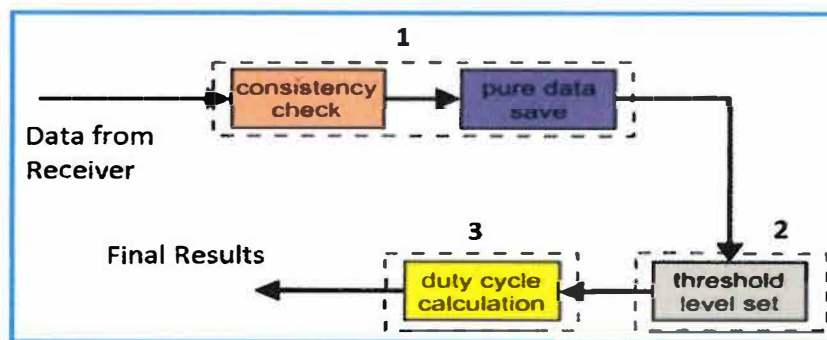


Figure 4-9: Flow Chart of Post-Processing.

4.5 Threshold Impact

With respect to the data analysis procedure, threshold setting is considered to be the most difficult part as well as being vital to success. There are several threshold techniques for energy based spectrum sensing, primarily based on empirical data analysis [91, 92], histogram analysis [93], computation of receiver properties [94] and complementary cumulative distribution function (CCDF) techniques. Also, there exists a second category of algorithms to determine the decision threshold without a priori knowledge of the noise properties. Some examples are Otsu’s algorithm [95] and the recursive one-sided hypothesis testing (ROSHT) algorithm proposed in [96,97]. The main drawback of these algorithms is that they are more complex and based on some assumptions that may not hold. Moreover, such assumptions are not necessary when noise properties are known as is often the case. Figure 4.10 illustrates the duty cycle dependence on the decision threshold for different inspected bands measured with our platform. As shown in Figure 4.10, the spectrum occupancy observed for various systems (expressed in terms of the duty cycle) may exhibit significant variations depending on the selected decision threshold (in some cases, with changes from 100% to 0% for a variation of 5 dB or less).

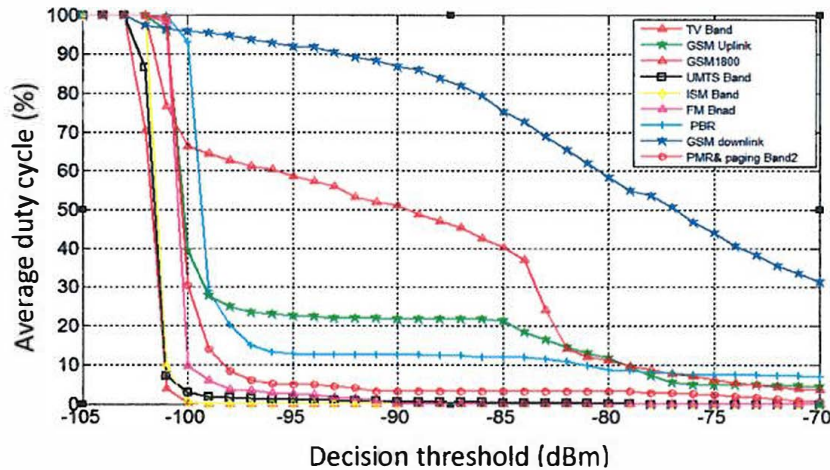


Figure 4-10: Average Duty Cycle as Function of the Decision Threshold for Different Systems.

Another method to determine the decision threshold is to fix the decision threshold m decibels above the average noise level. The decision threshold as in the recommendation of the ITU spectrum monitoring handbook is 10 dB above the average noise floor [98]. However in some of the studies as in [99] and [100], the decision threshold was 3 to 6 dB above the average noise floor. Calculation of an appropriate decision threshold has a great impact on the estimation of the duty cycle. In the following experiment we will illustrate different values of m dB criterion threshold and choose the most approximate one. For this purpose a signal with wide diversity of licensed systems, low power transmitters and high power transmitters were investigated. Five different threshold (m dB criterion) are applied to the generated samples. Table 4.5 summarises the calculated thresholds for the different cases m dB criterion.

Table 4.5: Calculate Thresholds and Corresponding Duty Cycles.

Threshold \ Frequency Band	8 dB above noise floor	7 dB above noise floor	6 dB above noise floor	5 dB above noise floor	4 dB above noise floor
108-400MHz	49.0 %	54.5 %	59.0 %	61.4 %	67.5 %
880-915MHz	4.7 %	5.1 %	5.6 %	6.9 %	13.6 %
470-850MHz	11.9%	12.7%	12.8	13.4%	15.4
880-960MHz	30.5%	31.2%	31.7	32.1%	33.7%

The comparison is performed based on the occupancy statistics obtained for several types of bands, namely bands allocated to a wide diversity of licensed systems (108-400 MHz and 470-850MHz), low power transmitters (880-915 MHz and 1900-2500MHz). For example, when the decision threshold is lowered from the 8dB criterion to the 7dB criterion, a maximum amount of noise samples are allowed to lie above the decision threshold, which may be detected

as signal samples. Table 4.5 shows that the average DC for the 108–400 MHz band and 880–915MHz band increases 5.5% (from 54.5% to 49.0%) and 0.4% (from 5.1% to 4.7.0%), respectively, when moving from 8dB criterion to the 7dB. Another trend is observed for further lowered threshold with the 6dB, 5dB and 4dB criteria as shown in table 4.5. In the band above 2500 MHz where signals are very weak the m-criterion increases the average DC by the nearly same amount. The absence of licensed signals in these bands indicates that such increase is not caused by the detection of true weak signals but noise samples above the threshold. A similar behavior is also observed for bands with high-power transmitters such as TV and GSM downlink. In this case, this means that in such bands lowering the decision threshold below the maximum noise level with the m-criterion does not result in the detection of some additional weak signals. Based on the obtained results at Table 4.5, the 5dB criterion can be considered as a reasonable trade-off between the improvement in the ability to detect weak signals and the overestimation error. This result has been used for our later measurements (Chapter5). However, Multi-bit hard Threshold using two-stage adaptive sensing is proposed in[Chapter8].

4.5.1 An Adaptive Threshold Setting Approach

The spectrum occupancy measurements performed in Chapter 5 are based on a fixed threshold to distinguish PU signals from noise. This may not be optimum in low SNR conditions where the performance of fixed threshold based detectors can vary from the targeted performance metrics substantially. Unlike the conventional fixed threshold based sensing algorithm, an adaptive spectrum sensing algorithm was proposed to dynamically adjust its energy threshold according to the signal to noise ratio in [Chapter8]. The goal of this technique is to select the upper and lower bounds of the detection threshold to be used with spectrum measurements (Digital TV pilot power measurements) for safe operation of cognitive radio devices that guarantees no harmful interference. For instance, if the detection threshold is continually raised, then at a point it will not be able to sense the legitimate TV signal, even a strong TV signal, and therefore with increasing detection threshold the rate of harm will go to 100%. If the detection threshold is continually lowered, then at a point it will begin to sense the noise floor and therefore with decreasing detection threshold the rate of false alarm will go to 100%. Clearly, one cannot be too conservative as a really low detection threshold will ensure “no harm”, but will also raise the rate of false alarm so high that the radio is never able to turn on and be of any practical use.

4.6 Chapter Summary

In this Chapter firstly we compare the results of spectrum measurement campaigns carried out by the SSC and other global research groups within the last decade. All presented results are based on real-life measurements. Overall, the comparison shows that the level of spectrum utilisation is consistently low. The obtained results demonstrated the existence of a significant amount of spectrum which is potentially available for the future deployment of cognitive radio systems. Next, we have discussed spectrum occupancy measurement setups in detail and have elaborated on the major design decisions and lessons learned. This part presented a comprehensive and in-depth discussion of several important methodological aspects that need to be taken into account when evaluating spectrum occupancy such as the influence of antenna selection, influence of spectrum analyser, influence of spectrum measurement and influence of frequency and time aspects. Finally, data post processing and the impact of threshold on the performance of spectrum detection was discussed. The results presented in this Chapter highlight the importance of carefully designing an appropriate methodology when evaluating spectrum occupancy in the context of cognitive radio. The outcome of this Chapter will be of great utility in the study outlined in following Chapters.

Chapter

5

Spectrum Occupancy Survey in Cognitive Radio: Measurement and Analysis

5.1 Introduction

Although several of spectrum occupancy measurements have been conducted worldwide as described in Chapter 4, an old management adage that is still accurate today says “you can’t manage what you can’t measure”. Therefore, to estimate the degree of radio spectrum utilisation in a geographical region and hence to consider principles of actual radio spectrum management, a campaign of experimental measurements has been conducted. This Chapter describes the set of spectrum occupancy measurements performed at different geographical locations, within the UK in 2012, 2013 and 2014 and proposes long-term studies in multiple locations. The measurement campaign was undertaken covering a wide range of frequency. Observations provide evidence that the licensed spectrum is far from fully utilised in frequency. Measurements provide evidence of the spectral efficiency benefits that might be accrued by the dynamic reuse of the available spectrum. Such improved usage could break the current spectrum availability bottleneck.

The remainder of this Chapter is organised as follows. Section 5.2 describes radio spectrum measurement, including spectrum measurement system, measurement sites and data acquisition. Section 5.3 describes the measurement setup. Section 5.4 describes the data processing, leading to the determination of occupancy metrics, spectrum occupancy and duty

cycle. Section 5.5 illustrates detailed analysis of spectrum occupancy measurement where results are presented and analysed. Section 5.6 summarises the conclusions.

5.2 Radio Spectrum Measurement

This section presents a sophisticated radio spectrum measurement platform specifically envisaged and designed for spectrum occupancy surveys in the context of cognitive radio. We start by introducing the measurement of radio spectrum usage in section 5.2.1. Additional detail associated with spectrum study is explained in section 5.2.2. Spectrum measurements system are discussed in section 5.2.3. Measurement sites and data acquisition are introduced in section 5.2.4 and 5.2.5 respectively.

5.2.1 Measuring Radio Spectrum Usage

To maximise the utility of the radio spectrum, knowledge of its current usage is beneficial. While some coarse information can be attained from spectrum licenses, essential details, including the location of transmitters, transmitter output power, and antenna type, are often unknown. Additionally, licenses do not specify how often the spectrum is being occupied if at all. Furthermore, the local environment affects the propagation of radio waves; while this effect can be simulated, the results offer only moderate precision. Hence, to categorise spectrum usage, measured data is vastly preferable to theoretical analysis. Several spectrum studies were performed to provide multidimensional usage information. These studies, improve upon past spectrum studies by resolving spectrum usage by nearly all of its possible parameters. Very few other wide bandwidth spectrum studies have been performed.

5.2.2 Spectrum Study

In these studies, spectrum usage was measured as a function of frequency, time and location type. The contiguous frequency range from 180MHz to 3000MHz was measured. This covers emitters from UHF TV, several land-mobile communication systems, radars (both air search and weather), satellites (uplink and downlink channels), fixed microwave services, and several passive bands. To measure spectrum usage in the time dimension, two schemes were employed. One measured the short-term usage of the spectrum, which provided a metric of spectrum usage over a span of a few minutes. This metric can aid in the identification of periodic spectrum users. The other method employed was designed to measure usage of the spectrum over the course of the day; determining if temporal variations exist and to what extent. To provide a statistically valid model of the spectral environment, a large number of data samples were taken. More than one thousand spectrum measurements have been taken over several months of

observation. The spectrum studies also determine the effects of the demographic location type. The degree of spectrum usage has been investigated in following region: Urban Hull city, suburban Hull city, and rural Humber region, UK.

5.2.3 Spectrum Measurement System

The spectrum studies conducted required the design and construction of a spectrum measurement system composed of several hardware and software subsystems. A block diagram of the hardware that composed the spectrum measurement system is shown in Figure 4.1 (Chapter 4), consisting of antenna sub-system, an RF-subsystem, a spectrum analyser, and finally a data acquisition and control system.

1) An antenna system involving both omnidirectional and directional antenna was used for spectrum occupancy measurement.. For the fixed high points used in urban studies, 10 m of Belden RG-8 9913 coaxial cable is used to connect the Bilog antenna. The rural and suburban sites offered the opportunity to mount the antenna on the roof of a car, hence shorter cable be used. In this case, 1 m of Belden RG-8 9913 coaxial cable is used to connect the DTA218 antenna.

2) Amplification was performed by the RF sub system shown in Figure 4.1(Chapter 4). From the antenna, signals pass through a low noise amplifier (LNA) with a high gain (+24 dBm). The LNA is needed to lower the total system's noise temperature, since the spectrum analyser used has a high noise figure (27 to 39 dB, depending on frequency). The noise figure of the RF- amplifier and spectrum analyser combination includes the antenna cabling. The LNA combination has an instantaneous spurious-free dynamic range that is better than that for the spectrum analyser alone as discussed in Chapter 4. For many of the spectrum measurements, the spectrum analyser limits the system's intermodulation performance and thus sensitivity, since the power of the intermodulation products is above the thermal noise floor.

3) A spectrum analyser, Agilent E4407B, was used in this system to provide spectral power measurement, over the complete frequency range. The setting for resolution bandwidth, detector type, span, sweep time, video bandwidth, reference level, attenuation level, and data collection method were chosen with the intent of maximising the probability of detection. Resulting from Chapter 4, a narrow 10 kHz resolution bandwidth was employed to maximise the detection of narrowband signals and to resolve the spectral content of wider bandwidth signals. Some measurements were

undertaken with 100 kHz resolution bandwidth to improve the ability to observe pulsed signals. It was determined that this wider bandwidth filter reduced sensitivity and spectral content information significantly with only an incremental benefit in the detection of pulsed signals; hence 10 kHz was employed for nearly all of the spectrum measurements. The span is the frequency range that the spectrum analyser covers in one sweep. While it would have been possible for the spectrum analyser's span to be set to cover the full range of measured frequencies, this would have produced coarse and inaccurate results. Spectrum analysers have a defined number of discrete frequency bins to store the results of a scan; for the Agilent E4407B we use 401 bins. To provide the maximum amount of valid data for analysis after collection, it was desired to transfer the measurements of every resolution bandwidth to the control and data collection system. The amount of time it takes the spectrum analyser to sweep through a span is known as the sweep time. The spectrum analyser can automatically select the minimum sweep time, which is limited by the rise time of resolution bandwidth filter being used. Shorter sweep times result in an understatement of received power. Larger sweep times increase the amount of time the resolution bandwidth filter rests at a given frequency. To eliminate this analogue form of averaging the video bandwidth was set to equal the resolution bandwidth.

5.2.4 Measurement Sites

There were several attributes used in the selection of the measurement sites. Most of previous spectrum occupancy studies are based on measurements performed in outdoor environments and more particularly in outdoor high points such as building rooftops and towers. The main advantage of high points is that they provide direct line-of-sight to various transmitters and therefore enable a more accurate measurement of the spectral activity. Nevertheless, this scenario may not be representative of the spectrum occupancy perceived by a secondary network in other more practical situations where the secondary antenna is not placed in a static high point (e.g., a mobile secondary user communicating inside a building or while walking in the street between buildings). The measurement of real network activities in additional scenarios of practical significance is therefore required for an adequate and full understanding of the use of spectrum. This study involves three scenarios. Two of the measurement sites urban/suburban are in the University of Hull and near to Hull city centre with the third rural site in the Humber region, UK. The high point urban measurement site (Location 1) is situated in Hull University, on the campus of the University. This site has direct line of sight with

several FM transmitters, analogue and DVB-T transmitter, GSM and UMTS base stations. Various base stations and telecommunication systems are already hosted in the University, including GSM and UMTS base stations which were a few tens of meters away from the measurement location. The urban/suburban spectrum study was performed in multiple places near to Hull city centre. The roof of the car was chosen since it offers a simple platform for the measurement system. For the rural measurements, multipoint measurement points located in the Humber region was chosen. At this locations, local population density is less. The measurement system was situated on the top of a car roof at the sites. The measurement equipment employed in this study is illustrated in Figure 5.1 & 5.2. The locations in terms of latitude, longitude and elevation are shown in Table 5.1 and Table 5.2. The locations of urban, suburban and rural sites were determined with a Global Positioning System (GPS) receiver. Figure 5.3 and Figure 5.4 shows the location of the urban, suburban and rural measurement sites with the map cropped.

Urban area
(Hull University)

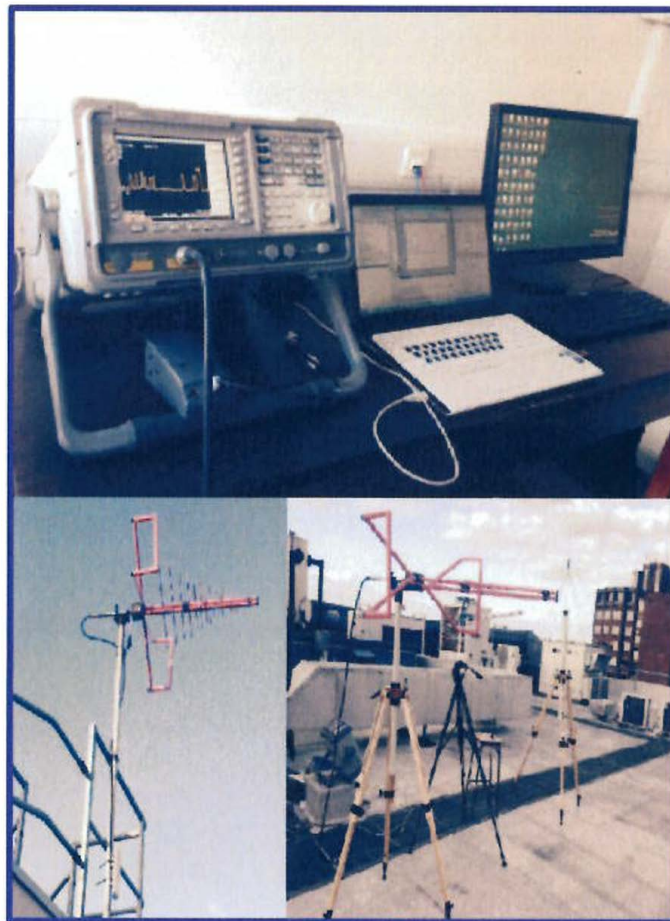


Figure 5-1: Measurement Equipment Employed in this Study: Antenna, Preamplifier and Spectrum Analyser at Urban Area (Hull University).

Rural area
(Humber region)



Figure 5-2: Measurement Equipment Employed in this Study: Antenna, Preamplifier and Spectrum Analyser at Rural Area (Humber region).

Table 5.1: Location of Measurement Sites Urban/Suburban Sites.

No	Locations	latitude	Longitude	Antenna height
1	Location1	53.7469444°N	0.3444444°E	23m(roof of building)
2	Location2	53.7869444°N	0.3644444°E	1.7m(roof of car)
3	Location3	53.7883333°N	0.3858333°E	1.7m(roof of car)
4	Location4	53.7736111°N	0.367524°E	1.7m(roof of car)
5	Location5	53.7716667°N	0.3716667°E	1.7m(roof of car)
6	Location6	53.7483333°N	0.3747222°E	1.7m(roof of car)
7	Location7	53.7466667°N	0.3505556°E	1.7m(roof of car)
8	Location8	53.7558333°N	0.3494444°E	1.7m(roof of car)
9	Location9	53.7650300°N	0.34697 °E	1.7m(roof of car)
10	Location10	53.7896691°N	0.303721°E	1.7m(roof of car)
11	Location11	53.7799565°N	0.277533°E	1.7m(roof of car)
12	Location12	53.8039620°N	0.332876°E	1.7m(roof of car)
13	Location13	53.7340707°N	0.399673°E	1.7m(roof of car)
14	Location14	53.7466513°N	0.255875°E	1.7m(roof of car)
15	Location15	53.7853486°N	0.3184622°E	1.7m(roof of car)

Table 5.2: Location of Measurement Sites Rural Sites.

No	Locations	latitude	Longitude	Antenna height
16	Location16	53.714768°N	0.4434872°E	1.7m(roof of car)
17	Location17	53.68002°N	0.46068°E	1.7m(roof of car)
18	Location18	53.623660 °N	0.430293°E	1.7m(roof of car)
19	Location19	53.5844444°N	0.3494444°E	1.7m(roof of car)
20	Location20	53.5508333°N	0.2841667°E	1.7m(roof of car)
21	Location21	53.4741667°N	0.2961111°E	1.7m(roof of car)
22	Location22	53.4172222°N	0.2386111°E	1.7m(roof of car)
23	Location23	53.349776°N	0.182547°E	1.7m(roof of car)
24	Location24	53.584146°N	0.421635°E	1.7m(roof of car)
25	Location25	53.5447667°N	0.6434167°E	1.7m(roof of car)
26	Location26	53.5706167°N	0.8293167°E	1.7m(roof of car)
27	Location27	53.5911167°N	0.9664167°E	1.7m(roof of car)
28	Location28	53.6721°N	0.9645167°E	1.7m(roof of car)
29	Location29	53.7355167°N	0.8641°E	1.7m(roof of car)
30	Location30	53.7706167°N	0.6928333°E	1.7m(roof of car)
31	Location31	53.73075°N	0.55015°E	1.7m(roof of car)

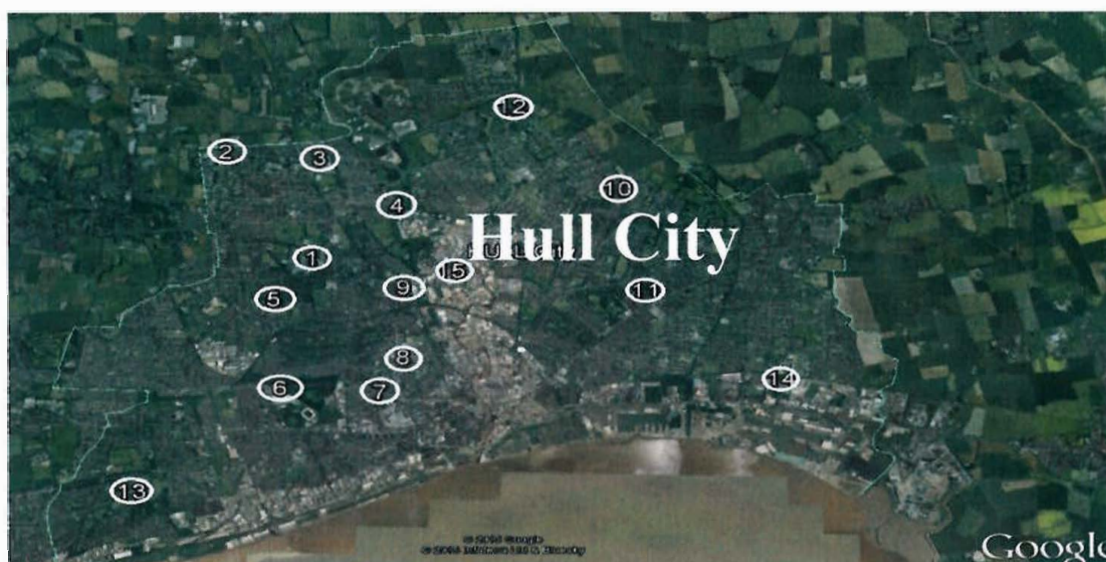


Figure 5-3: Measurement Locations in Urban Environment (Hull city).



Figure 5-4: Measurement Locations in Suburban/ Rural Environment (Humber region).

5.2.5 Data Acquisition

The objective of this part is to establish a real-time system between PC and spectrum analyser by using general purpose interface bus (GPIB). The spectrum analyser converted the received signal into power versus frequency traces using an internal mixer, sampler, and a computational Fast-Fourier Transform (FFT) engine. The traces collected from the spectrum analyser were transferred to a computer. Matlab program provides an environment, which is needed for creating a virtual instrument (VI). The VI can then write and read data to or from the spectrum analyser. The datasets are analysed in Matlab and the final result is displayed through the

monitor. The created VI in this study has the complete functions of the spectrum analyser. The recorder function has been developed to create an automated process for test and measurement. All data is saved in a database as a collection of objects, with each object containing one sweep from the spectrum analyser. This format retains all the data produced by the spectrum analyser in its raw form, thus allowing for later post-processing. This data was later processed using Matlab functions to estimate the occupancy statistics and to produce time-frequency occupancy plots.

5.3 Measurement Setup

The main configuration parameters for the spectrum analyser are listed in Table 5.3. The measurement frequency range was divided into several blocks according to the local spectrum allocations and taking into account the transmitter signal bandwidth for each band. For example, GSM/DCS bands were measured with frequency spans of 45 MHz, which results in a frequency bin of $45 \text{ MHz} / (401 - 1) = 122.5 \text{ kHz}$ (i.e., narrower than the 200 kHz RF bandwidth of GSM/DCS signal). Taking the result obtained in Chapter 4, a 10 kHz RBW was carefully chosen as an adequate trade-off between decision capabilities and required measurement periods. Each block was measured over a 10 min to 24 hour interval or several days, depending on the measurement locations. At the high point fixed location (University Campus) since the circumstance allowed untended option, a 24 hour measurement period was selected. In difficult locations, where the presence of an operator is required as well as an AC- power supply, measurement periods of hours were infeasible and were therefore shortened to 10-15 minutes. Furthermore, sweep time is automatically adjusted, and the reference level was adjusted in accordance with the maximum power observed in each frequency range.

Table 5.3: Spectrum Analyser Configuration.

Parameter	Value	
Frequency	Frequency Range	From (180 - 2700 MHz) Block1 180 : 400MHz Block2 470 : 850MHz Block3 880 :915MHz Block4 915 : 960MHz Block5 1710 :1800MHz Block6 1800 :1870MHz Block7 1900 :2500MHz Block8 2500 : 2700MHz
	Frequency blocks	Variable (45- 400)
	Frequency bins	122.5.8 - 1250 kHz)
	Resolution Bandwidth (RBW)	10 kHz
Time	Video Bandwidth (VBW)	10 kHz
	Measured period	1-24 hours or days
Amplitude	Sweep time	Auto (Selected by the SA)
	Reference level	-20 to -40dBm
	Scale	10 dB/division
	Input attenuation	0 dB

5.4 Data Processing

This section describes the steps taken to produce the spectrum occupancy graphs and values as shown in Figure 5.5. The numerical computational package Matlab was used for all processing after the signal capture. The whole process consists of four steps: raw data input, adaptive threshold setting, calculating the duty cycle of each channel and calculating the average duty cycle of the spectrum band.

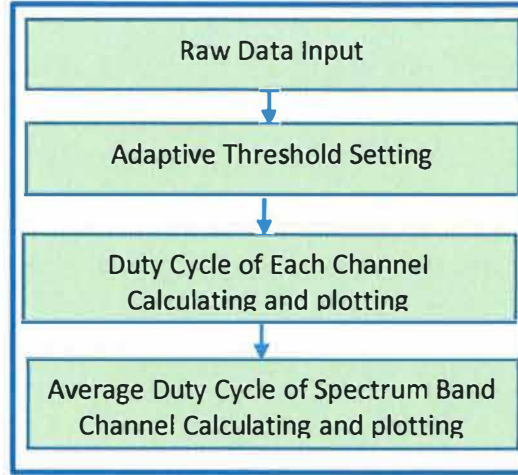


Figure 5-5: Data Processing Procedure.

The values of data are the received power level values in dBm at the antenna output without any processing. We read the raw data from the measurement files into a M by N matrix, each with elements values of which is denoted by P_{f_m, t_n} as

$$\begin{bmatrix} P_{f_1, t_1} & \cdots & P_{f_1, t_N} \\ \vdots & \ddots & \vdots \\ P_{f_M, t_1} & \cdots & P_{f_M, t_N} \end{bmatrix};$$

The subscripts of the powers are put into a two-dimensional array $[f_m][t_n]$. The rows subscript of the matrix f_m denotes frequencies or channels we measure. And the columns subscript of the matrix t_n records the time when channel m is swept for the n-th time. The dimensions of the matrix structure shown were computed based on the information stored in textual meta data file, enabling the data to be read into the computational environment or analysis toolkit. As each channel has a different power noise level, a threshold will be set for each band respectively. When the receive power is higher than this threshold a channel will be considered to be occupied and unavailable for use by a CR system. Given a time-series of channel power measurements, the duty cycle can be calculated using:

$$Duty\ Cycle(DC) = \frac{Signal\ Occupancy\ Period}{Total\ Measurement\ Duration} \times 100\% =$$

$$\frac{n_s t}{T} = \frac{n_s t}{Nt} = \frac{n_s}{N},$$

Where t denotes the interval of time (also known as slot) during which a frequency bin is monitored during a frequency sweep, T is total measurement duration, n_s is the number of slots in which a channel was deemed to be occupied, and N denotes the total number of frequency bins in the sweep. The band spectrum occupancy is defined to be the average duty cycle of the channels within a band. The amount of spectrum occupied is then the product of the band spectrum occupancy and the bandwidth. From a set of measurement data, assuming the energy detection model and measurements of power spectral density or received signal strength (RSS), we can determine the empirical duty cycle as follows. If an RSS sample at time t_i and frequency point f_i is denoted with $RSS(f_i, t_i)$, the DC for each frequency point f_i will simply be the empirical average. Mathematically, this can be expressed as following [80].

$$\psi_{f_i} = \frac{\sum_{t=1}^{N_i} \Omega(t_i, f_i)}{N_i}$$

Where the binary labels $\Omega(t_i, f_i)$ represent the spectrum occupancy at time t_i and frequency point f_i . The parameter γ is the threshold used.

$$\Omega(t_i, f_i) = \begin{cases} 0, & \text{if } RSS(t_i, f_i) < \gamma \\ 1, & \text{if } RSS(t_i, f_i) > \gamma \end{cases}$$

5.5 Analysis of Spectrum Occupancy

5.5.1 General View of Spectrum Occupancy

Before moving to our band by band spectrum occupancy analysis, in Figure 5.6, we show the received power versus frequency plot for the whole frequency range of the measurement study (180 MHz to 2700 MHz). Based on this first impression and following the local spectrum allocations, the entire frequency range can then be divided into smaller blocks/spans. The frequencies below 900 MHz are primarily allocated for broadcast communication. Because of the nature of the high power broadcast channels, the communication channels were easily detected by the equipment. It is interesting to note that the band below 1 GHz appears to some extent occupied, despite the fact that the band above 1 GHz appears to be unused. While the band below 1 GHz may be fully occupied, we know that many of these legacy broadcast systems are not the most efficient users of spectrum (television and radio can benefit from modern digital compression) and many include carrier waves which convey no information but are necessary for simple envelope detection. In the low portion of the band the high occupancy

recorded may not correlate to efficient utilisation. On the other hand, the low occupancy recorded above 1 GHz may not necessarily mean that the spectrum is unutilised. Although it indicates that overall spectrum utilisation in the whole frequency range of our study might be very low, it does not give us a detailed picture of how spectrum is utilised in different bands allocated to different services. Therefore, for a better view of the band by band occupancy pattern, we will consider selected bands in more detail.

The percentage time occupancy for every channel for each hour of the day was measured over full day period (start measurement at 29 October 2012 18:00PM and stop measurement at 30 October 2012 18:00PM). The mean and standard deviation of the hourly occupancy is studied in order to establish which channels' occupancy remain constant over each of the 24 hours in a day, and which have a more unpredictable occupancy (characterised by a higher standard deviation from the mean).

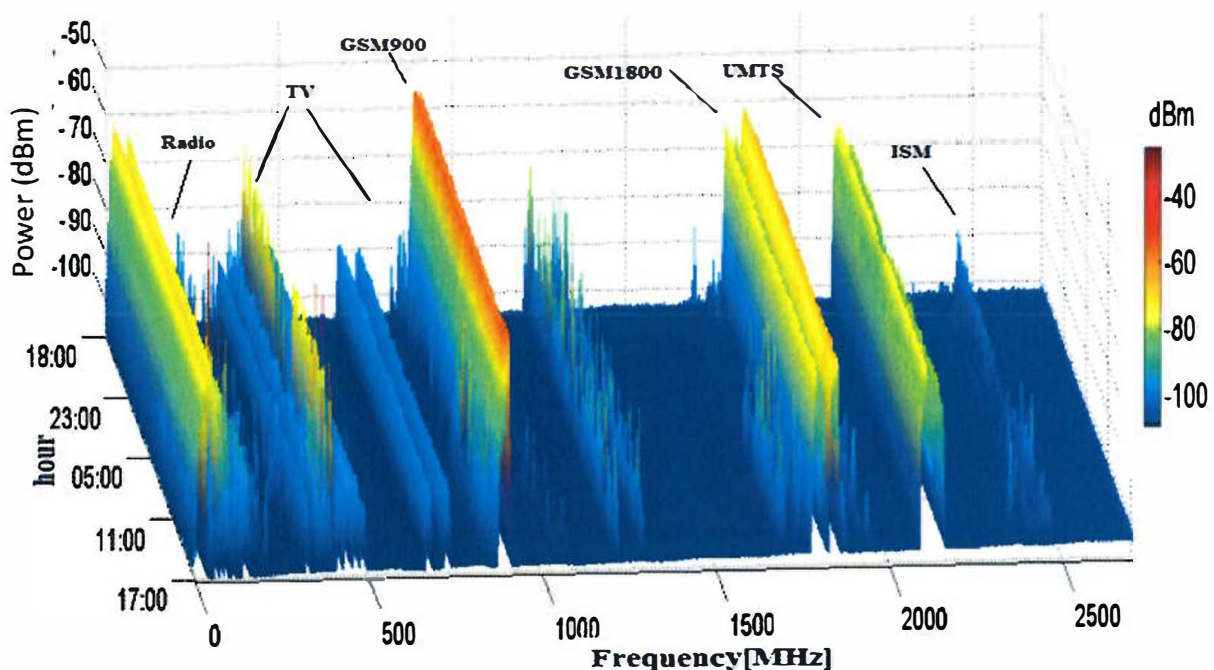


Figure 5-6: Received Power versus the Frequency Band (80 MHz-2700 MHz) for 24Hours Start Time 10/29/2012 18:00pm & Stop Time 10/30/2012 18:00pm.

5.5.2 Occupancy Metrics

Spectrum utilisation is characterised and quantified in the next section by means of three occupancy metrics, which are shown in the Figures presented in the following sections. The first graph in each Figure shows minimum, maximum and average values for each measured frequency. When considered together, minimum, maximum and average PSD provide a simple characterisation of the temporal behaviour of a channel. For example, if the three PSD values are quite similar, it suggests a single transmitter that is always on, experiences a low level of

fading and is probably not moving. At the other extreme, a large difference among minimum, maximum and average suggests a more intermittent use of the spectrum or a severely fading signal. The second occupancy metric, shown in the middle graph of each Figure, represents the instantaneous evolution of the temporal spectrum occupancy over the whole measurement period. Colour dots represent samples of busy channels, while the blue colour indicates the absence of licensed signals. The busy/idle state of each measured frequency is determined following an energy detection principle. The third considered occupancy metric (occupancy level), which is shown in the lower graph of each Figure. This metric, represents the fraction of time that a certain channel or frequency range is observed as busy over a specified period of time, thus providing a more precise quantification of spectrum occupancy. For instance, in the figures below (5.7-5.9), a duty cycle of 0% (DC=0) was obtained in almost band of Figures 5.6 & 5.7. This result signifies that the band is almost unoccupied. This is an indication of the low penetration of devices that operate in this band that has little or no wireless network infrastructures. However, in the Figure 5.9 the results show high occupancy level, a duty cycle of 100%, (DC=1) was obtained in almost band of Figure 5.9(GSM Downlink). This result signifies that the band is almost occupied (continuously broadcasts).

5.5.3 Urban Area High Point (Location 1)

The obtained measurement results which are shown in Figures 5.7, 5.8, 5.9, 5.10 and 5.11 at this location using Bilog antenna. As can be seen, the spectrum experiences a relatively moderate use below 1 GHz and a low usage between 1 and 2 GHz, whilst remaining mostly underutilised between 2 and 2.5 GHz. For example, Figure 5.7 shows the frequency band 180-400MHz. These bands are populated by a wide variety of narrowband systems, including Private/Professional and Public Access Mobile Radio (PMR/PAMR) systems, FM audio broadcasting, aeronautical radio navigation and communication systems, maritime systems such as the Global Maritime Distress and Safety System (GMDSS), paging systems and fixed links, audio applications such as wireless microphones, Digital Audio Broadcasting (DAB) systems and satellite systems. Although these bands exhibit an average duty cycle of 6.9%, there is no significant amount of white space due to the narrowband nature of the systems operating on them or due to weak signal reception of the signal broadcasting. Several TV broadcasting station can be noticed in Figure 5.8 between frequency bands 470-720MHz. The power level of some of these stations is higher than others, as the broadcasting station is located closer to our building where the measurement was performed. The amount of occupancy is quite low which might be due to that the Ofcom have already performed the introduction of

DVBT in UK. Corresponding signals can be noticed in Figure 5.8 on 582 MHz (channel 22), 514MHz (channel 26), 530 MHz (channel 28) and 56MHz (channel 30). In the frequency band 720 to 850 MHz only two channels were detected during measurement, broadcast station (730 MHz, channel 53) and broadcast station (785MHz, channel 60). Over all, the average duty cycle of this band is 13%.

Additionally, two interesting cases are observed above and below 1GHz. Below 1 GHz is observed in the frequency bands allocated to GSM, the Extended GSM (E-GSM) 900 system operates in the 880–910 MHz (uplink) and 915–960 MHz (downlink) bands as shown in Figure 5.9. Above 1 GHz the highest spectrum usage is observed for the bands allocated the DCS 1800 system operating on 1710–1785 MHz and 1805–1880 MHz (Figure 5.10). These two bands have average occupancy of 32.19% and 24.64 % respectively. Note that, the occupancy between the uplink and downlink sides are not identical. This result can be explained as follows. The control channels for GSM900, GSM1800 and WCDMA are constantly being broadcasted by the base stations on the Downlink (DL), thus the DL for these frequencies seems fully occupied as they are always transmitting with relatively high power. The uplink, on the other hand, for cellular system is based on active user communication through the network. If there is no active communication, there are still some periodic short-pulse transmissions on the uplink for location updating procedures which are too short to be picked up by analyser. Also note that GSM900 mobile stations have a higher transmit power than GSM1800, which explains the higher average duty cycle picked up by spectrum analyser. From Figure 5.10, it is observed that 3G uplink is totally unoccupied. The reason behind this outcome is the WCDMA is a spread spectrum system where the signal is modulated over larger bandwidth to give very low output transmission power, which might not be detectable with analyser and thus does not show any occupancy on the 3G uplink.

Furthermore, looking at Figure 5.11, it appears that most of the band from 1900 to 2500 MHz is almost unoccupied except UMTS system and ISM band. The average duty cycle of this band is 9.47%. The occupancy estimates of these bands might not be the representative of the actual occupancy. These results could be explained as follows: Wireless Broadband Alliance (WBA) signals might not be detected at measurement point if the access points are close enough, satellite signal power might be much lower than the ambient noise when it reaches the ground, and the short wavelength of ISM band signals cannot penetrate through walls. Additionally, the frequency band (2400-2483 MHz) was used by well-known unlicensed industrial, scientific and medical (ISM). Devices in this band include microwave ovens, cordless phones, wireless

networking and wireless instrumentation devices. The spectrum plot indicates that the band is used, but the occupancy (duty-cycle) is low. That may be due to the location of the receiver 30 m above the ground. Also there may have been low activity in the time period under study. The frequency band of 2500 to 2700 MHz appears completely unused at this point. The occupancy estimates of these bands might not be representative of actual occupancy due to issues such as weak signals and penetration. Finally, it is worth noting as well that some spectrum bands appear as idle when judged by their average duty cycle. Nevertheless, the maximum PSD reveals that some primary users, although difficult to detect, are present in such bands. Some examples are the uplink bands for mobile communications, radio navigation and the ISM band.

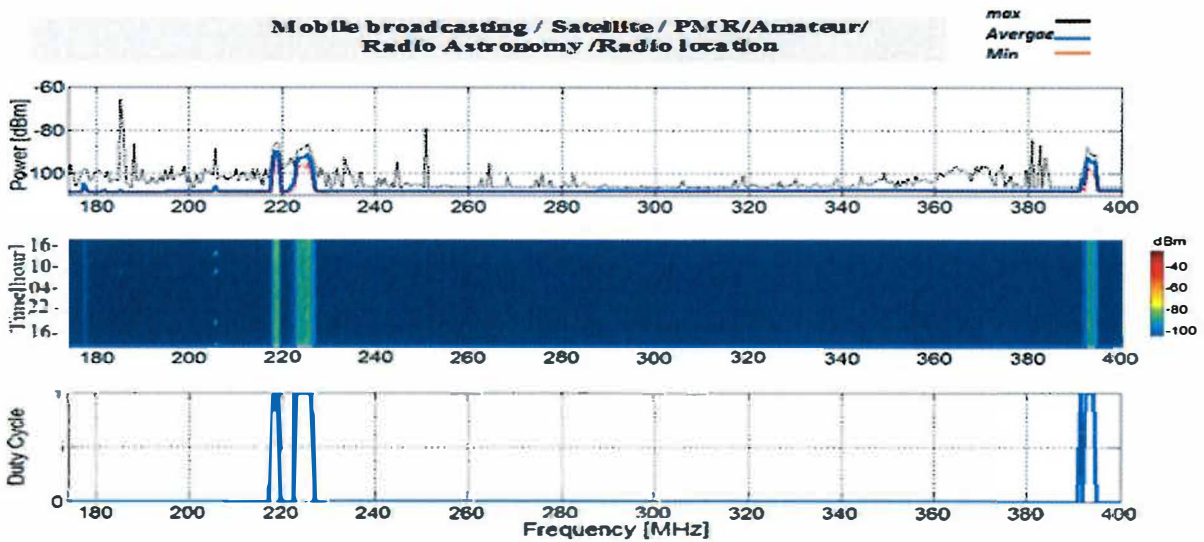


Figure 5-7: Occupancy Measurement from 180 MHz to 400 MHz.

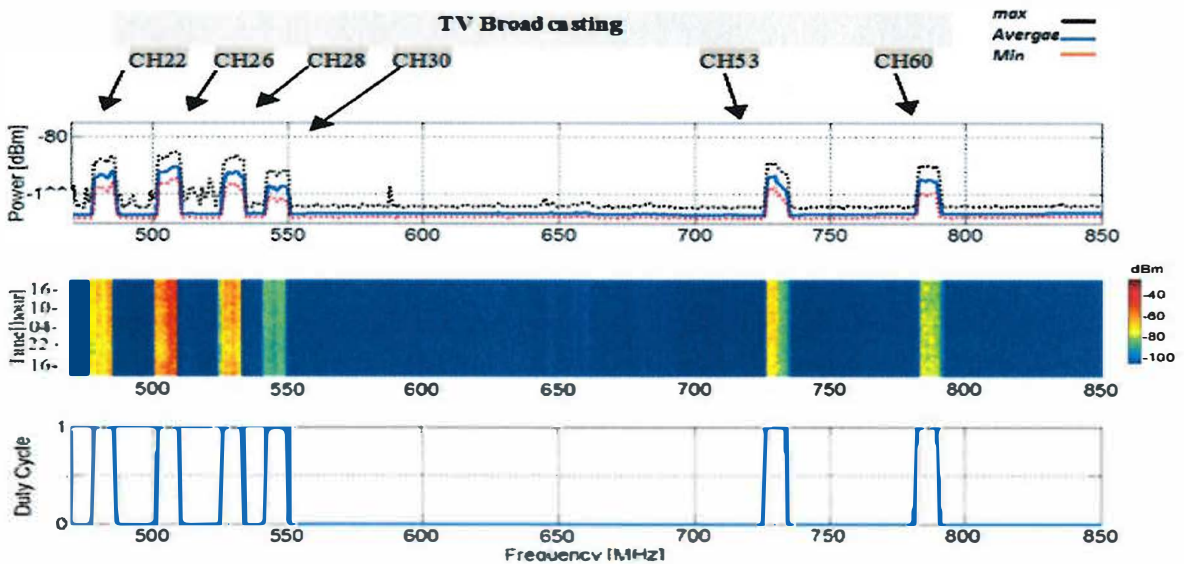


Figure 5-8: Occupancy Measurement from 470 MHz to 850 MHz.

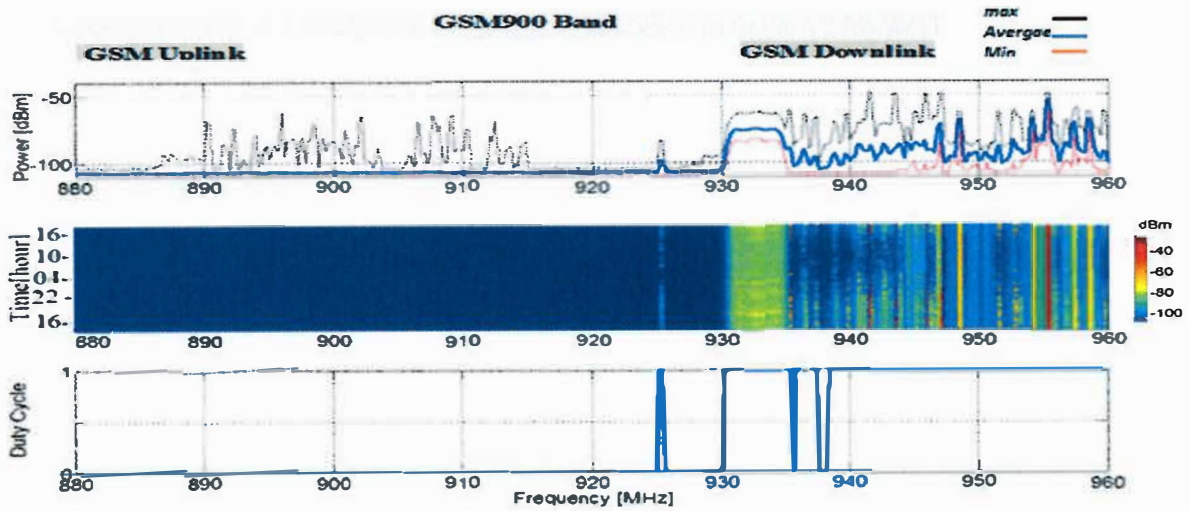


Figure 5-9: Occupancy Measurement from 880 MHz to 960MHz.

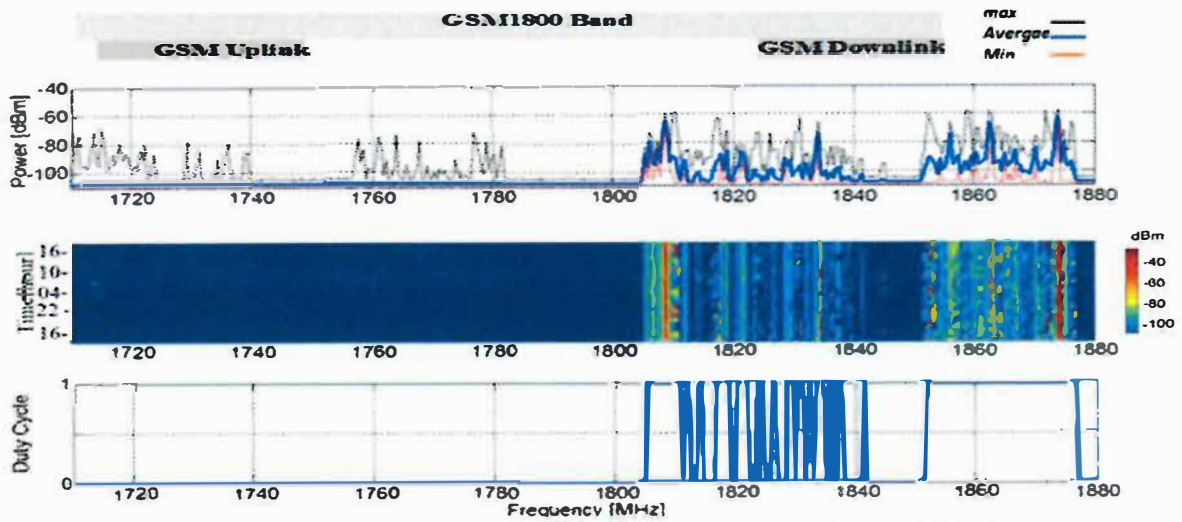


Figure 5-10: Occupancy Measurement from 1710 MHz to 1880MHz.

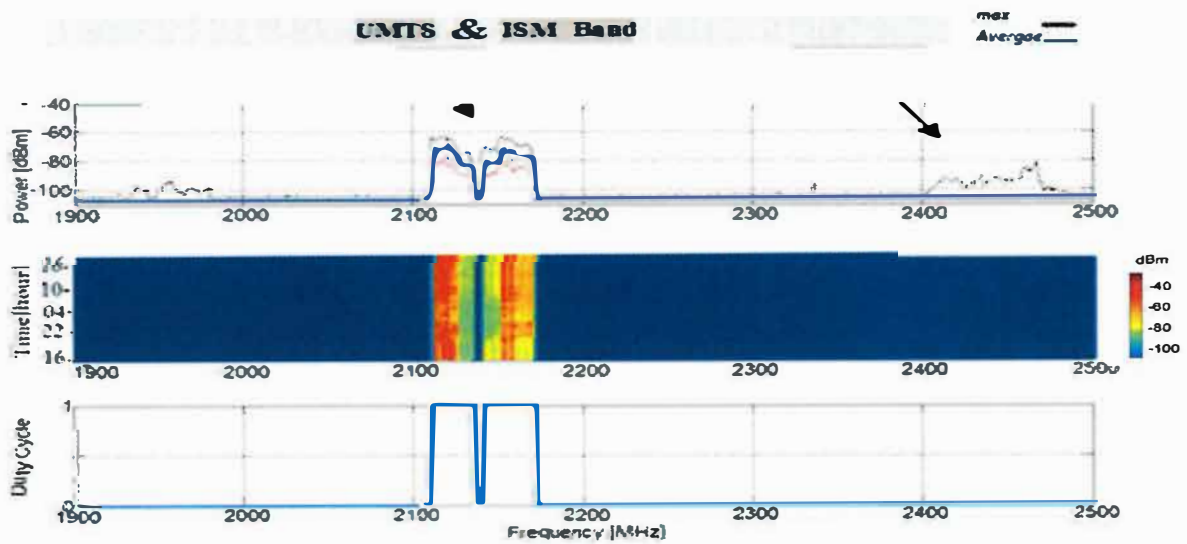


Figure 5-11: Occupancy Measurement from 1900MHz to 2500MHz

5.5.3.1 Result and Main Observations

In this section, we summarise the major observations from the occupancy results of this study and identify the channels for long term studies in order to provide the policy makers with the necessary information for taking proper initiative to facilitate dynamic spectrum access technologies such as cognitive radio. Graphical presentations of the band by band average spectrum occupancy as well as the average spectrum occupancy for the whole band of study are shown in Table 5.4 and Figure 5.12. The average occupancy plot for the whole 180 MHz to 2700 MHz band is determined as follows. First we determine the average spectrum usage (in MHz) of each band as shown in Table 5.4 by multiplying the average occupancy of each band by its corresponding bandwidth. For example, average spectrum usage of 470 MHz to 850 MHz band is $0.1346 \times (850-470) = 51.1$ MHz. Then, summing the spectrum usage of all bands and dividing it by the total available bandwidth $2700-80=2620$, we get the average spectrum occupancy of 11.0% for the whole frequency bands of study.

Table 5.4: Average Duty Cycle Statistics.

Frequency range (MHz)	Average duty Cycle (Measured occupancy %) TH 5dB above noise floor		
108-180	61.1%	12.4%	11.0%
180-400	6.9 %		
470-850	13.4%		
880-960	32.1%	9.9%	
1710-1880	24.6%		
1900-2500	9.4%		
2500-2700	0%		

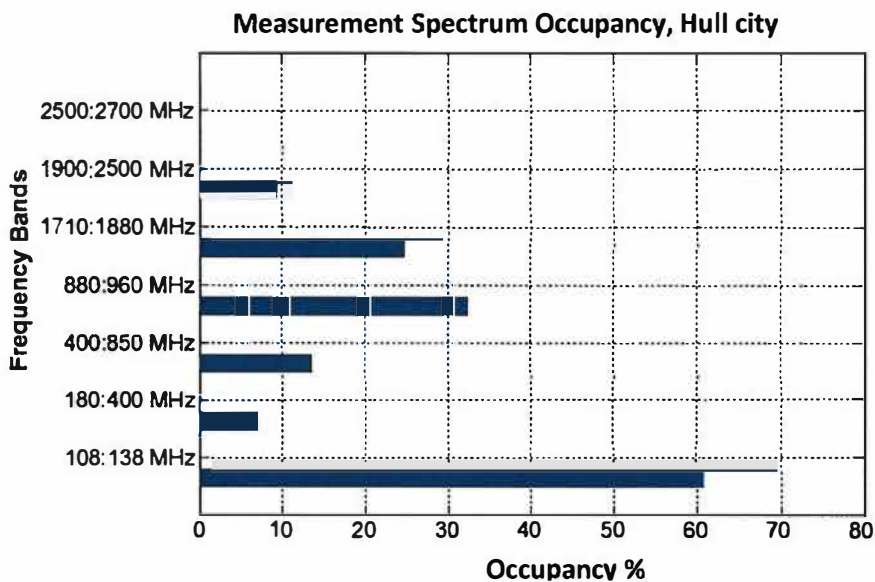


Figure 5-12:Band By Band Average Duty Cycle Statistics.

Now using Table 5.4 result, the following useful information can be extracted:

- ❖ Highest occupancy has been observed in the bands of GSM900 and GSM1800 due to broadcasting downlink.
- ❖ Low occupancy has been observed in the bands allocated for fixed/mobile services, and primary and secondary radar. But the lack of radar band occupancy might be due to the pulse rate of radar pulses not being captured by spectrum analyser sweep (if sweep is out of synchronisation with radar pulse it will never be seen).
- ❖ The bands allocated for aeronautical radio navigation, fixed satellite, WBA and ISM appear to have low utilisation. Also, TV bands provide interesting opportunities for secondary usage.
- ❖ Frequencies above 1GHz are relatively underutilised except for the cellular bands. Although some frequencies in some bands are appeared to be used, the duty cycle is quite low.

5.5.4 Urban, Suburban and Rural (Using Vehicle)

5.5.4.1 Urban Area Ground Points

This section focused on studies of white spaces in the UHF television broadcasting frequencies from 470MHz to 862MHz, since the results shown in section 5.5.3 indicate that TV spectrum remains mostly unused. The experimental campaign was performed at the multiple locations. Figure 5.2 shows photographs of the experimental setup. The vehicle used for the experiments was author's private Vauxhall Astra car. The instrument is controlled by a laptop connected via an Ethernet interface. The results obtained at urban area high point (Location 1) used a TV omnidirectional antenna instead of the directional Bilog antenna. An omnidirectional TV antenna with 3.5dBi gain is used to capture signals from all the directions. The measurement was conducted during a weekend to measure the spectrum occupancy around the Humber region, UK. Coverage goals were achieved for rural, suburban and urban areas of Humber region. During this time the trial vehicle covered a total of nearly 500km. These measurements were challenging and complex from both a technical and a logistical point of view. Sophisticated spectrum measurement equipment (spectrum analyser) and TV antenna were mounted on the vehicle to perform a preliminary spectrum utilisation survey. Table 5.5 gives an indication of the extent of the measurements undertaken.

The aim of this experiment is to measure TV bands and determine the impact of considering different outdoor locations at ground level on the spectral activity perceived by a secondary user with respect to that observed in an outdoor highpoint.

Table 5.5: Top Level Measurement Statistic.

Parameters	
Total distance covered by vehicles during measurement	nearly 500km
Number of individual spectrum measurement	15 locations urban and suburban 16 locations suburban/ rural
Total size of database created	832 Mbytes

Each location was measured at a different time instant. So, the random component introduced by the presence of different transmissions at different time instants could be averaged by considering a sufficiently long enough measurement period. However, since supply power converter from 12 Volts battery power to 230 Volts AC to operate the spectrum analysis platform (spectrum analyser and preamplifier) was required in these measurements, periods of 24 hours as in location 1 was infeasible and was therefore shortened to 10-15 minutes in locations (LOC2–LOC15). To reduce the impact of random components and make the results of locations 1 and 2-15 comparable, the average duty cycle obtained in locations 2-15 has been normalised by the average duty cycle in location 1 obtained when considering the samples corresponding to the same time interval. Therefore, if an average duty cycle DC_k is obtained for location k ($k = 2, 3, \dots, 15$) based on the samples captured during a 10 minute interval between time instants T_{start} and T_{stop} the samples captured at location 1 between the same T_{start} and T_{stop} values are used to compute an average duty cycle DC_1 . The normalised average duty cycle [80] for location k is then obtained as

$$\overline{DC_k} = DC_k/DC_1.$$

This procedure reduces the randomness of the obtained results and enables a fairer comparison between the outdoor high point and the rest of outdoor positions. As result, altogether bands and locations measured in this test obtained normalised average DC lower than unity, meaning that the average DC observed at the ground level is in general lower than at high points. This is a consequence of the radio propagation blocking caused by buildings and other obstacles: under non-line-of-sight conditions, the direct path is often lost; only multipath propagation components attenuated are received, thus resulting in lower received signal levels and therefore in lower average DCs. From a practical point of view, this indicates that a secondary user at the ground level would perceive a higher amount of spectrum opportunities. Nevertheless, it is worth highlighting that this observation should be interpreted carefully, taking into account the specific circumstances of each band. In the following, some particular bands of interest are

discussed. Figure 5.13 show the average duty cycle statistics in locations 1 to 15 for TV band (470-862MHz).

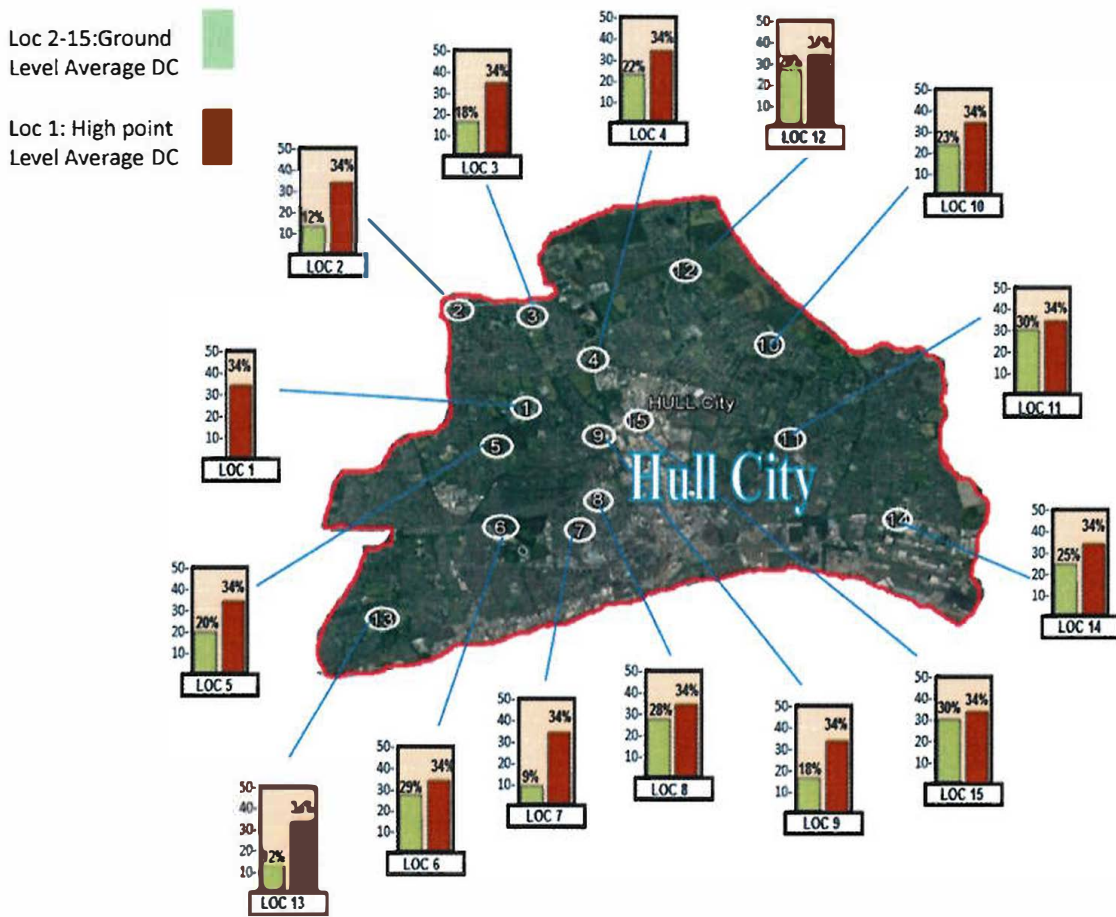


Figure 5-13: Average Duty Cycle Statistics in Locations 2-15 for TV Band Compared to Location 1.

Figure 5.14 shows the spatial distribution of the normalised average DC for the TV bands. In the TV band, it can be clearly appreciated that the normalised average DC is lower in closed regions: in locations 2, 7 and 13, where radio propagation blocking caused by buildings is more intense such as between house and narrow streets, its value is lower than in other less closed regions such as locations 6, 8, 11 and 12 where the measurement were taken in open fields. Comparing locations 6, 7 and 8, location 7 exhibits the lowest normalised average DC in the case of TV, as expected due to propagation blocking. For instance, the normalised average values of 0.8% and 0.75% respectively were measured in locations 6 & 8, which are about a ratio of 4:1 when compared to the normalised average values of 0.2% obtained in locations 7. The result is not far-fetched because the locations described as location 6 and location 8 are open field areas, while location 7 is a residential area with narrow street.

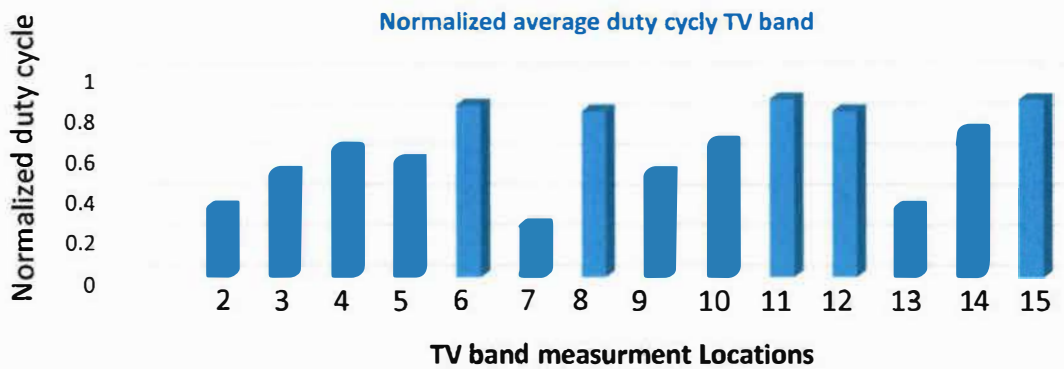


Figure 5-14: Normalised Average DC Statistics in Locations 2-15 for TV Bands (470-860 MHz).

5.5.4.2 Rural, Suburban Locations

This section presents the results obtained in suburban and rural locations based on measurements performed outdoors using a private Vauxhall Astra vehicle (the same platform used for urban location measurement). In this study, two identical measurement suites were deployed in suburban and rural locations, Humber region, UK. Each measurement involved multiple location measurements. Moreover, spectrum occupancy in this section is examined in the TV band as well, since the results shown in section 5.5.4 indicate that TV spectrum remains mostly unused. Normalised average duty cycle is no longer used in this section as there are several locations where spectrum occupancy is greater than at the urban high point (location 1) due to some measurement locations receiving from more than one transmitter broadcasting. The obtained results of average duty cycle per location are shown in Figure 5.15.

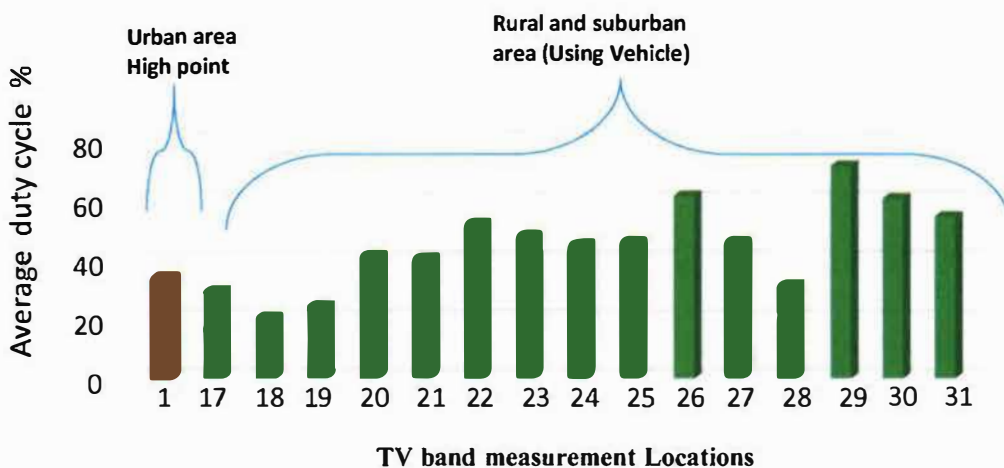


Figure 5-15: Average DC Statistics in Locations 17 To 31 for TV Bands: TV (470-862 MHz).

As can be seen, the overall spectrum occupancy is appreciably higher in the rural/suburban environment of the Humber region (average DC of 42.2%) than in the urban environment of Hull (average DC of 22.1%). In particular bands such as those allocated to broadcast services, e.g. TV (470–862 MHz) and DAB-T (195–223), where spectrum usage does not depend on the number of users of the service, the results should be similar in both environments. However, it is worth noting that some of the TV channels were observed in the same state (busy or idle) in some locations, which can be explained by the fact that the distance between them is shorter than the coverage areas usually intended for TV transmitters and, as a result, some locations observe the same transmitters (Belmont transmitter). An exception was noticed in some measuring locations (channels), which may be due to another strong signal TV station (Emely Moor Transmitter). This clarifies why the average DC between suburban and rural measurements was unequal. In summary, the results obtained in this study indicate that spectrum usage is generally lower in sparsely populated areas. This indicates the existence of more spectrum opportunities for DSA/CR systems in these environments, which is in accordance with the conclusions of previous spectrum measurement campaigns (section 5.5.3).

5.6 Chapter Summary

The first part of the work discussed in this Chapter, covers a set of long and short term observations of spectrum occupancy in the Humber region. The main aims of the work have been to discover which bands might be suitable for cognitive radio. Thus, powerful methods for the detection and exploitation of spectrum holes, based on observation of the radio's environment are essential for an efficient use of the wireless resource. The results obtained during the measurement campaign conducted in an urban environment (Urban High Points) demonstrated a significant amount of unused spectrum in these bands especially in the TV band region, as well between 1 GHz and 2 GHz except GSM1800 band. The unused spectrum could be potentially made available to future development of cognitive radio. Generally, the mean occupancy ratio over the whole band was as low as 11.0 %. The second part of work, section 5.5.4, presents and compares the results obtained in sub-urban and rural environments. As opposed to sections 5.5.3 where the spectrum occupancy in fixed location was evaluated at different time instants, the measurements reported in section 5.5.4, were performed at various locations. Moreover, spectrum occupancy in this section is examined in the TV band. The obtained results indicate that in some bands such as those allocated to broadcast services, e.g. TV (470–862 MHz), where spectrum usage does not depend on the number of users of the service, the results are more similar in both environments. An exception was noticed in some

measuring locations (channels), where average duty cycle was higher. This may be due to the spectrum analyser receiving signals from more than one TV station at the same location. Overall, our measurements showed that the spectrum occupancy highly depends on the sensing location. Variability between sensing locations is to be expected but clearly confirmed by 31 measurement locations. However, to determine more objective spectrum utilisation, additional and more sophisticated methods will have to be employed and various locations will have to be analysed. Although the results collected were exclusively in the Humber region environment, UK, future work should involve further measurement campaigns in different cities (suburban and rural environments) in order to obtain a complete picture of the perspectives for future cognitive radio application.

Part III: Spectrum Sensing and Analysis Using High Time Resolution (USRP2)

*Opportunities? They are all around us. . .
There is power lying latent everywhere
waiting for the observant eye to discover it.*

Orison Swett Marden

This part contains two chapters

CHAPTER 6: Spectrum Sensing Technology

CHAPTER 7: Cyclostationary Feature Detection

Chapter

6 **Spectrum Sensing Technology****6.1 Introduction**

Although spectrum licensing offers an effective way to guarantee adequate quality of service for license holders, nevertheless, exclusivity also leads to inefficient use of the spectrum. The FCC reported in [102] that “while some bands are heavily used many other bands are not in use or used only part of the time”. Indeed, in spite of the nominal absence of available spectrum, measurements of the radio frequency occupancy in previous Chapter (Figure 5.6) indicate that large portions of the frequency bands between 80 MHz-2700 MHz are not used for significant periods of time and locations. Cognitive radio technologies have been proposed for lower priority secondary user systems aiming at improving the spectral efficiency by sensing the environment and then filling the discovered gaps of unused licensed spectrum with their own transmissions [103]. The spectrum sensing is a crucial task and is by far the most important component for the establishment of cognitive radio. It is considered as the first step towards adaptive transmission in unused spectral bands without causing interference to primary users.

The goal of this Chapter is to point out several aspects of spectrum sensing. We start by introducing the concept of passive awareness and active awareness in section 6.2. Additional details associated with active awareness are explained in section 6.3. Primary transmitter detection (non-cooperative sensing) methods are studied in 6.4. Comparison of various spectrum sensing methods are illustrated in 6.5. The cooperative sensing and two stage adaptive sensing techniques are introduced in section 6.6 and our conclusions are presented in section 6.7.

6.2 Passive Awareness and Active Awareness

There are a number of ways in which cognitive radio system are able to perform spectrum sensing. These ways fall into one of two categories, active awareness and passive awareness. The classification of active and passive awareness presented in this Chapter are taken from a book about cognitive and cooperative networks [104]. Spectrum awareness is the task of obtaining awareness about spectrum usage and existence of primary users in a geographical area. This awareness can be classified into two forms: (1) an opportunistic one, where the secondary system recognises the spectrum use pattern individually by cooperative or by a non-cooperative sensing and (2) the sharing information approach where the spectrum knowledge is distributed through beacons or using a control channel or by sharing databases of existing users. CR systems may employ either or both forms of awareness, thus the discussed approaches should not be viewed as mutually exclusive. Both active and passive awareness methods are considered in the following subsections. Figure 6.1 presents the classification of spectrum sensing awareness.

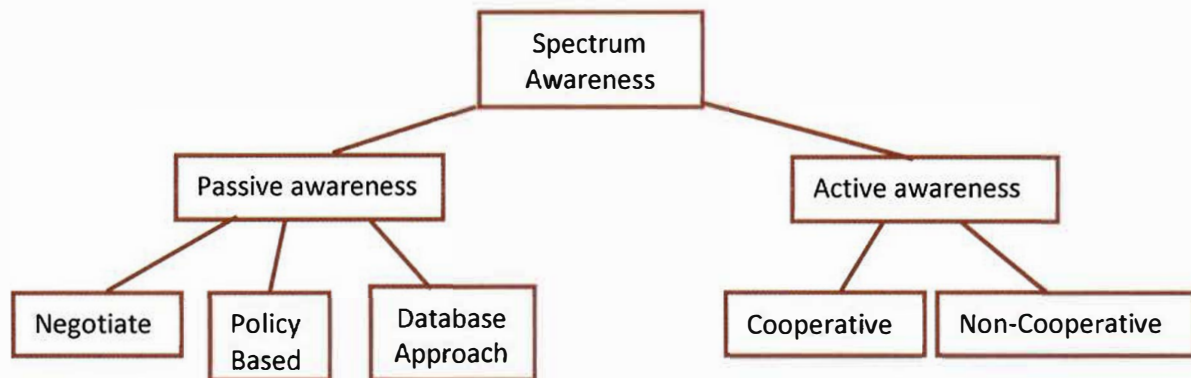


Figure 6-1: Spectrum Awareness.

6.2.1 Passive Awareness

In passive awareness, the spectrum use pattern is received from outside of one's own secondary communication system. Secondary Users (SUs) can obtain spectrum resources by negotiating with primary Users (PUs) [104], from Geolocation databases [105] or from a policy-based approach [107].

In systems based on negotiated spectrum use the primary system explicitly announces to secondary users information about the allocated frequencies and the available spectrum opportunities. For example, the base station of an existing (primary) communication system, such as television, broadcasts beacons that advertise the availability of licensed spectrum for secondary usage. This solution has a very high

infrastructural cost and requires some modifications of the current licensed systems. However, some CR networks implementations foresee the adoption of a Cognitive Pilot Channel (CPC) to support cognitive operations such as spectrum allocation [106]. This dedicated channel could also be adopted to convey sensing information towards the SU nodes.

In the policy-based approach, the radio regulation authority identifies a licensed band of the radio spectrum where use is low or the band is used with a deterministic pattern [107,108]. This band is then made available for secondary use. The authority assigns a set of policies that provide rules and constraints describing how this available band should be used.

In systems based on a data base, a primary system or the radio regulation authority can maintain a table or database of frequency resources in its server and both primary and secondary users can update this table. The database solution is based on the consultation by the SU network of a database that stores the information on the spectral occupancy in the nodes locations and additional information, such as the maximum permitted effective isotropic radiated power (EIRP) in each band. The advantage of this approach is that it is virtually error free and is not affected by radio channel characteristics. However, it is a quite expensive solution. Indeed the secondary nodes are required to incorporate some localisation technique (e.g. GPS) and an Internet connection in order to access the database information. Moreover, additional costs are related to the design, implementation, maintenance and administration of the database, and to the costs for gathering the PU occupancy information [111].

All these passive approaches are good in the sense that they can ensure interference-free communication for the primary system, since the spectrum use is defined a priori. However, passive awareness increases the amount of control information needed in the system. Furthermore, passive approaches are not compatible with existing licensed systems and need high costs for gathering the information [108].

6.2.2 Active Awareness

Active awareness, is defined by IEEE as “the act of measuring information indicative of spectrum occupancy” [112], it is also known as spectrum sensing. It consists therefore of the implementation of an autonomous process of the SUs that on the basis of the received signals analyse the spectrum. The idea of active awareness is to monitor spectrum by signal detection

methods so that we can identify those frequency bands which other systems are using. The method requires constant monitoring of the channel so that new primary users and possible vacant channels will be detected in near real time. When using spectrum sensing, the hidden terminal problem might cause problems when there is an obstacle between the secondary system and the primary transmitter. In this kind of situation the secondary user might have a good connection to a primary receiver but it cannot necessarily detect the primary transmitter. To overcome this kind of problem, we can use a longer sensing period to increase the measurement accuracy but this reduces the available time for transmission. Another method to overcome the hidden terminal problem is to use cooperative sensing. When a device operates in a cooperative mode, it shares the data, which it has collected from the spectrum environment, with other similar secondary users. Hence, the secondary user can have information about the primary user even though it cannot see it. The rest of this Chapter focuses on active awareness as the method for radio environment analysis. Techniques for active spectrum sensing have received much attention in recent years and so these will be discussed in more detail in following sections. The term spectrum sensing will be used in the remainder of this Chapter to refer to active awareness.

6.3 Spectrum Sensing Techniques

To be capable of sensing very weak signals, cognitive radios must have significantly better sensitivity than conventional radios [113]. Requirements for radio frequency (RF) frontend and analog-to-digital converters (ADC) are very demanding and have only recently become feasible. After reliable reception and sampling of the signal, digital signal processing techniques are utilised to further increase confidence in the data. Most of the recent spectrum sensing work focuses on primary transmitter detection based on local observations by secondary users. In [114], the spectrum has been classified into three types by estimating the incoming RF-stimuli, thus; black spaces, grey spaces and white spaces. Black spaces are occupied by high power local interferer some of the time and unlicensed users should avoid those spaces at those times. Grey spaces are partially occupied by low power interferers but they are still candidates for secondary use. White spaces are free of RF interferers except for ambient noise made up of natural and man-made forms of noise. White spaces are obvious candidates for secondary use. Before looking into the details of spectrum sensing methods, we summarise the typical grouping of spectrum sensing schemes in Figure 6.2 and highlight characteristic features of these sensing approaches.

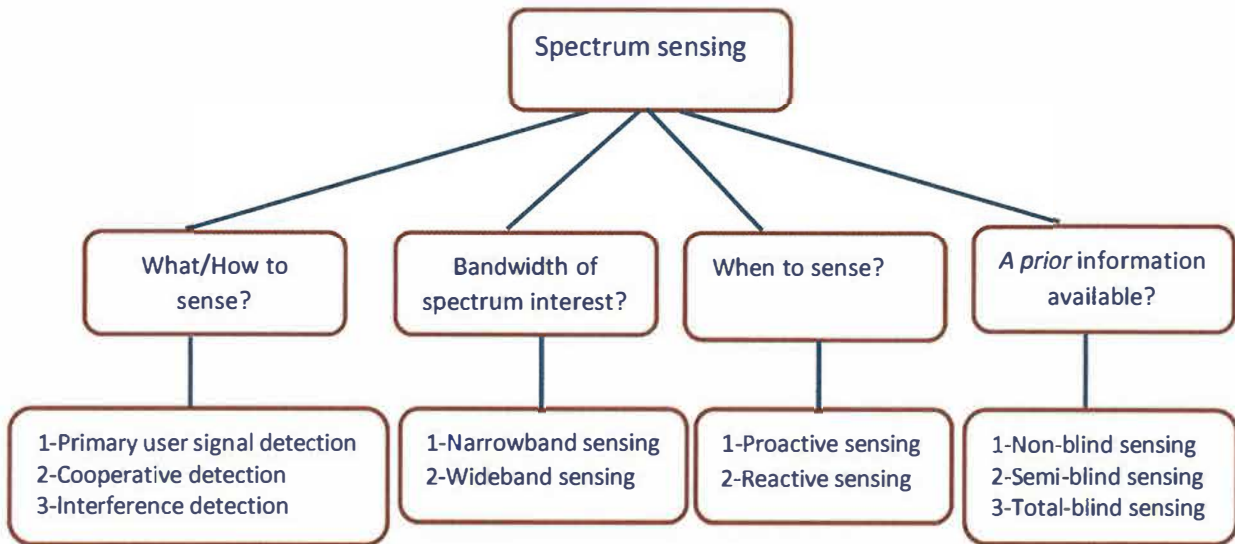


Figure 6-2: Classification of Spectrum Sensing Techniques.

Generally, spectrum sensing techniques can be classified into two main types, primary signal detection and interference detection. In addition, sensing techniques can be used both by cooperative and non-cooperative types of detection. Classification of spectrum sensing techniques presented in this section are partly based on [104,115]. In a non-cooperative primary-user signal detection approach, CR makes a decision about the presence or absence of PU based on its local observations of the spectrum. In comparison, cooperative detection refers to primary-user signal detection based spectrum sensing methods where multiple CRs cooperate in a centralised or decentralised manner to decide about the spectrum hole (in this context a “spectrum hole” is defined as an area of radio spectrum that is available for SU usage). Both of these approaches fall within the category of spectrum overlay wherein SUs only transmit over the licensed spectrum when PUs are not using that band. Conversely, the interference based detection approach, based on spectrum underlay, (wherein SUs are allowed to transmit concurrently with PUs under the stringent interference avoidance constraint) was analysed and declared to be non-implementable [116]. Depending on the application at hand, CR can opt for either narrowband or wideband sensing. Thus, the focus of CR will be on identifying narrow band spectrum holes or free wideband spectrum. To find spectrum opportunities, CR may adopt either a proactive (periodic) or reactive (on demand) sensing strategy. Either of the two approaches may be employed in the absence or presence of cooperation among CRs. A priori information required for PU detection is another important criterion upon which different spectrum sensing methods are classified. In this category, different primary-user signal detection based sensing techniques are categorised as non-blind, semi-blind or total-blind. Non-blind schemes require primary signal signatures as well as noise

power estimation to reliably detect PU. Semi-blind schemes are relaxed in the sense that they need only a noise variance estimate to detect a spectrum hole. However, most practical sensing techniques are generally total blind and semi-blind, requiring no a priori information to determine PU activity. Fundamental to all these classifications is the need to detect the presence or absence of PU signals. In the next sections, we will focus on primary-user signal detection sensing based on both non-cooperative and cooperative approaches.

6.4 Primary Transmitter Detection (Non-Cooperative Sensing)

In recent times, most of the researchers into CR have introduced sensing asserting that sensing algorithms can be classified in several detectors techniques. These techniques, indeed, are the strategies that can be adopted in sensing problems in the presence of single/multi receivers that operate on a single/ multiple frequency band. A variety of sensing methods are proposed in the literature to identify spectrum holes [117]. In general, the detection problem is analysed as a binary hypothesis model, defined as[118]:

$$x(t) = \begin{cases} n(t), & 0 < t \leq T \quad H_0 \\ h s(t) + n(t), & 0 < t \leq T \quad H_1 \end{cases} \quad (6.1)$$

where $x(t)$ is the signal received by CR during observation window T , $n(t)$ represents the additive white Gaussian noise (AWGN), $s(t)$ represents the transmitted signal from a primary user which is to be detected and h is the channel gain, H_0 and H_1 denote the hypothesis of the absence and the presence, respectively, of the PU signal in the frequency band of interest.

This is a classic binary signal detection problem in which the CR has to decide between two hypotheses, H_0 and H_1 . H_0 corresponds to the absence of a primary signal in the scanned frequency band while H_1 indicates that the spectrum is occupied. It is important to point out here that under H_1 , spectrum may be occupied by an incumbent or a secondary user. Hence, a sensing scheme is generally required not only to detect but also to differentiate between the primary and secondary user signals. Conventionally, the performance of a detection algorithm is restricted with its sensitivity and specificity [118] which are measured by the probability of detection P_d and the probability of false alarm P_f , respectively.

P_d is the probability of correctly detecting the PU signal present in the considered frequency band,

P_f is the probability that the detection algorithm falsely decides that PU is present in the scanned frequency band when it actually is absent.

A number of methods have been proposed for identifying any spectrum usage opportunity in the scanned frequency band ranging from very simple energy detection to quite advanced cyclostationary feature extraction and waveform based sensing. Recent work mainly focuses on further sophistication of these basic techniques with an aim to making sensing results more robust and accurate at the same time [119]. The following subsections provide a brief overview of spectrum sensing techniques. This review provides a single unified reference guide to both classical and emerging trends in spectrum sensing for CR.

6.4.1 Energy Detection

The energy detector based approach, also known as radiometry or periodogram, is the most common way of spectrum sensing because of its low computational and implementation complexities [121]. In practice, energy detection (ED) is especially suitable for spectrum sensing when the CR cannot gather sufficient information about the PU signal since it does not require any prior information about the primary signal. It measures the energy in the received waveform over an observation time window [122]. The block diagram of the energy detector is shown in Figure 6.3.

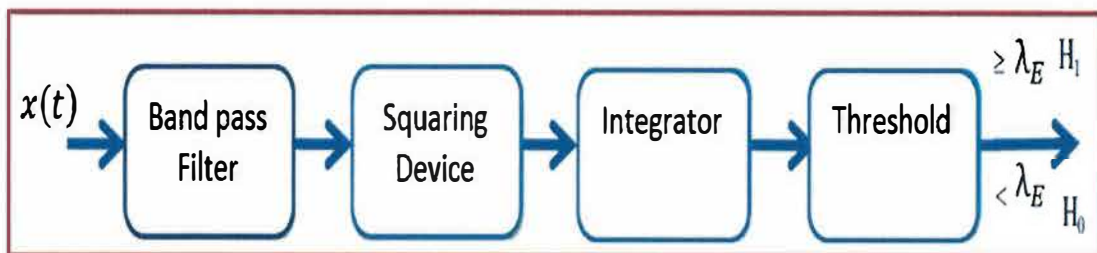


Figure 6-3: Block Diagram of Energy Detection.

First, the observed spectrum signal is pre-filtered with a band pass filter (BPF) of bandwidth W to select the desired frequency band. The filtered signal is then squared and integrated over observation window of length T . This gives an estimated energy content of the signal which is then compared with a threshold value depending on prevailing noise floor to decide about the presence of a PU signal in the scanned sub-band. Mathematically, this can be expressed with the following steps [121,122]. Let us assume that the received signal has the following simple form:

$$y(n) = s(n) + w(n) \quad (6.2)$$

where $s(n)$ is the signal to be detected, $w(n)$ is the additive white gaussian noise (AWGN) sample, and n is the sample index. Note that $s(n) = 0$ when there is no transmission by any primary user. The decision metric $M(y)$ for the energy detector can be written [121] as

$$M(y) = \frac{1}{N} \sum_{n=0}^{N-1} |y(n)|^2 \quad (6.3)$$

where N is the length of the observation sequence, referred to as sample complexity. This output signal $M(y)$ is compared to the threshold λ_E in order to decide whether a signal is present or not. The λ_E is set according to statistical properties of the output M when only noise is present. This is equivalent to distinguishing between the following two hypotheses: [122]

$$\begin{aligned} H_0 &: y(n) = w(n) \\ H_1 &: y(n) = s(n) + w(n) \end{aligned} \quad (6.4)$$

where H_0 is a null hypothesis stating that the received signal samples $y(n)$ correspond to noise samples $w(n)$ and therefore there is no primary signal in the sensed spectrum band, and hypothesis H_1 indicates that some licensed user signal $s(n)$ is present.

The performance of the detection algorithm can be summarised with three probabilities: $P_{f,E}$ and $P_{m,E}$. $P_{d,E}$ is the probability of detecting a signal on the considered frequency when it truly is present. Thus, a large detection probability is desired. It can be formulated as

$$P_{d,E} = P_r(M(y) > \lambda_E | H_1) \quad (6.5)$$

$P_{f,E}$ is the probability that the test incorrectly decides that the considered frequency is occupied when it actually is not, and it can be written as

$$P_{f,E} = P_r(M(y) > \lambda_E | H_0) \quad (6.6)$$

$P_{m,E}$ is the probability of not detecting a signal on the considered frequency when a signal is present. Consequently, large $P_{m,E}$ introduces unexpected interference to primary users.

$$P_{m,E} = P_r(M(y) < \lambda_E | H_1) \quad (6.7)$$

$P_{m,E}$ should be kept as small as possible in order to prevent underutilisation of transmission opportunities. The decision threshold λ_E can be selected for finding an optimum balance between $P_{d,E}$ and $P_{f,E}$. However, this requires knowledge of noise and detected signal powers. The noise power can be estimated, but the signal power is difficult to estimate as it changes depending on ongoing transmission characteristics and the distance between the cognitive radio

and primary user transmitter. In practice, the threshold is chosen to obtain a certain false alarm rate [123], where $P_{f,E}$ is fixed to a small value (e.g. $\leq 5\%$) and $P_{d,E}$ is maximised. This is referred to as constant false alarm rate (CFAR) detection principle. Hence, knowledge of noise variance is sufficient for selection of a threshold. Setting the right threshold value is of critical importance, which we have already discussed in Chapter 4. The key problem in this regard is illustrated in Figure 6.4 which shows probability density functions of received signal with and without active primary user.

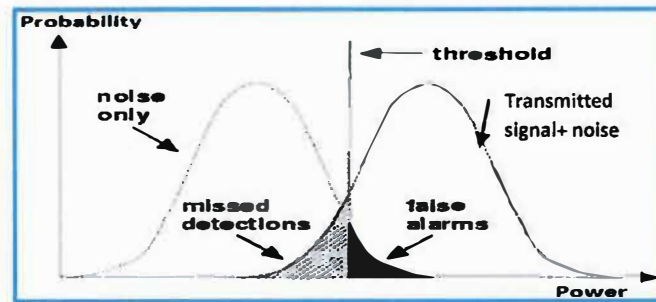


Figure 6-4: Threshold Setting in ED: Trade-off between Missed Detection and False Alarm.

The probability of detection $P_{d,E}$, and probability of false alarm $P_{f,E}$, of energy detection over the AWGN channel are approximated from [122] as

$$P_{d,E} = Q_m(\sqrt{2\gamma}, \sqrt{\lambda_E}) \quad (6.8)$$

$$P_{f,E} = \frac{\Gamma(m/2, \lambda_E/2)}{\Gamma(m)} \quad (6.9)$$

* $Q_m(.,.)$ is the generalised Marcum Q-function, which is widely used in radio communications and has important applications in error performance analysis of digital communication problems dealing with partially coherent, differentially coherent, and noncoherent detections.

* $\Gamma(.)$ and $\Gamma(.,.)$ are complete and incomplete gamma functions, respectively, where the gamma function is a component in various probability distribution functions, and as such it is applicable in the fields of probability and statistics.

* γ is the instantaneous SNR and λ_E is the decision threshold of the energy detector, $m = TW$ is the time bandwidth product, where samples were used to detect the presence of a signal of duration T and band limited to W.

Key positive features of energy detection are the implementation simplicity and low computational complexity, which have motivated most of the recent work in spectrum sensing

for CR towards enhanced energy detection and its combination with other robust and accurate spectrum sensing methods [125]. ED needs to estimate only the noise power to set its threshold and does not require any information on primary transmission characteristics. This makes energy detection based sensing a semi-blind technique. On the other hand, the limitations of energy detection are addressed in [126,128] and some hidden assumptions in conventional ED are unveiled more recently in [127,129]. The vital limitation of ED based spectrum sensing is the uncertainty in threshold setting to produce optimal sensing results, since it strongly depends on the accurate estimation of the noise power which changes temporally and spatially. Spectrum sensing results based on ED have limited reliability as energy observations are unable to differentiate between primary and secondary user signals which appears as a cost of semi-blind signal detection. Other limitations include poor performance under deep signal fades resulting from shadowing and fading and inability to detect spread spectrum signals. All these factors characterise ED with less robustness and low accuracy/reliability.

6.4.2 Cyclostationary Feature Detection

Cyclostationary Feature Detection (CFD) is a method for detecting primary user transmissions by exploiting the cyclostationary features of the received signals [130,131,132]. Wireless (digitally modulated) signals are in general coupled with sine wave carriers, pulse trains, repeating, spreading or hopping sequences or cyclic prefixes, which induce periodicity in the signal making them cyclostationary. This periodicity may result from modulation or even be deliberately generated to assist channel estimation (regularly transmitted pilot sequences) and synchronisation (preambles, mid-ambles etc.). Cyclostationary feature detection exploits the built-in periodicity of received signals to detect primary transmissions in a background of noise [133]. Features that can be extracted include RF carrier, symbol rate and modulation type. The inherent periodicity in cyclostationary signals causes key statistical characteristics of PU signal like mean and correlation to repeat after regular time intervals. This introduces correlation between widely separated frequency components of the received primary signal which is identified in cyclostationary detection by examining the Cyclic Autocorrelation Function (CAF), or, equivalently in the frequency domain by Cyclic Spectral Density (CSD), also known as Spectrum Correlation Function (SCF). An illustration of a cyclostationary feature detector is presented in Figure 6.5.

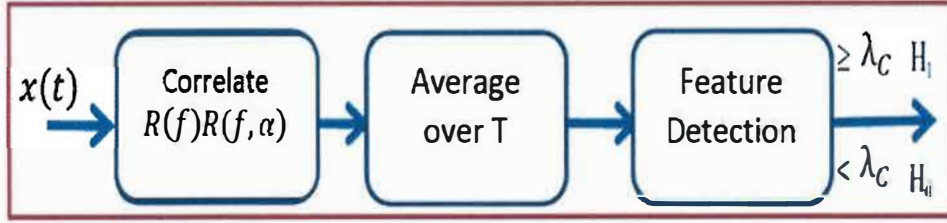


Figure 6-5: Block Diagram of Cyclostationary Feature Detection.

In general, a process is cyclostationary in the wide sense if its mean and autocorrelation are periodic or the sum of periodic functions of time. If there is more than one source of periodicity and the periods are not all commensurate, then the process is called almost cyclostationary since its parameters are almost periodic functions of time. An important characteristic property of a cyclostationary random process is that it exhibits spectral correlation, i.e., the complex envelopes of some pairs of frequency components have nonzero temporal correlation. This contrasts sharply with stationary processes, in which no pairs of distinct frequency components are correlated. It is the exploitation of this spectral correlation property of the signal of interest that leads to devices with superior tolerance to noise and interference as compared to radiometric devices. Mathematically, this can be expressed with the following steps [136,137]. The cyclic spectral density (CSD) function of a received signal can be written as

$$M(f, \alpha) = \sum_{\tau=-\alpha}^{\infty} R_y^{\alpha} e^{-j2\pi f\tau} \quad (6.10)$$

where

$$R_y^{\alpha}(\tau) = E[y(n + \tau)y^*(n - \tau)e^{-j2\pi\alpha n}] \quad (6.11)$$

is the cyclic autocorrelation function (CAF) and parameter α is the cycle frequency. It describes the frequency separation of the correlated spectral components [135]. The CSD function outputs peak values when the cyclic frequency is equal to the fundamental frequencies of the transmitted signal $x(t)$. Cyclic frequencies can be assumed to be known [136] or they can be extracted and used as features for identifying transmitted signals [137]. The probability of detection, P_d , and probability of false alarm, P_f , of cyclostationary detection over an AWGN channel are approximated as

$$P_{d,c} = 1 - [1 - Q_m(\frac{2\gamma}{\sigma_w}, \frac{\lambda_c}{\delta_A})]^L \quad (6.12)$$

$$P_{f,c} = 1 - (1 - e^{-\frac{\lambda_c}{2\delta_A^2}})^L \quad (6.13)$$

where σ_w^2 is the variance, $\delta_A^2 = \sigma_w^2(k_C + 1)$ in which k_C is the number of samples for detection, L is the number of diversity branches, γ is instantaneous SNR, $Q_m(\dots)$ is the generalised Marcum Q-function, and λ_c is a predetermined threshold.

The main positive point of feature detection is its ability to differentiate PU signals from interference and noise and even distinguish among different types of PUs. This derives from the fact that noise is in general (white) uncorrelated while every PU signal has a specific cyclostationary feature. Another important advantage is robustness to noise uncertainty which allows cyclostationary detector to identify primary transmissions more than 30 dB below the noise floor [136]. Therefore, feature detection outperforms ED especially in a low SNR regime. The hidden PU problem is much less likely to occur than with ED because of its high probability of detection. On the other hand, the limitations of feature detection arise from the cost of increased implementation complexity in terms of high processing requirements which results in a large sensing time. Specifically, this processing is required to extract cyclic frequencies (if not known a priori) from received primary transmissions which in turn also makes this approach non-blind. Also, short duration spectral opportunities cannot be exploited efficiently using this approach because of large observation time requirements.

6.4.3 Matched Filtering

When the secondary users know information about a primary users signal a priori, it can detect the PU signal by either passing the received signal at CR through matched filter (MF) having impulse response matched to the incoming signal or correlating it with a known copy of itself. The optimal detection method is matched filtering [138], since a MF can correlate the already known primary signal with the received signal to detect the presence of the primary user and thus maximise the SNR in the presence of additive stochastic noise. The output of MF is compared with a threshold to decide about the presence or absence of PU signal. Figure 6.6 depicts the block diagram of a matched filter.

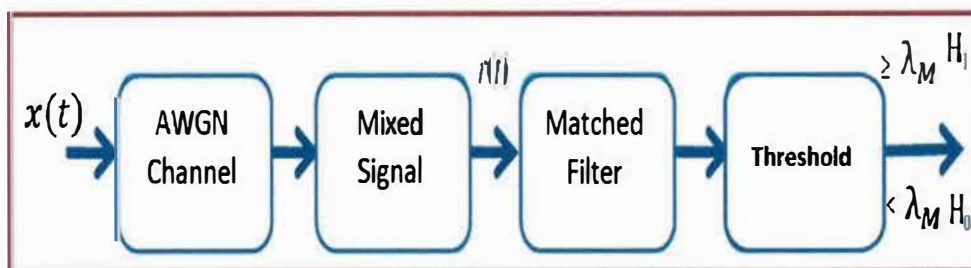


Figure 6-6: Block Diagram of Matched Filter Detection.

Mathematically, this can be expressed with the following steps [138]. The signal $r(t)$ received by CR is fed to the matched filter and is expressed mathematically as

$$r(t) = hs(t) + n(t) \quad (6.14)$$

where in general $s(t)$ is 0 if the PU is absent. The matched filter is equivalent to convolving the received signal $r(t)$ with a time-reversed version of the known signal or template as

$$r(t) * s(T - t + \tau) \quad (6.15)$$

where T is the symbol time duration and τ is the shift in the known signal. The probability of detection, P_d , and false alarm, P_f , of a matched filter are given as

$$P_{d,M} = Q\left(\frac{\lambda_M - E}{\sigma_w \sqrt{E}}\right) \quad (6.16)$$

$$P_{f,M} = Q\left(\frac{\lambda_M}{\sigma_w \sqrt{E}}\right) \quad (6.17)$$

where Q is the Gaussian complexity distribution function, E is the energy of the deterministic signal of interest, and σ_w^2 is the noise variance.

The main advantage of matched filtering is the short time to achieve a certain probability of false alarm or probability of mis-detection as compared to other methods, since a matched filter needs less received signal samples. Nevertheless, its implementation complexity and power consumption is too high [139], because matched-filtering requires cognitive radio to demodulate received signals. Hence, it requires perfect knowledge of the primary users signalling features such as bandwidth, operating frequency, modulation type and order, pulse shaping, and frame format. If wrong information is used for matched filtering, the detection performance will be degraded.

6.4.4 Other Sensing Methods

Other alternative spectrum sensing methods are waveform-based sensing, wavelet based spectrum sensing, filter bank and spectrum detection employing compressed sensing. In the following, we present a brief overview of these spectrum sensing methods.

Waveform-based sensing can be used to decide whether a primary user is transmitting or not, if only a certain pattern is known from the received signals. Known patterns are usually utilised in wireless systems to assist synchronisation or for other purposes. Such patterns include preambles, midambles, regularly transmitted pilot patterns, spreading sequences etc. A preamble is a known sequence transmitted before each burst and a midamble is transmitted in the middle of a burst or slot. In the presence of a known pattern, sensing can be performed by

correlating the received signal with a known copy of itself [90]. This method is only applicable to systems with known signal patterns, and it is termed waveform-based sensing or coherent sensing. In [90], it is shown that waveform-based sensing outperforms energy detector based sensing in reliability and convergence time. Furthermore, it is shown that the performance of the sensing algorithm increases as the length of the known signal pattern increases. The wavelet transform was proposed for spectrum sensing for detecting edges in the Power Spectral Density (PSD) of wideband spectrum in the frequency domain for detecting one or more narrowband users [142]. Wavelet transforms in general are used to detect irregularities/ singularities in the power spectral density and thus proposed to be used for detecting spectral irregularities or in other words varying power levels in the spectral bands over a wide portion of the spectrum. The wavelet detection method avoids the requirement to have complex band pass architectures in the receiver for detecting narrowband users for wideband sensing; however, it requires a high sampling rate when operating in the discrete domain.

A filter bank method is proposed in [143], where a set of band pass filters with low side-lobes are used to estimate the signal spectra. This is a very conventional method (with hardware antecedent) for spectral estimation and could also possibly be used for spectrum sensing in cognitive radios. The major disadvantage of this method is obviously the requirement for many band pass filters in the receiver; on the other hand, considering multicarrier communications with filter bank structures already in the receivers this method could be conveniently utilised for spectrum sensing without too many additional requirements.

Compressive sensing is a technique that can efficiently acquire a signal using relatively few measurements, by which unique representation of the signal can be found based on the signal's sparseness or compressibility in some domain. As the wideband spectrum is inherently sparse due to its low spectrum utilisation, compressive sensing becomes a promising candidate to realise wideband spectrum sensing by using subNyquist sampling rates. Spectrum detection based on compressed sampling is proposed in [144], where the authors have extended their approach of wavelets to wideband spectrum sensing using sub-Nyquist sampling by exploiting the sparse nature of wireless signals in frequency domain. This technique relies on the maximum sparsity order to determine the fundamental limit on the sampling rate which turns out to be unnecessarily high for the desired sensing performance and hence wasteful of sensing resources. To alleviate wasteful sampling, a Two-step compressed Spectrum Sensing (TS-CSS) scheme is proposed in [145].

6.4.5 Performance Assessment of Well-Known Spectrum Sensing Techniques ED, CFD, MF and Other Techniques

In this section, we compare the performance of three well-known algorithms; energy detectors, matched filtering, and cyclostationary detection. During the comprehensive study of these three models of spectrum sensing techniques, criteria which directly affect performance and accuracy of each technique are discussed. In particular, these aspects for energy detection, matched filtering and cyclostationary detection are presented in Figure 6.7A and 6.7B. A comparison has been made of time, cost, prior knowledge, and complexity for each technique in Figure 6.7A and how these aspects impact on the accuracy and performance as shown in Figure 6.7B. The performance comparison has been represented in three different values; low, medium and high. It can be clearly seen that the energy detection has short time, low cost, no prior knowledge and less complexity but correspondingly the accuracy and performance are low because these criteria rely on some factors such as suitable threshold selection and noise stability. It is unrealistic to expect to find these stationary factors in all the times and various places. On the other hand, the matched filter technique as illustrated in Figure 6.7B has good performance and high accuracy but at the expense of increasing the cost, more complexity and requiring perfect signal knowledge to operate these techniques. In contrast, cyclostationary analysis has slightly better performance and possesses higher accuracy than energy detection, but it needs long time, high cost and partial prior knowledge which makes it less complex than the matched filter. Therefore, each of these techniques has advantages and disadvantage where some advantages are at the expense of significant problems, which might impact directly on the technique working properly and effectively [146].

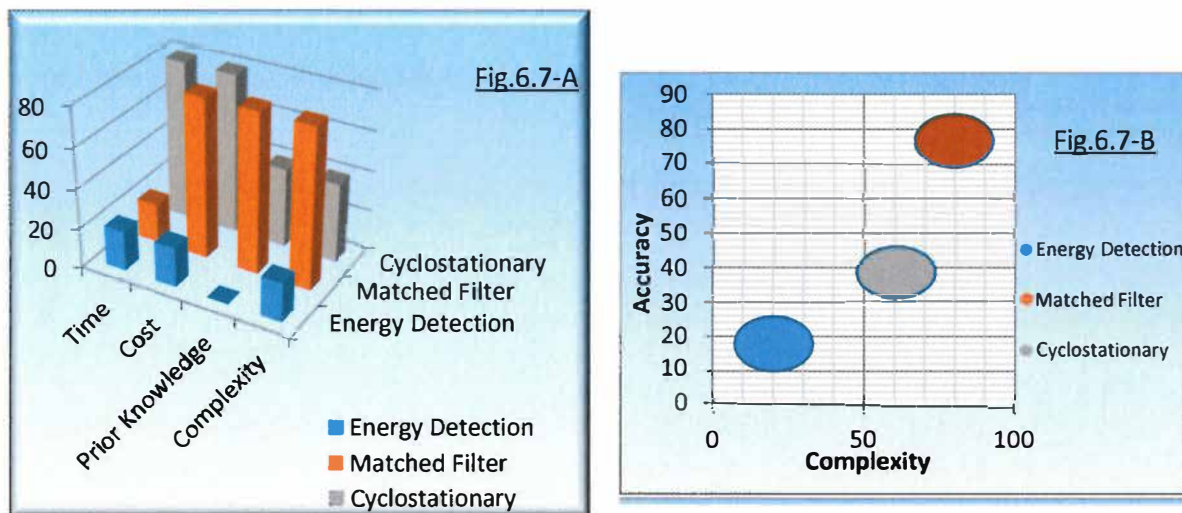


Figure 6-7: (A) Comparison of Spectrum Sensing and (B) Performance of the Spectrum Sensing [146]

6.4.6 Simulation Platform for Spectrum Sensing Techniques ED, CFD and MF

This simulation has been carried out by implementing equations 6.8 and 6.9 (ED), 6.12 and 6.13 (CFD) and 6.16 and 6.17 (MF) in Matlab code. Two different simulation processes are carried out. For the first simulation type, the SNR is kept at a fixed value of 0dB, and for the second simulation type, the SNR is kept at a fixed value of 6dB. The decision threshold range is varied between minimum and maximum threshold values. The two major parameters used as a performance measurement metrics to analyse the performance of the detection process are, probability of detection (P_d) and probability of false alarm (P_f). The performance of a spectrum sensing technique is illustrated by the receiver operating characteristics (ROC) curve which is a plot of P_f versus P_d . An extensive set of simulations have been conducted using the system model as described in the previous section. The emphasis is to analyse the comparative performance of the three well-known spectrum sensing techniques. The results are shown in Figure 6.8. It is constructed by plotting the detection rate versus the false alarm rate. The curve is created by assuming a large range of thresholds. In the plot we compare the performance of three different scenario energy detection, matched filter and cyclostationary detection. The simulation results of spectrum sensing techniques show in Figure 6.8 point out that the cyclostationary detector is better than the conventional energy detector. The cyclostationary feature detector does not assume full knowledge and therefore its performance cannot surpass that of the matched filter based. This is confirmed in the plot. However, the cyclostationary detector performance is comparable to that of the matched filter which is based on full prior knowledge. This is clearly difficult to implement, and will be very expensive and very complicate to build in. Additionally, Figure 6.8 indicates that when SNR is increased to 6dB, all the proposed methods have low probability of false alarm and high probability of detection compared with SNR=0dB. Overall, the results in this section show that probability of detection starts working well with high SNRs. Matched filter detection is better than energy detection even with low SNRs. Taking into account the complexity of matched filter and uncertainty of energy detection, cyclostationary feature detection is better than both the previous detection techniques since it produces respectable results[146].

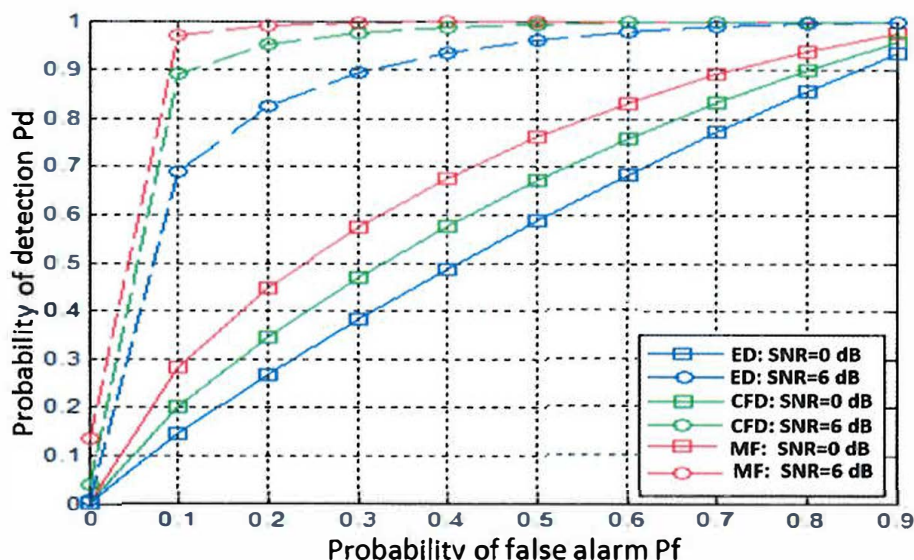


Figure 6-8: Probability of Detection vs Probability of False Alarm Spectrum Sensing Techniques ED, MF, CFD with SNR=0dB And SNR=6dB.

Similar results have been concluded in most of the previous published studies of performance comparison of spectrum sensing method relying on theoretical analysis and numerical simulations. However, real world noise can be different from AWGN, and there are other factors to consider such as path loss, shadowing, multipath fading, and interference. These facts have motivated the author to examine the performance comparison of energy detection and cyclostationary feature detection with real measurement signals in the next Chapter.

6.5 Comparison of Various Sensing Methods

Although in section 6.4.5 we compared the performance of three well-known algorithms; ED, MF and CFD, in this section we will compare the detection performance of several other representative spectrum sensing algorithms. The selection of a sensing method is always a trade-off between accuracy and complexity. The comparison of the sensing methods given in the previous section is summarised in Figure 6.9.

When nothing is known about the PU signal, ED happens to be most simple approach, but it fails in the presence of fading and noise uncertainties. Waveform-based sensing is more robust than energy detector and cyclostationarity based methods because of the coherent processing that comes from using deterministic signal component [147,148]. However, there should be a priori information about the primary user's characteristics and primary users should transmit known patterns or pilots. Advanced power spectrum estimation techniques such as wavelet based and filter bank spectrum achieve accuracy while sacrificing the simplicity of energy detection. As a matter of fact, some a priori knowledge about primary transmissions is

necessary to distinguish a primary signal from a secondary signal and interference/noise. Processing of this known information achieves reliability in detection at the cost of additional computational complexities. Such schemes are classified as non-blind and the type of the detection approach depends on the available information about primary signals. In particular, cyclostationary detection is suitable when cyclic frequencies associated with primary transmissions are known while coherent detection is preferred when pilot transmissions of the primary system are known. Blind sensing, based on received signal covariance matrix and other approaches achieves high accuracy with its computational complexity dependent on the sensing algorithm used.

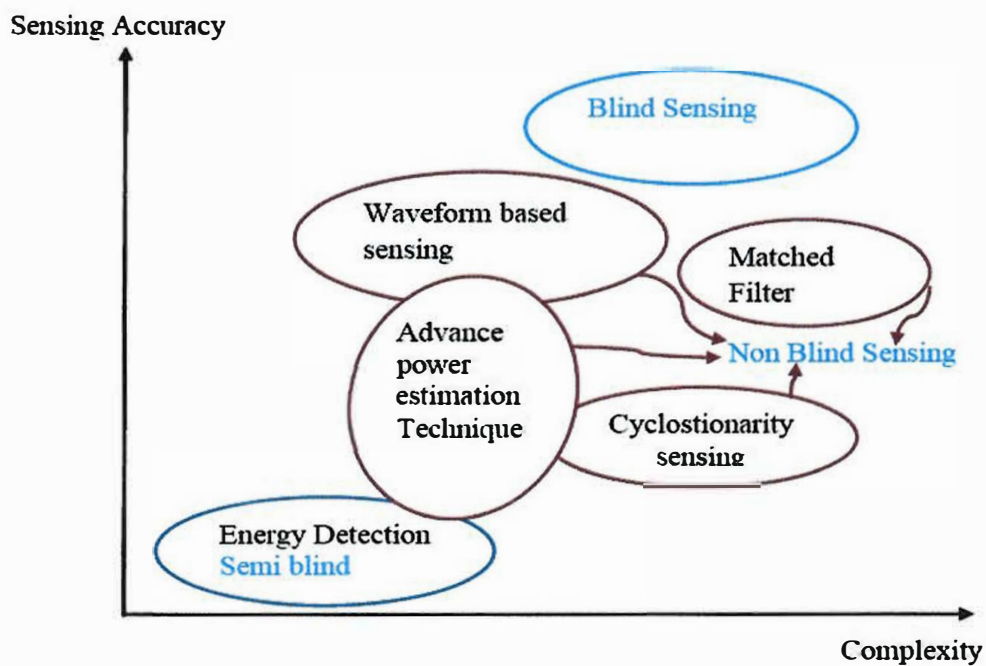


Figure 6-9: Comparison of Spectrum Sensing Methods

Overall, while selecting a sensing method, some trade-offs should be considered. The characteristics of primary users are the main factor in selecting a method. Cyclostationary features contained in the waveform, existence of regularly transmitted pilots, and timing/frequency characteristics are all important. Other factors include required accuracy, sensing duration requirements, computational complexity, and network requirements.

Estimation of traffic in a specific geographic area can be done locally (by one cognitive radio only) using one of the algorithms. However, information from different cognitive radios can be combined to obtain a more accurate spectrum awareness. In the following section, we present the concept of cooperative sensing where multiple cognitive radios work together to perform the spectrum sensing task collaboratively.

6.6 Cooperative and Two-Stage Adaptive Sensing

The key challenges associated with single-user-centric transmitter detection schemes, that prevent them achieving promised sensing performance under practical conditions include restricted sensing ability, high detection sensitivity requirements, vulnerability of primary receivers to secondary transmissions and spectrum sensing in multiuser environments. The above limitations of conventional spectrum sensing can be overcome by sharing the sensing information among spatially distributed CRs which leads to the concept of cooperative sensing [148]. It is well known from the theory of distributed detection that higher reliability and lower probability of detection error can be achieved when observation data from multiple, distributed sources is intelligently fused in a decision making algorithm, rather than using a single observation data set. Cooperation is proposed as a solution to problems that arise in spectrum sensing due to noise uncertainty, fading, and shadowing [149]. Cooperative sensing decreases the probabilities of misdetection and false alarm considerably. Also, cooperation can solve hidden primary user problem and can decrease sensing time.

To further improve the reliability of the detection, two-stage spectrum sensing scheme is designed, which has better performance than single-stage techniques with relatively low computational complexity. Recent work [150] has reported the combination of ED with feature detection to benefit from complementary advantages of both the schemes by doing coarse detection using ED which is then made more reliable by fine detection employing cyclostationary detection. In Chapter 8, the author will explain in more detail the challenge of non-cooperative sensing and cooperative spectrum sensing and analyse how it can guarantee improved sensing performance with minimum incurred cost.

6.7 Chapter Summary

Spectrum is a very valuable resource in wireless communication systems, and it has been a focal point for research and development efforts in recent decades. Cognitive radio, which is one of the efforts to utilise the available spectrum more efficiently through opportunistic spectrum usage, has become an exciting and promising concept. One of the important elements of cognitive radio is sensing the available spectrum opportunities. In this Chapter, passive awareness and active awareness concepts have been introduced. Active awareness of the spectrum sensing task are explained in detail. A variety of detection techniques were studied, compared and classified. Comparison of sensing algorithms revealed wide variability in their computational complexity for the targeted detection performance. Performance comparison of

basic spectrum sensing mechanisms such as, Energy Detection (ED) and Cyclostationary Feature Detection (CFD) along with the Matched Filter (MF) detection method is evaluated. From simulation results it is observed that the detection performance of the CFD method is a compromise technique, having better low SNR detection performance than energy detectors and less strict requirements than matched filters. Due to limitations of conventional spectrum sensing, and to mitigate the impact of such as multipath fading, shadowing and receiver uncertainty issues in spectrum sensing, cooperative spectrum sensing and two-stage adaptive sensing are introduced as a solution to come over these problems.

Chapter

7 Cyclostationary Feature Detection

7.1 Introduction

To mitigate the impact of harmful interference with licensed users, detection algorithms have been shown to be an effective method to improve the detection performance [151,152]. Wireless signal detection can be performed using many different techniques. Each of these techniques has advantages and disadvantages in terms of theoretical and real world performance, which have already been mentioned in previous Chapters. Among these techniques, cyclostationary feature detection (CFD) can be viewed as a compromise technique, having better low signal-to-noise ratio (SNR) detection performance than energy detectors and less strict requirements than matched filters. Therefore the CFD is regarded as a promising technique for signal detection.

Spectrum sensing at low SNR conditions is critical to mitigate the hidden transmitter problem and to enhance spectrum awareness. Cyclostationary feature detectors are considered to be one of the most robust detectors under noise uncertainties. CFD uses the cyclostationarity of a signal to detect its presence. Signals that have cyclostationarity exhibit correlations between widely separated spectral components. Functions that describe this cyclostationarity include the Spectral Correlation Function (SCF) and Spectral Coherence Function (SOF). In recent years, cyclostationary feature detection strategies have gained an increasing interest in the context of cognitive radio. This fact has been driven by the fact that CFD is able to differentiate PU signal from interference and noise and even distinguish among different types of PUs. This section reviews some of the campaigns performed in cyclostationary feature detection. In [154]

it was shown that the SCF floor gets lower as the observation time (and computation budget) gets longer (by simulation), which indicates that SCF features can be detected under lower SNR environment with longer observation time as shown in Figure 7.1.

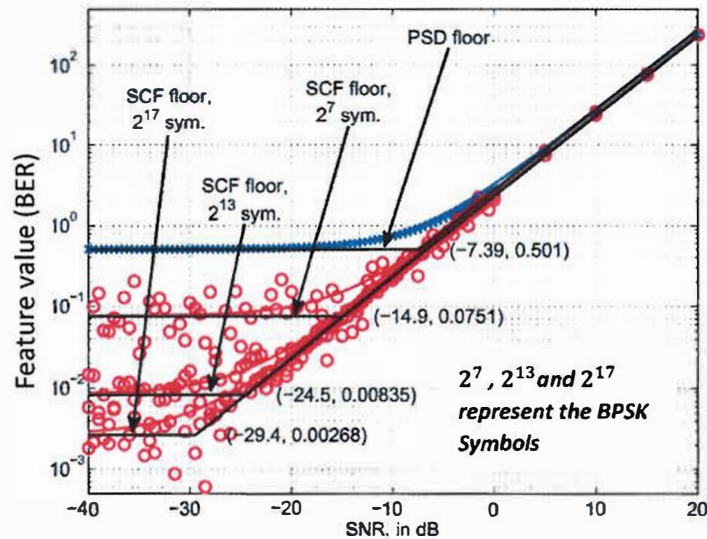


Figure 7-1: SCF of BPSK under different SNR/observation time compared with PSD, using 2^7 , 2^{13} and 2^{17} BPSK Symbols [154].

In [153], the authors used a cyclostationary signature which is a unique identifier or watermark intentionally embedded in the signal and identified through SCF. They proved, using simulation, that the cyclostationary signature is sensitive to time variant Rayleigh multipath. In [156], the authors propose a method to improve CFD using the fact that SCF is robust to slow multipath fading, low SNR environments and is insensitive to unknown prior knowledge of received signal gain by simulation. Other researchers have used real experiments to understand the SCF in a limited manner. In [157], the real world performance of CFD was presented in the form of SCF through hardware implementation, overcoming its hardware limitation such as sampling clock offset by partially coherent feature processing. The author in [157] tried to relate the performance of his CFD to an experimental approach. But the noise used in his research was synthetic stationary white noise. In addition, through empirical experiments, it was shown in [158] that under multipath fading with static and dynamic states the SCF still shows its cyclostationary features in the cyclic frequency (α) \neq 0 regions. Reference [157] focuses on implementing SCF in hardware and interpreting its limitations whereas [158] focuses more on stationary analysis under multipath and shadowing effects. The rest of the Chapter is organised as follows. In section 7.2 we address goals, framework and approach of Chapter. In section 7.3, we briefly describe the background to the cyclostationary process. Channel noise analysis is introduced in section 7.4. In section 7.5, we present

methodology aspects, describing the cyclostationary feature analysing system and experimental setup. In section 7.6, we present research analysis and research results. We conclude the Chapter in section 7.7.

7.2 Goals, Framework and Approach

The performance of SCF has not been investigated sufficiently under real-world noise conditions. Instead, it has been proven in analytic/simulation manner or with real experiments using AWGN (synthetic noise) as noise. But real world noise, which often includes low level interference can be different from AWGN, and there are other factors to consider such as path loss, shadowing, multipath fading, and interference [160]. Although the log-normal shadowing model is built based on empirical experiments using the PSD of the signal, showing the effects of noise on signal power, however, the PSD when used for energy detection is shown to have worse performance under those multiplicative noise conditions [161]. There has been very limited research on a SCF-based path model in the context of cyclostationary sensing to identify the effects of noise like the PSD based (energy detection) log-normal shadowing model above. Therefore, the features of SCF under path loss, shadowing, multipath need to be investigated by varying path length and receiver location. Consequently, the goals of this research are: Firstly, to identify and characterise the difference between the cyclostationary features and energy features of modulated signals under channel noise in term of path loss, shadowing and multipath under various locations and with various transmitter/receiver separations. Secondly, to determine the performance difference between SCF and PSD under low SNR conditions with real world signals.

During this research, frequency shift keying (2FSK) modulation is used with 20 kS/s symbol rate in the 2.415 GHz band. The signal is generated from a signal generator, Agilent E4438C, ESG vector signal generator. The universal software radio peripheral (USRP2), which is a software defined radio, is used as a receiver. The receiver and the transmitter are static (fixed locations) while taking measurements. To get the cyclostationary features of the modulated signal, SCF is used, and to get the energy features, PSD is used, both implemented using Matlab programs. Analysis of path loss is based on the “log-normal shadowing” for both indoor and outdoor experiments. Curve fitting to the measured data is performed using the Least Squares curve fitting method which minimises deviation from all data points. According to the goals stated above, an experimental approach was determined. To identify and characterise the SCF features of the modulated signal under real world channel noise, we measure the path loss

exponent of SCF and compare it to the path loss exponent of PSD. Experiments for path loss are performed by varying locations and distances. The resultant path loss for each location is analysed in terms of path loss exponents and variance of feature magnitudes. To observe the performance of SCF under low SNR environment with real world signals, the SNR is changed by controlling the transmitted signal strength. Performance of SCF under low SNR is compared with performance of the PSD. SNR and observation time are varied at a fixed distance and fixed location.

7.3 Cyclostationary Process

The cyclostationary process analysis transforms a signal into a frequency-cycle domain instead of the time-frequency domain. This represents the signal as a cyclic process rather than a stationary one which is accurate since most of the waveforms of interest are cyclic in nature. Cyclostationary feature detectors are based on the identification of second-order cyclostationary characteristics, which are present in most of the communication signals that contain pilot sequences, carrier tones and frame headers, which are transmitted on a recurrent basis. Stationary processes exhibit a time-invariant mean and auto-correlation function, whereas a cyclostationary process has a time periodical probability distribution function. Wide-sense stationary refers to time-invariant moments (such as mean, variance and higher order moments), while wide sense cyclostationarity means that the mean and the autocorrelation function of the signal are periodic [162]. From a mathematical point of view, if any higher order nonlinear transformation of a random signal generates a spectral line at cyclic frequencies other than zero, the signal is called cyclostationary [163]. A signal is said to be cyclostationary with a cycle frequency α , delay τ and period T_0 , if and only if its delay conjugate product $y(t) = x(t)\tilde{x}(t - \tau)$ produces a spectral line at frequency α .

The spectral correlation of a cyclostationary signal cannot be visible through use of conventional PSD function [164,165]. Cyclic spectral analysis or cyclostationary processing are the tools for investigating and extracting such cyclic features. A simple periodic signal with period (T_0) and fundamental frequency ($1/T_0$), can be expressed as eq. 7.1[166].

$$x(t) = x(t + T_0) \quad (7.1)$$

Periodic signals can be represented using Fourier series coefficients $x(t)$:

$$\text{The Fourier series expansion of } x(t) \text{ is; } x(t) = \sum_{k=-\infty}^{+\infty} a_k e^{jk\omega_0 t} \quad (7.2)$$

where, $a_k = \frac{1}{T_0} \int_{T_0} x(t) e^{-jk\omega_0 t} dt$ is the Fourier coefficient.

The Fourier series expansion extracts certain features, in this case the period of the periodic signal. This is illustrated in Figure 7.2, with a repeated sinc wave as the signal $x(t)$. In the frequency domain, the spectral lines of Figure 7.2 are related to the Fourier coefficients a_k . If we apply a quadratic transformation to our signal, we can extract its hidden periodicity due to the presence of modulation.

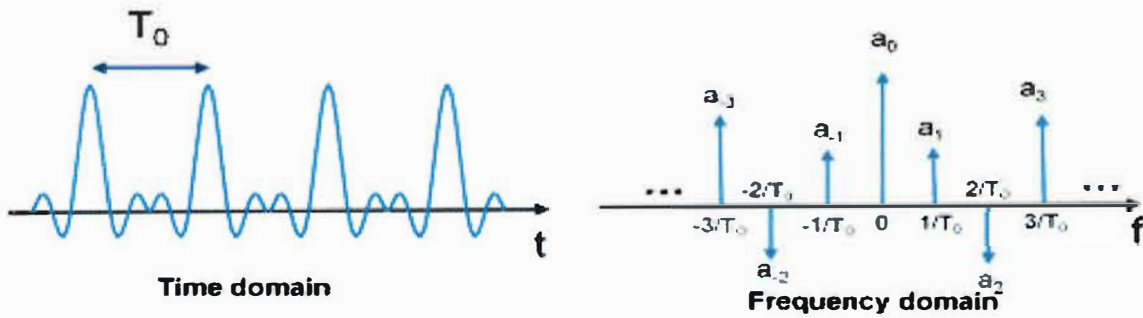


Figure 7-2: Fourier Expansion of Periodic Signal for Feature Extraction.

7.3.1 Model of the Cyclostationary Signal

The general properties of cyclostationary processes are derived starting from the Fourier series expansion of the autocorrelation function, which is periodic. The Fourier coefficient of the Fourier expansion of the periodic autocorrelation function of a cyclostationary signal is called the Cyclic Autocorrelation Function (CAF). The Fourier transform of CAF is called the Spectral Correlation Density Function (SCF). Mathematically, this can be expressed with the following steps [164,165,166,189,172].

7.3.1.1 Cyclic Autocorrelation Function (CAF)

The CAF is a measure of the spectral correlation between time shifted versions of a cyclostationary waveform. The periodic autocorrelation function for a cyclostationary signal can be written [164] as,

$$R_y(t, \tau) = E[x(t)\tilde{x}(t, \tau)] \quad (7.3)$$

Here in eq. (7.3), $E[.]$ stands for the statistical expectation operator, t is the time index, τ is a time delay, and \tilde{x} is the complex conjugate of $x(t)$. If the autocorrelation function $R_y(t, \tau)$ is periodic, then the Fourier series decomposition can be performed and it yields:

$$R_y(t, \tau) = \sum_{\alpha=-\infty}^{+\infty} R_y^\alpha(\tau) e^{2\pi j \alpha t} \quad (7.4)$$

where α is the cyclic frequency which ranges over all integer multiples of the fundamental frequency $\frac{1}{T_0}$. The Fourier coefficient $R_y^\alpha(\tau)$ is called CAF and it can be defined according to eq. (7.5),

$$R_y^\alpha(\tau) = \lim_{T \rightarrow \infty} \frac{1}{T} \int_{-T/2}^{T/2} R_y(t, \tau) e^{-j2\pi\alpha t} dt \quad (7.5)$$

where, T is an observation interval. The autocorrelation function of eq. (7.5) can be replaced by the symmetric delay conjugate product and expressed as in eq. (7.6),

$$R_y^\alpha(\tau) = \lim_{T \rightarrow \infty} \frac{1}{T} \int_{-T/2}^{T/2} x(t + \frac{\tau}{2}) x(t - \frac{\tau}{2}) e^{-j2\pi\alpha t} dt \quad (7.6)$$

CAF may be viewed as the correlation in the time domain between two frequency-shifted values of $x(t)$ separated in frequency by α as below in eq. (7.7).

$$R_y^\alpha(\tau) = \lim_{T \rightarrow \infty} \frac{1}{T} \int_{-T/2}^{T/2} u(t + \frac{\tau}{2}) v(t + \frac{\tau}{2})^* dt \quad (7.7)$$

Where $u(t) = x(t)e^{-j2\pi\alpha t}$ and $v(t) = x(t)e^{j2\pi\alpha t}$ are two time shifted versions of $x(t)$.

7.3.1.2 Spectral Correlation Density Function (SCF)

The Spectral Correlation Density Function (SCF) is defined as the Fourier transform of the cyclic autocorrelation function of $x(t)$. The SCF of a signal is given by [166],

$$S_y^\alpha(f) = \int_{-\infty}^{\infty} R_y^\alpha(\tau) e^{-j2\pi f \tau} d\tau \quad (7.8)$$

SCF having spectral components of $x(t)$ at frequencies $(f + \frac{\alpha}{2})$ and $(f - \frac{\alpha}{2})$ over an observation interval of T given below in eq. (7.9),

$$S_y^\alpha(f) = \lim_{\Delta t \rightarrow \infty} \lim_{T \rightarrow \infty} \frac{1}{\Delta t} \frac{1}{T} \int_{-\Delta t/2}^{\Delta t/2} X_T(t, f + \frac{\alpha}{2}) X_T^*(t, f - \frac{\alpha}{2}) dt \quad (7.9)$$

Above, the spectral component of $x(t)$ at frequency f with period T is:

$$X_T(t, f) = \int_{t-T/2}^{t+T/2} x(t) e^{-j2\pi f t} dt \quad (7.10)$$

The cyclic spectrum at a given cycle frequency represents the density of correlation between two spectral components of the process which are separated by an amount equal to the cycle frequency. The SCF is typically plotted on a bi-frequency plane as a function of spectral frequency f and cyclic frequency α . The range of values of f (normally, $-\frac{fs}{2}$ to $\frac{fs}{2}$, where fs is the sampling frequency) and α (normally, $-fs$ to fs) for which $S_y^\alpha(f)$ exists is referred to as the region of support on the bi-frequency plane. For a purely stationary random process, CAF reduces to the autocorrelation function $R_y(t)$ and SCF reduces to the PSD function $R_y(f)$ [167]. This corresponds to $\alpha = 0$. Starting from eq. (7.8), and choosing $\alpha = 0$, we get

$$S_y^\alpha(f) = \frac{1}{T_0} \int_{-\infty}^{\infty} \int_{-T_0/2}^{T_0/2} R_y(\tau) e^{-j2\pi f\tau} d\tau d\tau = \int_{-\infty}^{\infty} R_y(\tau) e^{-j2\pi f\tau} d\tau = S_y(f) \quad (7.11)$$

SCF of different modulated signals creates unique patterns which are modulation dependent (examples are given later in section 7.3.2). Thus, SCF can be used as a signal classifier based on signals' modulation scheme [172].

7.3.1.3 Spectral Coherence Function (SOF)

To derive a normalised version of the SCF, the spectral coherence function (SOF) is given by [172]:

$$C_y^\alpha(f) = \frac{S_y^\alpha(f)}{[S_y^0(f+\frac{\alpha}{2}) S_y^0(f-\frac{\alpha}{2})]^{1/2}} \quad (7.12)$$

The spectral coherence function (SOF) has been demonstrated to be insensitive to noise, and to produce highly distinct features for signals with different modulation schemes without requiring any a priori knowledge of the signal's carrier frequency, phase, or timing offset [168,169]. The resulting SOF is a three dimensional image. The amount of data is too large for any classifier to utilise in a reasonable amount of time, and must be reduced in some manner. In [168], the authors suggested using only the cycle frequency profile of the SOF, which was shown to achieve excellent classification results in AWGN channels at SNR levels down to -5dB. However, with only a modest gain in computational complexity, we could use the Spectral Frequency Profile (CFP). CFP defines the cycle frequency profile ($\overline{\alpha}$) and spectral frequency profile (\overline{f}) [179] as

$$\overline{\alpha} = \max_f |C_y^\alpha(f)| \quad (7.13)$$

$$\overline{f} = \max_\alpha |C_y^\alpha(f)| \quad (7.14)$$

In [169], it was shown that with only a marginal increase of computational complexity incurred by using both the spectral and cycle frequency profiles, the system can be significantly improved. Reference [169] extends this work to evaluate the ability of the SOF's performance as a reliable feature detector in multipath fading channels, and to compare its performance to that of the benchmark system given in [168]. By exploiting the SOF's insensitivity to additive noise as well as channel corruption, the resulting classifier is shown to be robust both to low SNR as well as multipath fading channels. The main three important functions derived in cyclostationary feature detection are presented in table 7.1 [164,165,166,189,172].

Table 7.1: Three Important Functions Derived in Cyclostationary Feature Detection.

Function Name	Equation	Characteristic
Cyclic Autocorrelation Function (CAF)	$R_y^\alpha(\tau) = \lim_{T \rightarrow \infty} \frac{1}{T} \int_{-T/2}^{T/2} R_y(t, \tau) e^{-j2\pi\alpha t} dt$	Fourier series of autocorrelation
Spectral Correlation Density Function (SCF)	$S_y^\alpha(f) = \int_{-\infty}^{\infty} R_y^\alpha(\tau) e^{-j2\pi f\tau} d\tau$	Fourier transform of the CAF
Spectral Coherence Function (SOF)	$C_y^\alpha(f) = \frac{S_y^\alpha(f)}{[S_y^0(f + \frac{\alpha}{2}) \cdot S_y^0(f - \frac{\alpha}{2})]^{1/2}}$	Normalised version of the SCF

7.3.2 Benefits of the SCF/SOF

Spectral correlation/coherence functions (SCF/SOF) have benefits which can be used in the practical situation over traditional PSD. One benefit is that stationary noise such as AWGN does not exhibit spectral correlation, because the spectral correlation comes from cyclostationarity which is special case of non-stationary process. Therefore, in the limit, the SCF/SOF of white noise is identically zero. Another benefit is that the SCF/SOF is robust to low SNR and multipath fading channels. A further benefit is that the SCF/SOF of same modulation type with different number of possible symbols, such as Binary Phase Shift Keying (BPSK) and Quaternary PSK (QPSK), have different unique features. This is in contrast to the PSD which has identical features for the same modulation type. This property helps to detect expected signals and classify signals according to modulation type. Graphically, in Figure 7.3 four peaks are shown, two of them are on the $\alpha = 0$ axis and the other two of them are $f = 0$ axis. Among the peaks, two peaks on $\alpha = 0$ and $f = \pm f_0$ are considered as common peak which come up in other schemes where same modulation type (PSK in this example) is used with different number of symbols, such as QPSK and Staggered QPSK (SQPSK).

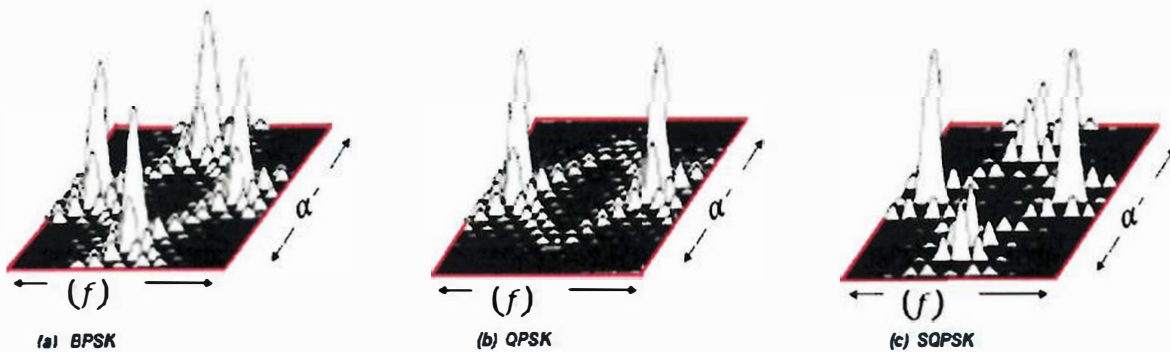


Figure 7-3: Theoretical SCF Magnitude for BPSK, QPSK and SQPSK with Carrier Frequency [170].

This points out that the two peaks are no longer distinct features of the BPSK signal. However, the other two peaks on $\alpha = \pm 2f_0$ and $f = 0$ are distinct compared to other modulation schemes. Figure 7.3 below shows SCFs of BPSK, QPSK and SQPSK. All plots show similar peaks where, $f = 0$ and $f = \pm f_0$. However, the other two peaks at $\alpha = \pm 2f$ and $f = 0$ in BPSK signal does not show up in QPSK and SQPSK signal or the height of the peaks are comparatively different from the peaks in SQPSK.

7.3.3 Evaluation of Cyclic Spectral Analysis Algorithms

Cyclic spectral analysis is used to detect the presence of a signal by use of the Spectral Correlation Density Function (SCDF). The detection algorithm based on cyclostationary detection has a high computational complexity in comparison to a detection algorithm based on Power Spectral Density (PSD). There is therefore a need to identify more efficient algorithms, which are still based on the cyclic spectral features, but which require less computational effort. As reported by Roberts [171], cyclic spectral analysis algorithms fall into two classes: those that average in frequency (frequency smoothing) and those that average in time (time smoothing). Although both classes of algorithms produce similar approximations to cyclic spectrum, time smoothing with an FFT Accumulation Method (FAM) and Strip Spectral Correlation Algorithm (SSCA) are considered to be more computationally efficient. These two computationally efficient algorithms for digital cyclic spectral analysis, the FAM and SSCA, are developed from a series of modifications on a simple time smoothing algorithm [172,173,174]. With computational efficiency for general cyclic spectral analysis as our primary motivation, we focus in this Chapter on the time smoothing algorithm. One algorithm based on this time smoothed method is called the time smoothed FFT method described in section 7.3.3.1. Further developments based on the time smoothed FFT method are the FFT Accumulation Method (FAM) and Strip Spectral Correlation Algorithm (SSCA) method and they will be described in section 7.3.3.2 and section 7.3.3.3 respectively.

7.3.3.1 Time Smoothed FFT Method

In the time smoothing FFT method, spectral components of signal $x(t)$ are determined over a data tapering windows of length TW , overlapping (L), sliding (short time) Fast Fourier Transform (FFT) over the entire observation time window Δt of the received signal. The practical approach for sliding the time window for determining frequency components of $x(t)$ is shown in Figure 7.4. The data-tapering window is used to reduce the cyclic leakage. A data tapering window with an observation length, T , slides over the data for Δt time span with a size of N' sliding point FFT and it produce two spectral components in each FFT window. It is

known that the frequency separation of certain spectral components which are correlated is called cyclic frequency. The cyclic frequency α is expressed as $\alpha = f_2 - f_1$, where f_1 and f_2 are the spectral frequencies of spectral components of $x(t)$. The spectral components are then down-converted to frequency shifted versions (one shifted with $+\alpha/2$ and the other one with $-\alpha/2$).

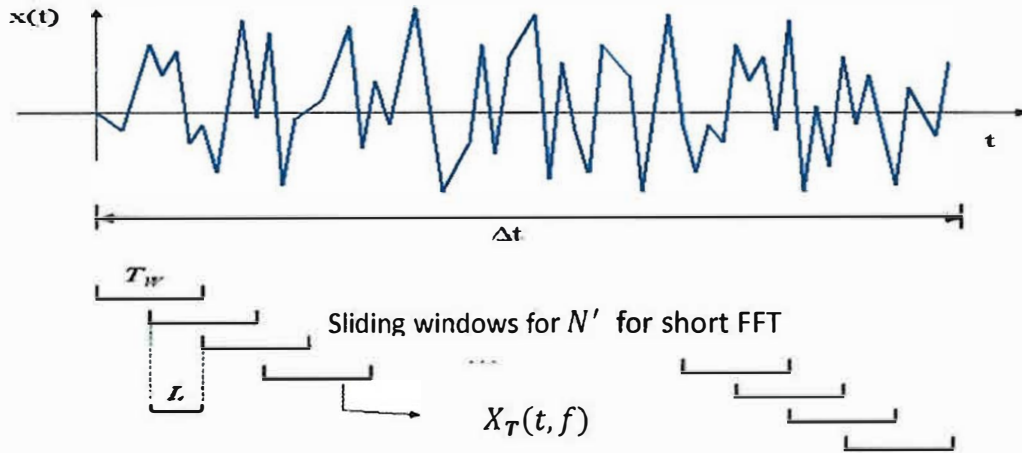


Figure 7-4: Practical Implementation of Time Smoothed FFT Method [176].

The time smoothed FFT method implementation is illustrated in the block diagram of Figure 7.5. According to the figure 7.5, after two frequency-shifted versions are produced, the conjugate of one frequency shifted version is multiplied with the other over the observation time Δt . They are both Fourier transformed (FFT) and after that, the multiplication product is passed through an LPF (average over time: time smoothing) to form SCF.

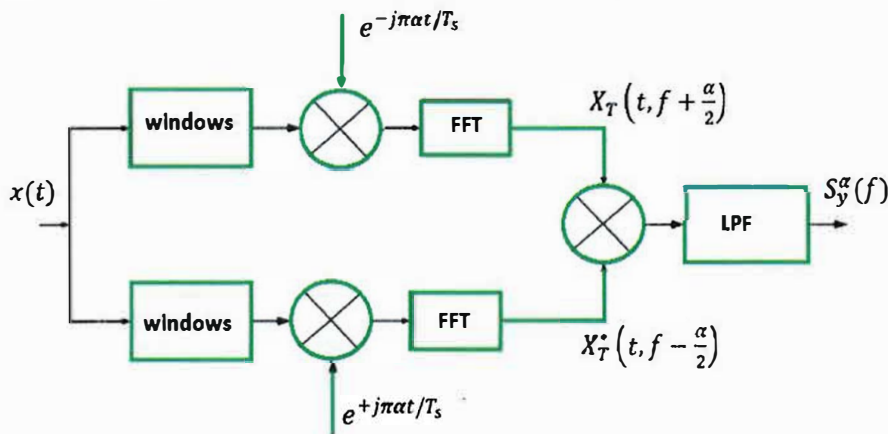


Figure 7-5: Time Smoothed FFT Method [143], [7].

7.3.3.2 FFT Accumulation Method (FAM)

The time smoothing FFT accumulation method was developed to reduce the number of computations required to estimate the cyclic spectrum [177]. This technique divides the bi-frequency plane into small regions called channel pair regions, and computes the estimates one

block at time using the fast Fourier transform. A block diagram of the FFT accumulation method is shown in Figure 7.6.

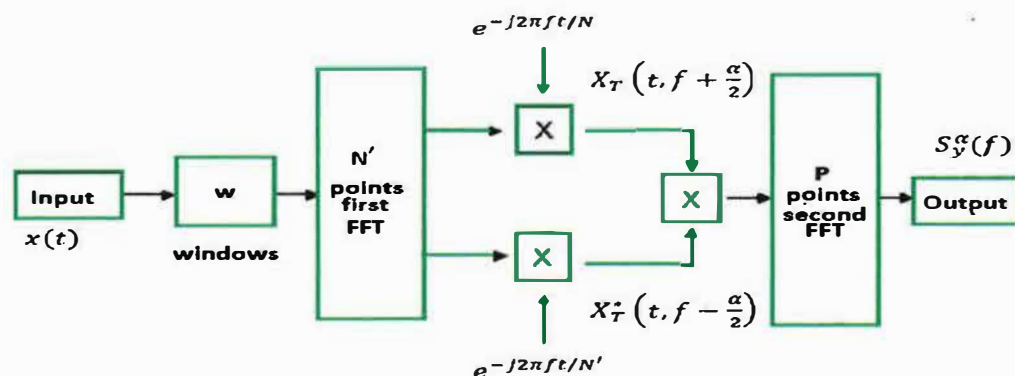


Figure 7-6: Description of the FFT Accumulation Method Algorithm [173].

The algorithms consist of three basic stages: computation of complex demodulation (divided into data time window, sliding N' point Fourier transform and baseband frequency translation sections), computation product sequences, and smoothing of product sequences. In FAM algorithms, spectral components of a sequence, $x(t)$ are computed using (eq. 7.17). Two components are multiplied to provide a sample of a cyclic spectrum estimate representing the finite channel pair regions in the bi frequency plane. A sequence of samples for any particular area may be obtained by multiplying the same two components of a series of consecutive short-time sliding FFTs along the entire length of the input sequence. After the channelisation performed by N' -point FFT sliding over the data with an overlap of L samples, the output of the FFTs are shifted in frequency in order to obtain the complex demodulated sequences. Instead of computing an average of product of sequences between the complex demodulated signals, they are Fourier transformed with a P -point (second) FFT to get the final version of SCF estimate.

7.3.3.3 Strip Spectral Correlation Algorithm (SSCA)

In SSCA, the complex demodulated signals are multiplied directly with the conjugate of the signal itself. Each multiplication is then smoothed with an N point FFT and then summed up. The SSCA method block diagram is presented in Figure 7.7. The design parameters for the cyclic spectral estimation are presented in Table 7.2 from time smoothing method point of view, which is used later in this Chapter for simulation modelling.

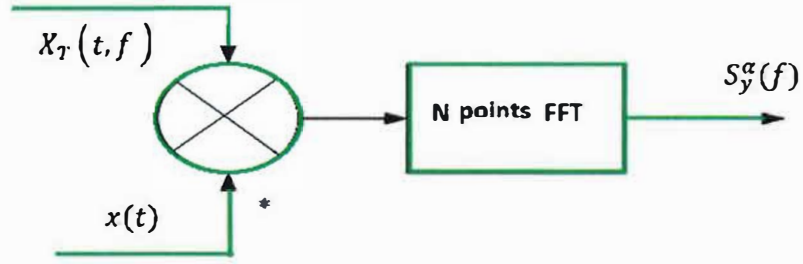


Figure 7-7: Description of the SSCA Method Algorithm [166], [167].

Table 7.2: Time Smoothed Method Design Parameters [167].

Name	Notation	Important criteria: at a glance
Time span or observation time	Δt	$T = N' T_s$ $T_s = 1/f_s$ $f = \left(\frac{f_1 - f_2}{2}\right)$ $\alpha = f_1 - f_2$ $\Delta f = \frac{1}{T} = \frac{1}{N' T_s} = \frac{1}{\Delta t}$ $\Delta t, \Delta f = \frac{N}{N'} \gg 1$ $\frac{1}{\Delta \alpha} \cong \Delta t \gg T \cong \frac{1}{\Delta f}$ $L \geq \frac{N'}{4}$ $N = PL$
Tapering window length	T	
Size of the sliding point FFT	N'	
Sample duration	T_s	
Sampling frequency	f_s	
Spectral frequency	f	
Cyclic frequency	α	
Frequency resolution of SCF	Δf	
Cyclic frequency resolution	$\Delta \alpha$	
Length of the sequence or size of the data vector	N	
Decimation overlap parameter	L	
Size of second FFT point	P	

7.4 Channel Noise Analysis

In a typical wireless communication channel, noise sources can be divided into two groups: multiplicative and additive [178]. Additive noise comes from different sources such as thermal agitation within the receiver, cosmic radiation and interference from other transmitters and other electrical appliances. Multiplicative noise comes from various processes encountered by the transmitted signal before reaching the receiver antenna. Fading is a physical phenomenon where the multiple signals that are reflected, refracted or diffracted from different sources sum up together causing time-varying attenuation/amplification of the signal power. In urban areas, signals are also blocked by buildings and trees which further deteriorate the received signal power. Fading can be broadly classified into three different subgroups [178,179] as follows. Path loss (also known as very slow variations) is mainly due to the change in the distance between the transmitter and receiver. Slow fading (also known as shadowing, long term variations or large-scale fading) is mainly due to the momentary blockage of the LOS signal by trees, mountains, building, etc. Fast fading (also known as multipath fading, short term

variations or small scale fading) is mainly due to the constructive and destructive nature of the multiple signals arriving at the antenna due to reflection, diffraction, refraction and scattering. Fig. 7.8 shows a graphical representation of different types of fading that occur in reality.

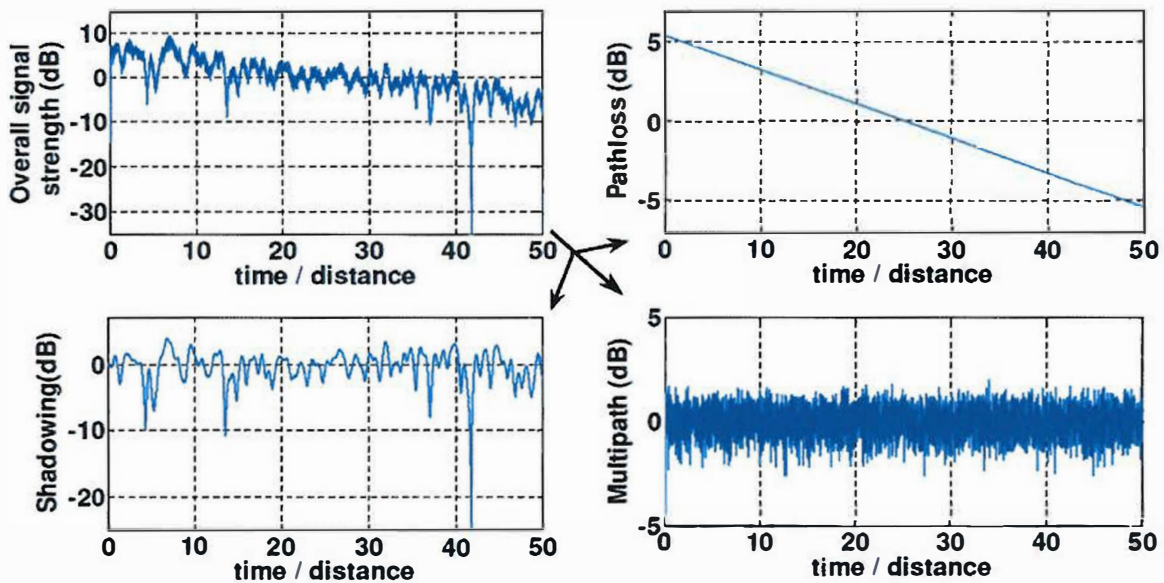


Figure 7-8: Different Kinds of Fading Processes Such as Path Loss, Shadowing and Multipath that can occur in a Real Scenario.

The different nature of those phenomena requires the use of various mathematical tools including, stationary and cyclostationary analysis. There has been very limited research on a SCF-based path model in the context of cyclostationary sensing to identify the effects of noise like the PSD based log-normal shadowing model above. Therefore, the features of SCF under path loss, shadowing and multipath need to be investigate by varying distance and locations.

7.4.1 Path Loss Model and Ranging

Path loss models are generally used to relate expected signal strength to path length in wireless applications. Such models have been widely implemented in ranging, localisation, and location tracking systems. A range of extension models have been proposed to enhance the performance for various environments and applications. Nevertheless, path loss exponent retains its significance at the main factor in the model regardless of how the model is varied. Based on the nature of the exponent of the model, an inaccurate path loss exponent amplifies the error if it is used to estimate distance from received signal strength. Therefore, measurement of an accurate value for path loss exponent becomes very important as it directly influences the output of distance estimation. The path loss can be determined in dB as [182]:

$$PL = \overline{PL}(d_0) + 10n \log_{10} \left(\frac{d}{d_0} \right) + X_\sigma \quad (7.18)$$

where \overline{PL} is the average path loss in decibels, n is the path loss exponent which is the rate at which the path loss increases with distance increases, d_0 is the close-in reference distance and d is the transmitter-receiver separation distance. X_σ is a zero-mean Gaussian distributed random variable (in dB) with standard deviation σ which also varies depending on environments [180]. This statistical distribution random variable is used to show unpredictable shadowing and multipath effects.

7.4.2 Path Loss Exponent Estimation

The estimation of path loss exponent relies on the measurements of the received signal strength together with the corresponding locations. There are two types of method used to investigate the path loss exponent. One method is to calculate the path loss exponent using a number of received powers and the corresponding distances. This method is called one-line measurement as the collection of RSSI values was done by locating the transmitter and receiver along a straight line, and varying the distance between them. Another method is to directly update the environmental parameters using a gradient descent technique which is named online-update measurement [181]. For one-line measurement, received powers must be collected along the line with distance marked on the line. The collected signal strength values represent the received power at each marked distance along the line. Theoretically, every room/area has only one set of environmental parameters. Note that a small change in path loss exponent n may leads to drastic change in distance estimation. Table 7.3 shows path loss exponent values for different environments [180]. From table 7.3 and equation (7.18), the fact that location (environment) and distance affect the path loss is easily noticed. Overall, the path loss exponent n and X_σ indicate the level of multipath and shadowing. The main determinate of path loss is distance.

Table 7.3: Path Loss Exponents for Different Environments [180].

Environment	Path Loss Exponent (n)
Free Space	2
Urban area cellular radio	2.7 to 3.5
Shadowed urban cellular radio	3 to 5
Inside a building – Line of Sight	1.6 to 1.8
Obstructed in building	4 to 6
Obstructed in Factory	2 to 3

7.5 Methodology

This section describes the methodology of the Chapter. A detailed methodology is discussed defining cyclostationary feature analysing system and their components, parameters and factors. Next, the test bed is described and the experimental design and evaluation techniques are covered.

7.5.1 Cyclostationary Feature Analysing System

The System Under Test (SUT) is a “Cyclostationary Feature Analysing System” and it consists of a receiver and a channel which is the propagation path of the signal. The receiver of the system receives a signal transmitted through the channel and analyses it using the SCF. The receiver includes a software defined radio (USRP2) which receives the signal and a laptop which runs SCF codes to analyse the received signal using Matlab programs. Figure 7.9 shows the framework structure which involves: system services and metrics, workload parameter and system parameters. System services and metrics are provided to analyse the cyclostationary features of the received signal using the SCF. Outcomes of system are PSD and SCF values of received signal at certain frequency f and cycle frequency α coordinates in area $\alpha \neq 0$ and $\alpha = 0$.

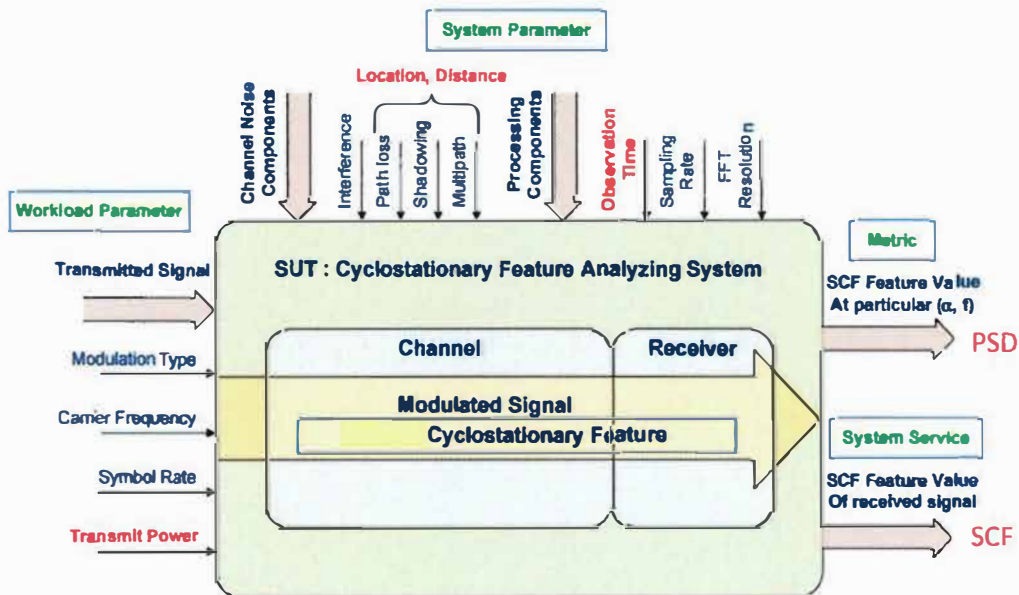


Figure 7-9: Framework Structure of Cyclostationary Feature Analysing System.

The outcome value would be used to determine the presence of expected signal in the channel. A workload parameter is a request for system services, which means that the workload in this system is a particular configuration of transmitted signals in a channel. In the research, the signal configuration is the set of parameters that define the signal, which includes modulation

type, carrier frequency, symbol rate and transmitted power. These parameters affect the SCF feature values of the received signal. All other things that affect the feature value but are not part of the workloads (such as observation time) belong to system parameters. System parameters are parameters within the system boundary that affect the SCF feature values of the received signals. System parameters include channel noise components (such as path loss, shadowing, multipath, interference) and processing components at receiver (such as observation time, FFT resolution, sampling rate etc.). Factors are a subset of the system parameters and workloads that are varied during the experiments. In order to identify the difference between real world and theoretical SCF features, that is, in order to identify effects of a real world transmission channel, we vary the levels of the transmitter/receiver separation distance as well as their locations. This is because separation distance and location affects the path loss, shadowing, and multipath resulting in separating out channel noise. The SNR is varied at the fixed distance and location to distinguish the performance of SCF and PSD under low SNR environments from theoretical and simulation based researches. Lastly, the observation time is changed to verify how it affects the statistic components of SCF feature values [182] and to verify that the noise floor of SCF is lowered as the observation time increases improving the performance of SCF under low SNR environments [183]. Observation time is related to the number of samples that are used to get one SCF value in the signal analysis, thus the observation time is controlled by the number of samples. As each type of environment has different path loss exponent n , the location factor here is varied corresponding to the environments in the Table 7.4.

Table 7.4: Location Factor.

Environment		Location	
In-door	In building line-of-sight	LOS	PhD Room School of Engineering
	Obstructed in building	non- LOS	Hall way School of Engineering
Out-door	Free space	LOS	Anechoic chamber Football field
	Shadowed	Non-	University Campus
	Urban area	LOS	

7.5.2 Experimental Setup

The measurement setup employed in this study, shown in Figure 7.10, is modular and capable of performing cyclostationary detection based on CFD of sensed signals. It consists of two main parts, IQ data acquisition (measurements part) and post-processing (implementation of the algorithms needed for cyclostationarity based detection). The goal of the IQ data acquisition phase is twofold; gather sufficient measurement data at the chosen spectrum band and prepare it for processing. The post processing stage is accomplished using Matlab programs containing functions for importing data from measurements acquired in the field and processing them. The Matlab system block diagram illustrated in Figure 7.11 describes how the data flows are analysed inside the Matlab program. The test bed setup uses the strip spectral correlation algorithm (SSCA) for CFD estimation. The SSCA algorithm is a computationally efficient algorithm suitable for practical implementations using measurements of the received signal at different positions and different environment from transmitter. The measurement was conducted using two elements: Receiver platform and Transmitter platform. The receiver platform used two types of commercially available spectrum sensing equipment: Agilent N9030A PXA signal analyser [184] and a USRP2 [185]. The transmitter platform was representing by using Agilent E4438C vector signal generator [184]. It generates 2-FSK signal with controllable symbol rate and transmit power. A symbol rate of 20 kS/s at a 2.415 GHz carrier frequency varying with transmit power was used.



Figure 7-10: Test Bed for Experiments.

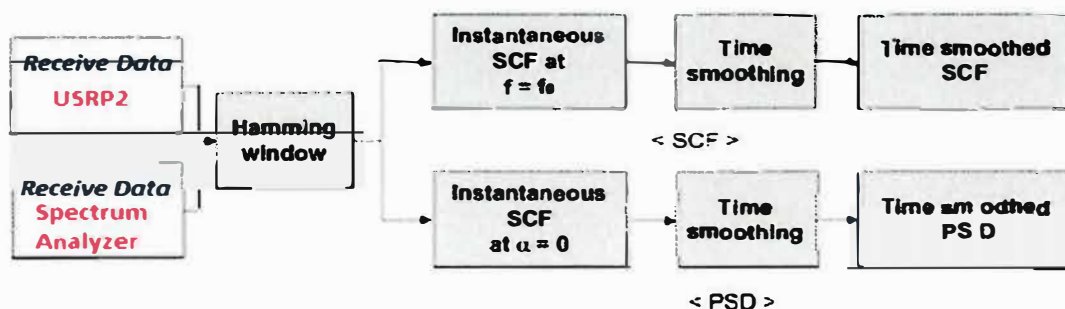


Figure 7-11: Matlab System Block Diagram.

The USRP2 is a software defined radio with capability to perform a limited number of high speed, high precision general purpose signal processing tasks such as decimation, interpolation, digital up conversion and down conversion. A daughterboard, the RFX 2400, which covers from 2.3 to 2.9 GHz frequency range, is used. In the experiments, USRP2 continuously receives a 2.415GHz signal at 100MS/s sampling rate and decimate the sampled signal with the decimation factor 125, resulting in 800 kS/s sampling rate. The host computer connected to the USRP2 is a laptop running the Matlab program, which receives transferred signal data in frame format, processes the data, and shows/records the SCF values in real time. During the research, the USRP2 block set receives data continuously from USRP2 and sends the data to signal blocks and embedded blocks which analyses the received data by calculating and recording the SCF values particular (f, α) position in real-time. The Simulink blocks in Appendix Figure A.3 describe how the data flows are analysed. The Simulink blocks in Appendix Figure A.3 describe how the data flows are analysed. Through the USRP2 receiver block, centre frequency, gain, decimation factor and output data type are controlled. The received samples go through the hamming window, and then its instantaneous SCF is calculated using equation 6.17. The instantaneous SCF is analysed both at particular frequency value, set to centre frequency of signal, which is for SCF and at particular alpha value set to 0, which is for PSD. The Simulink blocks in Appendix Figure A.3 describe how the data flows are analysed. Two things were investigated to validate the USRP2. Firstly, a frequency offset was found in the USRP2, which occurs from USRP2 hardware itself estimated to be related to a thermal issue and is different for each USRP2 and its decimation factor. This frequency offset was manually determined and manually compensated by specifying the centre frequency as (desired centre frequency – frequency offset). Secondly, the validation of correct working of USRP2 was done by comparing the PSD of transmitted signal from USRP2 with that from signal analyser.

7.6 Analysis and Results

The experiment are divided into the 4 separate parts, including performance measurement overview (section 7.6.1), path loss analysis (section 7.6.2), SNR analysis and observation time analysis (both in section 7.6.3).

7.6.1 Performance Measurement Overview

Figure 7.12, presents the results of the experimental detection using cyclostationary sensing for 2.415 MHz signals as well as energy sensing. The signal transmitted from Vector Signal Generator with (carrier frequency 2.415 GHz, frequency deviation 20 kHz and modulation 2-FSK), and received by USRP2 under two conditions: line of sight (LOS) and non-line of

sight (NLOS) conditions. It shows the received signal FSK plot for the signal transmitted by the vector signal generator. Figure (7.12-A) and (7.12-B) depicts the CPS (cycle power spectrum) estimates for the cyclostationary sensing of ISM signal in LOS conditions with two different signal to noise ratios (SNR=12dB and SNR=4dB) at 1m distance and 6m distance from transmitter respectively. CPS is presented at frequency of 2.415 GHz for a bandwidth of BW= 36 kHz. From both Figures, we clearly identify the different frequency and cyclic frequency components of the CPS. The cyclostationary feature is observed at the cyclic frequencies of $\alpha = \pm 20\text{kHz}$, where $\alpha = 0$ represents the standard power spectrum (energy sensing) of the received signal with respect to frequency f . Figure (7.12-C) depicts the CPS estimates for the cyclostationary sensing of ISM band signal in NLOS conditions with SNR= -3dB at 6m distance from transmitter. In comparison to Figure (7.12-A, B and C) we observe a similar cyclic feature of the spectrum but with a rough density surface due to signal fading and shadowing. Note that, although the signal peaks become indistinct between signal and noise as the SNR decreases, special at $\alpha = 0$, it can still detect the cyclic frequencies of $\alpha = \pm 0.2(\pm 20 \text{ kHz})$. Overall, in modulations with a purely real time-domain baseband signal, such as FSK, there will be a strong feature at $f = 0$ and $\alpha = \pm 0.2$. In the absence of noise, this feature is comparable to the PSD feature. In the presence of noise, the PSD is washed out, but this feature (and all other SCF points for $|\alpha| > 0$) is still defined.

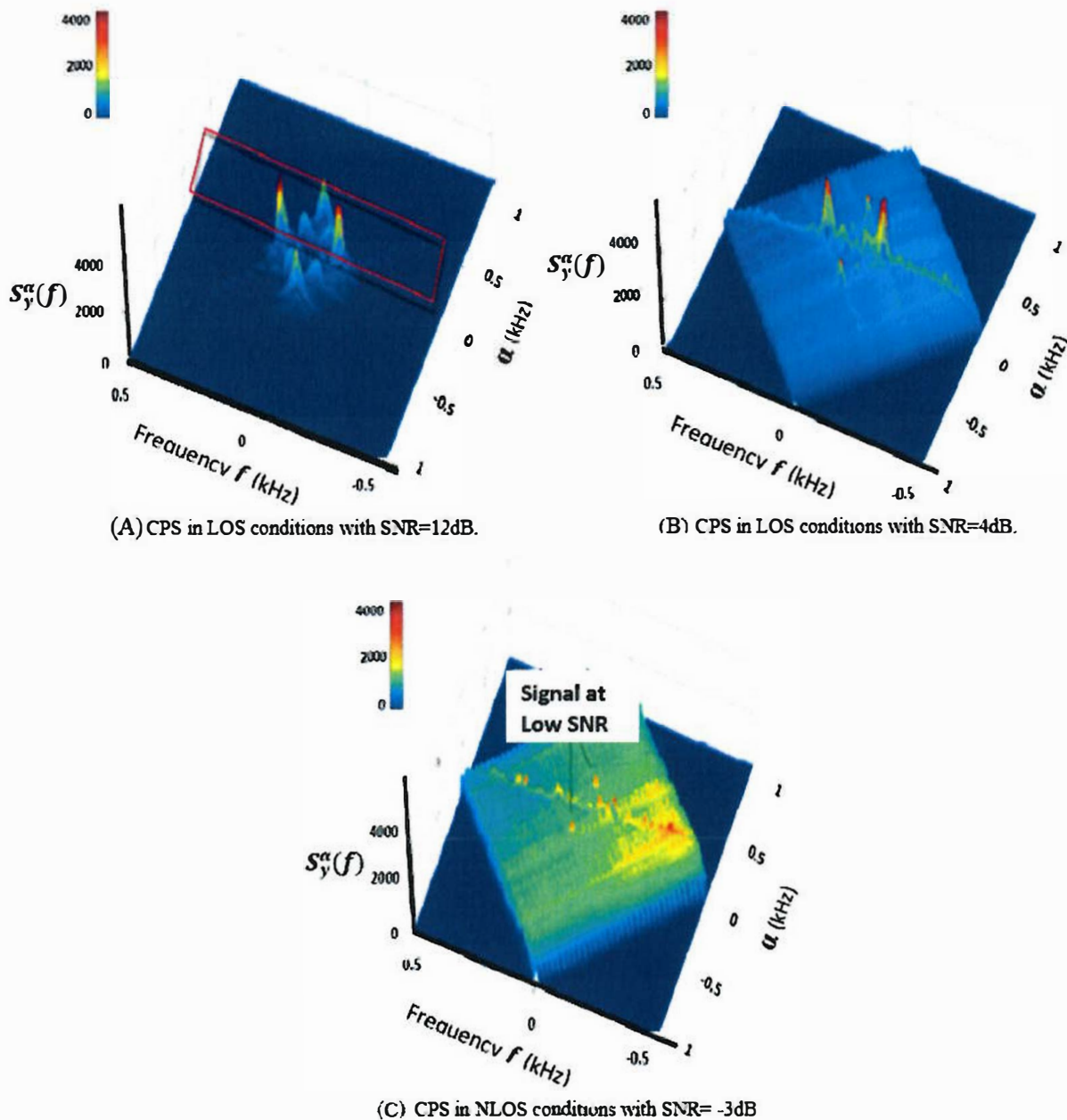


Figure 7-12: Received Power vs Frequency and Cyclic Frequency

7.6.2 Path Loss Exponent Analysis

In this section, the behaviour of path loss, path loss exponents and variances of the SCF/PSD obtained under different scenarios at the University of Hull, such as open sky scenario/outdoor and indoor scenario. Indoor measurement was undertaken on the second floor of the School of Engineering building. Outdoor measurements was undertaken at main entrance and on the football field of the University. The measurement locations and the building layout are shown in Figure 7.13. The SCF and PSD are investigated at the same time to compare their path loss

under the same conditions. To see the effects of noise, the path loss exponent and variance of the features are analysed. Firstly, path loss trends are analysed to see path loss exponent.



Figure 7-13: Experiment Setup for Path-Loss Measurement Locations at Hull University.

The two states are the "path loss state" (decreasing value) and the "noise floor state" (steady value), both are investigated by looking at the SCF/PSD feature value trends. Generally, transitions from the path loss state to noise floor happen smoothly as distances get longer. However, to analyse each state, the smooth trends are analysed into one path loss trend and one constant noise floor trend. That is, each of the states is expected to have one exponential line with distance which reflects trend of each state. Secondly, variances of the SCF/PSD measurements are obtained by averaging variances of measurements and comparing them. The reason why variance of the SCF/PSD is investigated is that it reflects small fluctuations which are mainly due to multipath. Additionally, during the experiments, observation times are varied in three different levels (512, 8192, 131072 samples) to see the effects of observation time on path loss by looking at path loss exponents at each observation time. Path loss exponents at each observation time are presented as Root Mean Squared Error (RMSE) of the LS fit to capture whether the LS fit of the path loss is comparatively accurate or not. For path loss plots, results at 8192 sample observation time are used.

7.6.2.1 Open Sky Scenario (LOS Football Field)

The first location investigated is football field, University of Hull, where reflection is minimised as well as external interference and noise. The place is close to 'free space' with nothing around apart from ground reflection and LOS guaranteed as seen in Figure 7.14-B. In other words, this football field is expected to have little multipath and shadowing effects compared to other environments with the exception of the anechoic chamber room. That is, results from other sites will be compared to the results from this location not for comparing

overall performance in certain area, but for comparing effects of multipath and shadowing. Figure 7.14-A shows that the SCF path loss exponent was smaller than the PSD path loss exponent by 0.1. By comparing Figure 7.1 it can be clearly observed that, path loss is the major contribution. This could mean that in the environment like the open sky scenario with almost no multipath and no shadowing, the SCF has more distinct features than the PSD. Figure 7.14-C shows Fit curve slopes. It is showed that for every length of observation time, the SCF had a lower path loss exponent than the PSD. Under open sky conditions, amplitude variance of the SCF is smaller than that of the PSD at every observation times. SCF variance from (-95dB to -110dB) and PSD variance from (-91dB to -102dB) with observation time (512 sample to 131072). It can be said that without any multipath and shadowing the SCF showed less variance than the PSD.

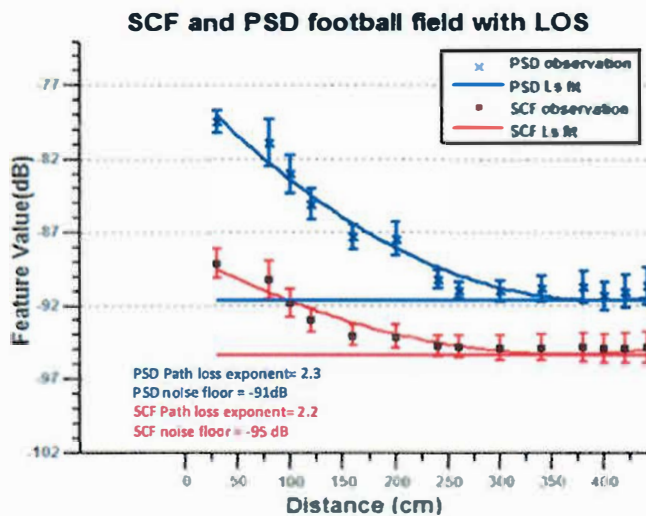


Fig.7.14-A



Football field

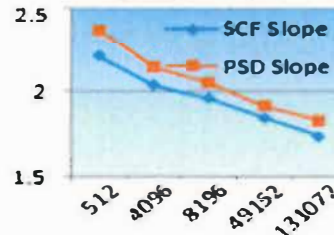


Fig.7.14-C: Fit curve slopes

Figure 7-14: A) SCF/PSD Path Loss at Football Field with LOS B) Photographs B) Fit Curve Slopes

7.6.2.2 Open Sky Scenario (Reflector and Shadowing)

Figure 7.15 shows a data collection setup that was performed in front (main entrance) of the Middleton Hall at the University of Hull. Two different data collections were performed; single LOS outside building position was chosen to model "urban area" with buildings around, and NLOS outside building position was chosen to model "shadowed urban area" with buildings around and LOS not guaranteed. Multiple datasets were collected on each location. In this location the Middleton Hall acts as reflector for those signals arriving from the right side of the building, as well from ground. The SCF path loss exponent was smaller than the PSD path loss exponent by 0.1 as in Figure 7.15. That is, overall, the SCF of path loss exponent demonstrated

better performance the PSD. When compared to the results of open sky scenario, the path loss exponent of the SCF increased by 0.1 and the PSD decreased by 0.1. Although SCF shows slightly greater path loss exponents than the PSD for every observation times, overall change of the observation time does not appear to affect either PSD or SCF path loss exponent. The slow variations cannot be attributed to the shadowing as there were no signal blocking elements during the entire data collection interval. In the shadowing scenario, shadowing is expected to affect the path loss more than LOS guaranteed cases. The SCF path loss exponent was smaller than the PSD path loss exponent by 0.1 as in Figure 7.16. Both the SCF and the PSD showed similar performance, in terms of overall noise effects such as distance dependent path loss, multipath, shadowing, because the 0.1 difference in the path loss exponents is small. However, when compared to the results of open sky scenario, the path loss exponent of the SCF increased by 1.7 and the PSD increased by 1.5. The SCF seems to have more noise effect than the PSD in this location. And, for every observation time the SCF keeps steeper than the PSD.



Outside Building with LOS



Outside Building with NLOS

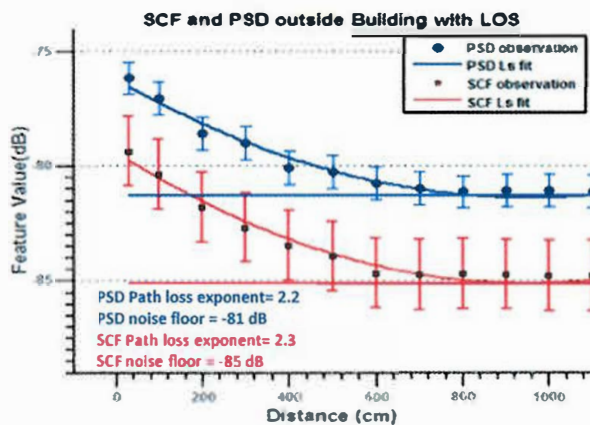


Figure 8-15: SCF/PSD Path Loss outside Building with LOS.

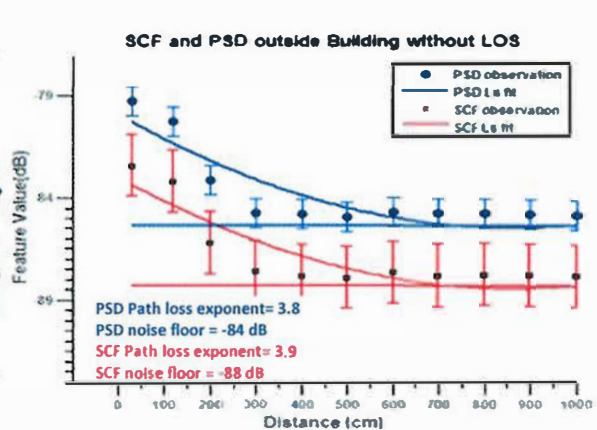
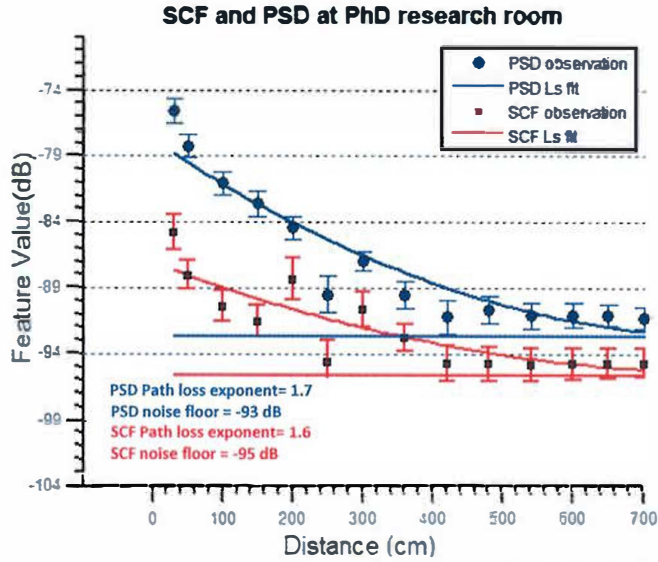


Figure 8-16: SCF/PSD Path Loss outside Building with NLOS.

7.6.2.3 Indoor Scenario (LOS/NLOS)

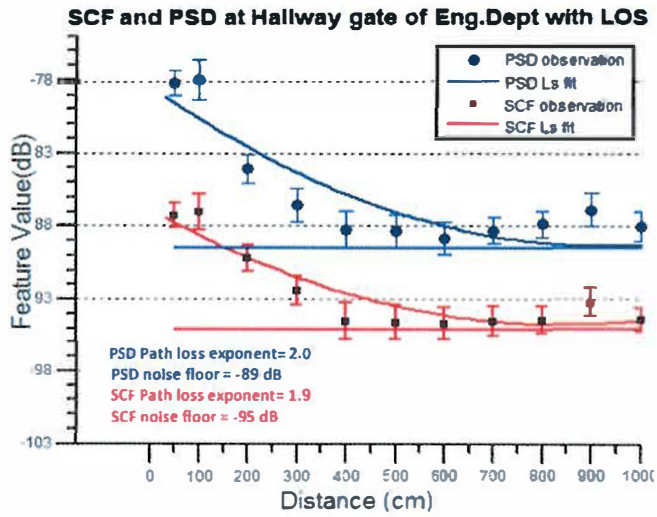
Figures 7.17, 7.18 and 7.19 show the data collection performed in an indoor scenario inside the School of Engineering at the University of Hull. Data collections were performed in two

different ways (LOS and NLOS). The first dataset was collected inside PhD Researcher Room. The second data collection, under LOS and NLOS conditions at The Hallway gate of School of Engineering. In an indoor scenario, the signal is strongly attenuated by the structures of the building. Therefore, long coherent integrations have to be performed for detecting the signals indoors. PhD Researcher Room was chosen to model "obstructed in factories" environment. This model includes the statistics of multipath propagation characteristics for cases of light and heavy clutter in a factory such as thin walls and desks. Obstruction between transmitter and receiver is same up to a certain point of distance, but with distance increased, obstructions between them increased. SCF path loss exponent at PhD Room measurement was smaller than the PSD path loss exponent by 0.1 as in Figure 7.17. By comparing PhD Researcher Room result with open sky scenario, both the SCF and the PSD had smaller path loss exponent than those in open sky scenario. Respectively, SCF and PSD decreased by 0.5 and nearly 0.6. Therefore, this might mean that such PhD Room environment the SCF is more robust to multipath and shadowing effects since the PSD path loss exponent decreased slightly further. The Hallway gate of School of Engineering (Eng.Dept with LOS) can be considered as indoor LOS environment with well-built multipath components. In this case, the SCF path loss exponent was smaller than the PSD path loss exponent. The path loss exponent of SCF decreased by 0.2 compared to open sky scenario result, whereas the path loss exponent of the PSD decreased by 0.3. With this result we could conclude that in an environment like the hallway with multipath, the SCF is slightly robust to multipath. Moreover, there are slight changes in path loss exponent for both SCF and PSD as the observation time changes. Also, the variance of the SCF was smaller than the PSD for every observation time. Hallway gate of Eng.Dept without LOS is considered to model "obstructed in building" environments. Obstructions at this point are thicker/denser obstructions than previous experiment at the PhD Room. Since the LOS is not guaranteed, shadowing is expected to affect the path loss more than in LOS-guaranteed cases. But, there are still multipath effects as well. In this case, the obstruction was a concrete wall which is dense, whereas in PhD Research Room, the obstruction was a cubicle wall which is sparse. In a Hallway gate without LOS, the SCF path loss exponent was less than the PSD path loss exponent by nearly 0.2 as in Figure 7.19. That is, overall, the SCF showed a small performance advantage over the PSD. When compared to the results of open sky scenario, the SCF increased by 0.4 and the PSD increased by nearly 0.5. This indicates that the SCF was slightly less affected by multipath and shadowing than the PSD in this location.



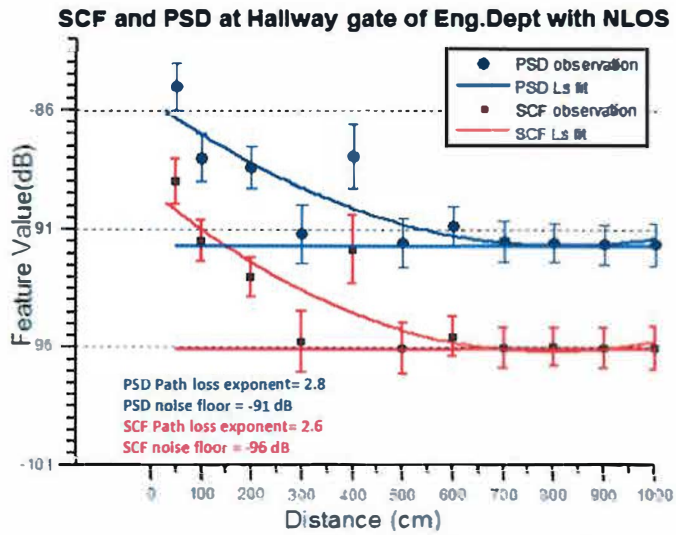
PhD Researcher Room

Figure 7-17: SCF/PSD Path Loss at PhD Researcher Room.



Hallway gate of Eng.Dept with LOS

Figure 7-18: SCF/PSD Path Loss at Hallway Gate with LOS.

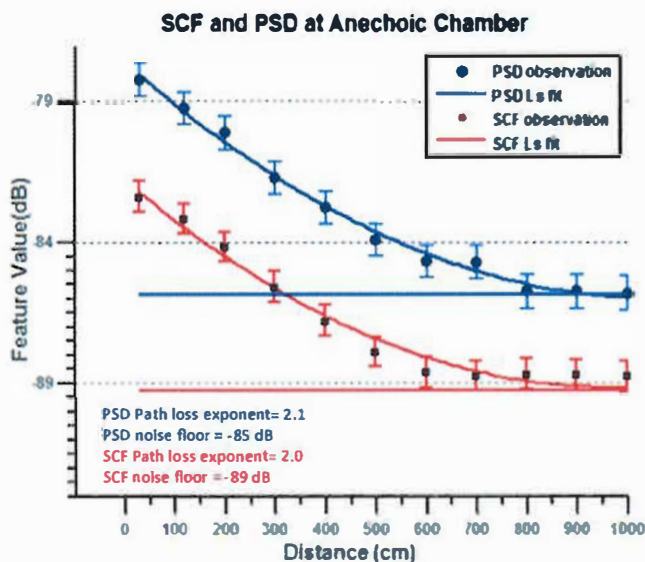


Hallway gate of Eng.Dept with NLOS

Figure 7-19: SCF/PSD Path Loss at Hallway Gate with NLOS.

7.6.2.4 RF Shielded Room

In the shielded room reflections were suppressed using Radio Observing Material (ROM) so it can be considered as nearly a quiet open space. Moreover, the USRP2 receiver surrounded by RAM to have the least amount of noise and reflections. This place is close to "free space" with nothing around and LOS guaranteed as seen in Figure 7.20. In other words, this place is expected to have very little multipath effects. In the RF Shielded Room, the SCF path loss exponent was similar to the PSD path loss exponent. That is, overall, the SCF showed better performance than the PSD. When compared to the results of football field, the path loss exponent of the SCF decreased by 0.1 and the PSD decreased by 0.2. And for every observation times, the SCF keeps less steep path loss exponents than the PSD.



RF Shielded Room

Figure 7-20: SCF/PSD Path Loss at Anechoic Chamber.

7.6.2.5 Brief summary

At seven respectively different radio propagation environment locations, measurements were taken varying distances. Table 7.5 shows path loss exponents of the SCF / PSD at each locations and path loss exponent differences between Open Sky Scenario (Football field with LOS) and each location, which may reflect performances of SCF/PSD. Because the performance can be different from robustness to noise effects, therefore, path loss exponent differences are investigated, which possibly reflect the robustness to noise effects. Positive values in the difference mean increase of path loss exponent and negative values mean decrease of path loss exponent related to the reference value. But, since we only look at magnitude of the differences as a result of noise effect, whether it is a positive value or a negative value doesn't matter. Green-colored cells in the table indicate smaller value when comparing between the values at

the SCF and the PSD. At four out of six locations, the SCF showed smaller path loss exponents which could indicate that, in these four places, the SCF showed better performance. Moreover, in terms of robustness to noise effects, three places out of six (Grey-colored cells in the table), the SCF showed smaller differences, which could indicate more robustness to noise effects. Since the path loss exponent differences of the SCF are consistently smaller than that of the PSD, we could say that SCF is more robust than PSD in general. However, in terms of variance at each location, the SCF exhibited smaller values than the PSD consistently, which could indicate robustness of SCF to noise effects, especially multi-path.

Table 7.5: Path Loss Exponents in Each Locations, Path Loss Exponent Difference & Variance.

		Football Field LOS	Outside Main Entrance LOS	PhD research Room	Hallway gat LOS	RF Shielded Room	Outside Main Entrance NLOS	Hallway gat NLOS
Path loss exponent	SCF	2.2	2.3	1.6	1.9	2.1	3.9	2.6
	PSD	2.3	2.2	1.7	2.0	2.1	3.8	2.8
Path loss exponent different	SCF	-	0.1	-0.6	-0.2	-0.1	1.7	0.4
	PSD	-	-0.1	-0.6	-0.3	-0.2	1.5	0.5
Smaller Variance	SCF	SCF	SCF	SCF	SCF	SCF	SCF	SCF

7.6.3 SNR and Observation Time

The performance of SCF over PSD is verified against real world signals and background noise by varying the SNR for each observation time to compare against previous simulation. SNR was varied by controlling the transmit power of signal. The receiver analysed the collected signal in terms of the SCF and PSD, the observation time was varied at four different levels. Figure 7.21-A shows SCF feature values of the experiments. The feature value decreases in dB scale as SNR decreases. From a certain point of SNR, the feature values are almost the same values, which is the noise floor. In terms of observation time, it is shown that the observation time affects the position of starting point of SCF floor (blue box in the Figure). That is, the noise floors of SCF features from every observation time start at slightly different SNR level. The observation time also decreases the SCF value both in high and low SNR environments. This result is also somewhat different from Figure 7.1 in section 7.1, which showed the same SCF features for different observation time under high SNR environment. Comparing to the PSD feature in Figure 7.21-B shows the almost same starting point position of PSD floor. It is

shown that the observation time does not affect the position of starting point of PSD floor (blue box in the Figure). That is, the noise floors of PSD features from every observation time start at nearly at same SNR level. These results provide evidence that show that the SCF outperforms the PSD. In conclusion, with real world signal and background noise, it appears that the SCF has better performance than the PSD and shows a distinct feature in low SNR environment.

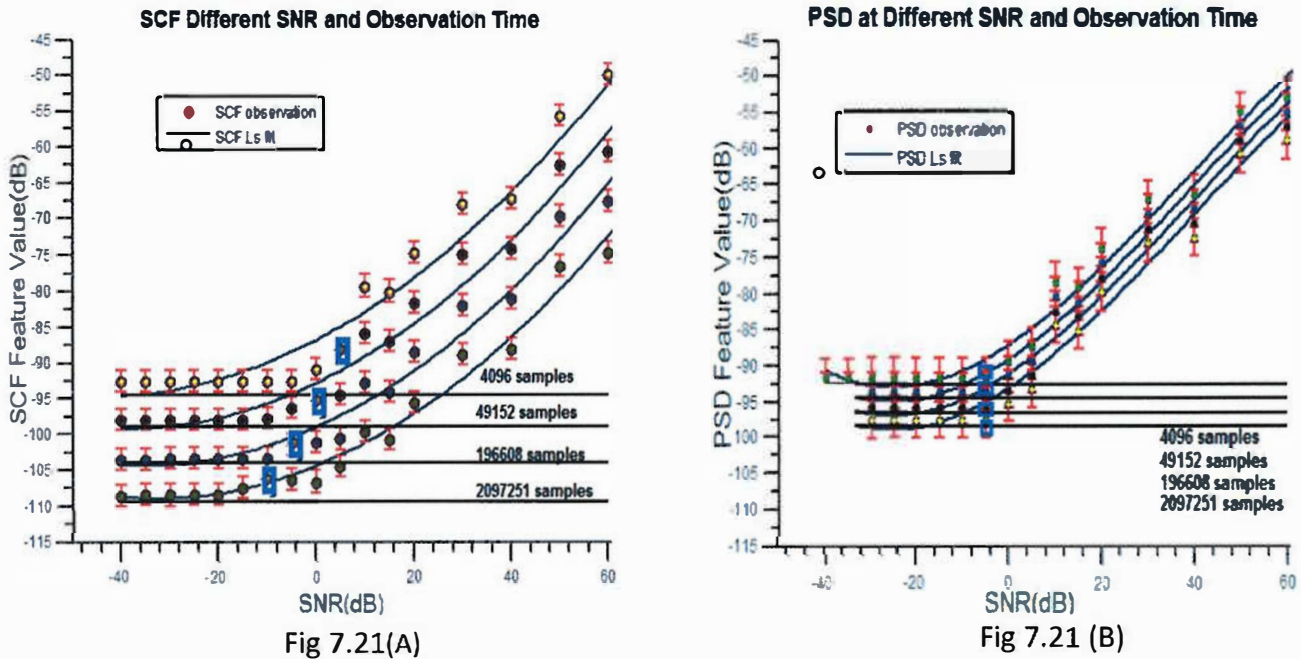


Figure 7-21: SCF Vs PSD with Varying SNR and Observation Time.

7.7 Chapter Summary

In this Chapter we have investigated the feasibility and performance of the cyclostationary feature detection for spectrum sensing, which included a theoretical background and experimental results for cyclostationary detection using SCF. Firstly, introduction and background of cyclostationary process was discussed. Then, we go into technique details of computationally efficient algorithms of SCD and channel noise analysis. The main goal of this Chapter was to identify cyclostationary features of digitally modulated signals through empirical measurements using features of the spectral correlation density function (SCF), compared with energy detection using features of the power spectral density (PSD). Overall, according to path loss measurement resulting process, the magnitude of the SCF features were obtained from many locations and compared to those from the PSD. The path loss exponent and variances of the SCF features were investigated. It was found that, from the path loss exponents, that it is conclusive that the SCF features are more robust to noise effects than the PSD features. Moreover, from the feature variances, it was found that the SCF does tend to be

more robust to noise effects, especially multipath, because it has smaller variance than the PSD features. According to SNR and observation time result, the SCF/PSD features were measured under varying SNR levels with different observation times. It was found that, under real world noise, SCF shows better performance under a low SNR environment compared with PSD.

Part IV: Simulation Phase, Cooperative Wideband Spectrum Sensing

*Unity is strength... when there is teamwork and collaboration,
wonderful things can be achieved.*

Mattie Stepanek

This part contain one chapter

CHAPTER 8: Cooperative Wideband Spectrum Sensing

Chapter

8

Cooperative Wideband Spectrum Sensing

8.1 Introduction

Several signal processing techniques are being used for spectrum sensing mentioned in the previous Chapter. In a cognitive radio network (CRN), the sensing performance of a single CR is often reduced by the presence of multipath fading, shadowing, and receiver uncertainty in the channel. To mitigate these effects, cooperative or multiuser sensing techniques are being used [186,187,188]. CR can detect the signals in a single/narrow frequency band or multiple/wide frequency bands. In the recent past, most studies have focused on cooperative/distributive detection approaches. However, they are confined to the detection of signals in a narrow band [189]. In order to improve the opportunistic throughput of the cognitive user network, a CR user must detect the signals in multiple frequency bands to reduce the sensing delay. This also provides better opportunities for CR users to transmit their signals without considerable delay in case the licensed user starts transmission in the channel suddenly. The study in [190] reports the sensing time required to achieve maximum throughput in multiband or wideband situations.

In this Chapter, we propose cooperative wideband spectrum sensing schemes with multi-bit hard decision in cognitive radio, which lead to energy-efficiency and time-saving using two stages in the spectrum sensing process. To check if the primary user exists or not in the wideband spectrum, only one stage of coarse spectrum sensing is needed, by which the sensing time and energy are saved. Then, the second stage of fine spectrum sensing will be performed

to increase the spectrum sensing accuracy. Furthermore, only multi-bit decisions are sent by each secondary user to minimise the communication overhead. The proposed algorithm fully utilises the local decisions of the coarse detection, and its energy consumption is further reduced with its sensing performance. Simulation results are presented to show that the sensing time and energy consumption are both reduced significantly in the proposed schemes. The distinct features and contributions of this Chapter are as follows:

- ❖ We propose a system model for wideband cooperative spectrum sensing with multi-bit hard decision in cognitive radio using a multi resolution spectrum sensing (MRSS) technique, where the power consumption and the time of sensing are considerably reduced.
- ❖ Based on the first proposal of wideband cooperative spectrum sensing with a multi-bit hard decision algorithm, another algorithm is proposed using a two-stage adaptive sensing technique. This algorithm uses an adaptive technique at the first stage coarse detection, which presents more sensing accuracy compared to the first algorithm, with reliable detection performance.
- ❖ The time-saving and energy-efficiency performance of the proposed two schemes are analysed and the sensing time and energy consumption of the proposed schemes are shown to be reduced significantly compared to the conventional cooperative sensing scheme.
- ❖ Extensive simulation results are presented to illustrate the effectiveness of the algorithms in reducing sensing time, energy consumption and the rules of parameters setting in the proposed algorithms.

The remainder of this Chapter is organised as follows. In section 8.2, the challenges in non-cooperative detection are described and cooperative spectrum sensing schemes are introduced on section 8.3. In sections 8.4 and 8.5 the wideband spectrum sensing and traditional cooperative spectrum sensing schemes respectively are presented. In Section 8.6, a proposed system model for wideband cooperative spectrum with multi-bit hard decision in cognitive radio using multi resolution spectrum sensing (MRSS) technique is introduced. In section 8.7, a proposed system model for two-stage adaptive spectrum sensing presented. In section 8.8, the proposed system model for wideband cooperative spectrum sensing with multi-bit hard decision using two-stage adaptive sensing are explained. Finally, we conclude this Chapter and present the main points in Section 8.9.

8.2 Challenges in Non-Cooperative Sensing

The key challenges associated with single-user-centric transmitter detection schemes that prevent them achieving the promised sensing performance under practical conditions are:

Firstly, restricted sensing ability, CRs need to sense their multidimensional radio environment with limited sensing resources. In general, CRs have no information regarding the possible primary communication over a licensed band. This makes spectrum sensing for cognitive radio a very challenging task. **Secondly**, high detection sensitivity requirements, where detection of low-power primary signals in itself is a difficult task, which becomes even more challenging under uncertain, channel conditions. In a typical wireless environment, severe multipath fading and shadowing cause high attenuation of the primary transmitted signal. For example, wireless microphones operating in the TV bands transmit signals with a power of only about 50 mW and a bandwidth of 200 kHz. If Secondary Users (SUs) are several hundred meters away from a microphone device, the received SNR may be well below -21 dB [191]. Poor CR sensitivity in this case results in missed detection of PU (transmitter), resulting up in secondary transmissions offering unacceptable interference to the PU receiver. **Thirdly**, vulnerability of primary receivers to secondary transmissions where the locations of PUs are unknown; the SU may lie outside the PU coverage area or it may be located within the PU's transmission range but primary signal is obscured due to deep fading or shadowing. These practical scenarios are referred to as the primary receiver uncertainty problem and the hidden primary transmitter problem. In both cases, the primary receiver may become vulnerable to harmful interference by secondary communications as such situations make CR incapable of picking up ongoing primary transmissions. **Fourthly**, spectrum sensing in multiuser environment, where CRs reside in a multiuser environment consisting of users with and without exclusive rights for frequency spectrum usage [192].

The above-discussed limitations of conventional spectrum sensing can be overcome by sharing the sensing information among spatially distributed CRs in a CR network, which leads to the concept of cooperative detection. In the following section, we explore various aspects of cooperative spectrum sensing and analyse how it can guarantee improved sensing performance with minimum incurred cost.

8.3 Cooperative Sensing

A very promising solution for improving the sensing performance of the SU networks is to exploit cooperation among secondary nodes. Cooperative spectrum sensing can not only decrease the probabilities of false alarm and missed detection, but can also mitigate multipath and shadowing, that cause the hidden node problem [192, 195]. Thus, multiple cognitive radios are often required to collaborate for spectrum sensing. Cooperative spectrum sensing has received increasing attention in the last few years, and many different schemes have been proposed. We refer to [193] and the references therein for an extended overview on cooperative techniques and their principal issues. Cooperative algorithms can be classified on the basis of how SUs share their sensing data and in which point of the network the final decision is taken. The following subsections highlight the distinguishing features of cooperation strategies.

8.3.1 Centralised and Distributed Sensing

In centralised cooperative strategies the sensing information from all the SUs is reported to a central identity, called the fusion centre that takes the global decision. This information is then provided to the cognitive manager of the network which will use it for supporting resource allocation strategies. In some cases the global decision must be sent back to the SUs by means, for example, of broadcasting [194, 195]. Distributed schemes differ from centralised ones in the absence of a specific fusion centre. In this case, the SUs communicate among themselves and converge to a unified decision taken by each SU on the basis of a common policy [196]. In addition, some mixed strategies can be adopted. For example, a relay assisted cooperative scheme can be used in situations in which some SUs experience a weak report channel and the remainder can be used for forwarding their sensing results to the fusion centre [196]. Another solution is the clustered sensing scheme, in which cluster-heads act as second level fusion centres, collecting the sensing results from the SUs within their cluster. Then this data can be shared among other cluster-heads or can be forwarded to a global fusion centre. An example of cluster based cooperative sensing can be found in [197].

8.3.2 Data and Decision Fusion

A control channel is required for sharing sensing information within a CRN to reach a cooperative decision on spectrum whole availability. The bandwidth of the control channel limits the amount of sensing information that can be reported to the fusion centre (FC) or shared among cooperating CRs. With respect to the information that is shared among the SUs,

cooperative strategies can be classified as hard fusion, quantised soft combining fusion and soft fusion as shown in Figure 8.1. If the entire local sensing data or the complete local test statistics are shared, joint processing of the raw sensing data offers the best detection performance at the cost of control channel communication overhead. This fundamental component of cooperative sensing is termed data fusion. A variety of signal combining techniques are reported in the literature to implement data fusion based on optimally combining the weighted local observations. In [192], the authors have proposed a generalised soft combining scheme that reduces to equal gain combining (EGC) at high SNR and boils down to maximal ratio combining (MRC) at low SNR. Furthermore, a two-bit quantised soft combining scheme is also presented in the same work to overcome the computational complexity of the data fusion scheme and relax the control channel bandwidth requirement. In comparison to quantised soft combining, hard combining is another alternative to perform cooperation under a control channel bandwidth constraint. In this approach, sensing data is processed locally before being transmitted over the control channel and the one-bit local decision from each of the cooperating secondary users is combined using linear fusion rules. This leads to decision fusion based cooperative detection which requires much less control channel bandwidth at the cost of depreciated sensing performance when compared with data fusion based cooperative spectrum sensing. Typically, OR, AND, and MAJORITY rules are used for decision fusion which can be considered as special instances of the generalised k out of N rule. Figure 8.1 comparison of the performance of proposed data fusion rules.

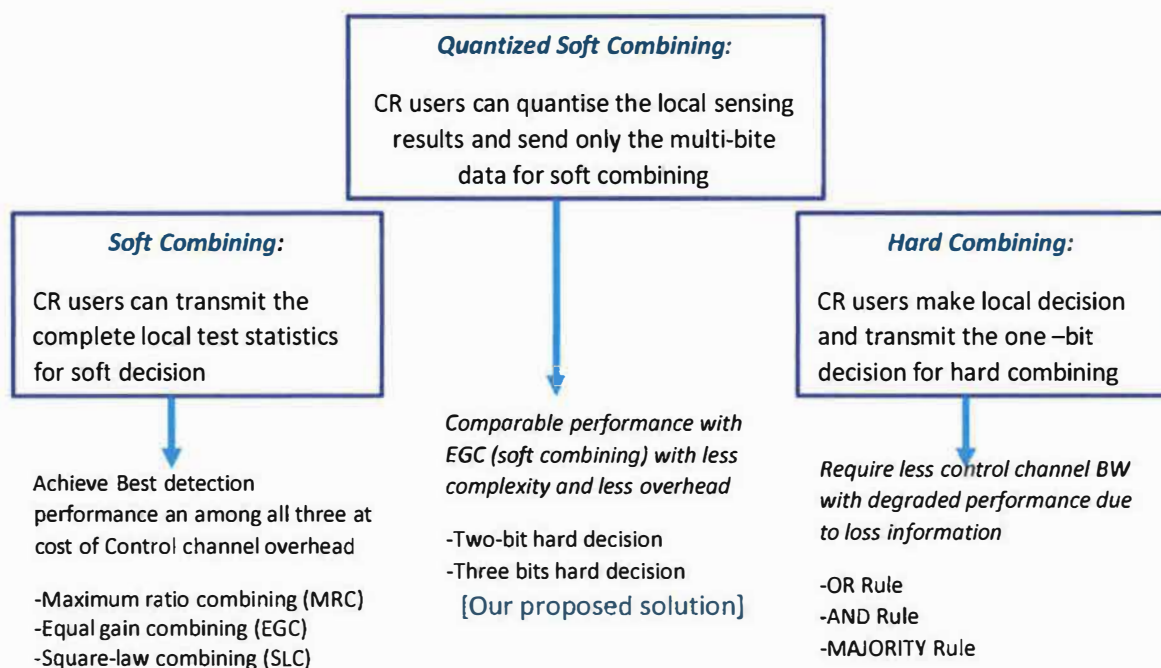


Figure 8-1: Comparison of the Performance of proposed Data Fusion Rules.

8.4 Wideband Spectrum Sensing

The successful deployment of CR relies on its ability to accurately sense the spectrum usage status over a wide frequency range serving various wireless communication standards. From the discussion in section 4.1, the average spectrum occupancy is less than 25%. Under such a circumstance, the cognitive radio can easily find spectrum holes by using a tunable narrowband bandpass filter (TNBF) [198] to search one narrowband portion of the spectrum at a given time. Traditional spectrum sensing algorithms can then be used for searching spectrum holes. Due to ongoing the explosive development of wireless products, the average spectrum occupancy is increasing. A wideband spectrum sensing structure should be adopted to search multiple bands simultaneously [199]. Moreover, cognitive radio networks will eventually be required to exploit spectral opportunities over a wide frequency range from hundreds of Megahertz (MHz) to several Gigahertz (GHz) for achieving higher opportunistic throughput. For example, to exploit spectral opportunities in the whole ultra-high-frequency TV band, wideband spectrum sensing techniques should be employed.

In practice, wideband spectrum sensing systems are difficult to design due to either high implementation complexity or high financial/energy costs [200]. The literature of wideband spectrum sensing is still in its early stages; five types of models are commonly discussed. They are: wavelet detection [201], filter bank detection [202], multicorset sampling based detection [205,206], compressed sampling based methods [203, 204,207], and multirate sampling based detection [208,209]. Furthermore, traditional cooperative sensing exploits the spatial diversity of cooperating CR users and focuses on the sensing of one frequency band during each round of cooperation. Therefore, to determine the availability of the spectrum in multiple channels or bands, CR users need to be synchronised to switch to another band and perform cooperative sensing separately in each band. This process can incur significant switching delay and synchronisation overhead. Alternatively, CR users can cooperatively sense multiple channels or frequency bands to reduce the total sensing time for all users.

To further improve the reliability of the detection, a novel two-stage spectrum sensing scheme is designed, which has better performance than one-stage schemes with relatively low computational complexity. In following subsection, we will give briefly discuss dual-stage spectrum sensing schemes [210,211] and wideband cooperative sensing [212].

8.4.1 Dual-stage Spectrum Sensing

The most crucial requirements are the sensing sensitivity and sensing time to protect incumbent users and to improve the data throughput. When SNR becomes lower, the gap between the information calculated in the hypothesis H_0 and hypothesis H_1 are getting smaller, hence the detection results become unreliable. To improve the performance of the detection based on spectrum sensing at low SNR, a dual stage detection scheme is proposed. A dual-stage spectrum sensing scheme [213] was suggested to meet the requirements for the sensing sensitivity and sensing time. Initially, an energy detector takes a snapshot of the current spectrum usage pattern over a wide bandwidth. In this stage, spectrum segments occupied by strong signals are identified and marked as occupied. Subsequently, energy detection or feature detection scrutinises the unidentified candidate spectrum segments where signals from primary users are weak or absent. By applying second method only to the selected segments, total detection time can be significantly reduced while preserving the sensitivity requirement for spectrum sensing.

A great deal of work on dual-stage spectrum sensing has been done recently. In [214], a coarse spectrum sensing technique adopts wavelet transforms to provide MRSS feature. Using the beneficial properties of auto correlation in the time domain, temporal signature detection is proposed as a fine spectrum sensing technique. However, the transition between the two sensing methods is not mentioned. Reference [217,218] propose two-stage spectrum sensing schemes based on different detection techniques. Unfortunately, the threshold of sensing is not discussed. In [219], the threshold of ED and CFD is deduced respectively according to sensing performance in single sensing stage. However, the thresholds are not optimal because the whole sensing performance is not considered. Reference [220] aims to design the thresholds based on the whole two-stage sensing accuracy. Although sensing speed is also considered, it is separated from sensing accuracy. Moreover, one threshold energy detection is used in the coarse sensing stage. Thus, the probability of implementing fine sensing is larger and sensing speed reduces correspondingly. The above existing dual-stage spectrum sensing schemes focus little on optimal thresholds which consider both the performance of spectrum sensing speed and accuracy jointly.

In this Chapter, two stage adaptive detection are chosen as the coarse sensing technique follow by fine sensing technique. Two thresholds are considered in first stage to improve the sensing speed and five thresholds to improve accuracy.

8.4.2 Wideband Cooperative Sensing

Wideband spectrum sensing is becoming increasingly important to cognitive radio systems as a means of identifying spectrum holes or characterising interference. Meanwhile, due to the effects of multipath fading and shadowing, the primary signal as received at cognitive radios may be severely degraded, leading to unreliable wideband sensing results in each cognitive radio. In this situation, future cognitive radio networks should employ cooperative strategies for improving the reliability of wideband sensing by exploiting spatial diversity. Actually, in cooperative cognitive radio network, the wideband spectra as observed by different cognitive radios could share some common spectral components, while each cognitive radio may observe some unique spectral components [221]. Thus, it is possible to fuse measurements from different nodes and exploit the spectra among cognitive radios in order to save the total number of measurements and thus the energy consumption in cellular networks. Such a data fusion-based cooperative technique, however, will lead to a heavy data transmission burden in the common control channels. It is therefore challenging to develop data fusion-based cooperative wideband sensing techniques subject to a relaxed data transmission burden. Moreover, the high sampling rates are problematic when the distributed cognitive radios are battery powered. An alternative is to develop decision fusion-based wideband sensing techniques, if each cognitive radio is able to detect the wideband spectrum independently. Furthermore, one of the problems in cooperation is in combining the results of various users which may have different sensitivities and sensing times. Some form of weighted combining needs to be performed in order to take this into account. In the following section, we will propose wideband cooperative spectrum sensing with multi-bit hard decision in cognitive radio using a multi resolution spectrum sensing (MRSS) technique and adaptive sensing techniques where the power consumption and the time of sensing are considerably reduced.

8.5 Proposed System Model for Wideband Cooperative Spectrum with Multi-Bit Hard Decision in Cognitive Radio using MRSS Technique.

This section presents the proposed cognitive radio networks based collaborative wideband spectrum sensing method to detect primary signals and determine their frequency bands in order to reuse unoccupied bands. Multi resolution spectrum sensing (MRSS), collaborative spectrum sensing and modified multi-bit hard combination schemes are considered. In the first stage, all nodes in the cognitive radio network apply coarse resolution sensing to achieve a fast

examination of the spectrum that is needed in the second stage; modified multi-bit hard combination combines the results of the coarse resolution sensing to detect the signal and to determine frequency bands that require further detailed examination. Then, fine resolution sensing is applied to these frequency bands to narrow down the spectral bands of the signals in the third stage. In the final decision stage, the channels are processed from every node through modified multi-bit combination stage to determine the primary signal channel and weak channel that are combined to provide occupied channels for the final list. To avoid interference to the primary and cognitive radio users (using vacant spectrum or frequency holes in the primary spectrum), information is reported to the decision node. Thus, the list of vacant channels will be used to allocate spectrum and distribute it to cognitive radio users in the unoccupied spectrum of primary users. With the integration technique mentioned above, the entire system bandwidth is not tested comprehensively, therefore the power consumption and the time of sensing are considerably reduced. In the following subsection, MRSS Method, performance analyse of multi threshold using the multi-bit hard combination technique and the proposed algorithm will described.

8.5.1 Multi-Resolution Spectrum Sensing Method

Given the wide variation in signal bandwidth and formats that must be reliably sensed, it is preferable to have flexibility in selecting detection bandwidth, just like spectrum analyser that can adjust its resolution bandwidth depending on the frequency span and sweep time. For these reasons, the multi-resolution spectrum sensing (MRSS) technique has been proposed as a type of energy detection method, which works like a simple spectrum analyser embedded into a receiver. This technique senses the spectrum at two different frequency resolutions. In such a way, the total sensing time of cognitive radio can be reduced, wherein the total system bandwidth is first sensed using a coarse resolution. A fine resolution sensing is then performed over a small range of frequencies. This technique not only reduces the total number of frequency blocks that must be sensed, it also allows the cognitive radio to avoid sensing the entire system bandwidth at the maximum resolution. One approach using the MRSS techniques is described in [222] using an FFT-based energy detector. Another MRSS approach with less hardware efforts to implement (antennas and ADC blocks) relies on analog wideband spectrum sensing and reconfigurable RF front end [223,224]. In order to provide the multi-resolution sensing feature the wavelet transform was adopted. This is method will discuss in the following section.

8.5.1.1 Wavelet-based MRSS

Wavelets are mathematical functions that cut up data into different frequency components, and then study each component with a resolution matched to its scale. Wavelet transform used for evaluating singularities and irregular structures and can able to describe the local regularity of signals. So the wavelet transform approach for spectrum sensing in Cognitive radio is well motivated to investigate the primary users. Using this wavelet transform technique the sensing time that taken to detect whether primary user using the spectrum or not is very less when compare to other type of spectrum sensing technique. A block diagram of this wideband analog wavelet-based MRSS technique is presented in Figure 8.2. In this wavelet-based MRSS technique, the pulse duration of the wavelet generator and frequencies of the sinusoidal functions are changed to sense the spectrum with different resolutions [4]. The building components are an analog wavelet waveform generator where the wavelet pulse is generated and modulated with I and Q sinusoidal carrier with the given frequency and a window with specific bandwidth is selected as the wavelet. The received signal and the wavelet are multiplied using an analog multiplier. The analog integrator computes the correlation of the wavelet waveform with the given spectral width, i.e. the spectral sensing resolution and the resulting correlation with I and Q components of the wavelet waveforms are inputted to the ADC where the values are digitised and recorded. If the correlation values are greater than a certain threshold level, the sensing scheme determines the reception of an interferer.

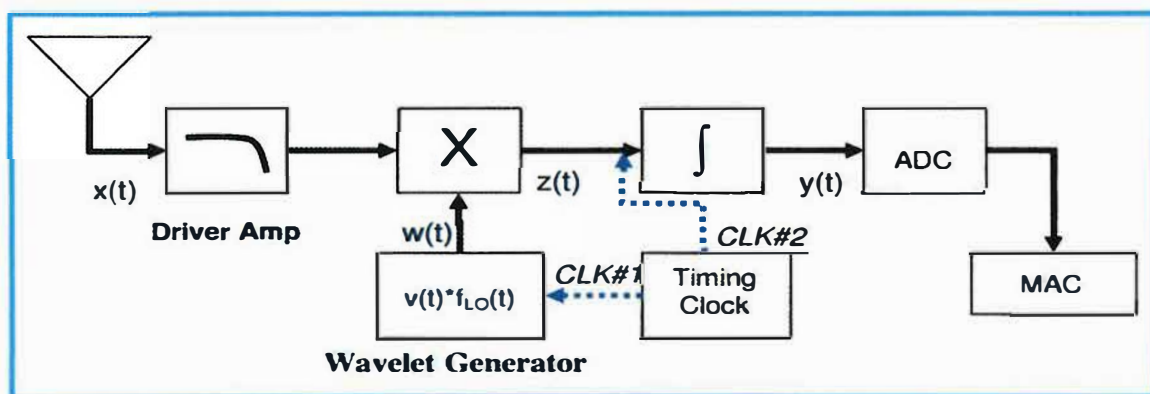


Figure 8-2: Block Diagrams for MRSS Wideband Sensing Algorithms.

Since the analysis is performed in the analog domain, high speed operation and low power consumption can be achieved. Furthermore, by applying the narrow wavelet pulse and a large tuning step size of the frequency of the local oscillator, the MRSS is able to examine a very wide spectrum span in the fast and sparse manner. On the contrary, very precise spectrum searching is realised with the wide wavelet pulse and the delicate adjusting of the local

oscillator frequency. In this manner, by virtue of the scalable feature of the wavelet transform, multi-resolution is achieved without any additional digital hardware burdens. The disadvantages of this sensing method consist in the difficulty of knowing the frequency information of received signals which imply relatively complicated hardware compared to the FFT method. Another disadvantage, still concerning the hardware implementation, is the need to generate a wavelet waveform which needs much more complex circuitry than a simple oscillator.

8.5.2 Performance Analysis of Multi Threshold using Multi-bit Hard Combination Technique

Figure 8.3 shows an energy distribution graph of a primary user signal and noise where the intersection area of upper bound threshold (λ_1) and lower bound threshold (λ_2) is known as the confused region. In the H_0 area a primary signal is absent whereas in the H_1 area noise is absent. In the confused region detection, between noise and PU signal, is difficult using a single threshold.

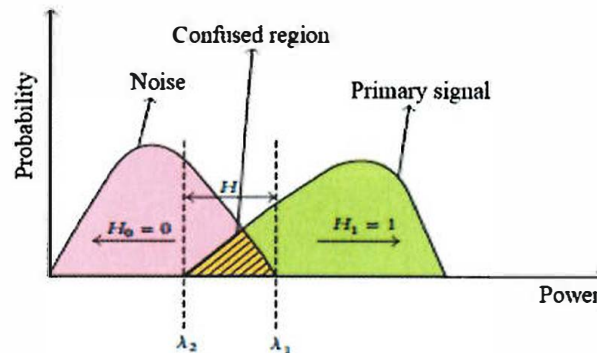


Figure 8-3: Energy Distribution of Primary User Signal and Noise.

To overcome the above challenge, the concept of soft and hard decision combination is introduced to solve problem, as follows.. Soft combination mean CR users can transmit the complete local test statistics and hard combination mean CR users make local decisions and transmit the one –bit decision for hard combining. Soft combination has excellent performance. However, it requires a significant communications overhead to feed back the observation. In contrast, the conventional hard combination scheme requires only one bit of overhead, but has worse performance because of the information loss caused by local hard decisions. Quantised Soft combination (Two bit hard combination) was proposed in [224]. Quantised soft combination mean CR users can quantise the local sensing results and send only the multi-bit data for soft combining. A proposed Softened 3-bit hard combination technique shown in

Figure 8.4 gives better performance than the one bit hard combination technique and needs less overhead than the soft combination technique.

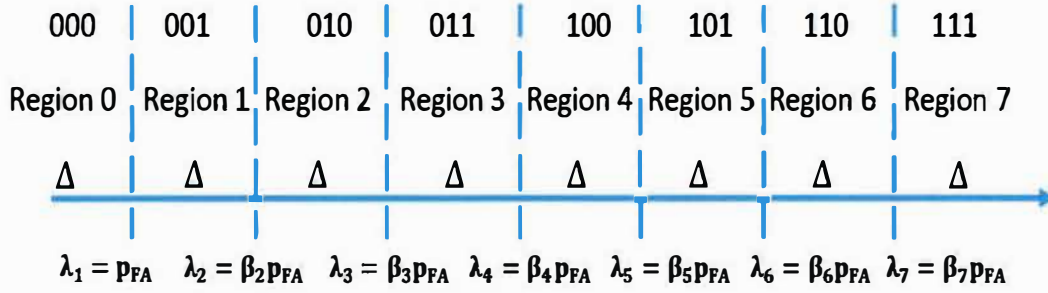


Figure 8-4: Energy Regions of Softened Three Bits Hard Combination.

In this section, we designed multi threshold using multi-bit hard combination scheme to determine local decision at CR user. In Figure 8.5, three-bit quantisation method divides confused region into eight equal quantisation intervals, Δ is the equal gap between each quantisation levels. $\lambda_7, \lambda_6, \lambda_5, \lambda_4, \lambda_3, \lambda_2$ and λ_1 are subthreshold (ST), and their values are chosen as

$$ST = \begin{cases} \text{region7, and } D_i = 111 \\ \text{region6, and } D_i = 110 \\ \text{region5, and } D_i = 101 \\ \text{region4, and } D_i = 100 \\ \text{region3, and } D_i = 011 \\ \text{region2, and } D_i = 010 \\ \text{region1, and } D_i = 001 \\ \text{region0, and } D_i = 000 \end{cases} \quad (8.2)$$

In this section three-bit hard combination scheme for wideband cooperative spectrum sensing is proposed. Seven thresholds are used to divide the whole range of observed energy into eight areas. The decision node collects three-bit information from each cognitive radio after taking measurements in the energy regions of interest. Compared to conventional hard combination with only one-bit exchange, less information is lost at each CR user in the proposed scheme and hence performance improvement is expectable. Thresholds of the three-bit hard combination scheme are determined by using the Neyman-Pearson criterion and optimising the detection performance [225]. In this criterion, while determining the threshold probability of false alarm p_{FA} is fixed to some value, the probability of detection p_D is maximised.

The three-bit hard combination scheme, and the weighted summation is given by $M = \sum_{h=1}^7 w_h N_h$, where N_h is the number of observed energies falling in region h and w_h is the

weight value of region h . Then, M is compared with the threshold, if $M \geq \text{Threshold}$, primary signal is declared present; otherwise, it is declared absent. For the three-bit hard combination scheme, we need to decide threshold values so that the given overall false alarm probability of the CR network is met. In our proposal, the p_{FA} chosen to determining the threshold values in three bit hard combination scheme is $\lambda_n = \beta_n p_{FA}$ where $n = 2, \dots, 7$, and for first threshold $\lambda_1 = p_{FA}$, and the coefficients β_n in Figure 8.5 are found by $\beta_n = (n - 1) \times 10^{-(n-1)}$.

8.5.3 Proposed Algorithm using MRSS technique

The proposed two-stage procedure with three-bit cooperative wideband spectrum sensing using the wavelet-based MRSS scheme is shown in Figure 8.5. The implementation of determination of seven thresholds, coarse resolution sensing and fine resolution sensing are carried out using Matlab programming represented by the following steps [Appendix] :

- ❖ Firstly, a node designated as the decision maker applies coarse resolution spectrum sensing to the entire bandwidth of interest and determines seven thresholds, which are used to divide the observation range into eight regions, as explained in section 8.5.1.
- ❖ Next, all other nodes are informed of these threshold values so that every node is able to apply the same thresholds. Then, all nodes, except for the decision maker node, apply coarse resolution spectrum sensing to the entire bandwidth of interest.
- ❖ After applying the thresholds, the nodes evaluate those frequency bands in which sensed energy exceeds the first threshold and determine the region of the sensed energy. Then, nodes send information about the observed energy regions as three-bit values to the decision maker.
- ❖ Next, the decision maker determines the spectrum bands on which fine resolution spectrum sensing will be applied by using the proposed three-bit hard combination scheme. The decision maker also decides which nodes will apply fine resolution spectrum sensing on the determined spectrum bands.
- ❖ In particular, nodes that sense the highest energies on the determined spectrum bands apply fine resolution sensing. After fine resolution sensing is applied at each selected node, each of the nodes applies the maximum of the seven threshold values that is below the maximum observed energy sensed by coarse

resolution sensing in the determined spectrum band. In this way, selected nodes determine the frequency bands of the signals.

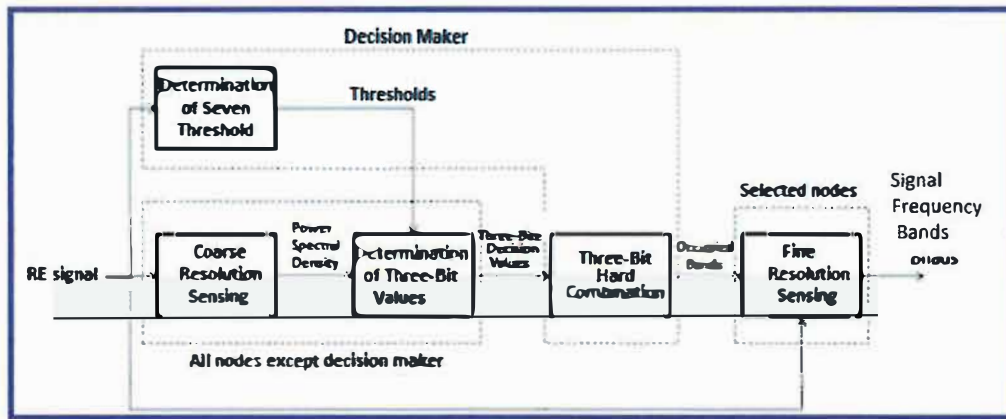


Figure 8-5: Block Diagram of the Cooperative Wideband Sensing of the Proposed Scheme.

8.5.4 Simulation Results and Discussion

To evaluate the performance of the proposed detection scheme, simulations have been carried out. In the following subsections, detection percentage is used as a detection performance measure. Steps used to evaluate the performance of the proposed sensor network based cooperative wideband spectrum sensing is presented in Appendix A.3.

8.5.4.1 Coarse and Fine Resolution Sensing Results for a Node

Figure 8.6 shows an example of seven thresholds that divide the whole range of observed coarse resolution sensing band between (430 MHz -530 MHz). Two peak values at 441 MHz and 461 MHz correspond to the two transmitters whose specifications are given during simulation with different power values. The observed energies at 441 MHz, 461 MHz are in regions 7 and 1 respectively. With this information, it can be deduced that radio will send a three-bit local observation value of “111” for 441 MHz and “001” for 461MHz. Since the observed energies at other frequencies are in region 0, no information will be sent to the decision maker for these frequencies.

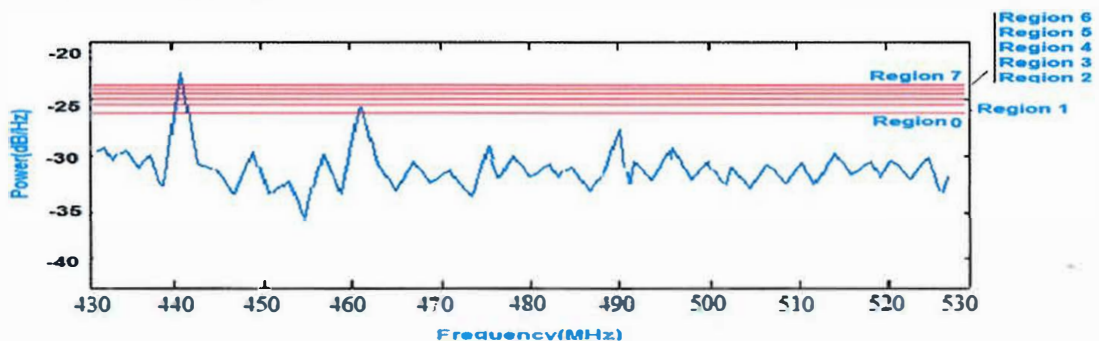


Figure 8-6: Result of Coarse Sensing Of 430-530 MHz Band.

8.5.4.2 Effect of Number of Nodes and Number of Transmitters

Figure 8.7 (A) depicts the effect of the number of nodes cooperating on detection percentage at various SNR values. Figure 8.7 (B) depicts the effect of the number of different received signals on detection percentage at various SNR values. As seen in Figure 8.7 (A), a maximum detection percentage is obtained when there are more nodes participating in the cooperative wideband spectrum sensing. Figure 8.7 (B), shows the performance of the proposed scheme on the detection of the signal emitted by transmitter 3 (assumed transmitter) for the following scenarios: Only transmitter 3 is present, transmitter 1 and transmitter 3 are present and transmitter 1, transmitter 2 and Transmitter 3 are present. As shown in Figure 8.7 (B), when other transmitters are present in the medium, the detection percentage of detecting the signal emitted by Transmitter 3 decreases. This is an expected result since the signals of transmitter 1 and Transmitter 2 contribute to the channel noise while the signal of Transmitter 3 is being detected.

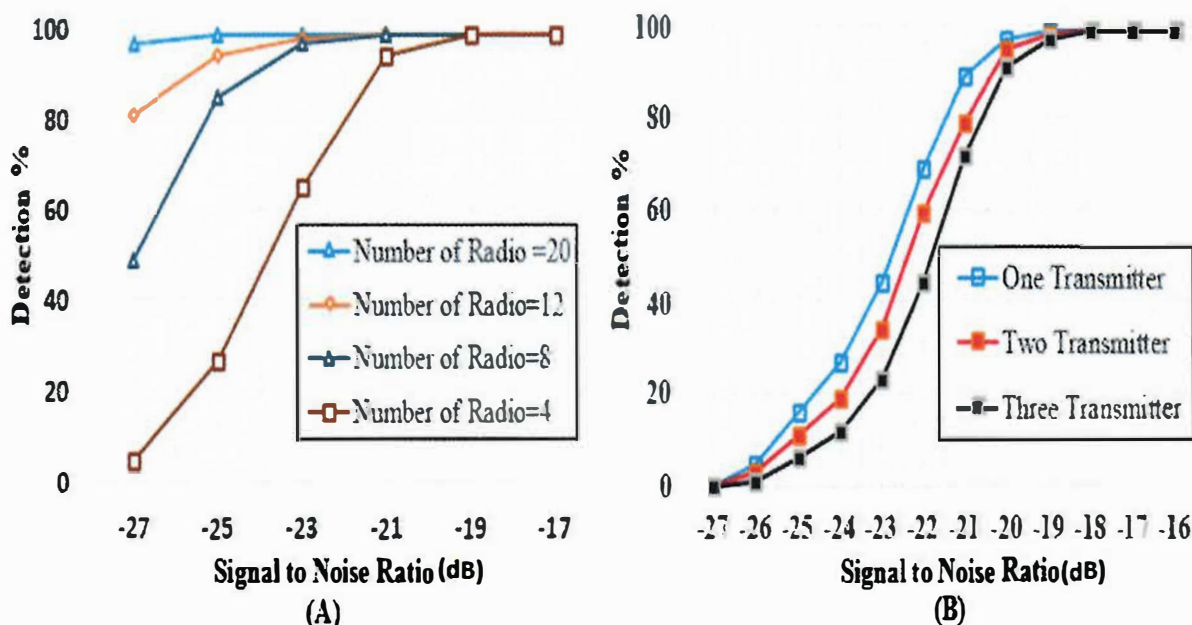


Figure 8-7: (A) Detection versus SNR for Four Different Numbers of Nodes, (B) Detection of Transmitter 3 versus SNR for Three Different Scenarios.

The MATLAB code used to evaluate the performance of the proposed sensor network based cooperative wideband spectrum sensing is presented in Appendix A.5. This code used to study the effect of number of nodes on detection percentage of the cooperative wideband spectrum sensing part of the proposed scheme. The code corresponds to the discussion of the experimental results in Figure 8.7-A.

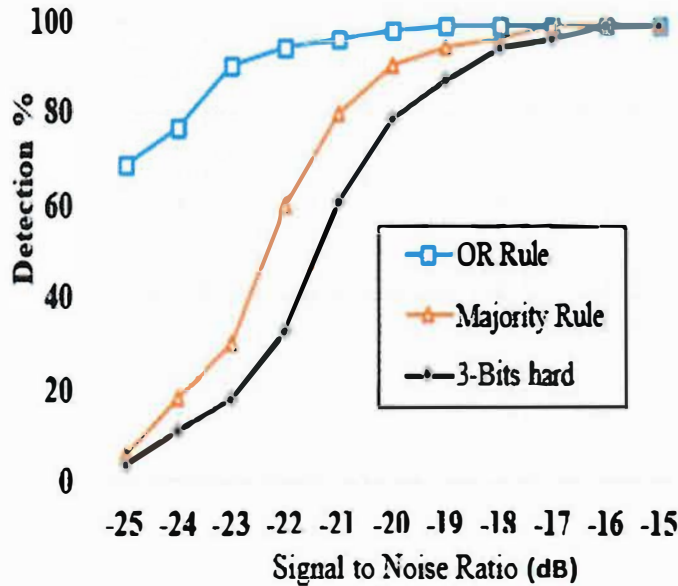
8.5.4.3 Comparing Three-Bit Hard Combination with traditional Hard Combination.

The traditional combination schemes and proposed three-bit hard combination scheme were explained in Section 8.5.2. As mentioned in Section, two of the decision rules used by the traditional hard combination scheme are logical-OR rule and majority rule. This section compares the detection and false alarm performances of the proposed three-bit hard combination scheme and the traditional hard combination schemes using logical-OR rule and majority rule.

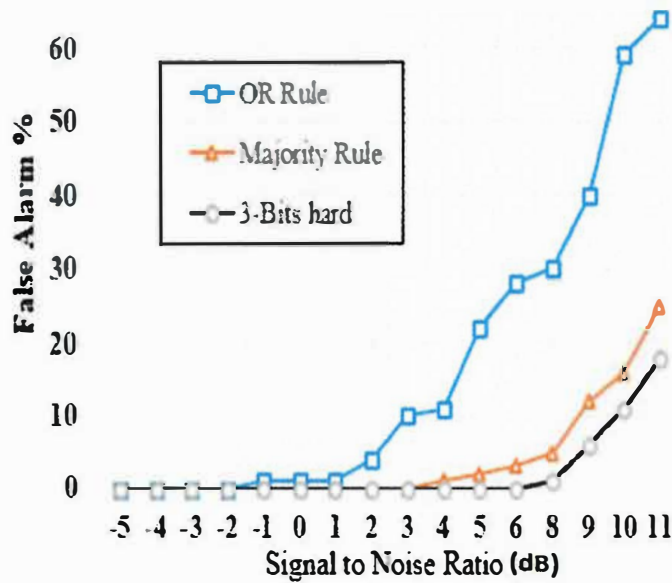
Figure 8.8 (A) shows the detection percentage versus SNR, for three combination schemes. The simulation results indicate that OR and Majority Rule algorithms' results are very close to each other and unmatched well with three-bit hard combination at a low SNR. Implemented with the proposed three-bit hard combination setting algorithm, the detection probability P_d comparison between the OR and Majority Rule algorithms is shown in Figure 8.8 (A). With the proposed threshold setting algorithm, OR and Majority Rule methods can achieve higher detection probabilities than the three-bit hard combination at lower SNR levels. However, three-bit hard combination algorithms could achieve about 30% improvement at $\text{SNR} = -18\text{dB}$ in terms of detection probability P_d . Overall, it shows that when the SNR is between -25 dB and -15 dB , the traditional hard combination schemes have a better detection percentage than the proposed three-bit hard combination scheme. In particular, the traditional hard combination scheme here using logical-OR rule is fairly superior to the other two schemes for $\text{SNR} < -18\text{ dB}$. This is due to the fact that for declaring the presence of the signal of interest, only one node sensing energy above the threshold is enough. The disadvantage of this approach can be seen when false alarm performances are compared.

Figure 8.8 (B) shows the false alarm performances of the three combination schemes. In particular, the y-axis denotes the percentage of the scanned frequencies in coarse resolution sensing that contributes to false alarm for more than 50% of the simulation. It can be seen from Figure 8.8(B) that the proposed three-bit hard combination scheme presents robust false alarm performance compared to the two traditional hard combination schemes. For example, with the traditional hard combination scheme using logical-OR rule, at $\text{SNR} = 10\text{ dB}$, 60% of the scanned frequencies in coarse resolution sensing will be sent to the fine resolution sensing block redundantly. When the results of Figure 8.8 (B) are analysed, the following conclusions can be made. The higher percentage of the scanned frequencies in coarse resolution sensing

that contribute to false alarms means that some of the nodes will apply fine resolution sensing unnecessarily. This is a waste of scarce battery energy for redundant computations and communications between the node and the decision maker. The detection performance of the three-bit hard combination scheme can be improved by using two stage adaptive sensing, where energy detection used when SNR high, and cyclostationary detection used when SNR low. This will explained in more detail in the following section.



(8.8-A)-Detection versus SNR for Three Different Combination Schemes



(8.8-B)-False Alarm versus SNR for Three Different Combination Schemes.

Figure 8-8: (A)Detection versus SNR (B) False Alarm versus SNR

8.6 Proposed System Model for Two-stage Adaptive Spectrum Sensing

Two sensing techniques that have been considered in previous chapters (6 & 7) are energy detection and cyclostationary detection. From simulation results in section 6.4 it is observed that the detection performance of the cyclostationary detection method is a compromise technique, having better low SNR detection performance than energy detectors and less strict requirements than matched filters. In section 7.6, Chapter 7 the performance of SCF has been investigated under real-word noise conditions. It was found that, from the path loss exponents, that it is conclusive that the cyclostationary features are more robust to noise effects than the energy features. However, it is more complex than energy detection and needs a much higher sensing time. Thus, dual-stage adaptive spectrum sensing is proposed to obtain the trade-off between speed and accuracy combining the advantages of different detection techniques. Figure 8.9 shows the system model of the proposed two-stage spectrum sensing detectors having one energy detector and one cyclostationary detector. As show in Figure 8.9, two-threshold ED is adopted with detector with fixed dual thresholds λ_1 and λ_7 the first spectrum sensing stage, and CFD is used within threshold λ_1 and λ_7 in to judge the confused area in the second spectrum sensing stage. In the adaptive dual-stage sensing model, two-threshold energy detection is adopted as the first stage sensing. If $X \geq \lambda_7$, the SU regards the sensing result as H_1 . If $X < \lambda_1$, the SU regards the sensing result as H_0 . If $\lambda_1 \leq X \leq \lambda_7$, the SU cannot judge whether PU is using the spectrum or not. Where three-bit quantisation method divides region into eight equal quantisation intervals as shown in Figure 8.10, $\Delta_{1,\dots,n}$ is the gap between each quantisation levels. $\lambda_7, \lambda_6, \lambda_5, \lambda_4, \lambda_3, \lambda_2$ and λ_1 are subthreshold (ST). Consequently, the second stage sensing is activated to sense the confused area. So CFD is not necessarily to implement unless X locates in the confused area. In this way, the spectrum sensing speed is guaranteed by ED and sensing accuracy is ensured by CFD.

Based on the detection and false alarm probabilities derived in the Chapter 6 on the subject of energy detection and cyclostationary detection, we seek to minimise the average detection time of an available channel for secondary users. A higher average detection time leads to longer delay to allocate a feasible channel for an incoming secondary user, hence decreasing their throughput. Therefore, in this section, we will investigate the sensing performance of our proposed scheme with respect to detection performance.

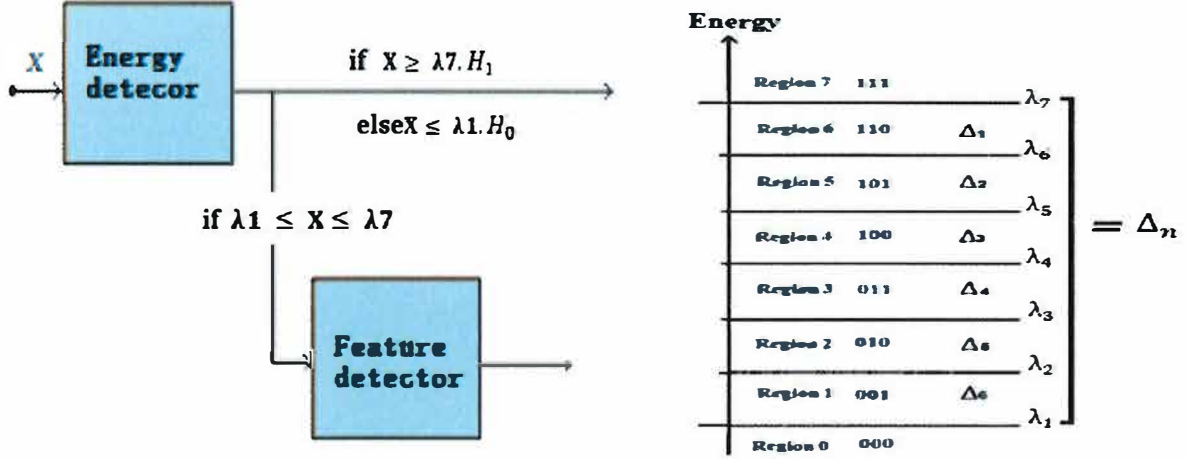


Figure 8-9: Two-Stage Adaptive Spectrum Sensing Detectors.

The overall probability of false alarm and probability of detection of two-stage spectrum sensing scheme are given in (8.3) and (8.4).

$$P_f = P_r P_f^E + (1 - P_r) P_f^C = P_r (P_f^E - P_f^C) + P_f^C \quad (8.3)$$

$$P_d = P_r P_d^E + (1 - P_r) P_d^C = P_r (P_d^E - P_d^C) + P_d^C \quad (8.4)$$

where

- P_d Probability of detection of two-stage adaptive sensing
- P_f Probability of false alarm of two-stage adaptive sensing
- P_d^E Probability of detection for bi-threshold energy detector
- P_f^E Probability of false alarm for bi-threshold energy detector
- P_d^C Probability of detection for cyclostationary detector
- P_f^C Probability of false alarm for cyclostationary detector
- P_r Probability that channel would sense by ED
- $1 - P_r$ Probability that channel would sense by CFD

In order to evaluate agility of the proposed adaptive two-stage spectrum sensing scheme, its mean detection time is compared with the energy detection and the cyclostationary detection, respectively. The mean detection time of proposed two-stage sensing is:

$$\bar{T} = \bar{T}_E + \bar{T}_C \quad (8.5)$$

where \bar{T}_E and \bar{T}_C are the sensing times of energy detection and cyclostationary detection, respectively. \bar{T}_E and \bar{T}_C can be derived as follows:

$$\bar{T}_E = E[K_1]T_1 \quad \& \quad \bar{T}_C = E[K_2]T_2 \quad (8.6)$$

where $E[K_1]$ and $E[K_2]$ represents the mean number of channels reported to energy detector and cyclostationary detector and $T_1 = \frac{M_E}{2w}$ and $T_2 = \frac{M_C}{2w}$ is the mean sensing time for each channel, in which M_E and M_C are the number of samples during the observation interval for energy detection and cyclostationary detection, respectively. w is the channel bandwidth. K_1, K_2 are a random variable which follows a binomial distribution, with parameters N and P_r , where N is the number of channels to be sensed and P_r is the probability that a channel would be reported to the energy detector and $1-P_r$ is the probability that a channel would be reported to the cyclostationary detector. Hence, the mean detection time of the energy detection and cyclostationary detection are

$$\bar{T}_E = NP_r T_1 \quad \& \quad \bar{T}_C = N(1 - P_r)T_2 \quad (8.7)$$

The total mean detection time is found by substituting (8.7) for \bar{T}_E and \bar{T}_C in (8.5):

$$\bar{T} = N(P_r T_1 + (1 - P_r)T_2) \quad (8.8)$$

We can investigate the following two limiting cases on the basis of P_r . For the proposed algorithm P_r ranges from 0 to 1; it indicates the probability that a channel would be sensed using an adaptive strategy. There are two distinct scenarios to be evaluated:

Case 1: When $0 \leq P_r \leq 0.5$, most of the channels are very noisy. SU will perform cyclostationary detection for sensing the majority of the channels. The detection time will increase when more channels are being sensed by the cyclostationary because it consumes a longer detection time than the energy detector. In the worst case when $P_r=0$, the probability of false alarm, the probability of detection and the total mean detection time can be evaluated by putting $P_r \approx 0$ in equation (8.3), (8.4) and (8.8):

$$\begin{aligned} P_f &\approx P_f^C \\ P_d &\approx P_d^C \\ \bar{T} &\approx NT_2 \end{aligned} \quad (8.9)$$

Case 2: When $0.5 \leq P_r \leq 1$, the majority of the channels have a very good SNR. Therefore, SU will perform energy detection for sensing most of the channels because the performance of the energy detector is excellent under good SNR. The mean detection time of energy detection is the least, and therefore it will be the best case for the detection time when majority of the

channels are sensed by the energy detector. The best scenario is when $P_r \approx 1$ and the probability of false alarm, the probability of detection and the total mean detection time can be found by putting $P_r \approx 1$ in equation (8.3), (8.4) and (8.8):

$$\begin{aligned} P_f &\approx P_f^E \\ P_d &\approx P_d^E \\ \bar{T} &\approx NT_1 \end{aligned} \quad (8.10)$$

8.6.1 Performance Assessment and Comparison of Two-stage Detector with One Stage Detector.

The performance of our proposed two stage detector using energy and cyclostationary detection has been evaluated by simulation (performed within Matlab). For each simulation we computed the detection probability as a function of the signal-to-noise ratio, by fixing the false alarm probability P_f . In the following simulations, the false alarm constraint is assumed to be $P_f \leq 0.1$. A comparison between the proposed two-stage and other detection simulations are carried out as shown in Figure 8.10. In Figure 8.10, the detection probability of these detectors is compared as function of SNR with background noise fixed. The thresholds of the two-stage combined spectrum sensing is $\lambda_1, \lambda_2, \lambda_3, \lambda_4, \lambda_5, \lambda_6$ and λ_7 with Δ_n set to small (0.1), Medium (0.6) and larger (0.8) values respectively. From Figure 8.10, we can see that, the detection performance of the cyclostationary detection is better than that of the energy detection. The two-stage detection has the best performance, and the performance becomes better when Δ_n is larger. The detection performance of cyclostationary detection is nearly better than two-stage detection when SNR is lower than -19dB and P_d smaller than 0.54. However, we do not care much about the detection performance when P_d is smaller than 0.54, for in this case, the detection probability is relatively not so high, and missed detection is very likely. From the simulations above, we can see that the detection performance of the cyclostationary detector is better than energy detectors, at the price of complexity and increasing the detection time. As well, the cyclostationary detectors are robust to the noise uncertainty while the energy detection is very sensitive to the variation of the background noise.

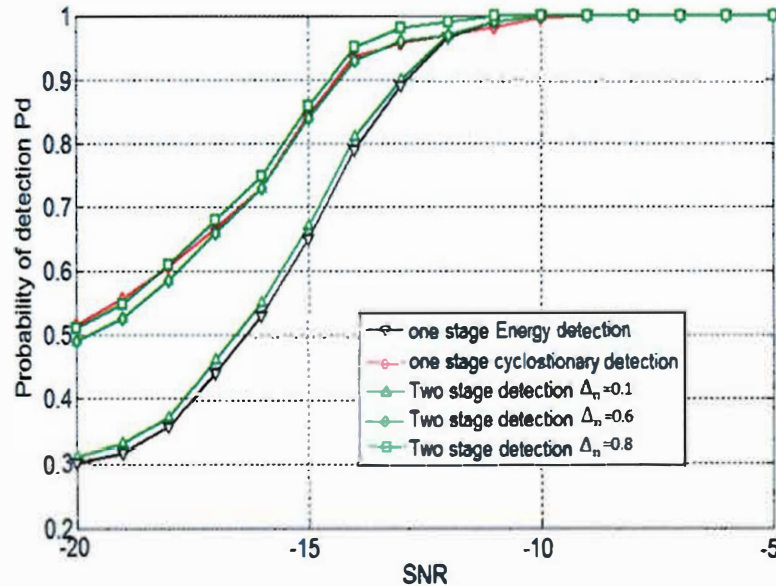


Figure 8-10: Detection Performance against SNR Comparison of the Two Stage Detector with One Stage Detector.

Overall, by considering the time taken by the two-stage detection process, it becomes evident that the cost of improving the detection performance is high. A close look at Figure 8.10 reveals a hidden redundancy in the two-stage sensing scheme. We can see that at high SNRs, the improvement in the detection performance of the two-stage detector is negligible as compared to an ED stage. Hence at high SNRs, where the ED is not constrained by the SNR wall, sensing the spectrum a second time whenever the ED calculates the energy to be less than the threshold seems to be overkill. In other words, activating the channel the CR is in will lead to an unnecessary evaluation by the time-consuming second stage. Thus, with these insights obtained, in the next section we propose a modification to the conventional two-stage spectrum sensing algorithms to optimise the usage of the second stage.

8.6.2 Performance of Adaptive Two-Stage Combined Sensing

The advantage of the adaptive two-stage method is that the second stage of the detector will not be activated always and hence the detection time will be reduced substantially. The second stage will be activated only at low SNR where the noise in the device environment is very high. The ED will work with very high accuracy at high SNR values and with low complexity and very less detection time. If the SNR is very low, then ED will fail to operate correctly and the second stage will be activated. Even though the complexity of cyclostationary detection is high, accuracy of this detector is very high at low SNR values. Furthermore, the sensing time is crucial in spectrum sensing techniques, which is defined as the sensing time taken by CR user

to detect a licensed PU signal. The sensing time is proportional to the number of samples taken by the signal detector. The more time is devoted to sensing, the less time is available for transmissions and thus reducing the CR user throughput. This is known as the sensing efficiency problem [227] or the sensing-throughput trade-off [228] in spectrum sensing.

Figure 8.11 shows detection performance of energy detection, cyclostationary and adaptive two stage detection versus SNR. As we can see, for SNR that is less than -12 dB, the two-stage sensing scheme performs better than energy detection, at the price of increasing the detection time. In addition, from Figure 8.11 we can see that the second stage can be totally switched off at high SNR regimes without having any impact on the detection performance of the CR system. Figure 8.11 shows the comparison between the percentages of the times the second stage is activated in the two-stage detector. It can be clearly seen that by incorporating an estimate of the SNR of the channel, the activation of the second stage can be avoided at high-SNR regimes. For the set of parameters used in this simulation, the critical SNR is -12 dB and hence we can see that once the SNR of the channel is more than -12 dB, the algorithm switches to the ED stage alone.

Furthermore, mean detection time versus SNR of energy detector, cyclostationary detector and two stage adaptive detector are demonstrated in Figure 8.12, where all the channels are sensed at the same probability of false alarm. It is illustrated that if all the channels are in good SNR conditions, then the mean sensing time is equal to the time taken by the energy detector and vice versa. The sensing time of $T_1 = 1.8$ ms for energy detection, $T_2 = 24$ ms for cyclostationary detection and T_3 range is between $T_3 > 1.8$ ms and $T_3 < 24$ ms for proposed adaptive two stage sensing. The mean time detection of adaptive sensing depend on SNR condition. The key advantage of the proposed adaptive spectrum sensing is that its reliable results equal those of the cyclostationary detection and can be achieved in less mean sensing time. It is apparent that the second stage consumes most time for detection and analysis and hence any reduction in the usage of the second stage would lead to savings in the mean detection time of the CR.

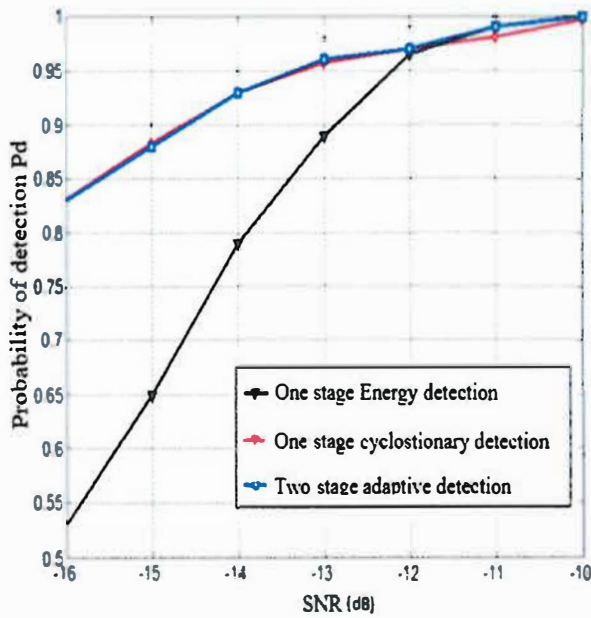


Figure 8-11: Probability Of Detection of the Proposed Two-Stage Adaptive Detector As Compared to A Single Stage ED And Cyclostationary Detector.

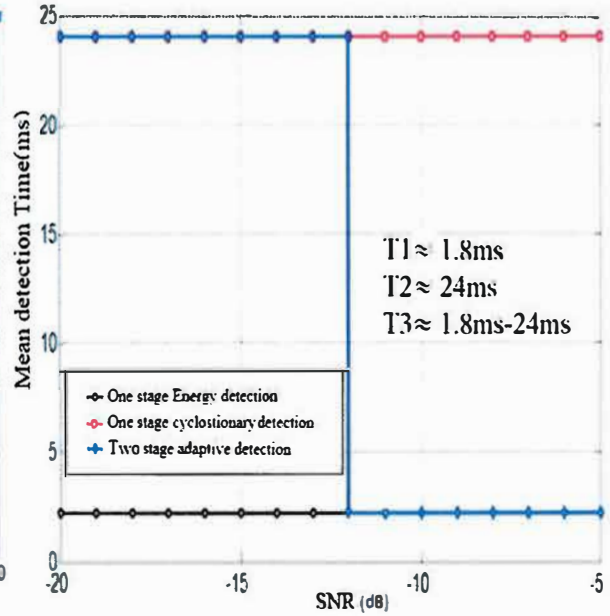


Figure 8-12: Mean Detection Time Comparison of Proposed Spectrum Sensing Cyclostationary Detector, Energy Detector and Two-Stage Adaptive

In this section, throughput performance of the proposed two stage-adaptive sensing has been analysed. Overall, the proposed scheme above chooses either the energy detection or the cyclostationary detection based on SNR. We observed that at low SNRs where energy detector is not reliable, the proposed scheme provides improved detection at the cost of mean detection time. At high SNRs, the proposed scheme provides fast detection using the energy detector. This section showed from simulation results that the mean detection time of the two-stage adaptive scheme is lower than that of the cyclostationary detection. Even in the worst case, it may be equal to the cyclostationary detection. In the best case, the total mean detection time is reduced dramatically to achieve the same accuracy. The results showed that the reliability of detection is also as high as that of the cyclostationary detection with reduced total mean detection time.

8.6.3 Optimisation of Mean Detection Time using Two-Stage Adaptive Sensing

The sensing time may be optimised by utilising the derived P_d and P_f of the signal detector. Based on the detection and false alarm probabilities derived in section (8.6), we jointly optimise two fundamental parameters of the detector, i.e., the sensing threshold and the integration time, to minimise the mean time to detect an available channel. Although the total detection time

involves channel switching time and integration time in the two-stage adaptive detector as \bar{T} and \bar{T}_s respectively, the \bar{T}_s not consider in this research, since \bar{T}_s is determined by the phase locked loop (PLL) design in the receiver circuitry and is also known as the PLL settling time . Therefore, in order to clarify how the detection time looks like for the two-stage adaptive sensing compared to energy and cyclostationary detectors , we present the mean detection time of the two-stage adaptive sensing , energy detection and cyclostationary which is derived in section (8.6),with varying P_K and Δ as shown in Figure 8.13. P_K is the Probability that the channel would be sensed by combined energy and cyclostationary detector and Δ representes change of range of thresholds values between λ_1 and λ_7 ,increasing λ_7 and decreasing λ_1 will increase the overall probability P_d detection at the cost of increase detection time.

The mean detection time of all the detection systems remains constant regardless of P_K , except for the adaptive two stage. If P_K is low, most of the channels are sensed by the energy detection, and the mean detection time is almost equal to the time taken by energy detection. When P_K is high, the adaptive two stages do not always have a smaller mean detection time in comparison with the energy detection because the majority of channels are sensed by cyclostationary detection. Figure 8.13, shows the graph of mean detection time with varying P_K from 0 to 1, and Δ is taken as 0.2, 0.5 and 0.8, respectively. When Δ is 0.2, most of channels sensed by energy detection. When Δ is 0.5, it means detection processing of some of the channels is concluded at the energy detection stage, and others need to pass through cyclostationary detection. When Δ is 0.8, most of the channels are sensed by cyclostationary detection. Overall, the mean detection time of two stage adaptive is much less in comparison with cyclostationary detection, and has nearly the same accuracy of detection. This improves the utilisation efficiency of the radio spectrum by increasing detection reliability and decreasing sensing time. A change in the probability that channels are sensed by a combined energy and cyclostationary detector means that the thresholds of the detector also change.

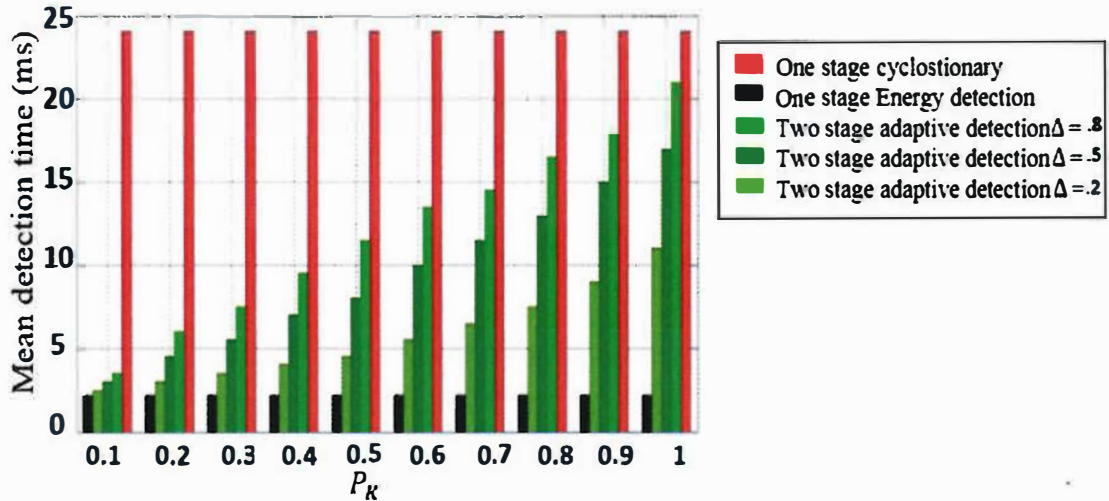


Figure 8-13: Mean Detection Time Comparison for Varying P_K and Δ .

8.7 Proposed System Model for Wideband Cooperative Spectrum Sensing with Multi-Bit Hard Decision using Two-stage adaptive sensing.

In the previous proposed scheme in section 8.5, wideband cooperative spectrum sensing using MRSS technique has been used as a type of energy detection method, which works like a simple spectrum analyser embedded into a receiver. Although, this method provides faster sensing time and simpler implementation than those of feature detection; it is well known that such method lacks the capability to differentiate different signal types. Also, the sensing the performance for energy detector will be more likely to be degraded due to the noise uncertainty. To meet the time and sensitivity requirement and to improve the performance of the detection at low SNR a two-stage adaptive method, collaboration spectrum sensing and modified multi-bit hard combination schemes are considered. Multi-bit hard decision using two-stage adaptive with adaptive mode sensing algorithms are presented with more sensing accuracy, and their sensing time and energy consumption are reduced greatly especially when the SNR is high or no PU exists. In the proposed algorithms, we try to increase sensing accuracy, reduce the energy consumption of wideband cooperative spectrum sensing with N_s samples by designing two stage adaptive sensing schemes with αN_s -sample first stage detection and $(1 - \alpha)N_s$ -sample second stage detection. We assume that, in the N_s -sample detection of these algorithms, the presence/absence status of the PU does not change. In other words, the received signal is stationary within the observation time T (i.e., N_s samples); this assumption is commonly used in the literature [214-217].

8.7.1 System Description

In this section we propose two-stage adaptive spectrum sensing scheme to further improve the wideband cooperative spectrum sensing performance as shown in Figure 8.14. Each secondary user reports three-bits, which can be calculated from the adaptive two-stage detection results. Although the same technique used in previous proposed algorithm of MRSS in section 8.6.3 will be used here again, the difference is that the two stage adaptive technique which switches between energy detection and cyclostationary detection depend on energy value of PU signal will using as coarse sensing. Furthermore, in this proposal the cyclostationary detection will used instead of energy detection as fine detection.

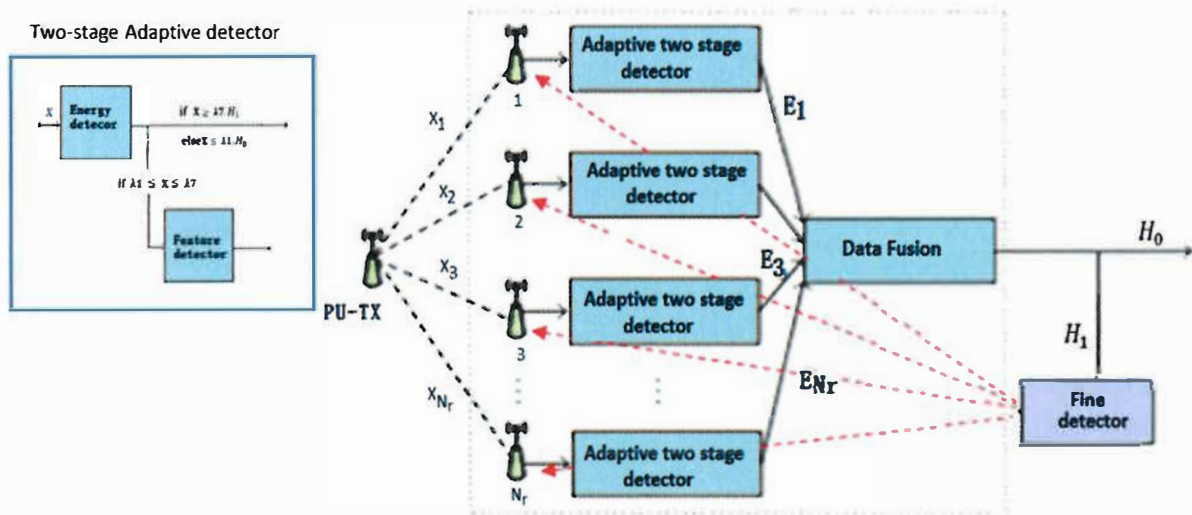


Figure 8-14:Architecture of Wideband Cooperative Sensing Using Two Stage Adaptive Detection.

The proposed wideband cooperative spectrum sensing scheme using two-stage adaptive technique can be represented by the following steps:

Step 1: at the i th secondary user, perform the first stage coarse energy detection with αN_s samples at each SU, and we can get the value E_{Nr} . Figure 8.14 shows the architecture of wideband cooperative sensing with first double thresholds λ_1 and λ_2 . If the detection result of SU_i ($i = 1, 2, \dots, K$), $X > \lambda_2$, the decide $D1_i$ is set to 111, and go to 2, indicating PUs exist; if $X < \lambda_1$, the decide $D1_i$ is set to 000, and go to 2, indicating no PUs exist; if $\lambda_1 \leq X \leq \lambda_2$, nothing sent, go to step 3 to perform second stage detection. When the received signal energy between λ_2 (upper threshold) and λ_1 (lower threshold), it is consider in the region uncertainty (UN), and the energy detector is not reliable for PU detection. Local decision $D1_i$ ($i = 1, 2, \dots, K$) is obtained through the first stage coarse energy detection as

$$D1_i = \begin{cases} 000 & X < \lambda_1, \quad \text{go to 2} \\ 111 & X > \lambda_7, \quad \text{go to 2} \\ \lambda_1 \leq X \leq \lambda_7 & , \text{nothing sent, go to step 3} \end{cases} \quad (8.11)$$

Step 2: The first stage local decisions $D1_i$ are fused at the fusion centre, and the final decision DF can be obtained as

$$DF = \sum_{i=1}^K D1_i \begin{cases} \geq k, H_1 \\ < k, H_0 \end{cases} \quad (8.12)$$

where H_0 and H_1 denote the decision made by the decision node that the PU is present or absent, respectively. The threshold k is an integer, representing the “n-out-of-K” rule [212]. If the final decision DF can be obtained, DF is sent to each SU to request fine sensing (cyclostationary detection). If the final decision DF cannot be obtained, nothing will be done.

Step 3: If the final decision DF is received by the SUs, it goes to step 6. If the final decision DF is not received by the SUs after τ period, it performs the second stage cyclostationary detection with $(1 - \alpha)N_s$ samples, and the sensing result of the SU_i , and we can get the value Y .

Step 4: Local decision $D2_i$ ($i = 1, 2, \dots, K$) is obtained through the second stage cyclostationary detection as

$$D2_i = \begin{cases} Y < \lambda_7, \text{ final decision } D2_i \\ Y > \lambda_1, \text{ final decision } D2_i \end{cases} \quad (8.13)$$

where Y is the second stage local sensing result of SU_i using cyclostationary detection. To transmit it easily and save the spectrum resource, the $D2_i$ is three-bit binary, which can be 110, 101, 100, 011, 010 and 001. At the common receiver, to fuse the decisions of all the secondary users together, $D2_i$ should be changed into signed integer F_i according to

$$F_i = \begin{cases} \text{region6, when } D2_i = 110 \\ \text{region5, when } D2_i = 101 \\ \text{region4, when } D2_i = 100 \\ \text{region3, when } D2_i = 011 \\ \text{region2, when } D2_i = 010 \\ \text{region1, when } D2_i = 001 \end{cases} \quad (8.14)$$

Step 5: The second stage local decisions $D2_i$ are fused at the fusion centre, and the final decision DF can be obtained according to of all the secondary users in (8.14) as follows.

$$DF = \sum_{h=1}^7 F_i \begin{cases} > M & H_1 \\ < M & H_0 \end{cases} \quad (8.15)$$

If the final decision DF can be obtained, goes to step 6.

Step 6: After the final decision DF is received by the SUs, apply fine cyclostationary spectrum sensing on these spectrum bands. The CR radios that apply fine cyclostationary spectrum sensing, determine the primary transmitted frequency bands. Finally, the report is sent to the decision maker again to determine the occupied, vacant and weak channels.

Overall, in the two-stage adaptive scheme described above, if the energy value in the first stage X is outside λ_7 (upper threshold) and λ_1 (lower threshold), the solution is located in the undoubted region. The final decision is made immediately based upon $D1_i$, and the decision is quite accurate. This situation is equal to the one-stage detection with N samples. If X is in $\lambda_1 \leq X \leq \lambda_7$, the solution is located in the doubted region, and a second stage cyclostationary feature detection will be performed. The final decision is based upon both $D1_i$ and $D2_i$. Therefore, the two-stage detection scheme can greatly improve the detection performance and make the decision more reliable.

8.7.2 Simulation Results and Discussion

To evaluate the detection performance of the proposed detection scheme, numerous of simulations are carried out as depicted in Figure 8.15 and Figure 8.16. We present the performance of the hard combining schemes compare to non-cooperative users. Furthermore, the two bit and the three-bit quantised schemes are compared in terms of detection performance. Next, detection performance against SNR comparison of two-stage adaptive detection non-cooperative detector with cooperative detector are demonstrated.

Figure 8.15 present ROC curves (probability of detection P_d vs probability of false alarm P_f), to compare the hard decision and quantised decision. ROC involve 'AND' rule, quantised data fusion with 2-bit and 3-bit quantised combination and compare it to the detection performance of a single CR user. Although the AND rule has better detection performance than the single CR user, the quantised data fusion still desirable. For quantised data fusion with 2-bit and 3-bit quantised combination, the Figure 8.15 indicates that the proposed 3-bit combination scheme shows much better performance than the 2-bit combination scheme at the cost of one more bit of overhead for each CR user, this scheme can achieve a good trade-off between detection performance and overhead.

Figure 8.16, compared the probability of detection (P_d) performance of wideband cooperative spectrum sensing schemes, when $P_f=0.1$ and SNR is varying from -20dB to -5dB . From the simulation results in Figure 8.16, we can see that the P_d performance of the proposed wideband cooperative two-stage adaptive detection scheme is much better than the traditional cooperative detection schemes. As the Figure 8.16 indicates, all fusion methods outperform the single node sensing using two stage adaptive, the quantised 3-bits scheme based on quantised combination rule outperforms the hard combination at the cost of control channel overhead, the 3-bit quantised combination scheme shows a comparable detection performance with the hard decision, with more overhead.

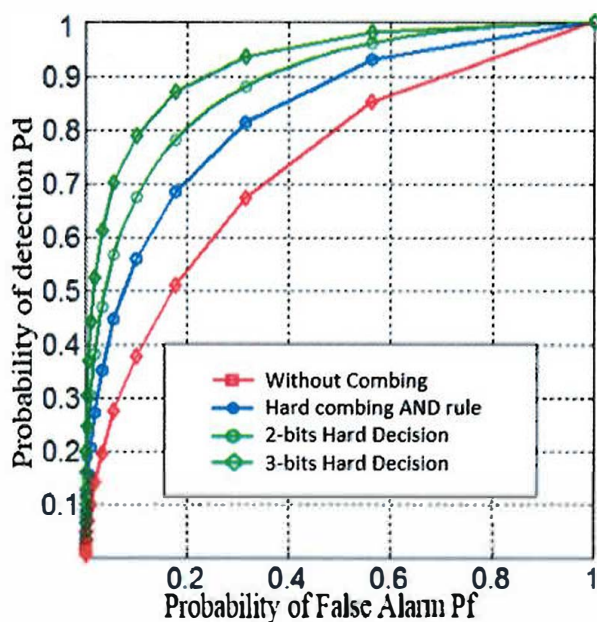


Figure 8-15: ROC Curves Comparison of Non- Wideband Cooperative Detector With Wideband Cooperative Detector under Different Fusion Rule.

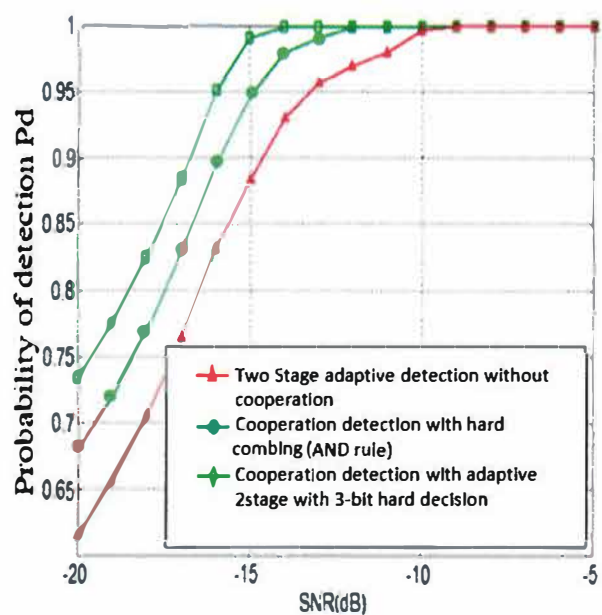


Figure 8-16: Detection Performance against SNR Comparison of Two-Stage Adaptive Detection Non-Cooperative Detector with Cooperative Detector.

8.8 Chapter Summary

In this Chapter, we first addressed the challenges in non-cooperative sensing, followed by presentation of an overview of cooperative spectrum sensing, where we discussed a general background of cooperative spectrum sensing schemes. Moreover, motivated by the fact that wideband spectrum sensing is critical for reliably finding spectral opportunities and achieving opportunistic spectrum access, we presented a brief survey of the state-of-the-art wideband spectrum sensing. To further improve the reliability of the detection, a novel two-stage spectrum sensing scheme is designed, which has better performance than one-stage solutions

with relatively low computational complexity. To meet the objectives, three proposed systems have investigated.

Firstly, a wideband cooperative spectrum sensing with multi-bit hard decision in cognitive radio using Multi Resolution Spectrum Sensing (MRSS) technique was proposed. The proposed scheme is appropriate for sensor networks for cognitive radio since it senses a wide spectrum band in an energy efficient manner. Energy efficiency comes from the usage of MRSS and the proposed three-bit hard combination scheme. In particular, redundant exhaustive sensing on empty bands is avoided with MRSS, and less overhead in collaboration with respect to the soft combination is provided by three-bit hard combination. The proposed system showed that a three-bit hard combination scheme is superior to the traditional hard combination schemes in false alarm reduction. Although the traditional hard combination schemes are shown to have a better detection percentage than the proposed three-bit hard combination scheme, the detection performance of the three-bit hard combination scheme can be improved by using two stage adaptive sensing.

Secondly, a system model for two-stage detectors with an adaptive technique using ED in the first stage and a CFD in the second stage and using seven thresholds scheme was proposed. The use of cyclostationary detection aims to mitigate the problems caused by noise uncertainty faced by ED at low SNRs. We pre-compute the lower bound of the SNR using first double thresholds (λ_1 and λ_7) at which the ED still works satisfactorily and show that by estimating the SNR of the channel the CR is in, we can switch off the second stage of a two-stage detector when the channel SNR is higher than the lower bound of the SNR level of the ED. This scheme improves performance, reduces computational complexity and overcomes the sensing failure problem. Numerical results show that the proposed two-stage adaptive spectrum sensing scheme outperforms the one stage detector schemes. Performance was also measured in terms of sensing time. It is shown that the proposed scheme yields smaller sensing time than cyclostationary detection and also increases throughput. Our results indicate that the proposed scheme performs better than previous schemes in terms of spectrum detection and spectrum sensing time.

Thirdly, wideband cooperative spectrum sensing with multi-bit hard decision using two-stage adaptive sensing was proposed to improve the reliability of wideband cooperative sensing. It has been shown that the proposed detection algorithm using adaptive detection can detect the wideband cooperative spectrum efficiently. In addition, it has also been shown that the

detection algorithm using seven thresholds with an adaptive technique can sense the spectrum efficiently and that it outperforms the traditional cooperative detection method. Simulation results reveal that the wideband cooperative sensing algorithm based on the adaptive technique can detect the low SNR signals up to -17 dB with 90% detection probability, 10% false alarm probability. In contrast, the traditional method can detect only -14.5 dB signals under same environment. In conclusion, the proposed sensing method achieves 2.5 dB better performance compared to the traditional technique.

Part V: Conclusions and Future Work

There is a way to do it better – find it.

Thomas A. Edison

This part contain one chapter

CHAPTER 9: Conclusion and Future Work

Chapter

9 Conclusion and Future Work

Spectrum is an incredibly precious finite and, in the short term, non-renewable resource. Its efficient use has been the focus of research and development efforts over many decades. Dynamic spectrum access (DSA) and cognitive radio (CR) are promising new techniques that aim to increase spectrum efficiency by allowing unlicensed (secondary) users to access licensed bands temporarily unoccupied by the licensed (primary) users, in an opportunistic and non-interfering manner. This conceptually simple but innovative and challenging spectrum access paradigm is expected to enable more efficient use and exploitation of the spectrum bands with commercially attractive radio characteristics. However, the resource available to the secondary user depends upon the spectrum occupancy patterns of the primary systems. Realistic modelling of the spectral activity of primary user systems is vital when designing and evaluating the performance of DSA/CR systems. Potential spectrum usage assessment tools range from measurement and analytical studies to the design and dimensioning of secondary networks as well as the development of innovative simulations and more efficient DSA/CR techniques. However, the utility of such tools depends on their realism and accuracy.

This chapter summarizes the main conclusions derived from the investigations carried out in this thesis and discusses possible directions for future work. Part I presented an overview of the radio spectrum today in terms of regulation and spectrum usage. It also studied the value of system evolution around future radio platforms given the introduction of software defined radio (SDR), dynamic spectrum access (DSA) and cognitive radio (CR) technologies. Part II reviewed the past spectrum measurement campaigns carried out by SSC groups and presented

recent spectrum measurements that were performed in the framework of a broadband spectrum measurement campaign, in the Humber Region, UK. Part III presented the characterisation of cyclostationary feature detectors through theoretical analysis, implementation and experiments under real noise and interference conditions, and compared them with energy detection methods. Part IV presented a wideband cooperative sensing method using adaptive sensing techniques and multi-bit soft decisions.

Part I of this thesis has presented an overview of radio spectrum today including regulation methods and spectrum usage. We conclude that the current spectrum management models operating today on both national and international level leave much to be desired in term of efficiency of use of the radio spectrum in reality. The command and control approach used in traditional spectrum licensing tends to predicate the idea of unlicensed access to licensed bands (called dynamic spectrum access (DSA) being introduced. The objective of DSA is to achieve a more efficient utilisation of radio spectrum without interfering with primary users. This flexibility could be achieved through the use of cognitive radio implemented within software defined radio systems. Various microelectronic technologies that are currently available would allow DSA to be implemented as part of a SDR hardware prototype. Furthermore, different a dynamic spectrum access strategies have been presented and categorised. Finally, an architecture for a cognitive radio network (CRN) and cognition capability was discussed.

Part II of this thesis has reviewed historical spectrum occupancy measurements, particularly the Shared Spectrum Company measurement campaigns, and compared global spectrum occupancy measurement. Additionally, this part addressed the development of a unified methodological framework for spectrum measurements in the context of DSA/CR. In this sense, this part has presented a comprehensive and in-depth discussion of several important methodological aspects that need to be carefully taken into account when evaluating spectrum occupancy. Next, we presented an investigation of spectrum white space availability for opportunistic cognitive radio access in the frequency range 180–2700 MHz over a wide variety of scenarios in urban, suburban and rural areas of the Humber region, UK. The spectrum occupancy analysis is based on a measurement campaign within results in several bands, specifically, cellular and TV broadcasting bands. To the best of the author's knowledge with the exception of that undertaken by Ofcom, this is the first study of these characteristics performed under the scope of the UK spectrum regulation at Humber region. The analysis indicates a significant amount of unused spectrum in these bands. Some spectrum bands are

subject to intensive usage while others show moderate utilisation levels, some are sparsely used and other are not used at all. Overall, the level of utilisation has been verified to be significantly low. This can provide useful information for the regulator in consideration of opportunistic spectrum access, which can bring both economic and social benefits to the country, as most of the allocated TV bands are below 13.4% utilisation.

Part III of this thesis has dealt with the study of various specific aspects related to spectrum sensing techniques. Several spectrum sensing techniques have been discussed. The performance of ED, CFD and MF (the most widely employed spectrum sensing techniques in DSA/CR) has been presented and assessed experimentally. The first spectrum sensing technique is based on an energy detector (ED), which has low computation complexity but minimum probability of detection in the case of low SNR. The matched filter (MF) technique is more complex but has a better probability of detection for low SNR. CFD is the most efficient algorithm, but it requires a priori information for detection. The results show that cyclostationary-feature-based detection can be robust compared to an energy-based technique for low signal-to-noise ratio levels with less complexity compared to matched filter technique. The outcome of this study has highlighted important practical aspects to more characterise in more detail and compare with CFD and ED under real world noise. Furthermore, we investigated the feasibility and performance of cyclostationary feature detection for spectrum sensing, which included a theoretical background and experimental results for cyclostationary detection using SCF. Overall, and including the path loss measurement process, the magnitude of the SCF features were obtained from many locations and compared to those from the PSD. It was found that, from the path loss exponents, it is conclusive that the SCF features are more robust to noise effects than the PSD features. Additionally, it was found that, under real world noise, SCF feature detection shows outperformed PSD feature detection under low SNR condition.

The findings of the aforementioned studies have shown that detection performance in practice is often compromised by multipath fading, shadowing and receiver uncertainty issues. To mitigate the impact of these issues, Part IV a proposed wideband cooperative spectrum sensing method with multi-bit hard decision using a two-stage adaptive technique to improve the detection performance by exploiting spatial diversity with minimum cooperation overhead.

Part IV of this thesis has presented and addressed the challenges in non-cooperative sensing, following by an overview of cooperative spectrum sensing, where the general background of

the cooperative spectrum sensing scheme is discussed. Moreover, motivated by the fact that wideband spectrum sensing is critical for reliably finding spectral opportunities and achieving opportunistic spectrum access for next generation cellular networks, we present a brief survey of state-of-the-art wideband spectrum sensing. To further improve the reliability of the detection, a novel two-stage spectrum sensing scheme is designed, which has better performance than the one-stage with relatively low computational complexity. To meet the objectives of wideband cooperative sensing, three proposed systems are investigated. The three proposed cooperative wideband spectrum sensing schemes all sense a wide spectrum band in an energy efficient manner whilst providing resilience to fading, shadowing, and noise. Energy efficiency comes from the usage of MRSS or two-stage adaptive techniques and the proposed three-bit hard decision combination scheme. Resilience to fading, shadowing, and noise is due to the cooperation of the nodes. Furthermore, the proposed three-bit hard decision combination scheme is superior to the traditional hard combination schemes.

9.1 Future Research Directions

The work that is presented in this thesis can be extended in several directions, focusing on either spectrum measurement, spectrum sensing or wideband cooperative sensing applications.

In the spectrum measurement direction, as part of our future work we plan to undertake measurements at further locations using cheaper receiver platforms such as software defined radio RTL-SDR and continue to investigate our results statistically in order to develop modelling strategies for spectrum occupancy. Our further work will differ from existing spectrum measurement platforms that require specialized and costly spectrum analysers. The use of a low-cost mobile platform is a key factor in attracting a large volume of crowdsourcing users without significant infrastructure cost. Furthermore, our current two testbeds are not well suited to indoor measurements because of the generally bad reception of the GPS signals indoors. However, GPS receivers specially designed for such reception conditions can often still provide a pulse-per-second based on a single GPS satellite to bridge complete lack of GPS reception. Those could be integrated into our testbeds easily.

In the spectrum sensing direction, we may consider compressive sensing methods to reduce the computational complexity of wideband CR applications. Although this problem usually assumes sparse RF signals in the frequency domain, it is nevertheless worth addressing in cyclostationary detection applications. Cyclostationary feature detection is one of the most

powerful spectrum sensing techniques used for cognitive radio (CR) systems. This is because of its robustness against noise uncertainties. However, this technique needs a high sampling rate, which is limited by the state-of-the-art analog to digital converters (ADCs), especially in the wideband regime. However, the compressive sensing method solves the high sampling rate problem. In particular, compressive sensing can be applied to cyclostationary feature detection due to the sparsity of the SCF in two-dimensions. Therefore, compressive sensing can be a perfect candidate for cyclostationary detection of wideband signals and can help to reduce both the computational burden and the hardware cost of such techniques.

1

References

1. Mishra, A., Varshney, G., & Karandikar, A. Analysis of the 3G and BWA Auctions in India. Proceedings of ITS India 2012.
2. Sicker, D. C., & Doerr, C. (2008, June). The 700 MHz Auction. In Sensor, Mesh and Ad Hoc Communications and Networks Workshops, 2008. SECON Workshops' 08. 5th IEEE Annual Communications Society Conference on (pp. 1-6). IEEE.
3. Van Damme, E. (2001, May). The Dutch UMTS auction in retrospect. cpb Report, 2.
4. Peha, J. M. (2009). Sharing spectrum through spectrum policy reform and cognitive radio. Proceedings of the IEEE, 97(4), 708-719.
5. Jones, S. D., Jung, E., Liu, X., Merheb, N., & Wang, I. J. (2007, April). Characterization of spectrum activities in the US public safety band for opportunistic spectrum access. In New Frontiers in Dynamic Spectrum Access Networks, 2007. DySPAN 2007. 2nd IEEE International Symposium on (pp. 137-146). IEEE.
6. Taher, T. M., Bacchus, R. B., Zdunek, K. J., & Roberson, D. (2011, May). Long-term spectral occupancy findings in Chicago. In New Frontiers in Dynamic Spectrum Access Networks (DySPAN), 2011 IEEE Symposium on (pp. 100-107). IEEE.
7. Petrin, A., & Steffes, P. G. (2005, March). Analysis and comparison of spectrum measurements performed in urban and rural areas to determine the total amount of spectrum usage. In Proc. International Symposium on Advanced Radio Technologies (ISART 2005) (pp. 9-12).
8. FCC, Unlicensed Operation in the TV Broadcast Bands Notice of Proposed Rulemaking (NPRM), ET Docket No. 04-186, May, 2004.
9. Ofcom "Statement on Cognitive Access to Interleaved Spectrum", July 2009.
10. The Global Transmission Market - A Screen Digest Report for DVB, September 2010, Available: www.screendigest.com.

11. Chiang, R. I., Rowe, G. B., & Sowerby, K. W. (2007, April). A quantitative analysis of spectral occupancy measurements for cognitive radio. In Vehicular Technology Conference, 2007. VTC2007-Spring. IEEE 65th (pp. 3016-3020). IEEE.
12. Wellens, M., Wu, J., & Mähönen, P. (2007, August). Evaluation of spectrum occupancy in indoor and outdoor scenario in the context of cognitive radio. In Cognitive Radio Oriented Wireless Networks and Communications, 2007. CrownCom 2007. 2nd International Conference on (pp. 420-427). IEEE.
13. Mitola III, J. (1999). Cognitive radio for flexible mobile multimedia communications. In Mobile Multimedia Communications, 1999.(MoMuC'99) 1999 IEEE International Workshop on (pp. 3-10). IEEE.
14. Mitola, J. Cognitive Radio, licentiate proposal. KTH, Stockholm, Sweden.
15. Sahai, A., Tandra, R., Mishra, S. M., & Hoven, N. (2006, August). Fundamental design trade-offs in cognitive radio systems. In Proceedings of the first international workshop on Technology and policy for accessing spectrum (p. 2). ACM.
16. Sutton, P. D., Nolan, K. E., & Doyle, L. E. (2008, Jan). Cyclostationary signatures in practical cognitive radio applications. Selected Areas in Communications, IEEE Journal on, 26(1), 13-24.
17. Gardner, W. A. (1994). Cyclostationarity in communications and signal processing. STATISTICAL SIGNAL PROCESSING INC YOUNTVILLE CA.
18. Akyildiz, I. F., Lo, B. F., & Balakrishnan, R. (2011). Cooperative spectrum sensing in cognitive radio networks: A survey. Physical communication, 4(1), 40-62.
19. Lee, W. Y., & Akyildiz, I. F. (2008). Optimal spectrum sensing framework for cognitive radio networks. Wireless Communications, IEEE Transactions on, 7(10), 3845-3857.
20. Hatfield, D. (1995). Spectrum Issues for the 1990s: New Challenges for Spectrum Management. Annenberg Washington Program, Communications Policy Studies, Northwestern University.
21. Maxwell, J. C. (1865). A dynamical theory of the electromagnetic field. Philosophical Transactions of the Royal Society of London, 459-512.
22. Hertz, H. (1893). Electric waves: being researches on the propagation of electric action with finite velocity through space. Dover Publications.
23. Lucky, R. W. (2001). The precious radio spectrum [Reflections]. Spectrum, IEEE, 38(9), 90-90.
24. Krasnow, E., Longley, L., & Terry, H. (1991). The Politics of Broadcast Regulation. In Regulation of the Electronic Mass Media: Law and Policy for Radio, Television, Cable and the New Video Technologies.
25. Federal Communications Commission. Spectrum Policy Task Force, "Report of the Spectrum Efficiency Working Group," Nov. 2002.
26. Peha, J. M. (2005). Approaches to spectrum sharing. Communications Magazine, IEEE, 43(2), 10-12.
27. Berlemann, L., & Mangold, S. (2009). Front Matter, in Cognitive Radio and Dynamic Spectrum Access. John Wiley & Sons, Ltd.
28. Kolodzy, P., & Avoidance, I. (2002). Spectrum policy task force. Federal Commun. Comm., Washington, DC, Rep. ET Docket, (02-135).
29. Hazlett, T. W. (2005). Spectrum tragedies. Yale J. on Reg., 22, 242.
30. Peha, J. M. (2009). Sharing spectrum through spectrum policy reform and cognitive radio. Proceedings of the IEEE, 97(4), 708-719.

31. Zhao, Q, & Ananthram S. "A survey of dynamic spectrum access: signal processing and networking perspectives," in Proceedings of the IEEE International Conference on Acoustics, Speech and Signal Processing (ICASSP 2007), vol. 4, Apr. 2007, pp. IV/1349–IV–1352.
32. Hatfield, D. N., & Weiser, P. J. (2005, November). Property rights in spectrum: Taking the next step. In *New Frontiers in Dynamic Spectrum Access Networks*, 2005. DySPAN 2005. 2005 First IEEE International Symposium on (pp. 43-55). IEEE.
33. Xu, L., Tönjes, R., Paila, T., Hansmann, W., Frank, M., & Albrecht, M. (2000). DRiVE-ing to the Internet: Dynamic radio for IP services in vehicular environments. In *Local Computer Networks*, 2000. LCN 2000. Proceedings. 25th Annual IEEE Conference on (pp. 281-289). IEEE.
34. Leaves, P., Moessner, K., Tafazolli, R., Grandblaise, D., Bourse, D., Tönjes, R., & Breveglieri, M. (2004, May). Dynamic spectrum allocation in composite reconfigurable wireless networks. *Communications Magazine*, IEEE, 42(5), 72-81.
35. Goldsmith, Andrea, Syed Ali Jafar, Ivana Maric, and Sudhir Srinivasa. "Breaking spectrum gridlock with cognitive radios: An information theoretic perspective." *Proceedings of the IEEE* 97, no. 5 (2009): 894-914.
36. Santivanez, C., Ramanathan, R., Partridge, C., Krishnan, R., Condell, M., & Polit, S. (2006, August). Opportunistic spectrum access: Challenges, architecture, protocols. In *Proceedings of the 2nd annual international workshop on Wireless internet* (p. 13). ACM.
37. ECC-CEPT's "Cognitive Radio Systems and Software Defined Radio", December 2016.
38. Mitola III, J. (1993). Software radios: Survey, critical evaluation and future directions. *Aerospace and Electronic Systems Magazine*, IEEE, 8(4), 25-36.
39. Mitola III, J., & Maguire Jr, G. Q. (1999). Cognitive radio: making software radios more personal. *Personal Communications*, IEEE, 6(4), 13-18.
40. Tabaković, Ž. A Survey of Cognitive Radio Systems. Post and Electronic Communications Agency, Jurišićeva, 13.
41. Wyglinski, A. M., & Pu, D. (2013). *Digital Communication Systems Engineering with Software-Defined Radio*. Artech House.
42. Zvonar, Z. (Ed.). (2001). *Software radio technologies: selected readings*. IEEE Press.
43. James, J. F. (2011). *A student's guide to Fourier transforms: with applications in physics and engineering*. Cambridge university press.
44. Cook, P. G., & Bonser, W. (1999). Architectural overview of the SPEAKEasy system. *IEEE Journal on Selected areas in Communications*, 17(4), 650-661.
45. Eyermann, P., & Powell, M. (2001). Maturing the software communications architecture for JTRS. In *Military Communications Conference, 2001. MILCOM 2001. Communications for Network-Centric Operations: Creating the Information Force*. IEEE (Vol. 1, pp. 158-162). IEEE.
46. Tarver, B., Christensen, E., Miller, A., & Wing, E. R. (2001). Digital modular radio (DMR) as a maritime/fixed Joint Tactical Radio System (JTRS). In *Military Communications Conference, 2001. MILCOM 2001. Communications for Network-Centric Operations: Creating the Information Force*. IEEE (Vol. 1, pp. 163-167). IEEE.
47. Oldham, D. R., & Scardelletti, M. C. (2007, October). JTRS/SCA and custom/SDR waveform comparison. In *Military Communications Conference, 2007. MILCOM 2007*. IEEE (pp. 1-5). IEEE.
48. Reed, J. H. (2002). *Software radio: a modern approach to radio engineering*. Prentice Hall Professional.

49. Ramm S & Leon A, ((2006, October). Selecting Architectures for Signal Processing in Military Applications. *The journal of Military Electronics & Computing* (pp. 1-2).
50. Dardaillon, M., Marquet, K., Risset, T., & Scherrer, A. (2012, August). Software defined radio architecture survey for cognitive testbeds. In *Wireless Communications and Mobile Computing Conference (IWCMC), 2012 8th International* (pp. 189-194). IEEE.
51. Dhar, R., George, G., Malani, A., & Steenkiste, P. (2006, September). Supporting integrated MAC and PHY software development for the USRP SDR. In *Networking Technologies for Software Defined Radio Networks, 2006. SDR'06. 1st IEEE Workshop on* (pp. 68-77). IEEE..
52. Minden, G. J., Evans, J. B., Searl, L., DePardo, D., Petty, V. R., Rajbanshi, R., ... & Agah, A. (2007, April). Kuar: A flexible software-defined radio development platform. In *New Frontiers in Dynamic Spectrum Access Networks, 2007. DySPAN 2007. 2nd IEEE International Symposium on* (pp. 428-439). IEEE.
53. Murphy, P., Sabharwal, A., & Aazhang, B. (2006, September). Design of WARP: a wireless open-access research platform. In *Signal Processing Conference, 2006 14th European* (pp. 1-5). IEEE.
54. Chang, C., Wawrzynek, J., & Brodersen, R. W. (2005). BEE2: A high-end reconfigurable computing system. *IEEE Design & Test of Computers*, (2), 114-125.
55. Harada, H. (2005, November). Software defined radio prototype toward cognitive radio communication systems. In *New Frontiers in Dynamic Spectrum Access Networks, 2005. DySPAN 2005. 2005 First IEEE International Symposium on* (pp. 539-547). IEEE.
56. Fernandes, V. N. (2012). Implementation of a radar system using Matlab and the USRP (Doctoral dissertation, California State University, Northridge).
57. González, C. R. A., Dietrich, C. B., Sayed, S., Volos, H., Gaeddert, J. D., Robert, P. M., ... & Kragh, F. E. (2009). Open-source SCA-based core framework and rapid development tools enable software-defined radio education and research. *Communications Magazine, IEEE*, 47(10), 48-55.
58. Hunter, C., Camp, J., Murphy, P., Sabharwal, A., & Dick, C. (2006, October). A flexible framework for wireless medium access protocols. In *Signals, Systems and Computers, 2006. ACSSC'06. Fortieth Asilomar Conference on* (pp. 2046-2050). IEEE.
59. Newman, T. R., Hasan, S. S., DePoy, D., Bose, T., & Reed, J. H. (2010). Designing and deploying a building-wide cognitive radio network testbed. *Communications Magazine, IEEE*, 48(9), 106-112.
60. Federal Communications Commission. (2005). Notice of proposed rule making and order: Facilitating opportunities for flexible, efficient, and reliable spectrum use employing cognitive radio technologies. *ET docket*, (03-108), 73.
61. Arslan, H. (Ed.). (2007). *Cognitive radio, software defined radio, and adaptive wireless systems* (Vol. 10). Berlin: Springer.
62. Mitola III, J., & Maguire Jr, G. Q. (1999). Cognitive radio: making software radios more personal. *Personal Communications, IEEE*, 6(4), 13-18.
63. Haykin, S. (2005). Cognitive radio: brain-empowered wireless communications. *Selected Areas in Communications, IEEE Journal on*, 23(2), 201-220.
64. Mitola, J. (2000). *Cognitive Radio: An Integrated Agent Architecture for Software Defined Radio*.
65. Akyildiz, I. F., Lee, W. Y., Vuran, M. C., & Mohanty, S. (2006). Next generation/dynamic spectrum access/cognitive radio wireless networks: a survey. *Computer Networks*, 50(13), 2127-2159.

66. Haykin, S. (2005). Cognitive radio: brain-empowered wireless communications. *Selected Areas in Communications, IEEE Journal on*, 23(2), 201-220.
67. Jondral, F. K. (2005). Software-defined radio: basics and evolution to cognitive radio. *EURASIP journal on wireless communications and networking*, 2005(3), 275-283.
68. Vilimpoc, M., & McHenry, M. (2003). Dupont circle spectrum utilisation during peak hours. The New America Foundation and the Shared Spectrum Company.
69. McHenry, M. A., McCloskey, D., & Bates, J. (2005). Spectrum Occupancy Measurements, Location 6 of 6: Shared Spectrum Building Roof, Vienna, Virginia, December 15-16, 2004. Shared Spectrum Company Report.
70. McHenry, M. A., & McCloskey, D. (2005). Spectrum Occupancy Measurements: Chicago, Illinois, November 16-18, 2005. Shared Spectrum Company. Technical report.
71. Erpek, T., Steadman, K., & Jones, D. (2007). Dublin Ireland spectrum occupancy measurements collected on April-16-18, 2007. The Shared Spectrum Company.
72. SSC (2009). Vienna spectrum occupancy measurements collected on September 23, 2010. The Shared Spectrum Company
73. Akyildiz, I. F., Lee, W. Y., Vuran, M. C., & Mohanty, S. (2008). A survey on spectrum management in cognitive radio networks. *Communications Magazine, IEEE*, 46(4), 40-48.
74. FCC. Spectrum Policy Task Force Report, ET Docket No. 02-135, Nov. 2002.
75. Matheson, R. J. (1988, August). Strategies for spectrum usage measurements. In *Electromagnetic Compatibility, 1988. Symposium Record., IEEE 1988 International Symposium on* (pp. 235-241). IEEE.
76. López-Benítez, M., & Casadevall, F. (2012). Spectrum usage models for the analysis, design and simulation of cognitive radio networks (pp. 27-73). Springer Netherlands.
77. Sanders, F. H. (1998, August). Broadband spectrum surveys in Denver, CO, San Diego, CA, and Los Angeles, CA: methodology, analysis, and comparative results. In *Electromagnetic Compatibility, 1998. 1998 IEEE International Symposium on* (Vol. 2, pp. 988-993). IEEE.
78. McHenry, M. A., Tenhuła, P. A., McCloskey, D., Roberson, D. A., & Hood, C. S. (2006, August). Chicago spectrum occupancy measurements & analysis and a long-term studies proposal. In *Proceedings of the first international workshop on Technology and policy for accessing spectrum* (p. 1). ACM.
79. Islam, M. H., Koh, C. L., Oh, S. W., Qing, X., Lai, Y. Y., Wang, C., ... & Toh, W. (2008, May). Spectrum survey in Singapore: Occupancy measurements and analyses. In *Cognitive Radio Oriented Wireless Networks and Communications, 2008. CrownCom 2008. 3rd International Conference on* (pp. 1-7). IEEE.
80. López-Benítez, M., Umbert, A., & Casadevall, F. (2009, April). Evaluation of spectrum occupancy in Spain for cognitive radio applications. In *Vehicular Technology Conference, 2009. VTC Spring 2009. IEEE 69th* (pp. 1-5). IEEE.
81. McHenry, M. A., & Steadman, K. (2005). Spectrum occupancy measurements, location 2 of 6: Tyson's Square centre, Vienna, Virginia, April 9, 2004. Shared Spectrum Company Report.
82. Ellingson, S. W. (2005, September). Spectral occupancy at VHF: implications for frequency-agile cognitive radios. In *IEEE Vehicular Technology Conference* (Vol. 62, No. 2, p. 1379). IEEE; 1999.
83. Sanders, F. H. (1998, August). Broadband spectrum surveys in Denver, CO, San Diego, CA, and Los Angeles, CA: methodology, analysis, and comparative results. In *Electromagnetic Compatibility, 1998. 1998 IEEE International Symposium on* (Vol. 2, pp. 988-993). IEEE.

84. McHenry, M. A., Tenhula, P. A., McCloskey, D., Roberson, D. A., & Hood, C. S. (2006, August). Chicago spectrum occupancy measurements & analysis and a long-term studies proposal. In Proceedings of the first international workshop on Technology and policy for accessing spectrum (p. 1). ACM.
85. Bacchus, R. B., Fertner, A. J., Hood, C. S., & Roberson, D. (2008, October). Long-term, wide-band spectral monitoring in support of dynamic spectrum access networks at the IIT spectrum observatory. In *New Frontiers in Dynamic Spectrum Access Networks, 2008. DySPAN 2008. 3rd IEEE Symposium on* (pp. 1-10). IEEE.
86. López-Benítez, M., & Casadevall, F. (2012). Spectrum usage models for the analysis, design and simulation of cognitive radio networks (pp. 27-73). Springer Netherlands.
87. Urkowitz, H. (1967). Energy detection of unknown deterministic signals. *Proceedings of the IEEE*, 55(4), 523-531.
88. McHenry, M. A. (2005). NSF spectrum occupancy measurements project summary. Shared spectrum company report.
89. Patil, K., Prasad, R., & Skouby, K. (2011, February). A survey of worldwide spectrum occupancy measurement campaigns for cognitive radio. In *Devices and Communications (ICDeCom), 2011 International Conference on* (pp. 1-5). IEEE.
90. Yücek, T., & Arslan, H. (2009). A survey of spectrum sensing algorithms for cognitive radio applications. *Communications Surveys & Tutorials, IEEE*, 11(1), 116-130.
91. Wellens, M., & Mähönen, P. (2010). Lessons learned from an extensive spectrum occupancy measurement campaign and a stochastic duty cycle model. *Mobile networks and applications*, 15(3), 461-474.
92. Islam, M. H., Koh, C. L., Oh, S. W., Qing, X., Lai, Y. Y., Wang, C., ... & Toh, W. (2008, May). Spectrum survey in Singapore: Occupancy measurements and analyses. In *Cognitive Radio Oriented Wireless Networks and Communications, 2008. CrownCom 2008. 3rd International Conference on* (pp. 1-7). IEEE.
93. [93]W. K. Pratt(2001), *Digital Image Processing*, John Wiley & Sons,
94. Petrin, A. J. (2005). Maximizing the utility of radio spectrum: Broadband spectrum measurements and occupancy model for use by cognitive radio(Doctoral dissertation, Georgia Institute of Technology).
95. Otsu, N. (1975). A threshold selection method from gray-level histograms. *Automatica*, 11(285-296), 23-27.
96. Datla, D., Wyglinski, A. M., & Minden, G. J. (2009). A spectrum surveying framework for dynamic spectrum access networks. *Vehicular Technology, IEEE Transactions on*, 58(8), 4158-4168.
97. López-Benítez, M., & Casadevall, F. (2010). Methodological aspects of spectrum occupancy evaluation in the context of cognitive radio. *European Transactions on Telecommunications*, 21(8), 680-693.
98. *Handbook Spectrum Monitoring*, H. S. (2010). ITU Radiocommunication Bureau.
99. Chiang, R. I., Rowe, G. B., & Sowerby, K. W. (2007, April). A quantitative analysis of spectral occupancy measurements for cognitive radio. In *Vehicular Technology Conference, 2007. VTC2007-Spring. IEEE 65th* (pp. 3016-3020). IEEE.
100. Mehdawi, M., Riley, N., Paulson, K., Fanan, A., & Ammar, M. (2013). Spectrum occupancy survey in Hull-UK for cognitive radio applications: measurement & analysis. *International Journal of Scientific & Technology Research*, 2(4), 231-236.

101. Amanna, A. E., Ali, D., Gadhiok, M., Price, M., & Reed, J. H. (2012). Cognitive radio engine parametric optimization utilizing Taguchi analysis. *EURASIP Journal on Wireless Communications and Networking*, 2012(1), 1-13.
102. Zhang, Y, and Mohsen, G, eds. *Game theory for wireless communications and networking*. CRC press, 2011.
103. Sum, C, Gabriel, P, Mohammad, A, Tuncer, B, Ha N, Tran, Z, Chen,S et al((2013). Cognitive communication in TV white spaces: An overview of regulations, standards, and technology. *IEEE Communications Magazine* 51, no.7: 138-145.
104. Fitzek, F. H., & Katz, M. D. (Eds.). (2007). *Cognitive wireless networks: concepts, methodologies and visions inspiring the age of enlightenment of wireless communications*. Springer Science & Business Media.
105. Anius, D. (2003). Enhancing innovation within a regional wireless grid. In *International Conference on Computer, Communication and Control Technologies (CCCT'03)*.
106. Tonelli, O., Berardinelli, G., Cattoni, A. F., Sorensen, T. B., & Mogensen, P. (2011, August). Software architecture design for a dynamic spectrum allocation-enabled cognitive radio testbed. In *Signal Processing Conference, 2011 19th European (pp. 2294-2298)*. IEEE.
107. Matinmikko, M., Höyhty, M., Mustonen, M., Sarvanko, H., Hekkala, A., Katz, M., ... & Kautio, A. (2008). *Cognitive radio: An intelligent wireless communication system*. VTT Technical Research Centre of Finland, Tech. Rep.
108. Ghasemi, A., & Sousa, E. S. (2008). Spectrum sensing in cognitive radio networks: requirements, challenges and design trade-offs. *Communications Magazine, IEEE*, 46(4), 32-39.
109. Brown, T. X. (2005, November). An analysis of unlicensed device operation in licensed broadcast service bands. In *New Frontiers in Dynamic Spectrum Access Networks, 2005. DySPAN 2005. 2005 First IEEE International Symposium on (pp. 11-29)*. IEEE.
110. Raman, C., Yates, R. D., & Mandayam, N. B. (2005, November). Scheduling variable rate links via a spectrum server. In *New Frontiers in Dynamic Spectrum Access Networks, 2005. DySPAN 2005. 2005 First IEEE International Symposium on (pp. 110-118)*. IEEE.
111. Challapati, K. Philips Research North America (private communication). FAQ on CogNeA Alliance, K. Kimyacioglu, Philips.
112. Wyglinski, A. M., Nekovee, M., & Hou, T. (Eds.). (2009). *Cognitive radio communications and networks: principles and practice*. Academic Press.
113. Cabric, D., Mishra, S. M., & Brodersen, R. W. (2004, November). Implementation issues in spectrum sensing for cognitive radios. In *Signals, systems and computers, 2004. Conference record of the thirty-eighth Asilomar conference on (Vol. 1, pp. 772-776)*. IEEE.
114. Haykin, S. (2005). Cognitive radio: brain-empowered wireless communications. *Selected Areas in Communications, IEEE Journal on*, 23(2), 201-220.
115. Höyhty, M., Hekkala, A., Katz, M. D., & Mämmelä, A. (2007). Spectrum awareness: techniques and challenges for active spectrum sensing. In *Cognitive Wireless Networks (pp. 353-372)*. Springer Netherlands.
116. FCC, ET Docket No. 03-237,07-78 Termination order, 2007
117. Yücek, T., & Arslan, H. (2009). A survey of spectrum sensing algorithms for cognitive radio applications. *Communications Surveys & Tutorials, IEEE*, 11(1), 116-130.

118. Yücek, T., & Arslan, H. (2009). A survey of spectrum sensing algorithms for cognitive radio applications. *Communications Surveys & Tutorials, IEEE*, 11(1), 116-130.
119. Axell, E., Leus, G., Larsson, E. G., & Poor, H. V. (2012). Spectrum sensing for cognitive radio: State-of-the-art and recent advances. *Signal Processing Magazine, IEEE*, 29(3), 101-116.
120. Ganesan, G., & Li, Y. (2005, December). Agility improvement through cooperative diversity in cognitive radio. In *Global Telecommunications Conference, 2005. GLOBECOM'05. IEEE (Vol. 5, pp. 5-pp)*. IEEE.
121. Cabric, D., Mishra, S. M., & Brodersen, R. W. (2004, November). Implementation issues in spectrum sensing for cognitive radios. In *Signals, systems and computers, 2004. Conference record of the thirty-eighth Asilomar conference on (Vol. 1, pp. 772-776)*. IEEE.
122. Urkowitz, H. (1967). Energy detection of unknown deterministic signals. *Proceedings of the IEEE*, 55(4), 523-531.
123. Lehtomaki, J. J., Juntti, M., Saarnisaari, H., & Koivu, S. (2005). Threshold setting strategies for a quantized total power radiometer. *IEEE Signal Processing Letters*, 12(11), 796.
124. Fitzek, F. H., & Katz, M. D. (Eds.). (2007). *Cognitive wireless networks: concepts, methodologies and visions inspiring the age of enlightenment of wireless communications*. Springer Science & Business Media.
125. Maleki, S., Pandharipande, A., & Leus, G. (2010, March). Two-stage spectrum sensing for cognitive radios. In *Acoustics Speech and Signal Processing (ICASSP), 2010 IEEE International Conference on (pp. 2946-2949)*. IEEE.
126. Hoven, N., Tandra, R., & Sahai, A. (2005). Some fundamental limits on cognitive radio. *Wireless Foundations EECS, Univ. of California, Berkeley*.
127. Umar, R., Sheikh, A. U., & Deriche, M. (2014). Unveiling the hidden assumptions of energy detector based spectrum sensing for cognitive radios. *Communications Surveys & Tutorials, IEEE*, 16(2), 713-728.
128. Tandra, R., & Sahai, A. (2008). SNR walls for signal detection. *Selected Topics in Signal Processing, IEEE Journal of*, 2(1), 4-17.
129. Ye, Z., Memik, G., & Grosspietsch, J. (2008, March). Energy detection using estimated noise variance for spectrum sensing in cognitive radio networks. In *Wireless Communications and Networking Conference, 2008. WCNC 2008. IEEE (pp. 711-716)*. IEEE.
130. Öner, M., & Jondral, F. (2004, September). Cyclostationarity based air interface recognition for software radio systems. In *Radio and Wireless Conference, 2004 IEEE (pp. 263-266)*. IEEE.
131. Ghozzi, M., Marx, F., Dohler, M., & Palicot, J. (2006, June). Cyclostationarity-based test for detection of vacant frequency bands. In *Cognitive Radio Oriented Wireless Networks and Communications, 2006. 1st International Conference on (pp. 1-5)*. IEEE.
132. Han, N., Shon, S., Chung, J. H., & Kim, J. M. (2006, February). Spectral correlation based signal detection method for spectrum sensing in IEEE 802.22 WRAN systems. In *Advanced Communication Technology, 2006. ICACT 2006. The 8th International Conference (Vol. 3, pp. 6-pp)*. IEEE.
133. Lundén, J., Koivunen, V., Huttunen, A., & Poor, H. V. (2007, August). Spectrum sensing in cognitive radios based on multiple cyclic frequencies. In *Cognitive Radio Oriented Wireless Networks and Communications, 2007. CrownCom 2007. 2nd International Conference on (pp. 37-43)*. IEEE.
134. Cabric, D., Chen, M. S., Sobel, D. A., Wang, S., Yang, J., & Brodersen, R. W. (2006). Novel radio architectures for UWB, 60 GHz, and cognitive wireless systems. *EURASIP Journal on Wireless Communications and Networking*, 2006(2), 22-22.

135. Gardner, W. A. (1992). A unifying view of coherence in signal processing. *Signal Processing*, 29(2), 113-140.
136. Fehske, A., Gaeddert, J., & Reed, J. H. (2005, November). A new approach to signal classification using spectral correlation and neural networks. In *New Frontiers in Dynamic Spectrum Access Networks, 2005. DySPAN 2005. 2005 First IEEE International Symposium on* (pp. 144-150). IEEE.
137. Ghozzi, M., Marx, F., Dohier, M., & Palicot, J. (2006, June). Cyclostationarity-based test for detection of vacant frequency bands. In *Cognitive Radio Oriented Wireless Networks and Communications, 2006. 1st International Conference on* (pp. 1-5). IEEE.
138. Sklar, B. (2001). *Digital communications (Vol. 2)*. NJ: Prentice Hall.
139. Tandra, R., & Sahai, A. (2005, June). Fundamental limits on detection in low SNR under noise uncertainty. In *Wireless Networks, Communications and Mobile Computing, 2005 International Conference on (Vol. 1, pp. 464-469)*. IEEE.
140. Tang, H. (2005, November). Some physical layer issues of wide-band cognitive radio systems. In *New frontiers in dynamic spectrum access networks, 2005. DySPAN 2005. 2005 first IEEE international symposium on* (pp. 151-159). IEEE.
141. Zeng, Y., & Liang, Y. C. (2009). Spectrum-sensing algorithms for cognitive radio based on statistical covariances. *Vehicular Technology, IEEE Transactions on*, 58(4), 1804-1815.
142. Zeng, Y., & Liang, Y. C. (2009). Eigenvalue-based spectrum sensing algorithms for cognitive radio. *Communications, IEEE Transactions on*, 57(6), 1784-1793.
143. Farhang-Boroujeny, B. (2008). Filter bank spectrum sensing for cognitive radios. *Signal Processing, IEEE Transactions on*, 56(5), 1801-1811.
144. Tian, Z., & Giannakis, G. B. (2007, April). Compressed sensing for wideband cognitive radios. In *Acoustics, Speech and Signal Processing, 2007. ICASSP 2007. IEEE International Conference on (Vol. 4, pp. IV-1357)*. IEEE.
145. Wang, Y., Tian, Z., & Feng, C. (2010, December). A two-step compressed spectrum sensing scheme for wideband cognitive radios. In *Global Telecommunications Conference (GLOBECOM 2010), 2010 IEEE* (pp. 1-5). IEEE.
146. Fanan, A. M, Riley, N, Mehdawi, M., Ammar, M., and Zolfaghari, M.. Survey: A Comparison of Spectrum Sensing Techniques in Cognitive Radio. In *Int'l Conference Image Processing, Computers and Industrial Engineering (ICICIP'2014) Jan, pp. 15-16. 2014.*
147. Tang, H. (2005, November). Some physical layer issues of wide-band cognitive radio systems. In *New frontiers in dynamic spectrum access networks, 2005. DySPAN 2005. 2005 first IEEE international symposium on* (pp. 151-159). IEEE.
148. Ganesan, G., & Li, Y. (2007). Cooperative spectrum sensing in cognitive radio, part I: Two user networks. *Wireless Communications, IEEE Transactions on*, 6(6), 2204-2213.
149. Ganesan, G., & Ye, L. (2007). Cooperative spectrum sensing in cognitive radio, part II: Multiuser networks. *Wireless Communications, IEEE Transactions on*, 6(6), 2214-2222.
150. Maleki, S., Pandharipande, A., & Leus, G. (2010, March). Two-stage spectrum sensing for cognitive radios. In *Acoustics Speech and Signal Processing (ICASSP), 2010 IEEE International Conference on* (pp. 2946-2949). IEEE.

151. Cabric, D., Mishra, S. M., & Brodersen, R. W. (2004, November). Implementation issues in spectrum sensing for cognitive radios. In *Signals, systems and computers, 2004. Conference record of the thirty-eighth Asilomar conference on* (Vol. 1, pp. 772-776). IEEE.
152. Cabric, D., Tkachenko, A., & Brodersen, R. W. (2006, October). Spectrum sensing measurements of pilot, energy, and collaborative detection. In *Military communications conference, 2006. MILCOM 2006*. IEEE (pp. 1-7). IEEE.
153. Dang, Z., Howitt, I., McKinney, R., & Conrad, J. (2010, March). First and second order statistics analysis for the RSS measurement in an indoor environment. In *IEEE SoutheastCon 2010 (SoutheastCon), Proceedings of the*(pp. 298-301). IEEE.
154. Martin, R. K., Thomas, R. W., & Wu, Z. (2011, June). Using spectral correlation for non-cooperative RSS-based positioning. In *Statistical Signal Processing Workshop (SSP), 2011 IEEE* (pp. 241-244). IEEE.
155. Ge, F., & Bostian, C. W. (2008, October). A parallel computing based spectrum sensing approach for signal detection under conditions of low snr and rayleigh multipath fading. In *New Frontiers in Dynamic Spectrum Access Networks, 2008. DySPAN 2008. 3rd IEEE Symposium on* (pp. 1-10). IEEE.
156. Like, E., Chakravarthy, V., Husnay, R., & Wu, Z. (2008, November). Modulation recognition in multipath fading channels using cyclic spectral analysis. In *Global Telecommunications Conference, 2008. IEEE GLOBECOM 2008*. IEEE (pp. 1-6). IEEE.
157. Tkachenko, A., Cabric, D., & Brodersen, R. W. (2007, April). Cyclostationary feature detector experiments using reconfigurable BEE2. In *New Frontiers in Dynamic Spectrum Access Networks, 2007. DySPAN 2007. 2nd IEEE International Symposium on* (pp. 216-219). IEEE.
158. Satyanarayana, Shashank. "Stationary, Cyclostationary and Nonstationary Analysis of GNSS Signal Propagation Channel." *Proceedings of the 23rd International Technical Meeting of The Satellite Division of the Institute of Navigation (ION GNSS 2010)*. 2011.
159. Häser, M., & Ahlrichs, R. (1989). Improvements on the direct SCF method. *Journal of Computational Chemistry*, 10(1), 104-111.
160. Qi, Y., Wang, W., Peng, T., & Qian, R. (2008, August). Spectrum sensing combining time and frequency domain in multipath fading channels. In *Communications and Networking in China, 2008. ChinaCom 2008. Third International Conference on* (pp. 142-146). IEEE.
161. Ghasemi, A., & Sousa, E. S. (2005, November). Collaborative spectrum sensing for opportunistic access in fading environments. In *New Frontiers in Dynamic Spectrum Access Networks, 2005. DySPAN 2005. 2005 First IEEE International Symposium on* (pp. 131-136). IEEE.
162. Izenman, A. J. (1987). *Introduction to Random Processes, With Applications to Signals and Systems*. *Technometrics*, 29(2), 245-246.
163. Gardner, W. A. (1986). The spectral correlation theory of cyclostationary time-series. *Signal processing*, 11(1), 13-36.
164. Kim, K. W. (2008). *Exploiting Cyclostationarity for Radio Environmental Awareness in Cognitive Radios Awareness in Cognitive Radios*, PhD thesis, Virginia Polytechnic Institute and State University, Blacksburg, VA, USA, 2008.
165. Gardner, W. A. (1994). *Cyclostationarity in Communications and Signal Processing*. Ed. W. A. Gardner. IEEE Press, New York, 1994.
166. Tom, C. (1995). *Cyclostationary Spectral Analysis of Typical Satcom Signals using the FFT Accumulation Method* (No. DREO-1280). DEFENCE RESEARCH ESTABLISHMENT OTTAWA (ONTARIO).

167. Gillman, A. M. (1999). Non Co-Operative Detection of LPI/LPD Signals Via Cyclic Spectral Analysis (No. AFIT/GE/ENG/99M-11). Air force inst of tech wright-pattersonafb oh school of engineering.
168. Fehske, A., Gaeddert, J., & Reed, J. H. (2005, November). A new approach to signal classification using spectral correlation and neural networks. In *New Frontiers in Dynamic Spectrum Access Networks, 2005. DySPAN 2005. 2005 First IEEE International Symposium on* (pp. 144-150). IEEE.
169. Wu, Z., Like, E., & Chakravarthy, V. (2007). Reliable modulation classification at low SNR using spectral correlation. In *2007 4th IEEE Consumer Communications and Networking Conference*.
170. Gardner, W., Brown, W., & Chen, C. K. (1987). Spectral correlation of modulated signals: Part II--digital modulation. *Communications, IEEE Transactions on*, 35(6), 595-601.
171. Roberts, R. S., Brown, W., & Loomis Jr, H. H. (1991). Computationally efficient algorithms for cyclic spectral analysis. *Signal Processing Magazine, IEEE*, 8(2), 38-49.
172. Guenther, B. E. (2010). *Multi-User Signal Classification Via Cyclic Spectral Analysis* (Doctoral dissertation, Wright State University).
173. Roberts, R. S., Brown, W., & Loomis Jr, H. H. (1991). Computationally efficient algorithms for cyclic spectral analysis. *Signal Processing Magazine, IEEE*, 8(2), 38-49.
174. Brown, W., & Loomis Jr, H. H. (1993). Digital implementations of spectral correlation analysers. *Signal Processing, IEEE Transactions on*, 41(2), 703-720.
175. Costa, E. L. (1996). *Detection and Classification of Cyclostationary Signals* (Doctoral dissertation, Master thesis, Naval Postgraduate School, Monterey, CA, US).
176. Da Costa, E. L. (1996). *Detection and Identification of Cyclostationary Signals*. NAVAL POSTGRADUATE SCHOOL MONTEREY CA.
177. Pace, P. E. (2009). *Detecting and classifying low probability of intercept radar*. Artech House.
178. Aragon-Zavala, A. (2008). *Antennas and propagation for wireless communication systems*. John Wiley & Sons.
179. Fontán, F. P., & Espiñeira, P. M. (2008). *Modelling the wireless propagation channel: a simulation approach with Matlab* (Vol. 5). John Wiley & Sons.
180. Rappaport, T. S. (1996). *Wireless communications: principles and practice* (Vol. 2). New Jersey: prentice hall PTR.
181. Pu, C. C., Lim, S. Y., & Ooi, P. C. (2012, December). Measurement arrangement for the estimation of path loss exponent in wireless sensor network. In *Computing and Convergence Technology (ICCC), 2012 7th International Conference on* (pp. 807-812). IEEE.
182. Song, M. (2011). *Characterizing cyclostationary features of digital modulated signals with empirical measurements using spectral correlation function* (No. AFIT/GCE/ENG/11-09). AIR FORCE INST OF TECH WRIGHT-PATTERSON AFB OH SCHOOL OF ENGINEERING AND MANAGEMENT.
183. Martin, R. K., Thomas, R. W., & Wu, Z. (2011, June). Using spectral correlation for non-cooperative RSS-based positioning. In *Statistical Signal Processing Workshop (SSP), 2011 IEEE* (pp. 241-244). IEEE.
184. Peterson, B. (2013) *Spectrum Analysis Basics*. Agilent Application Note 150, literature number5952-0292.

185. Ettus Research LLC, USRP2, The Next Generation of Software Radio Systems, http://www.ettus.com/downloads/ettus_ds_usrp2_v5.pdf.
186. Kolodzy, P., & Avoidance, I. (2002). Spectrum policy task force. Federal Commun. Comm., Washington, DC, Rep. ET Docket, (02-135).
187. Akyildiz, I. F., Lo, B. F., & Balakrishnan, R. (2011). Cooperative spectrum sensing in cognitive radio networks: A survey. *Physical communication*, 4(1), 40-62.
188. Lee, W. Y., & Akyildiz, I. F. (2008). Optimal spectrum sensing framework for cognitive radio networks. *Wireless Communications, IEEE Transactions on*, 7(10), 3845-3857.
189. Quan, Z., Cui, S., Sayed, A. H., & Poor, H. V. (2009). Optimal multiband joint detection for spectrum sensing in cognitive radio networks. *Signal Processing, IEEE Transactions on*, 57(3), 1128-1140.
190. Pei, Y., Liang, Y. C., Teh, K. C., & Li, K. H. (2009). How much time is needed for wideband spectrum sensing?. *Wireless Communications, IEEE Transactions on*, 8(11), 5466-5471.
191. Cabric, D., Mishra, S. M., & Brodersen, R. W. (2004, November). Implementation issues in spectrum sensing for cognitive radios. In *Signals, systems and computers, 2004. Conference record of the thirty-eighth Asilomar conference on* (Vol. 1, pp. 772-776). IEEE.
192. Umar, R., & Sheikh, A. U. (2013). A comparative study of spectrum awareness techniques for cognitive radio oriented wireless networks. *Physical Communication*, 9, 148-170.
193. Zhao, Z., Peng, Z., Zheng, S., & Shang, J. (2009). Cognitive radio spectrum allocation using evolutionary algorithms. *Wireless Communications, IEEE Transactions on*, 8(9), 4421-4425.
194. Kandeepan, S., & Giorgetti, A. (2012). *Cognitive Radios and Enabling Techniques*.
195. Ghasemi, A., & Sousa, E. S. (2005, November). Collaborative spectrum sensing for opportunistic access in fading environments. In *New Frontiers in Dynamic Spectrum Access Networks, 2005. DySPAN 2005. 2005 First IEEE International Symposium on* (pp. 131-136). IEEE.
196. Akyildiz, I. F., Lo, B. F., & Balakrishnan, R. (2011). Cooperative spectrum sensing in cognitive radio networks: A survey. *Physical communication*, 4(1), 40-62.
197. Saad, W., Han, Z., Başar, T., Debbah, M., & Ørnunges, A. (2011). Coalition formation games for collaborative spectrum sensing. *Vehicular Technology, IEEE Transactions on*, 60(1), 276-297.
198. Harada, H. (2008, October). A feasibility study on software defined cognitive radio equipment. In *New Frontiers in Dynamic Spectrum Access Networks, 2008. DySPAN 2008. 3rd IEEE Symposium on* (pp. 1-12). IEEE.
199. Tian, Z., & Giannakis, G. B. (2006, June). A wavelet approach to wideband spectrum sensing for cognitive radios. In *Cognitive radio oriented wireless networks and communications, 2006. 1st international conference on* (pp. 1-5). IEEE.
200. Hossain, E., & Bhargava, V. K. (Eds.). (2007). *Cognitive wireless communication networks*. Springer Science & Business Media.
201. Tian, Z., & Giannakis, G. B. (2006, June). A wavelet approach to wideband spectrum sensing for cognitive radios. In *Cognitive radio oriented wireless networks and communications, 2006. 1st international conference on* (pp. 1-5). IEEE.
202. Farhang-Boroujeny, B. (2008). Filter bank spectrum sensing for cognitive radios. *Signal Processing, IEEE Transactions on*, 56(5), 1801-1811.
203. Farhang-Boroujeny, B., & Kempter, R. (2008). Multicarrier communication techniques for spectrum sensing and communication in cognitive radios. *Communications Magazine, IEEE*, 46(4), 80-85.

204. Tian, Z., & Giannakis, G. B. (2007, April). Compressed sensing for wideband cognitive radios. In *Acoustics, Speech and Signal Processing, 2007. ICASSP 2007. IEEE International Conference on* (Vol. 4, pp. IV-1357). IEEE.
205. Polo, Y. L., Wang, Y., Pandharipande, A., & Leus, G. (2009, April). Compressive wide-band spectrum sensing. In *Acoustics, Speech and Signal Processing, 2009. ICASSP 2009. IEEE International Conference on* (pp. 2337-2340). IEEE.
206. Feng, P., & Bresler, Y. (1996, May). Spectrum-blind minimum-rate sampling and reconstruction of multiband signals. In *Acoustics, Speech, and Signal Processing, 1996. ICASSP-96. Conference Proceedings., 1996 IEEE International Conference on* (Vol. 3, pp. 1688-1691). IEEE.
207. Mishali, M., & Eldar, Y. C. (2009). Blind multiband signal reconstruction: Compressed sensing for analog signals. *Signal Processing, IEEE Transactions on*, 57(3), 993-1009.
208. Rosenthal, A., Linden, A., & Horowitz, M. (2008). Multirate asynchronous sampling of sparse multiband signals. *JOSA A*, 25(9), 2320-2330.
209. Fleyer, M., Linden, A., Horowitz, M., & Rosenthal, A. (2010). Multirate synchronous sampling of sparse multiband signals. *Signal Processing, IEEE Transactions on*, 58(3), 1144-1156.
210. Quan, Z., Cui, S., Sayed, A. H., & Poor, H. V. (2009). Optimal multiband joint detection for spectrum sensing in cognitive radio networks. *Signal Processing, IEEE Transactions on*, 57(3), 1128-1140.
211. Xie, S., Liu, Y., Zhang, Y., & Yu, R. (2010). A parallel cooperative spectrum sensing in cognitive radio networks. *Vehicular Technology, IEEE Transactions on*, 59(8), 4079-4092.
212. Tian, Z. (2008, November). Compressed wideband sensing in cooperative cognitive radio networks. In *Global Telecommunications Conference, 2008. IEEE GLOBECOM 2008. IEEE* (pp. 1-5). IEEE.
213. Benko, J., Cheong, Y. C., Cordeiro, C., Gao, W., Kim, C. J., Kim, H. S., ... & Liang, Y. C. (2006). A PHY/MAC Proposal for IEEE 802.22 WRAN Systems Part 1: The PHY. *IEEE802*, 22-01.
214. Hur, Y., Park, J., Woo, W., Lim, K., Lee, C. H., Kim, H., & Laskar, J. (2006, May). A wideband analog multi-resolution spectrum sensing (MRSS) technique for cognitive radio (CR) systems. In *ISCAS*.
215. Yi, Z., Yin, H., & Xikai, Z. (2012, August). Joint spectrum sensing method based on energy and covariance matrix theory. In *Instrumentation & Measurement, Sensor Network and Automation (IMSNA), 2012 International Symposium on* (Vol. 1, pp. 205-208). IEEE.
216. Smitha, K. G., Vinod, A. P., & Nair, P. R. (2012, March). Low power DFT filter bank based two-stage spectrum sensing. In *Innovations in Information Technology (IIT), 2012 International Conference on* (pp. 173-177). IEEE.
217. Nair, P. R., Vinod, A. P., & Krishna, A. K. (2011, September). A fast two stage detector for spectrum sensing in cognitive radios. In *Vehicular Technology Conference (VTC Fall), 2011 IEEE* (pp. 1-5). IEEE.
218. Chang, K., & Senadji, B. (2011, November). Spectrum sensing using two-stage detection to compensate for reduced primary user duty cycle. In *Wireless, Mobile & Multimedia Networks (ICWMMN 2011), 4th IET International Conference on* (pp. 149-154). IET.
219. Yi, Z., Lingling, Z., & Chengkai, T. (2010). Joint detection of cyclostationary and energy in cognitive radio. *Intelligent Systems and Knowledge Engineering (ISKE)*. In *2010 International Conference on* (pp. 182-186).
220. Maleki, S., Pandharipande, A., & Leus, G. (2010, March). Two-stage spectrum sensing for cognitive radios. In *Acoustics Speech and Signal Processing (ICASSP), 2010 IEEE International Conference on* (pp. 2946-2949). IEEE.

221. Sun, H., Nallanathan, A., Wang, C. X., & Chen, Y. (2013). Wideband spectrum sensing for cognitive radio networks: a survey. *Wireless Communications, IEEE*, 20(2), 74-81.
222. Neihart, N. M., Roy, S., & Allstot, D. J. (2007, May). A parallel, multi-resolution sensing technique for multiple antenna cognitive radios. In *Circuits and systems, 2007. ISCAS 2007. IEEE international symposium on* (pp. 2530-2533). IEEE.
223. Chang, S. Y. (2006). Analysis of Proposed sensing schemes. *IEEE P802*, 22.
224. Neihart, N. M., Roy, S., & Allstot, D. J. (2007, May). A parallel, multi-resolution sensing technique for multiple antenna cognitive radios. In *Circuits and systems, 2007. ISCAS 2007. IEEE international symposium on* (pp. 2530-2533). IEEE.
225. Viswanathan, R., & Varshney, P. K. (1997). Distributed detection with multiple sensors I. *Fundamentals. Proceedings of the IEEE*, 85(1), 54-63.
226. Hur, Y., Park, J., Woo, W., Lim, K., Lee, C. H., Kim, H., & Laskar, J. (2006, May). A wideband analog multi-resolution spectrum sensing (MRSS) technique for cognitive radio (CR) systems. In *ISCAS*.
227. Lee, W. Y., & Akyildiz, I. F. (2008). Optimal spectrum sensing framework for cognitive radio networks. *Wireless Communications, IEEE Transactions on*, 7(10), 3845-3857.
228. Liang, Y. C., Zeng, Y., Peh, E. C., & Hoang, A. T. (2008). Sensing-throughput trade-off for cognitive radio networks. *Wireless Communications, IEEE Transactions on*, 7(4), 1326-1337.

Note: A few References not referred to in the text

Spectrum Measurement Platform, Simulink Model and Matlab Code

The utilization of appropriate equipment and software for the evaluation of spectrum occupancy are essential to ensure accurate and reliable results. This appendix presents a sophisticated radio spectrum measurement /sensing platform that has been explicitly designed for spectrum surveys and studies in the context of DSA/CR. The developed platform constitutes a flexible measurement tool that combines a powerful RF measurement system with intelligent computer control and data processing (SectionA.1); as well, Matlab code and Simulink block diagrams (SectionA.2, SectionA.3). The description of this appendix corresponds to the measurement platform considered in Part II, III and IV.

A.1 Control Subsystem (Spectrum Analyser)

The platform experiment used in Chapter 5 is to investigate spectrum occupancy measurements in the Hull Region. The control subsystem, shown in Figure A.1, is in charge of supervising the measurement process, retrieving the measurement data from the spectrum analyser and saving the results in an appropriate format for off-line data post-processing. The control subsystem is mainly composed of a laptop, which is connected to the spectrum analyser via an Ethernet interface. The laptop runs a tailor-made script under Matlab's software environment, which controls the measurement process.

The control script communicates with the spectrum analyser by means of the Matlab's Instrument Control Toolbox and making use of commands in SCPI (Standard Commands for Programmable Instruments) format with the VISA (Virtual Instrument Standard Architecture)-TCP/IP interface.

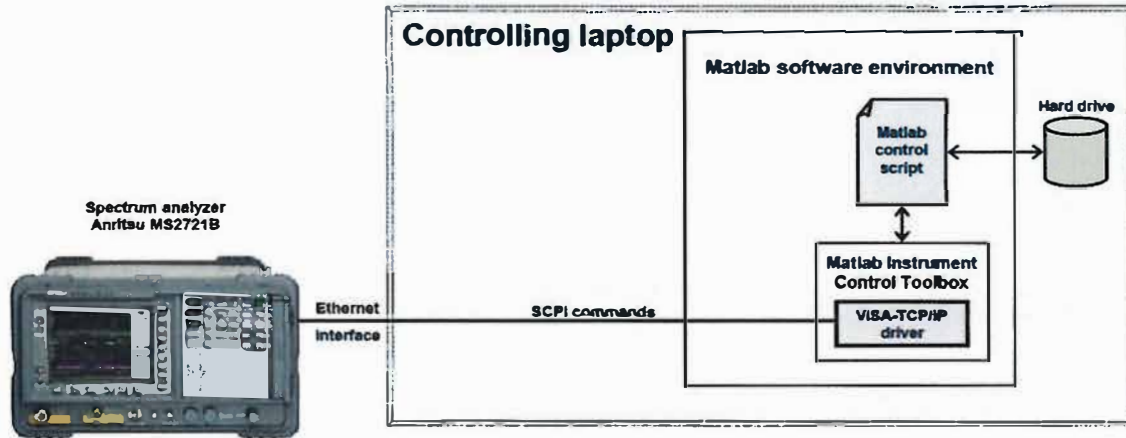


Figure A.1: Control Subsystem

The script receives the following data as input parameters from the user:

- `ip_address`: The IP address configured in the spectrum analyser.
- `f_start`: The lowest frequency in MHz of the band/span to be measured.
- `f_stop`: The highest frequency in MHz of the band/span to be measured.
- `t_start`: The time instant to begin measurements, specified in year-month-day hour-minute- second (YYYY/MM/DD/HH/MM/SS) format.
- `t_stop`: The time instant to end measurements, specified in year-month-day-hourminute- second (YYYY/MM/DD/HH/MM/SS) format.
- `file_name`: The root/base name for the generated data files.
- `nof_traces_per_file`: Number of traces/sweeps saved in each generated file. To avoid excessively large (computationally intractable) files when the measurement period is long (e.g., hours or days), the data are split into several files.

Based on the received input information, the measurement process is controlled as follows (see Algorithm control script).

A.1.2 Algorithm Control Script (Spectrum Analyser)

Input: ip_address, f_start, f_stop, t_start, t_stop, file_name, nof_traces_per_file

Output: power_file, time_file, frequency_file

1: Establish communication with the spectrum analyser → ip_address

2: Send configuration to the spectrum analyser → ip_address

{Including f_start, f_stop and others}

3: file_counter ← 0

4: trace_counter ← 0

5: power_matrix ← [] {Empty}

6: time_matrix ← [] {Empty}

7: frequency_vector ← Set of 551 frequency points between f_start and f_stop

8: next_sweep_time ← start_time

9: **while** current_time < t_start **do**

10: **while** current_time < t_stop **do**

11: Nothing {Wait for t_start}

12: **end while**

13: t ← current_time

14: next_sweep_time ← t + T_sweep

15: Initiate new sweep → ip_address

16: **while** Performing sweep ← ip_address **do**

17: Nothing {Wait for the sweep to be completed}

18: **end while**

19: Retrieve sweep data ← ip_address

20: power_values ← Retrieved sweep data

21: power_matrix ← [power_matrix; power_values]

22: time_matrix ← [time_matrix; t]

23: trace_counter ← trace_counter + 1

24: **if** trace_counter == nof_traces_per_file **then**

25: file_counter ← file_counter + 1

26: Save file power_file(file_counter) ← power_matrix

27: Save file time_file(file_counter) ← time_matrix

28: trace_counter ← 0

29: power_matrix ← [] {Empty}

30: time_matrix ← [] {Empty}

31: **end if**

32: **end while**

33: **if** trace_counter > 0 **then**

34: file_counter ← file_counter + 1

35: Save file power_file(file_counter) ← power_matrix

36: Save file time_file(file_counter) ← time_matrix

37: **end if**

38: Save file frequency_file ← frequency_vector

39: Close communication with the spectrum analyser → ip_address

A.2 Cyclostationary Feature Detection)

A.2.1 Design of Experiments (USRP2)

The experiments described in Chapter 7 is to investigate SCF values at every configuration. Two kinds of experiment were performed. One is about changing the environment-distance, location- which is done by full-factorial design. Another is about varying SNR levels and observation time with fixed distance and location. Replication is done by one long measurement and dividing it to 40 sub- measurements based on a regenerative simulation technique assuming all sub-measurements are independent and identically distributed.

The first experiment varying distance and location needs minimum measurements of:

$$10 \text{ (distance)} \times 6 \text{ (location)} \times 1 \text{ (fixed transmit power)} \times 1 \text{ (fixed observation time)} \times 1 \text{ (40 replications)} = 60$$

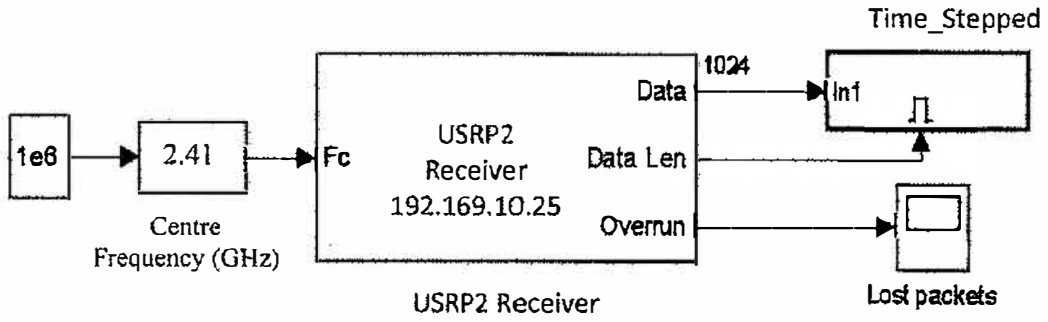
Next, Observation time is varied at each SNR levels. It requires, at a minimum, measurements of:

$$1 \text{ (fixed distance)} \times 1 \text{ (fixed location)} \times 17 \text{ (transmit power)} \times 4 \text{ (observation time)} \times 1 \text{ (40 replications)} = 68$$

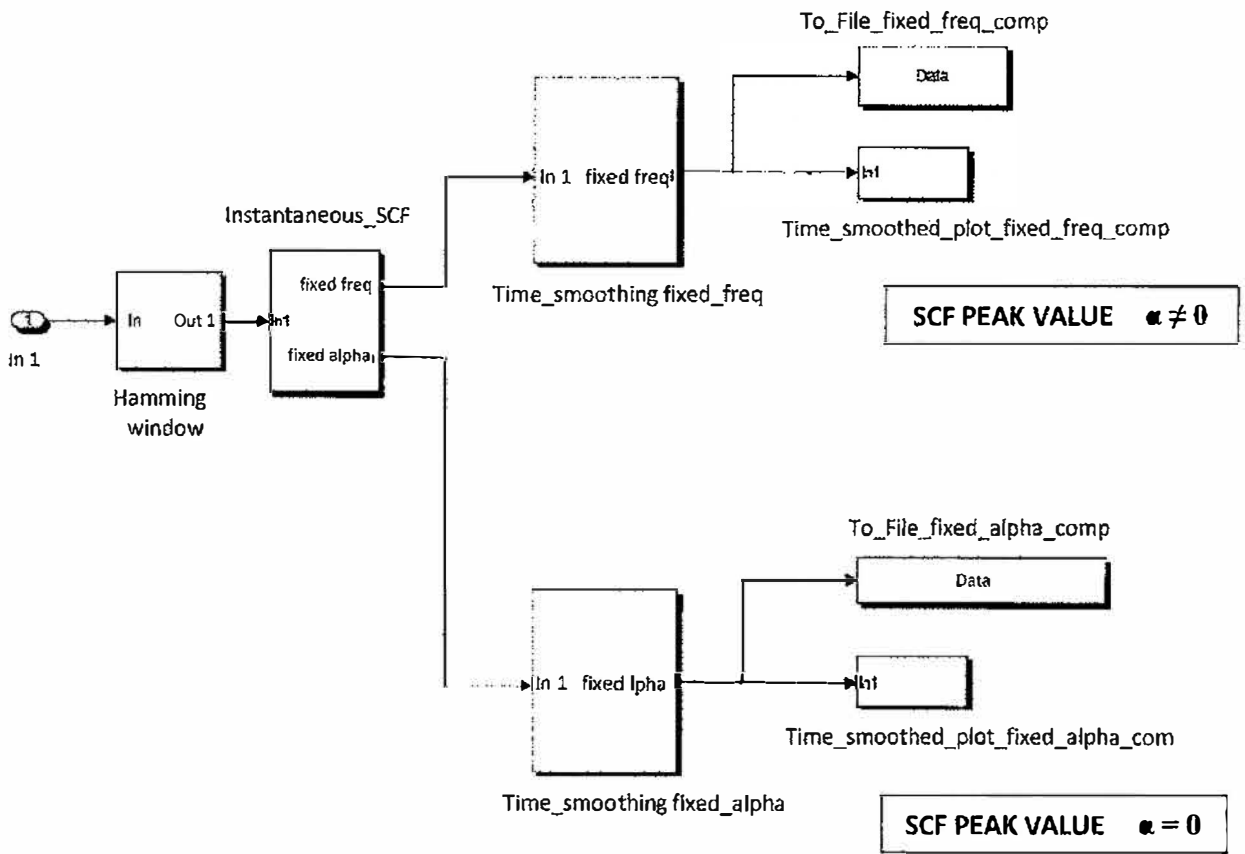
Therefore, a total of 128 measurements are required for the research

A.2.2 Simulink Model

The simulink blocks in Figure A.2 describe how the data from the experiment is analysed. Figure A.2(a) is an overall model of simulink. The block on the left is USRP2 receiver, which masks a real USRP2 device and transmits samples in a frame in complex value to SCF an analyser. Through the USRP2 receiver block, centre frequency, gain, decimation factor and output data type are controlled. Figure A.2 (b) is a detailed block diagram of the SCF analyser. Received samples go through the hamming window, and then its instantaneous SCF is calculated using Equation (7.9). The instant SCF is analysed both at particular frequency, set to the centre frequency of signal, which is for SCF and at particular alpha value set to 0, which is for PSD. The SCF values coming from the instant SCF are transferred to Time smoothing block, which takes n sets of instantaneous SCF values and computes the mean of the n sets to get time-smoothed SCF values, which is characterized as a time smoothing degree in Equation (7.13). The Time smoothing block outputs the time smoothed SCF values, plotting and recording them simultaneously.



(a) Overall Simulink Test Bed



(b) SCF/PSD Analyser

Figure A.2: Simulink Block Sets

A.3 System Model (Cooperative Wideband Sensing using Multi-Bit Hard Decision using MRSS Technique)

The experiment platform used in Chapter 8 is to investigate cooperative wideband spectrum sensing using Multi-Bit Hard Decision using two-stage adaptive sensing. Figure A.3 depicts the block diagrams of the cooperative wideband spectrum sensing part of the proposed sensor network based cooperative wideband spectrum-sensing scheme.

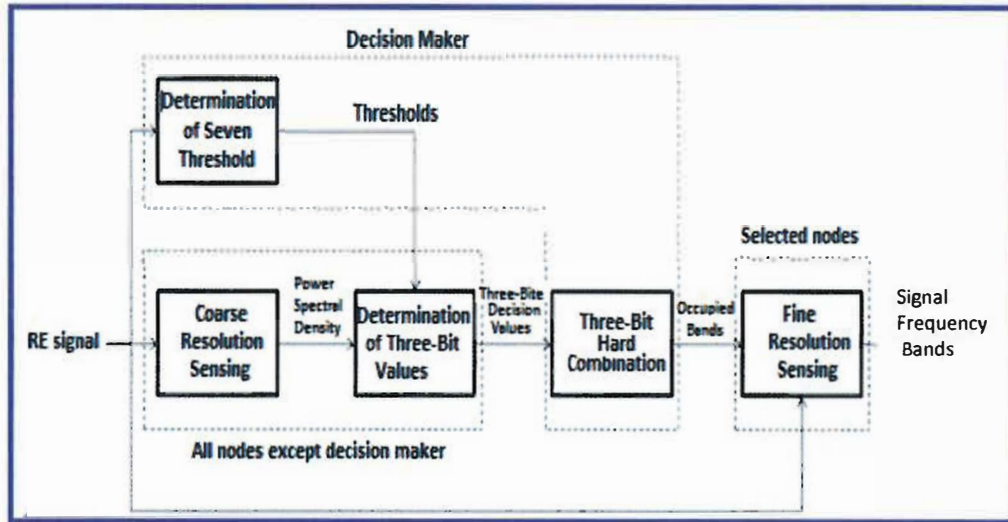


Figure A.3: Block Diagram of the Cooperative Wideband Sensing of the Proposed Scheme

The implementation of the “determination of seven thresholds,” “coarse resolution sensing,” and “fine resolution sensing” blocks in Figure A.3 is carried out by using the wavelet-based MRSS scheme discussed in section 8.5.1. Threshold determination takes place at the decision maker. Coarse resolution sensing is applied by all nodes except the decision maker, whereas only selected nodes apply fine resolution sensing. The implementation of the “determination of the three-bit values” and “three-bit hard combination” blocks in Figure 8.4 is carried out by using the proposed three-bit hard combination scheme discussed in section 8.5.3. Three-bit values are determined by the nodes after the coarse resolution sensing. Three-bit hard combination takes place at the decision maker. The “fine resolution sensing” block is applied to determine the frequency band of the signal. The following subsection describe as wavelet-based MRSS as well as each of the blocks shown in Figure A.3.

A.3.1 Wavelet-based MRSS

In wavelet-based MRSS technique, the pulse duration of the wavelet generator and frequencies of the sinusoidal functions are changed to sense the spectrum with different resolutions [229].

In particular, to obtain different sensing resolutions, wavelet pulse width T_g and frequency increment f_{sweep} are adjusted, and to scan the frequency band of interest, inspected frequency value kf is changed.

The use of a large T_g or a smaller f_{sweep} provides fine resolution sensing, whereas the use of a smaller T_g or a large f_{sweep} provides coarse resolution sensing. As shown in Figure A.4, first, a wavelet pulse with duration T_g is multiplied by a cosine and sine functions having the same frequency as the inspected frequency. Then, the results of these multiplications are multiplied by the received RF signal. After that, integration and digitization are applied in the analog correlators. The outputs of the analog correlators are first squared and then summed. Coarse resolution sensing and fine resolution sensing concepts can be better understood by an examination of the results of this technique presented in [229]. Figure A.5-b shows the spectrum of an input RF signal to the system shown in Figure A.5-a. In Figure A.5-b, there are three signals in the medium having carrier frequencies: 597 MHz, 615 MHz and 633 MHz, with bandwidths: 200 kHz, 6 MHz and 7 MHz, respectively.

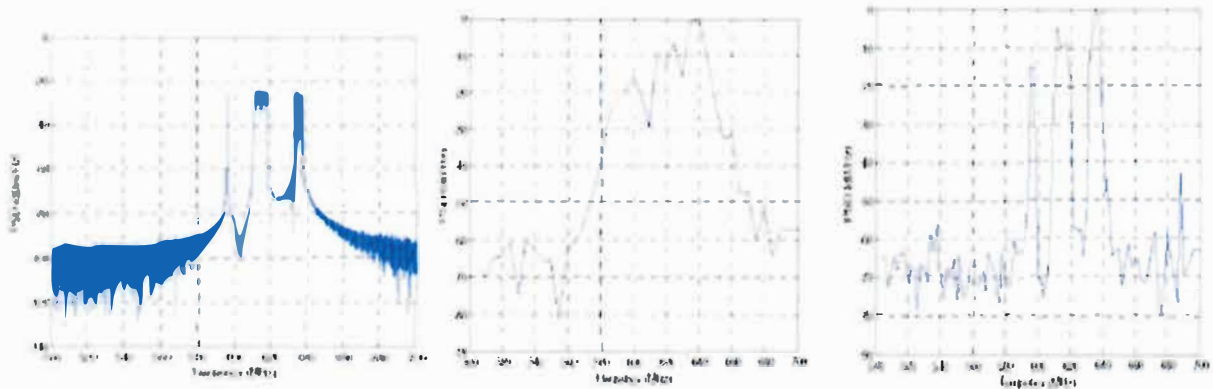


Figure A.5: Shows the result of coarse resolution spectrum sensing with a window pulse width T_g of $0.1 \mu s$ and a frequency increment f_{sweep} of 5 MHz. Figure A.5-c shows the result of fine resolution spectrum sensing with a window pulse width T_g of $1 \mu s$ and a frequency increment f_{sweep} of 2 MHz. Window pulse width T_g and frequency increment f_{sweep} determine the resolution of this scheme. Note that the lower the f_{sweep} value and the higher the T_g value, the higher the sensing resolution. By comparing Figure A.5-b and Figure A.5-c, sharp peaks for each input signal in Figure 9 show that fine resolution sensing gives better detection performance in terms of sensing resolution [229].

A.3.2 Determination of Seven Thresholds

Figure A.4 shows the multi-resolution spectrum-sensing diagram for the implementation of the “determination of seven thresholds” block of Figure A.3. This block diagram consists of a low noise amplifier (LNA), a window (wavelet) generator, a cosine function generator, multipliers, integrators and an envelope detector.

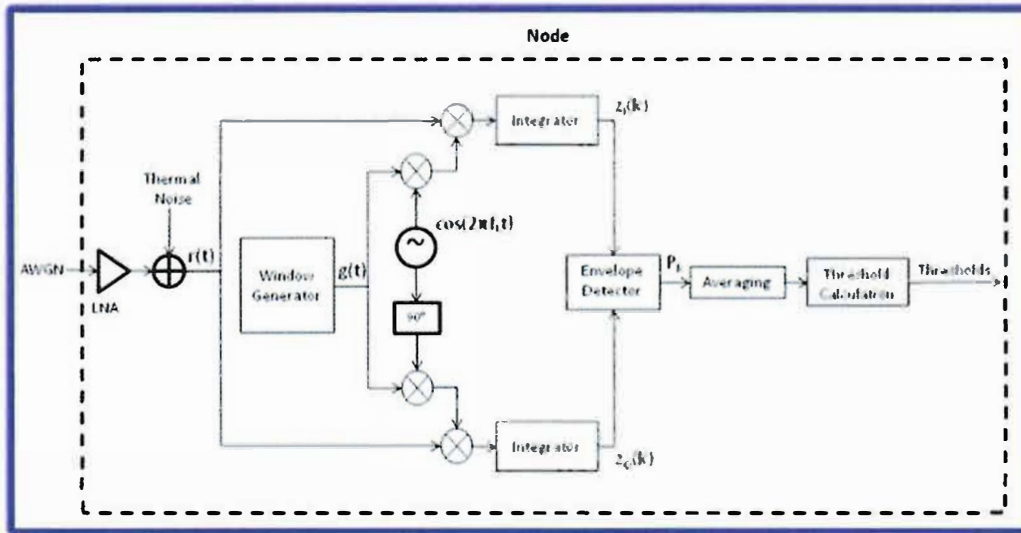


Figure A.4: Multi-Resolution Spectrum Sensing Diagram for the Implementation of Determination of Seven Thresholds Block.[229]

A.3.3 Coarse Resolution Sensing

After the thresholds are determined and the Radio nodes are informed about these threshold values, the coarse resolution-sensing block is implemented by using the diagram shown in Figure A.5 to quickly examine the spectrum. Parameters wavelet pulse width and frequency increment are chosen as 2MHz and 2 μ s, respectively. Power spectral density (PSD) is obtained from the output of Figure A.5.

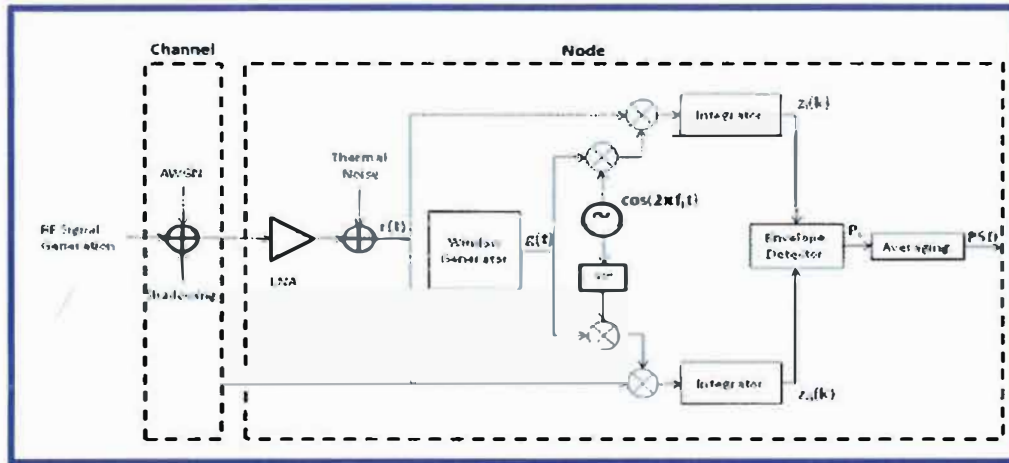


Figure A.5: Multi-Resolution Spectrum Sensing Diagram for the Implementation of “Coarse Resolution Sensing” Block[229].

A.3.4 Determination of Three-bit Values

After the coarse resolution sensing, the “determination of three-bit values” block follows. The result of the coarse resolution sensing is compared with the seven thresholds and three-bit values are determined for each frequency value at every node. Figure 8.4 shows the energy regions with the corresponding three-bit local observation values that will be sent to the decision maker when there is an observed energy in that region.

A.3.5 Three-bit Hard Combination

The function of the “three-bit hard combination” block in Figure A.3 is to combine the sensing results of the radio nodes and to detect the signals in the air by using the proposed three-bit hard combination scheme at the decision maker. The decision criterion given by Equation 8.2 and the weights given are used to determine the presence of the signal

A.3.6 Fine Resolution Sensing

As a last stage, the “fine resolution sensing” block is implemented with the same diagram used for the “coarse resolution sensing” block shown in Figure A.5. The objective of fine resolution sensing is to determine the frequency band of the signal. The differences from coarse resolution sensing are the values of wavelet pulse width and frequency increment, which are chosen as 500 kHz and $4\mu\text{s}$, respectively. The result of the three-bit hard combination scheme determines the spectrum bands on which fine resolution sensing will be applied, and the nodes that will apply fine resolution sensing. Then, fine resolution sensing is applied on these spectrum bands by the Radio nodes that sense the highest energies in these bands.